Photochemistry and organic complexation of iron: Interactions in the Southern Ocean

RIJKSUNIVERSITEIT GRONINGEN

Photochemistry and organic complexation of iron: Interactions in the Southern Ocean

Proefschrift

ter verkrijging van het doctoraat in de
Wiskunde en Natuurwetenschappen
aan de Rijksuniversiteit Groningen
op gezag van de
Rector Magnificus, dr F. Zwarts,
in het openbaar te verdedigen op
vrijdag 13 mei 2005
om 16:15 uur

door

Michaël Johannes Adrianus Rijkenberg

geboren op 3 juni 1972
te Amsterdam

Promotor: Prof. dr ir H.J.W. de Baar

Copromotores: Dr L.J.A. Gerringa
Dr A.G.J. Buma

Beoordelingscommissie: Prof. dr P.J. Neale
Prof. dr H.P. van Leeuwen
Prof. dr J. Huisman

Contents

Chapter 1

Introduction and objectives

1.1 Iron, the case for the Southern Ocean

Iron (Fe) is the fourth most abundant element in the earth crust (~ 5.6%) and was present in high concentrations in seawater during the anoxic past of the earth (Sternberg, 1974; Fallows and Raven, 1997; Turner et al., 2001). Given its abundance and capacity to transfer electrons, Fe evolved into a key element in many biochemical reactions, e.g. nitrogen fixation and photosynthesis (Reuters and Ads, 1987; Guider et al., 1993; de Bar and la Roche, 2003). With the oxygenation of the atmosphere and oceans (Holland, 1984) the Fe was removed from the oceans by precipitation, resulting in the Precambrian "banded iron formations" as have been found in North America, Asia and Australia (Evans, 1980). Fe became a "hard to get essential" (Gran, 1931; Martin and Fitzwater, 1988) inducing the evolution of specialized Fe harvesting strategies in biology (Price and Morel, 1998).

The Southern Ocean, making up 17% of the world oceans, is together with the Northeast Pacific and the Equatorial Pacific, known as a high-nutrient low-chlorophyll (HNLC) area. In HNLC areas the major nutrients such as phosphate, nitrate and silicate are in ample supply and apparently cannot be fully used by phytoplankton (Martin and Fitzwater, 1988; de Baar et al., 1990; Martin et al., 1990; Martin et al., 1994). The extremely low Fe concentrations (de Baar et al., 1990; Martin et al., 1990) together with factors such as irradiance and grazing (Mitchell et al., 1991; Nelson and Smith, 1991; Sunda and Huntsman, 1997; de Baar et al., 1999; de Baar and Boyd, 2000; Lancelot et al., 2000) limit and thus regulate primary production, species composition (Buma et al., 1991) and carbon cycling within Southern Ocean planktonic communities.

The Fe concentrations as measured in surface waters of the open Southern Ocean ranged from 0.05 – 0.4 nM as measured in 1996 in the Polar Front in the eastern part of the Atlantic sector (de Jong et al., 1998). Low Fe concentrations are the result of low Fe input rates. Sources of Fe for the open Southern Ocean surface waters were suggested to be: i) contact of waters with continental margin sediments of e.g. the Argentine Basin (de Baar et al., 1995) or archipelagos like the Kerguelen Islands (Blain et al., 2001), ii) aeolian sources of Fe originating from e.g. the South American continent (Duce and Tindale, 1991), iii) transport by melting sea-ice (Sedwick and DiTullio, 1997), iv) upwelling (de Baar and de Jong, 2001; Hoppema et al., 2003) and v) extraterrestrial dust (Johnson, 2001). Next to the above described sources of "new" Fe, regeneration and recycling of biological Fe may be very important in supporting the primary production in an open ocean Fe limited environment such as the Southern Ocean (Hutchins and Bruland, 1994; Hutchins et al., 1995).

In the austral spring, phytoplankton has to deal with significantly increased levels of ultraviolet B radiation (UVB: 280-315 nm) due to stratospheric ozone depletion (Frederick and Snell, 1988; Solomon, 1990), this in addition to limiting factors such as Fe. In the clear Southern Ocean waters UVB penetrates to significant depths (60 m) (Smith et al., 1992). Biological effects of enhanced UVB, detected to maximum depths of 20-30 m (Karentz and Lutze, 1990; Smith et al., 1992), negatively affect the marine Antarctic primary producers. It has been demonstrated that enhanced UVB increases photoinhibition (Neale et al., 1998), by decreasing photosystem II efficiency (Schofield, 1995), and modifying the RUBISCO pool (Lesser et al., 1996). Also much information is available on UVB-related accumulation of DNA damage, as demonstrated by the formation of cyclobutane pyrimidine dimers (CPD) in marine phytoplankton (Buma et al., 1996; Buma et al., 2001). So far, research mainly focused on evaluating the potentially harmful effects of enhanced UVB radiation on biological systems in this region. However, little is known about the effects of UVB on marine chemistry, in particular the iron photochemistry.

Ever since the onset of the industrial revolution, large scale burning of fossil fuels due to human activities causes a rapid rise of atmospheric carbon dioxide concentration. Carbon dioxide, acting as a global blanket, prevents the heat transport from the atmosphere into space, thereby increasing the temperature and largely determining the climate on earth. The Southern Ocean plays an important role in controlling this CO_2 concentration in the atmosphere (Hoppema et al., 1999). Here biological fixation of CO_2 by phytoplankton in surface waters (de Baar and Boyd, 2000) exceeds the expected outgassing of CO_2-rich upwelling waters.

Past global climate changes as correlated with dust input (and hence iron) in the Southern Ocean coincide with lower temperatures and lower atmospheric CO_2 concentrations (Jouzel et al., 1993; Edwards et al., 1998). The "Iron hypothesis" (Martin, 1990) suggests that high Fe-rich dust input, as a result of a dry climate and strong winds in combination with a weakened hydrological cycle (Yung et al., 1996), enhanced primary production and consequently the drawdown of atmospheric CO_2 during glacial maxima. It is not known as yet whether these correlations are an indirect result of Southern Ocean Fe enrichment, subsequent phytoplankton bloomforming, resulting in enhanced CO_2 sequestration, or that other mechanisms play a role (Arimoto, 2001; Ridgwell, 2002). Model calculations show that only about a third of the glacial-interglacial CO_2 change can be explained by dust deposition (Popova, 2000; Ridgwell and Watson, 2002; Fennel et al., 2003).

Large scale Fe enrichment experiments have been performed to investigate the possibility of climate regulation via the induction of phytoplankton blooms in the Southern Ocean (Boyd et al., 2000; Gervais et al., 2002; Boyd et al., 2004; Coale et al., 2004; de Baar et al., 2005). Biological sequestration of CO_2 into the deep ocean, via the sinking of particulate material (the biological pump), may prevent CO_2 from entering the atmosphere for

a long period of time. Recently, two Fe enrichment experiments, one in the Gulf of Alaska (Boyd et al., 2004) and one in the Southern Ocean (Buesseler et al., 2004) demonstrated that organic material resulting from an Fe induced phytoplankton bloom is exported to the deep ocean. Yet, the results suggest that the carbon export to the deep ocean was small and that the majority of the particulate organic carbon (POC) was remineralized by bacteria. The remineralization of POC results in an increase in pCO_2 in the surface seawater which eventually might lead to outgassing of the previously biologically fixed CO_2 back to the atmosphere. Minor carbon sequestration and export and subsequently the amount of Fe needed to add to the ocean in order to have an impact on the annual anthropogenic CO_2 released would make Fe enrichment an expensive tool (Buesseler and Boyd, 2003). Moreover, Fe enrichment as a tool for climate regulation should not be used until ecological consequences and possible unintended climatic feedbacks are investigated (Buesseler and Boyd, 2003; Turner et al., 2004).

Nevertheless, Fe is the dominant limiting nutrient of the ecosystem in the Southern Ocean. Not only phytoplankton, but also organisms higher up in the hierarchy of the foodchain will suffer the consequences. Hence a detailed knowledge of the chemistry of Fe in seawater and its biological availability is important to address the many questions relating with Fe metabolism in high nutrient low chlorophyll regions.

1.2 Fe chemistry in seawater

The chemistry of Fe in seawater is very complex (Figure 1). Fe(III) is the thermodynamically stable form in oxygenated waters. It has a very low solubility in seawater (Millero, 1998; Liu and Millero, 2002). The inorganic speciation of Fe(III) is dominated by its hydrolysis behavior (Waite, 2001). The Fe(III) has a low solubility product: ~ 0.07 nM in seawater of 4°C (pH = 8, S =36) (Liu and Millero, 1999). It tends to form particulate iron oxyhydroxides. Little is known about the kind of particulate iron oxyhydroxides present in seawater or formed upon addition of low concentrations of Fe(III). Moffett (2001) suggests, based on model studies, that in aqueous alkaline media Fe(III) polymerizes into amorphous Fe(III) hydroxides. With aging, these solids loose water and develop crystalline structures leading to two principal products, lepidocrocite (γ-FeOOH) (Tipping et al., 1989) and a more amorphous solid, ferrihydrite ($Fe_5HO_8 \cdot 4H_2O$) (Schwertmann and Thalmann, 1976). The final crystalline form is depending on the chemical environment of the Fe, e.g. in the presence of relatively high concentrations of $Si(OH)_4$ (Si/Fe ratios > 0.05), as found in the
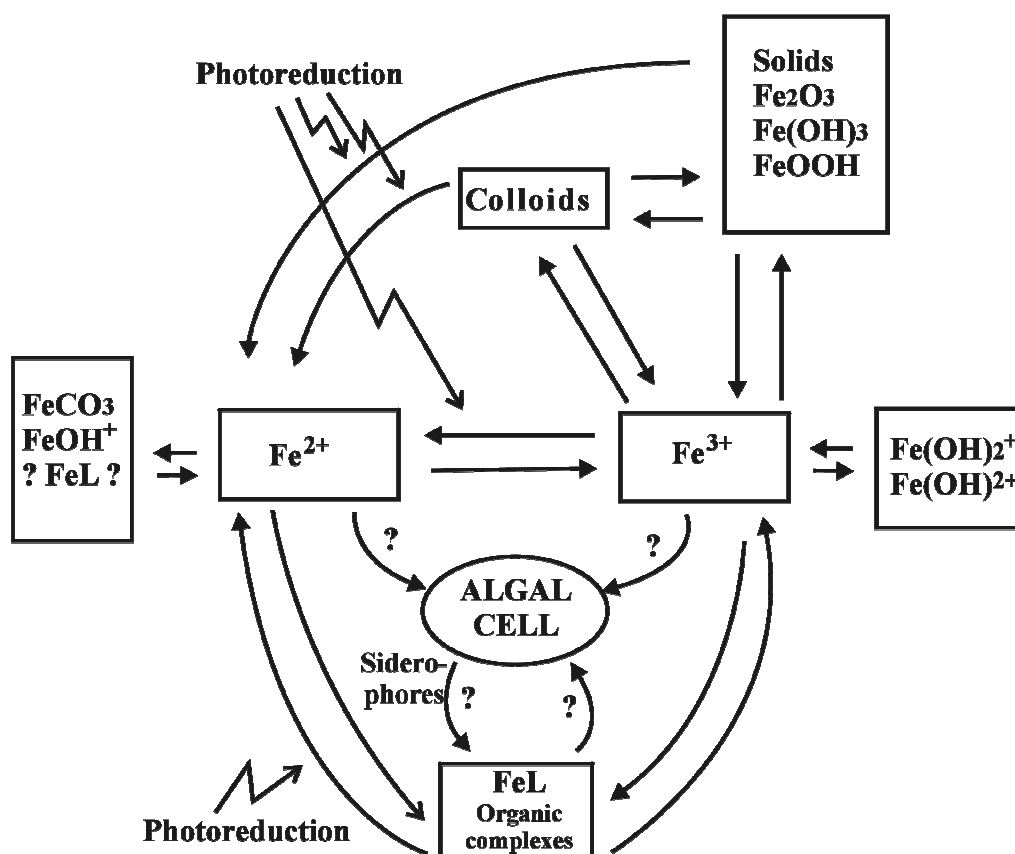
Figure 1. Model of the chemistry of Fe in seawater (Gerringa *et al.*, 2000).

Southern Ocean, Fe will form ferrihydrite (Schwertmann and Thalmann, 1976; Tipping et al., 1989). Ultimately these oxyhydroxide minerals will loose additional water with aging, and become more refractory minerals such as hematite (α-Fe_2O_3) and goethite (α-FeOOH) (Schwertmann and Taylor, 1972; Schwertmann and Fischer, 1973; Cornell and Schwertmann, 1996).

Organic complexation of iron in seawater increases the Fe solubility (Kuma et al., 1996; Johnson et al., 1997). Over 99% of the dissolved iron in the ocean is organically complexed (Gledhill and van den Berg, 1994; van den Berg, 1995). These organic ligands are found in excess over the dissolved Fe pool (Boye et al., 2001). The organic ligands are presumed to be of biological origin (Johnson et al., 1997; Hutchins et al., 1999). Nevertheless, the identity, origin, and chemical characteristics of the organic Fe binding ligands in the oceans are largely unknown. The conditional stability constants of FeL complexes range in magnitude between 10^{18} and 10^{23} as measured in the North Atlantic (Gledhill and van den Berg, 1994; Wu and Luther, 1995; Witter and Luther, 1998), the North Sea (Gledhill et al., 1998), the Mediterranean Sea (van den Berg, 1995), the Arabian Sea (Witter et al., 2000), the North Central and equatorial Pacific Ocean (Rue and Bruland, 1995;

Rue and Bruland, 1997) and the Southern Ocean (Nolting et al., 1998; Boye et al., 2001; Boye, in press). Although there is five orders of magnitude difference in the K'_{FeL} of organic complexes between different ocean regions, it has not been possible to use the K'_{FeL} to identify organic ligands using the K'_{FeL} of known model ligands (Witter et al., 2000). However, comparison of formation- and dissociation rate constants between model ligands and field samples suggests that most of the unknown ligands in seawater originate from porphyrin and siderophore-like compounds (Witter et al., 2000). Siderophores are low-molecular weight, high affinity Fe(III) binding ligands, which are secreted by e.g. Fe limited marine cyanobacteria and heterotrophic bacteria to scavenge and transport Fe (Wilhelm and Trick, 1994; Martinez et al., 2000; Barbeau et al., 2002). Siderophores have shown to be present in the marine environment: hydroxamate and catecholate Fe-binding functional groups, characteristic for siderophores, were present in different size classes of samples taken along the Californian coast (Macrellis et al., 2001). Furthermore, Gledhill et al. (2004) confirmed the presence of siderophores in coastal seawater by detecting 7 siderophore type compounds among which one was identified as desferrioxamine B.

For a long time it was thought that organic iron binding ligands were not photodegradable. There were no reports of vertical gradients in depth profiles of Fe(III) chelators (Gledhill and van den Berg, 1994; Rue and Bruland, 1995; Wu and Luther, 1995), i.e. exhibiting minima within the shallow mixed layer, or any other feature which would suggest a surface/photochemical sink (Moffett, 2001). However, recently, a surface low ligand concentration followed by higher ligand concentrations at depth suggested photochemical breakdown, as observed by (Boye et al., 2001) in the Southern Ocean. Powell and Wilson-Finelli (2003) reported that photodegradation of ligands appears to occur in a size class smaller than 1 kDa in the Gulf of Mexico. The hydroxamate and catecholate Fe-binding functional groups found by Macrellis et al. (2001) and present in the low molecular weight classes (< 300 Da) was suggested to be caused by UV induced degradation of larger Fe-binding siderophores in surface waters. Furthermore, Barbeau et al. (2001) showed for the first time the direct photolysis of marine Fe(III)-siderophore complexes (Trick, 1989; Wilhelm and Trick, 1994; Granger and Price, 1999) leading to the formation of lower-affinity Fe(III) ligands and the reduction of Fe(III) to Fe(II).

The Fe(II) is better soluble in seawater than Fe(III). However, the Fe(II) concentration is always the result of the reduction of Fe(III) counteracted by the oxidation of Fe(II). There are several possible mechanisms for the production of Fe(II) within oxic seawater: i) photochemical reduction of inorganic oxyhydroxides (Waite and Morel, 1984; Wells and Mayer, 1991) and organically complexed Fe (Barbeau et al., 2001), ii) dark reduction of Fe by superoxide (Voelker and Sedlak, 1995) or free radial organic ligand species (Ross and Neta, 1982; Faust, 1994), iii) reduction of Fe by intra- or extracellular enzymes (Maldonado and Price, 1999; Maldonado and Price, 2000), iv) reduction of Fe in microenvironments as

e.g. the acidic food vacuoles of protozoan grazers (Barbeau et al., 1996), and v) the deposition of photochemically altered aerosols (Behra and Sigg, 1990; Zhuang et al., 1992; Erel et al., 1993; Zhu et al., 1993). During the Fe enrichment experiment SOIREE in the Southern Ocean photo(induced) Fe reduction was the main mechanism explaining the retaining measurement of high Fe(II) concentrations (Croot et al., 2001).

The Fe(II) concentrations in seawater are expected to be very low due to low total iron concentrations and because Fe(II), although well soluble in seawater, becomes rapidly oxidized by O_2 and H_2O_2 (Millero et al., 1987; Millero and Izaguirre, 1989; Millero and Sotolongo, 1989; King et al., 1991; King et al., 1995; King, 1998). Yet, significant and remarkably stable levels of Fe(II) have been determined in the Northeast Atlantic (Boye et al., 2003), the East-equatorial Atlantic (Bowie et al., 2002) and during a Southern Ocean Fe enrichment experiment (Croot et al., 2001). The option of Fe(II) stabilization through the involvement of organic ligands has been hypothesized to explain the presence of these relative high concentrations of Fe(II) (Croot et al., 2001; Boye et al., 2003).

1.3 Fe photo(induced) redox cycle

1.3.1 *Fe(III) photoreduction*

The photoreduction of dissolved and synthetic colloidal Fe(III) has been measured in seawater under laboratory and field conditions (Waite and Morel, 1984; Rich and Morel, 1990; Wells and Mayer, 1991; Waite and Szymczak, 1993; Miller and Kester, 1994). The shortest wavelength of light in the terrestrial solar spectrum is ~300 nm. Many Fe species absorb at wavelengths greater than 300 nm including Fe with ligands such as OH^- (Faust and Hoigne, 1990; Faust, 1994), H_2O (Langford and Carey, 1975), HO_2^- (Evans et al., 1949), HSO_3^-/SO_3^{2-} (Faust and Hoffmann, 1986; Faust et al., 1989), Cl^- (Langford and Carey, 1975; Nadtochenko and Kiwi, 1998), carboxylates and polycarboxylates (Parker, 1954; Parker and Hatchard, 1959; Cunningham et al., 1988; Zuo and Hoigne, 1992; Faust and Zepp, 1993), and O^{2-} in Fe(III) (hydrous) oxides (Sherman and Waite, 1985; Faust and Hoffmann, 1986; Faust et al., 1989). Rich and Morel (1990) have shown that iron was not photoreduced at wavelengths higher than 560 nm. Correspondingly, Wells et al. (1991) observed increasing lability of colloidal iron in seawater, with a spectral dependency that generally increased with decreasing wavelength. In addition to wavelength dependency, a strong relation has been found between irradiance level and the iron photoreduction rate (Waite et al., 1995).

Diurnal variations of Fe(II) and reactive Fe(III) species have been observed in the field (Hong and Kester, 1986; O'Sullivan et al., 1991; Johnson et al., 1994). However, most information so far has been collected under artificial conditions in the laboratory. Laboratory

studies show that the rate of Fe(III) photoreduction is strongly dependent on the pH, decreasing rapidly with increasing pH (Waite and Morel, 1984; Sulzberger and Laubscher, 1995; Sulzberger and Laubscher, 1995) and the thermodynamic stability of the Fe(III)-(hydr)oxide phase present (Wells and Mayer, 1991; Wells et al., 1991). Direct reduction of Fe^{3+} and $Fe(OH)^{2+}$ has been shown to be the dominant Fe(II) producing photo-reactions at low pH (David, 1976) with the more hydrolyzed species $Fe(OH)_2^+$, being photo-chemically less reactive (Mulay and Selwood, 1955). The photoreduction of Fe(III) hydrolysis complexes, as studied in NaCl solutions, occurs via a ligand-metal charge transfer (LMCT) reaction (Eq. 1) (King et al., 1993):

$$Fe(OH)^{2+} \xrightarrow{\ hv\ } Fe-OH* \longrightarrow Fe^{2+} + OH\cdot, \qquad (1)$$
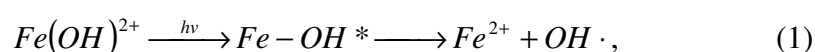
where Fe-OH* is an excited state intermediate.

Yet, direct photo-reduction of these dissolved inorganic Fe(III) species is not a significant source of Fe(II) in natural waters with a pH above 6.5 (King et al., 1993). Increasing pH, changing solubility and hydrolyzed Fe species, decreases the solubility product of Fe and induces the formation of colloidal Fe oxides. The mineralogy of these oxides affects the photoinduced dissolution of Fe. The ability of photochemically produced Fe(II) to detach from the oxide surface decreases with increasing stability of the crystalline form (Sulzberger and Laubscher, 1995). Waite and Morel (1984) could detect photoreduced iron from amorphous Fe hydroxides at pH is 6.5 but not at pH 8. They proposed that a hydroxylated ferric surface species is the primary chromophore (light absorbing compound), analogous to the photoreduction of $Fe(OH)^{2+}$, and that at pH 8 the Fe(III) surface complex was more strongly hydrolyzed and less prone to photoreduction.

Knowing that most Fe in seawater is complexed or coupled to organic material it is assumed that most observed photoredox reactions in marine waters are likely to be associated with absorption of light by Fe(III)-organic chromophores. These chromophores undergo ligand to metal charge transfers (LMCT) reactions (Eq. 2) resulting in the production of Fe(II) and, as shown in most Fe-ligand model systems, in a non-reversible decomposed organic ligand (Waite and Morel, 1984). However, the absorption of light does not necessarily results in the production of Fe(II) and the decomposition of the complex. The resulting excited state situation upon light absorption can be reversed by thermal relaxation (Eq. 3).

$$Fe(II)-L* \longrightarrow Fe(II) + L_{ox} \qquad (2)$$

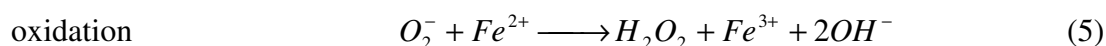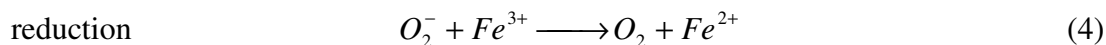$$Fe(III)-L \xleftarrow{\ hv\ } Fe(II)-L* \qquad (3)$$
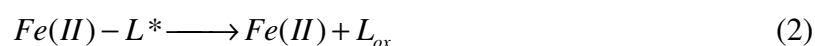
Organic matter does have the potential to increase the rate of Fe(III) photoreduction (Waite and Morel, 1984; Zuo and Hoigne, 1992) depending on the type and concentration of the reductants (e.g. oxalate, citrate, fulvic acid, sulphite) adsorbed to the Fe(III)-(hydr)oxide surface (Waite and Morel, 1984; Waite and Morel, 1984; Faust and Hoffmann, 1986; Siffert and Sulzberger, 1991; Pehkonen et al., 1993; Sulzberger and Laubscher, 1995; Sulzberger and Laubscher, 1995). Oxalate is a commonly found Fe chelator in atmospherically transported dust (Saydam and Senyuva, 2002). Complexation by oxalate extends the absorption band of Fe(III) into the visible part of the light spectrum (Zuo, 1995) and may enhance the pH range over which Fe may be photoreduced (Sulzberger and Laubscher, 1995). Kuma et al. (1992) detected high concentrations of Fe(II) during spring blooms in Funka Bay (Japan) and related this to the release of organic components from phytoplankton, thereby inducing the photoreduction of Fe. The presence of various dissolved organic substances, generally considered to be organic components released from phytoplankton such as sugar acids indeed improved the photoreduction of Fe (Kuma et al., 1995). In addition, Hudson et al. (1992) saw a similar effect when *Thalassiosira weissflogii* was added to seawater.

Marine siderophore Fe(III) complexes have shown to be photo-reactive, because they produce Fe(II) in the light (Barbeau et al., 2001; Barbeau et al., 2002; Barbeau et al., 2003). The photoreactivity of these complexes is depending on the non-reversible oxidation of the complexing functional group in the short time (≤ 1 ns) that the photoinduced excited state exists. Most photo-reactive complexes are characterized by the presence of carboxylate and aminocarboxylate ligands which are oxidized irreversibly through cleavage of the carboxylate as CO_2. Hydroxamate siderophores do not possess carboxyl groups involved in Fe coordination and do not undergo photoreactions, e.g. desferrioxamine B (Finden et al., 1984; Gao and Zepp, 1998). The oxidation of catechols is reversible and they are thus not photoreactive when complexed to iron (Barbeau et al., 2003). Iron-siderophore complexes using α-hydroxy carboxylate functional groups to bind iron are photoreactive, whereas its free form is not photodegraded (Barbeau et al., 2003). The presence of organic photosensitisers, organically complexed Fe catalyzing Fe reduction via the photoproduction of oxygen radicals as superoxide (see below), may further increase the rate of photochemical Fe reduction (Jickells and Spokes, 2001).

The reduction of Fe(III) by photochemically produced species, called secondary photoinduced Fe redox reactions, is also possible. Superoxide (O_2^-), reducing Fe(III) to Fe(II) has been studied by Voelker and Sedlak (1995). Superoxide and its conjugate acid, hydroperoxyl radical (HO_2), are produced in sunlit waters through photochemical reactions of organic chromophores (Cooper et al., 1989). The bimolecular dismutation of superoxide has been postulated as the main source of hydrogen peroxide in the open ocean (Petasne and Zika, 1987). However, in seawater reduction or oxidation reactions with transition metals
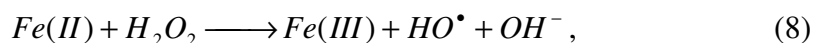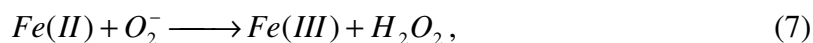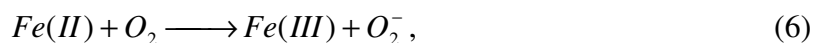
(Me), such as iron, could be the dominant mechanism of superoxide dismutation (and hydrogen peroxide formation) (Voelker and Sedlak, 1995). The reduction of iron by superoxide is faster than the oxidation (Eq. 4, 5).

reduction $\qquad\qquad\qquad O_2^- + Fe^{3+} \longrightarrow O_2 + Fe^{2+}$ $\qquad\qquad\qquad$ (4)

oxidation $\qquad\qquad\qquad O_2^- + Fe^{2+} \longrightarrow H_2O_2 + Fe^{3+} + 2OH^-$ $\qquad\qquad$ (5)

Furthermore, photo-oxidation of polycarboxylates results in decarboxylation producing CO_2 and carbon-centered radicals. These carbon-centered radicals can also react with Fe(III) to form Fe(II) (Faust, 1994).

1.3.2 Fe(II) oxidation

In O_2 saturated seawater oxidation of Fe(II) follows immediately upon the photoinduced production of Fe(II). The Fe(II) becomes rapidly oxidized by O_2 and H_2O_2 (Millero et al., 1987; Millero and Izaguirre, 1989; Millero and Sotolongo, 1989; King et al., 1991; King et al., 1995; King, 1998). The oxidation of Fe(II) by O_2 can be described by four reactions (Weiss, 1935):

$$Fe(II) + O_2 \longrightarrow Fe(III) + O_2^-,\qquad\qquad (6)$$

$$Fe(II) + O_2^- \longrightarrow Fe(III) + H_2O_2,\qquad\qquad (7)$$

$$Fe(II) + H_2O_2 \longrightarrow Fe(III) + HO^\bullet + OH^-,\qquad\qquad (8)$$

$$Fe(II) + HO^\bullet \longrightarrow Fe(III) + OH^-,\qquad\qquad (9)$$

where the reactions 7 and 9 are much faster than the rate determining reactions 6 and 8.

The oxidation of Fe(II) with H_2O_2 is the dominant oxidation pathway of Fe(II) (Moffett and Zika, 1987; Miller and Kester, 1994). The concentration of H_2O_2, important for the Fenton reaction (Eq. 8) (Goldstein et al., 1993; Wardman and Candeias, 1996), is dependent on spectrally determined photochemical reactions (Plane et al., 1987; Yocis et al., 2000). Primary sources of H_2O_2 are the reaction sequence (Eq. 6-7), the iron catalyzed mechanism of superoxide dismutation resulting in hydrogen peroxide formation (Eq. 5) (Voelker and Sedlak, 1995) and the bimolecular dismutation of superoxide (Petasne and Zika, 1987).

The main source of superoxide is photochemical reactions of colored dissolved organic matter (CDOM) involving O_2 (Cooper, 1983). Photobleaching of CDOM in natural waters has an inverse exponential relationship with wavelength (Osburn et al., 2001; Del Vecchio and Blough, 2002). The concentration of produced Fe(II) is not only spectrally dependent via the reduction but also via the oxidation of the Fe redox cycle.

The oxidation of Fe(II) is not only strongly dependent on the concentrations of oxygen and its radicals but also on many other factors. The pH (Singer, 1969; Millero et al., 1987), ionic strength/interactions (Millero et al., 1987; Millero, 1988; Millero and Izaguirre, 1989), temperature (Millero and Sotolongo, 1989) and the presence of surfaces (Tamura et al., 1976) play an important role in Fe(II) oxidation. These factors make the half live of Fe(II) ranging from 72 seconds (laboratory experiments by Millero et al. (1987), to several hours, as shown for the cold Antarctic waters (Croot and Laan, 2002). Furthermore, Sung and Morgan (1980) demonstrated the autocatalytic Fe(II) oxidation via oxidative precipitation of iron. Also bacteria can increase the Fe(II) oxidation rate by O_2 (Sulzberger et al., 1990; Barry et al., 1994). Depending on the relative stability of the Fe(II)-organic and Fe(III)-organic complexes, organic complexation can either enhance (Sedlak and Hoigne, 1993; Voelker and Sulzberger, 1996; Emmenegger et al., 1998) or slow down the rate of Fe(II) oxidation (Theis and Singer, 1974). Extensive literature on the influence of organic complexation of Fe on the oxidation kinetics is available (Theis and Singer, 1974; Millero et al., 1987; Voelker et al., 1997; Santana-Casiano et al., 2000; Rose and Waite, 2002; Santana-Casiano et al., 2004).

1.4 Biological uptake of iron

There are several reasons to study Fe chemistry in seawater and to elucidate its biological availability for the marine biota. These include: i) the recognition that iron is a bioactive element necessary for e.g. photosynthesis (Chereskin and Castelfranco, 1982; Greene et al., 1992; Geider et al., 1993), nitrate metabolism (Timmermans et al., 1994; de Baar et al., 1997; van Leeuwe et al., 1997), N_2 fixation (Mills et al., 2004) and detoxification of reactive oxygen species (Sunda and Huntsman, 1995), in concert with ii) the paradox that the biota, notably as phytoplankton needs relatively high quantities of such a scarce element in the marine environment (Boye, 2000).

At various stations in the oceans, the vertical distribution of concentrations of dissolved iron and major nutrients (N and P) are closely correlated, suggesting control by biological uptake and regeneration cycles (Martin and Gordon, 1988; Sunda and Huntsman, 1995; Johnson et al., 1997). However, at other stations such correlations have not been observed. There are still many uncertainties about the identity of the Fe species available for biological uptake by eukaryotic phytoplankton as well as their responsible uptake mechanisms.

Redox reactions and speciation are shown to be important for the bioavailability of Fe for phytoplankton. The Fe redox cycle initiated by photochemical processes is mentioned as an important mechanism by which colloidal and chelated Fe are converted into more kinetically labile inorganic species of Fe(II) and Fe(III), resulting in a higher bioavailability to phytoplankton (Finden et al., 1984; Wells and Mayer, 1991; Johnson et al., 1994; Miller and Kester, 1994). The Fe(II) is assumed to be a Fe fraction suitable for biological uptake (Anderson and Morel, 1980; Anderson and Morel, 1982; Takeda and Kamatani, 1989; Maldonado and Price, 2001).

Organic complexation increases iron solubility with respect to the formation of iron hydroxides and oxides. At the same time, it minimizes the adsorption of iron to particles, thereby maximizing the iron retention time in seawater, which benefits the biological community (Johnson et al., 1997; Sunda, 1997).

Once available for biological uptake, two common systems to transport iron over a membrane are: i) siderophore systems in which released strong Fe(III)-organic chelators are transported into the cell, and ii) ferrous or ferric ion membrane transporters binding external Fe(II) or Fe(III) upon ligand exchange with reactive iron species.

The siderophore system is well known and extensively described for marine bacteria (Hutchins et al., 1999; Yoshida et al., 2002; Martinez et al., 2003; McCormack et al., 2003; Weaver et al., 2003; Gledhill et al., 2004). Yet, there is no conclusive evidence for siderophore production in eukaryotic marine phytoplankton, although there are some studies indicating the release of siderophores or iron chelators by dinoflagellates, diatoms, *Emiliania huxleyi* and a green alga (Trick et al., 1983; Boye and van den Berg, 2000). Also, other studies have demonstrated uptake of organically complexed Fe by phytoplankton (Soriadengg and Horstmann, 1995; Hutchins et al., 1999; Maldonado and Price, 2001).

The second Fe uptake mechanism in eukaryotic marine phytoplankton is by membrane transporters that directly access dissolved monomeric inorganic iron species (Sunda, 2001). A direct relationship was found between the concentration of kinetically labile inorganic Fe species and iron uptake by the diatoms *Thalassiosira weissflogii* and *T. pseudonana* and the coccolithophore *Pleurochrysis carterae* (Anderson and Morel, 1982; Hudson and Morel, 1990; Sunda and Huntsman, 1995). According to Morel et al. (1991) the effectivity of the process is depending on the loss of water from the inner coordination sphere of the inorganic Fe species resulting in a ligand exchange between the inorganic Fe species and the receptor ligand sites on the membrane-bound iron transporters. Thus, the Fe(III) chelates and colloids are not directly available for uptake because their ligand exchange kinetics is too slow.

Equal uptake rates of dissolved inorganic Fe(III) and Fe(II) in *Thalassiosira weissflogii* (Anderson and Morel, 1982) in concert with the suggestion of Hudson and Morel (1990) that Fe(III) is the actual species transported over the membrane hint to a mechanism in

which Fe(II) is oxidized first, followed by binding to the transporter and transport over the membrane (Sunda, 2001). Supporting this idea is the similar rate constant for the loss of coordinated water, controlling ligand-association rate kinetics, for both Fe(III) and free Fe(II) in seawater (Hudson, 1998).

Not only does the chemistry of iron in seawater regulate its biological uptake and utilization by phytoplankton, conversely the activity of the phytoplankton also influences the speciation and cycling of iron (Wells et al., 1994; Price and Morel, 1998). Complexation of Fe by organic iron binding ligands not only increases Fe solubility but also influences the photochemistry and subsequently the bioavailability of Fe (Barbeau et al., 2003). Another option to examine is the role of the phytoplankton itself in generating stable Fe(II) levels or in inducing Fe(II) producing processes. Various reports describe high Fe(II) concentrations coinciding with chlorophyll-*a* maxima (O'Sullivan et al., 1991; Emmenegger et al., 2001; Shaked et al., 2002). The ability of different phytoplankton species to enzymatically reduce Fe(III) at the cell surface is known for a long time (Allnut and Bonner, 1987; Jones and Morel, 1988; Maldonado and Price, 2000), yet the underlying mechanism being poorly understood. Furthermore, Kuma et al. (1992) noticed high concentrations Fe(II) during spring blooms in Funka Bay and related this to the release of organic components from phytoplankton inducing the photoreduction of Fe. The presence of various dissolved organic substances, generally considered to be organic components released from phytoplankton, such as sugar acids, indeed improved the photoreduction of Fe (Kuma et al., 1995).

1.5 Rationale of the thesis

The redox-cycle of iron, initiated by photochemical processes, is mentioned as an important mechanism by which Fe is made more available for biological uptake by phytoplankton (Wells and Mayer, 1991; Johnson et al., 1994; Miller and Kester, 1994; Barbeau et al., 2001). This means that, theoretically, increased levels of UVB, related to the stratospheric ozone depletion occurring every Antarctic spring, could positively affect phytoplankton growth via the chemistry of iron.

The main scope of this thesis is to investigate the influence of irradiance and particularly UV radiation on the chemistry of Fe in seawater. The Fe chemistry is not only spectrally dependent via the reduction but also via the oxidation of the Fe redox cycle. Hydrogen peroxide is the main Fe(II) oxidant in sunlit waters. Therefore the influence of UV radiation on the photochemical production of H_2O_2 (Chapter 2) and the photoproduction of Fe(II) was investigated first. Photoreduction was the most likely candidate mechanism to explain the retained high Fe(II) concentrations during the iron enrichment experiment SOIREE in the Southern Ocean. Here, suggested maximal photoreduction rates at 20 m depth were as high as 370 pM hr^{-1}, despite cloudy skies (Croot et al., 2001). Therefore, the role of

UVB, UVA and VIS in driving the Fe redox cycle was investigated in deck-incubations during the *in situ* iron enrichment experiment EisenEx (Gervais et al., 2002) in the Southern Ocean (Chapter 3). To be able to accurately investigate and predict the relative impact of enhanced UVB on the photoproduction of Fe(II) in the Southern Ocean a spectral weighting function for Fe(II) photo-production from amorphous Fe hydroxides was established. A weighting function is a set of coefficients described by a mathematical expression that weighs the energy of a discrete wavelength with its biological or chemical effect, in this case Fe(II) photoproduction. This even allows prediction of the impact of natural variability of irradiance, as well as the anthropogenic effect of increased levels of UVB due to springtime stratospheric ozone depletion (Chapter 4).

Organic complexation of Fe influences the photo(induced) redox cycle. Inspired by the article of Witter et al. (2000) the influence of five model Fe-chelating ligands on the photoproduction of Fe(II) was studied including: tetrapyrrole ligands (phaeophytin and protoporphyrin IX), terrestrial hydroxamate siderophores (ferrichrome and desferrioxamine B) and the terrestrial Fe-complexing storage ligand inositol hexaphosphate (phytic acid) (Chapter 5).

It is known that phytoplankton releases organic substances to the environment. Furthermore it has been suggested that they produce siderophores (see above section 1.2). Phytoplankton could therefore actively alter the chemical environment of the Fe. This and subsequent possible photodegradation of organically bound Fe could, in this way, influence the biogeochemical cycle of iron. To study this, the influence of two Southern Ocean phytoplankton species, *Thalassiosira* sp. and *Chaetoceros brevis*, on the dissolved Fe concentration, the organic complexation of Fe and on Fe(II) photoproduction under three different optical treatments, UVB+UVA+VIS, UVA+VIS and VIS, was investigated (Chapter 6).

There is much discussion about the susceptibility of natural organic Fe binding ligands for photodegradation resulting in Fe(II). At the moment the importance of photodegradation of organic Fe binding ligands occurring in the marine environment is based on suggestions to explain datasets (Boye et al., 2001; Macrellis et al., 2001), laboratory experiments with single ligand species (Barbeau et al., 2001; Barbeau et al., 2002; Barbeau et al., 2003) and some field data showing marginal photo induced effects on the concentration of Fe binding ligands (Powell and Wilson-Finelli, 2003). On the contrary, Moffett (2001) concluded from the lack of publications describing shallow mixed layer minima and other features suggesting a surface, photochemical sink that photodegradation is not an important mechanism in marine Fe chemistry. To address the importance of the photodegradation of organic Fe binding ligands we performed experiments with estuarine Marsdiep and Scheldt water, containing high concentrations of organic Fe-binding ligands. Investigated was the presence of a weak Fe-binding ligand keeping dissolved Fe concentrations higher then the

concentrations of strong organic ligands and the solubility product of Fe (Chapter 7) and the influence of UV on this weak Fe-binding ligand and on the photodegradation of the strong organic Fe-binding ligands (Chapter 8).

References

Allnut, F.C.T. and Bonner, W.D., 1987. Evaluation of reductive release as a mechanism for iron uptake from ferrioxamine B by *Chlorella vulgaris*. Plant Physiol., 85: 751-756.

Anderson, M.A. and Morel, F.M.M., 1980. Uptake of Fe(II) by a diatom in oxic culture medium. Mar. Biol. Let., 1: 263-268.

Anderson, M.A. and Morel, F.M.M., 1982. The influence of aqueous iron chemistry on the uptake of iron by the coastal diatom *Thalassiosira weissflogii*. Limnol. Oceanogr., 27(5): 789-813.

Arimoto, R., 2001. Eolian dust and climate: relationships to sources, tropospheric chemistry, transport and deposition. Earth-Sci. Rev., 54(1-3): 29-42.

Barbeau, K., Moffett, J.W., Caron, D.A., Croot, P.L. and Erdner, D.L., 1996. Role of protozoan grazing in relieving iron limitation of phytoplankton. Nature, 380(6569): 61-64.

Barbeau, K., Rue, E.L., Bruland, K.W. and Butler, A., 2001. Photochemical cycling of iron in the surface ocean mediated by microbial iron(III)-binding ligands. Nature, 413(6854): 409-413.

Barbeau, K., Rue, E.L., Trick, C.G., Bruland, K.T. and Butler, A., 2003. Photochemical reactivity of siderophores produced by marine heterotrophic bacteria and cyanobacteria based on characteristic Fe(III) binding groups. Limnol. Oceanogr., 48(3): 1069-1078.

Barbeau, K., Zhang, G.P., Live, D.H. and Butler, A., 2002. Petrobactin, a photoreactive siderophore produced by the oil- degrading marine bacterium *Marinobacter hydrocarbonoclasticus*. J. Am. Chem. Soc., 124(3): 378-379.

Barry, R.C., Schnoor, J.L., Sulzberger, B., Sigg, L. and Stumm, W., 1994. Iron oxidation-kinetics in an acidic Alpine lake. Water Res., 28(2): 323-333.

Behra, P. and Sigg, L., 1990. Evidence for redox cycling of iron in atmospheric water droplets. Nature, 344: 419-421.

Blain, S., Treguer, P., Belviso, S., Bucciarelli, E., Denis, M., Desabre, S., Fiala, M., Jezequel, V.M., Le Fevre, J., Mayzaud, P., Marty, J.C. and Razouls, S., 2001. A biogeochemical study of the island mass effect in the context of the iron hypothesis: Kerguelen Islands, Southern Ocean. Deep Sea Res. I, 48(1): 163-187.

Bowie, A.R., Achterberg, E.P., Sedwick, P.N., Ussher, S. and Worsfold, P.J., 2002. Real-time monitoring of picomolar concentrations of iron(II) in marine waters using automated flow injection-chemiluminescence instrumentation. Environ. Sci. Technol., 36(21): 4600-4607.

Boyd, P.W., Law, C.S., Wong, C.S., Nojiri, Y., Tsuda, A., Levasseur, M., Takeda, S., Rivkin, R., Harrison, P.J., Strzepek, R., Gower, J., McKay, R.M., Abraham, E., Arychuk, M., Barwell-Clarke, J., Crawford, W., Crawford, D., Hale, M., Harada, K., Johnson, K., Kiyosawa, H., Kudo, I., Marchetti, A., Miller, W., Needoba, J., Nishioka, J., Ogawa, H., Page, J., Robert, M., Saito, H., Sastri, A., Sherry, N., Soutar, T., Sutherland, N., Taira, Y., Whitney, F., Wong, S.K.E. and Yoshimura, T., 2004. The decline and fate of an iron-induced subarctic phytoplankton bloom. Nature, 428(6982): 549-553.

Boyd, P.W., Watson, A.J., Law, C.S., Abraham, E.R., Trull, T., Murdoch, R., Bakker, D.C.E., Bowie, A.R., Buesseler, K.O., Chang, H., Charette, M., Croot, P., Downing, K., Frew, R., Gall, M., Hadfield, M., Hall, J., Harvey, M., Jameson, G., LaRoche, J., Liddicoat, M., Ling, R., Maldonado, M.T., McKay, R.M., Nodder, S., Pickmere, S., Pridmore, R., Rintoul, S., Safi, K., Sutton, P., Strzepek, R., Tanneberger, K., Turner, S., Waite, A. and Zeldis, J., 2000. A mesoscale phytoplankton bloom in the polar Southern Ocean stimulated by iron fertilization. Nature, 407(6805): 695-702.

Boye, M., 2000. Organic complexation and biogeochemistry of iron in the marine system: field data and culture experiments. PhD Thesis, University of Liverpool, Liverpool, 225 pp.

Boye, M., Aldrich, A.P., van den Berg, C.M.G., de Jong, J.T.M., Veldhuis, M. and de Baar, H.J.W., 2003. Horizontal gradient of the chemical speciation of iron in surface waters of the northeast Atlantic Ocean. Mar. Chem., 80(2-3): 129-143.

Boye, M. and van den Berg, C.M.G., 2000. Iron availability and the release of iron-complexing ligands by Emiliania huxleyi. Mar. Chem., 70(4): 277-287.

Boye, M., van den Berg, C.M.G., de Jong, J.T.M., Leach, H., Croot, P.L. and de Baar, H.J.W., 2001. Organic complexation of iron in the Southern Ocean. Deep Sea Res. I, 48(6): 1477-1497.

Boye, M.e.a., in press. Major deviations of iron complexation during 22 days of a mesoscale iron enrichment in the open Southern Ocean. Marine Chemistry.

Buesseler, K.O., Andrews, J.E., Pike, S.M. and Charette, M.A., 2004. The effects of iron fertilization on carbon sequestration in the Southern Ocean. Science, 304(5669): 414-417.

Buesseler, K.O. and Boyd, P.W., 2003. Will ocean fertilization work? Science, 300(5616): 67-68.

Buma, A.G.J., de Baar, H.J.W., Nolting, R.F. and van Bennekom, A.J., 1991. Metal enrichment experiments in the Weddell-Scotia Seas - effects of iron and manganese on various plankton communities. Limnol. Oceanogr., 36(8): 1865-1878.

Buma, A.G.J., de Boer, M.K. and Boelen, P., 2001. Depth distributions of DNA damage in Antarctic marine phyto- and bacterioplankton exposed to summertime UV radiation. J. Phycol., 37(2): 200-208.

Buma, A.G.J., van Hannen, E.J., Veldhuis, M.J.W. and Gieskes, W.W.C., 1996. UV-B induces DNA damage and DNA synthesis delay in the marine diatom *Cyclotella* sp. Sci. Mar., 60: 101-106.

Chereskin, B.M. and Castelfranco, P.A., 1982. Effects of iron and oxygen on chlorophyll biosynthesis.2. Observations on the biosynthetic-pathway in isolated *Etiochloroplasts*. Plant Physiol., 69(1): 112-116.

Coale, K.H., Johnson, K.S., Chavez, F.P., Buesseler, K.O., Barber, R.T., Brzezinski, M.A., Cochlan, W.P., Millero, F.J., Falkowski, P.G., Bauer, J.E., Wanninkhof, R.H., Kudela, R.M., Altabet, M.A., Hales, B.E., Takahashi, T., Landry, M.R., Bidigare, R.R., Wang, X.J., Chase, Z., Strutton, P.G., Friederich, G.E., Gorbunov, M.Y., Lance, V.P., Hilting, A.K., Hiscock, M.R., Demarest, M., Hiscock, W.T., Sullivan, K.F., Tanner, S.J., Gordon, R.M., Hunter, C.N., Elrod, V.A., Fitzwater, S.E., Jones, J.L., Tozzi, S., Koblizek, M., Roberts, A.E., Herndon, J., Brewster, J., Ladizinsky, N., Smith, G., Cooper, D., Timothy, D., Brown, S.L., Selph, K.E., Sheridan, C.C., Twining, B.S. and Johnson, Z.I., 2004. Southern Ocean iron enrichment experiment: Carbon cycling in high- and low-Si waters. Science, 304(5669): 408-414.

Cooper, W.J., 1983. Photochemical formation of hydrogen peroxide in surface and ground waters exposed to sunlight. Science, 220: 711-712.

Cooper, W.J., Zika, R.G., Petasne, R.G. and Fischer, A.M., 1989. Sunlight-induced photochemistry of humic substances in natural- waters - major reactive species. In: I.H. Suffet (Editor), Aquatic Humic Substances: Influence on fate and treatment of pollutants. Adv. Chem. Ser. American Chemical Society, Washington D.C., pp. 333-362.

Cornell, R.M. and Schwertmann, U., 1996. The Iron Oxides. VCH Publishers, New York.

Croot, P.L., Bowie, A.R., Frew, R.D., Maldonado, M.T., Hall, J.A., Safi, K.A., la Roche, J., Boyd, P.W. and Law, C.S., 2001. Retention of dissolved iron and Fe-II in an iron induced Southern Ocean phytoplankton bloom. Geophys. Res. Lett., 28(18): 3425-3428.

Croot, P.L. and Laan, P., 2002. Continuous shipboard determination of Fe(II) in polar waters using flow injection analysis with chemiluminescence detection. Anal. Chim. Acta, 466(2): 261-273.

Cunningham, K.M., Goldberg, M.C. and Weiner, E.R., 1988. Mechanisms for aquaeos photolysis of adsorbed benzoate, oxalate, and succinate on iron oxyhydroxide (goethite) surfaces. Environ. Sci. Technol., 22(9): 1090-1097.

David, F.and David, P.G., 1976. Photoredox chemistry of iron(III) chloride and iron(III) perchlorate in aqueous media. A comparative study. J. Phys. Chem., 80: 579-583.

de Baar, H.J.W. and Boyd, P.W., 2000. The role of iron in plankton ecology and carbon dioxide transfer of the global oceans. In: R.B. Hanson, H.W. Ducklow and J.G. Field (Editors), The dynamic ocean carbon cycle; A midterm synthesis of the joint global ocean flux study. University Press Cambridge, Cambridge.

de Baar, H.J.W., Boyd, P.W., Coale, K. and Tsuda, A., 2005. Synthesis of eight *in-situ* iron fertilizations in high nutrient low chlorophyll waters confirms the control by wind mixed layer depth of phytoplankton blooms. J. Geophys. Res., *in press*.

de Baar, H.J.W., Buma, A.G.J., Nolting, R.F., Cadee, G.C., Jacques, G. and Treguer, P.J., 1990. On iron limitation of the Southern Ocean - experimental- observations in the Weddell and Scotia seas. Mar. Ecol. Progr. Ser., 65(2): 105-122.

de Baar, H.J.W. and de Jong, J.T.M., 2001. Distributions, sources and sinks of iron in seawater. In: D.R. Turner and K.A. Hunter (Editors), The biogeochemistry of iron in seawater. John Wiley & sons, New York, pp. 123-253.

de Baar, H.J.W., de Jong, J.T.M., Bakker, D.C.E., Loscher, B.M., Veth, C., Bathmann, U. and Smetacek, V., 1995. Importance of iron for plankton blooms and carbondioxide drawdown in the Southern Ocean. Nature, 373(6513): 412-415.

de Baar, H.J.W., de Jong, J.T.M., Nolting, R.F., Timmermans, K.R., van Leeuwe, M.A., Bathmann, U., van der Loeff, M.R. and Sildam, J., 1999. Low dissolved Fe and the absence of diatom blooms in remote Pacific waters of the Southern Ocean. Mar. Chem., 66(1-2): 1-34.

de Baar, H.J.W. and la Roche, J., 2003. Trace metals in the oceans: evolution, biology and global change. In: G. Wefer, F. Lamy and F. Mantoura (Editors), Marine Science Frontiers for Europe. Springer-Verlag, pp. 79-105.

de Baar, H.J.W., van Leeuwe, M.A., Scharek, R., Goeyens, L., Bakker, K.M.J. and Fritsche, P., 1997. Nutrient anomalies in *Fragilariopsis kerguelensis* blooms, iron deficiency and the nitrate/phosphate ratio (A. C. Redfield) of the Antarctic Ocean. Deep Sea Res. II, 44(1-2): 229-&.

de Jong, J.T.M., den Das, J., Bathmann, U., Stoll, M.H.C., Kattner, G., Nolting, R.F. and de Baar, H.J.W., 1998. Dissolved iron at subnanomolar levels in the Southern Ocean as determined by ship-board analysis. Anal. Chim. Acta, 377(2-3): 113-124.

Del Vecchio, R. and Blough, N.V., 2002. Photobleaching of chromophoric dissolved organic matter in natural waters: kinetics and modeling. Mar. Chem., 78(4): 231-253.

Duce, R.A. and Tindale, N.W., 1991. Atmospheric transport of iron and its deposition in the ocean. Limnol. Oceanogr., 36: 1715-1726.

Edwards, R., Sedwick, P.N., Morgan, V., Boutron, C.F. and Hong, S., 1998. Iron in ice cores from Law Dome, East Antarctica: implications for past deposition of aerosol iron. Ann. Glaciol., 27: 365-370.

Emmenegger, L., King, D.W., Sigg, L. and Sulzberger, B., 1998. Oxidation kinetics of Fe(II) in a eutrophic Swiss lake. Environ. Sci. Technol., 32(19): 2990-2996.

Emmenegger, L., Schonenberger, R.R., Sigg, L. and Sulzberger, B., 2001. Light-induced redox cycling of iron in circumneutral lakes. Limnol. Oceanogr., 46(1): 49-61.

Erel, Y., Pehkonen, S.O. and Hoffmann, M.R., 1993. Redox chemistry of iron in fog and stratus clouds. J. Geophys. Res., 98: 18,423-18,434.

Evans, A.M., 1980. An introduction to ore geology. Elsevier North Holland Inc., New York.

Evans, M.G., George, P. and Uri, N., 1949. The $[Fe(OH)]^{2+}$ and $[Fe(O_2H)]^{2+}$ complexes. Trans. Faraday Soc., 34: 230.

Falkowski, P.G. and Raven, J.A., 1997. Aquatic Photosynthesis. Blackwell Science, Malden, MA.

Faust, B.C., 1994. Photochemistry of clouds, fogs, and aerosols. Environ. Sci. Technol., 28(5): A217-A222.

Faust, B.C., 1994. A review of the photochemical redox reactions of iron(III) species in atmospheric, oceanic, and surface waters: Influences on geochemical cycles and oxidant formation. In: G.R. Helz, R.G. Zepp and D.G. Crosby (Editors), Aquatic Surface Photochemistry. CRC Press, Inc., London, pp. 3-37.

Faust, B.C. and Hoffmann, M.R., 1986. Photoinduced reductive dissolution of alpha-Fe_2O_3 by bisulfite. Environ. Sci. Technol., 20(9): 943-948.

Faust, B.C., Hoffmann, M.R. and Bahnemann, D.W., 1989. Photocatalytic oxidation of sulfurdioxide in aqueous suspensions of alpha-Fe_2O_3. J. Phys. Chem., 93(17): 6371-6381.

Faust, B.C. and Hoigne, J., 1990. Photolysis of Fe(III)-hydroxy complexes as sources of OH radicals in clouds, fog and rain. Atmos. Environ., 24(1): 79-89.

Faust, B.C. and Zepp, R.G., 1993. Photochemistry of aqueous iron(III) polycarboxylate complexes - roles in the chemistry of atmospheric and surface waters. Environ. Sci. Technol., 27(12): 2517-2522.

Fennel, K., Abbott, M.R., Spitz, Y.H., Richman, J.G. and Nelson, D.M., 2003. Impacts of iron control on phytoplankton production in the modern and glacial Southern Ocean. Deep Sea Res. II, 50(3-4): 833-851.

Finden, D.A.S., Tipping, E., Jaworski, G.H.M. and Reynolds, C.S., 1984. Light-induced reduction of natural iron(III) oxide and its relevance to phytoplankton. Nature, 309(5971): 783-784.

Frederick, J.E. and Snell, H.E., 1988. Ultraviolet-radiation levels during the Antarctic spring. Science, 241(4864): 438-440.

Gao, H.Z. and Zepp, R.G., 1998. Factors influencing photoreactions of dissolved organic matter in a coastal river of the southeastern United States. Environ. Sci. Technol., 32(19): 2940-2946.

Geider, R.J., la Roche, J., Greene, R.M. and Olaizola, M., 1993. Response of the photosynthetic apparatus of *Phaeodactylum tricornutum* (Bacillariophyceae) to nitrate, phosphate, or iron starvation. J. Phycol., 29(6): 755-766.

Gerringa, L.J.A., de Baar, H.J.W. and Timmermans, K.R., 2000. A comparison of iron limitation of phytoplankton in natural oceanic waters and laboratory media conditioned with EDTA. Mar. Chem., 68(4): 335-346.

Gervais, F., Riebesell, U. and Gorbunov, M.Y., 2002. Changes in primary productivity and chlorophyll a in response to iron fertilization in the Southern Polar Frontal Zone. Limnol. Oceanogr., 47(5): 1324-1335.

Gledhill, M., McCormack, P., Ussher, S., Achterberg, E.P., Mantoura, R.F.C. and Worsfold, P.J., 2004. Production of siderophore type chelates by mixed bacterioplankton populations in nutrient enriched seawater incubations. Mar. Chem., 88(1-2): 75-83.

Gledhill, M. and van den Berg, C.M.G., 1994. Determination of complexation of iron(III) with natural organic complexing ligands in seawater using cathodic stripping voltammetry. Mar. Chem., 47(1): 41-54.

Gledhill, M., van den Berg, C.M.G., Nolting, R.F. and Timmermans, K.R., 1998. Variability in the speciation of iron in the northern North Sea. Mar. Chem., 59(3-4): 283-300.

Goldstein, S., Meyerstein, D. and Czapski, G., 1993. The Fenton reagents. Free Radical Biol. Med., 15(4): 435-445.

Gran, H.H., 1931. On the conditions for production of plankton in the sea. Conseil International pour l'exploration de la Mer, Rapports et proces verbaux de Reunions.(75): 37-46.

Granger, J. and Price, N.M., 1999. The importance of siderophores in iron nutrition of heterotrophic marine bacteria. Limnol. Oceanogr., 44(3): 541-555.

Greene, R.M., Geider, R.J., Kolber, Z. and Falkowski, P.G., 1992. Iron-induced changes in light harvesting and photochemical energy-conversion processes in eukaryotic marine-algae. Plant Physiol., 100(2): 565-575.

Holland, H.D., 1984. The chemical evolution of the atmosphere and oceans. Princeton University Press, Princeton, NJ.

Hong, H. and Kester, D.R., 1986. Redox state of iron in the offshore waters of Peru. Limnol. Oceanogr., 31: 512-524.

Hoppema, M., de Baar, H.J.W., Fahrbach, E., Hellmer, H.H. and Klein, B., 2003. Substantial advective iron loss diminishes phytoplankton production in the Antarctic Zone. Glob. Biogeochem. Cycle, 17(1): art. no.-1025.

Hoppema, M., Fahrbach, E., Stoll, M.H.C. and de Baar, H.J.W., 1999. Annual uptake of atmospheric CO_2 by the Weddell Sea derived from a surface layer balance, including estimations of entrainment and new production. J. Mar. Syst., 19(4): 219-233.

Hudson, R.J.M., 1998. Which aqueous species control the rates of trace metal uptake by aquatic biota? Observations and predictions of non-equilibrium effects. Sci. Total Environ., 219(2-3): 95-115.

Hudson, R.J.M., Covault, D.T. and Morel, F.M.M., 1992. Investigations of iron coordination and redox reactions in seawater using Fe-59 radiometry and ion-pair solvent-extraction of amphiphilic iron complexes. Mar. Chem., 38(3-4): 209-235.

Hudson, R.J.M. and Morel, F.M.M., 1990. Iron transport in marine-phytoplankton - kinetics of cellular and medium coordination reactions. Limnol. Oceanogr., 35(5): 1002-1020.

Hutchins, D.A. and Bruland, K.W., 1994. Grazer-mediated regeneration and assimilation of Fe, Zn, and Mn from planktonic prey. Mar. Ecol. Prog. Ser., 110: 259-269.

Hutchins, D.A., Wang, W.X. and Fisher, N.S., 1995. Copepod grazing and the biogeochemical fate of iron. Limnol. Oceanogr., 40(5): 989-994.

Hutchins, D.A., Witter, A.E., Butler, A. and Luther, G.W., 1999. Competition among marine phytoplankton for different chelated iron species. Nature, 400(6747): 858-861.

Jickells, T.D. and Spokes, L.J., 2001. Atmospheric iron inputs to the oceans. In: D.R. Turner and K.A. Hunter (Editors), The biogeochemistry of iron in seawater. IUPAC series on analytical and physical chemistry of environmental systems. John Wiley & Sons, LTD, New York, pp. 85-122.

Johnson, K.S., 2001. Iron supply and demand in the upper ocean: Is extraterrestrial dust a significant source of bioavailable iron? Glob. Biogeochem. Cycle, 15(1): 61-63.

Johnson, K.S., Coale, K.H., Elrod, V.A. and Tindale, N.W., 1994. Iron photochemistry in seawater from the equatorial Pacific. Mar. Chem., 46(4): 319-334.

Johnson, K.S., Gordon, R.M. and Coale, K.H., 1997. What controls dissolved iron concentrations in the world ocean? Mar. Chem., 57(3-4): 137-161.

Jones, G.J. and Morel, F.M.M., 1988. Plasmalemma redox activity in the diatom *Thalassiosira*. Plant Physiol., 87: 143-147.

Jouzel, J., Barkov, N.I., Barnola, J.M., Bender, M., Chappellaz, J., Genthon, C., Kotlyakov, V.M., Lipenkov, V., Lorius, C., Petit, J.R., Raynaud, D., Raisbeck, G., Ritz, C., Sowers, T., Stievenard, M., Yiou, F. and Yiou, P., 1993. Extending the Vostok ice-core record of paleoclimate to the penultimate glacial period. Nature, 364(6436): 407-412.

Karentz, D. and Lutze, L.H., 1990. Evaluation of biologically harmful ultraviolet-radiation in Antarctica with a biological dosimeter designed for aquatic environments. Limnol. Oceanogr., 35(3): 549-561.

King, D.W., 1998. Role of carbonate speciation on the oxidation rate of Fe(II) in aquatic systems. Environ. Sci. Technol., 32(19): 2997-3003.

King, D.W., Aldrich, R.A. and Charnecki, S.E., 1993. Photochemical redox cycling of iron in NaCl solutions. Mar. Chem., 44(2-4): 105-120.

King, D.W., Lin, J. and Kester, D.R., 1991. Spectrophotometric determination of iron(II) in seawater at nanomolar concentrations. Anal. Chim. Acta, 247(1): 125-132.

King, D.W., Lounsbury, H.A. and Millero, F.J., 1995. Rates and mechanism of Fe(II) oxidation at nanomolar total iron concentrations. Environ. Sci. Technol., 29(3): 818-824.

Kuma, K., Nakabayashi, S. and Matsunaga, K., 1995. Photoreduction of Fe(III) by hydroxycarboxylic acids in seawater. Water Res., 29(6): 1559-1569.

Kuma, K., Nakabayashi, S., Suzuki, Y., Kudo, I. and Matsunaga, K., 1992. Photo-reduction of Fe (III) by dissolved organic-substances and existence of Fe (II) in seawater during spring blooms. Mar. Chem., 37(1-2): 15-27.

Kuma, K., Nishioka, J. and Matsunaga, K., 1996. Controls on iron(III) hydroxide solubility in seawater: The influence of pH and natural organic chelators. Limnol. Oceanogr., 41(3): 396-407.

Lancelot, C., Hannon, E., Becquevort, S., Veth, C. and De Baar, H.J.W., 2000. Modeling phytoplankton blooms and carbon export production in the Southern Ocean: dominant controls by light and iron in the Atlantic sector in Austral spring 1992. Deep Sea Res. I, 47(9): 1621-1662.

Langford, C.H. and Carey, J.H., 1975. The charge transfer photochemistry of the hexaaquoiron(III) ion, the chloropentaaquoiron(III) ion, and the mu-dihydroxo dimer explored with *tert*-butyl alcohol scavenging. Can. J. Chem., 53: 2430.

Lesser, M.P., Neale, P.J. and Cullen, J.J., 1996. Acclimation of Antarctic phytoplankton to ultraviolet radiation: Ultraviolet-absorbing compounds and carbon fixation. Mol. Mar. Biol. Biotechnol., 5(4): 314-325.

Liu, X.W. and Millero, F.J., 1999. The solubility of iron hydroxide in sodium chloride solutions. Geochim. Cosmochim. Acta, 63(19-20): 3487-3497.

Liu, X.W. and Millero, F.J., 2002. The solubility of iron in seawater. Mar. Chem., 77(1): 43-54.

Macrellis, H.M., Trick, C.G., Rue, E.L., Smith, G. and Bruland, K.W., 2001. Collection and detection of natural iron-binding ligands from seawater. Mar. Chem., 76(3): 175-187.

Maldonado, M.T. and Price, N.M., 1999. Utilization of iron bound to strong organic ligands by plankton communities in the subarctic Pacific Ocean. Deep Sea Res. II, 46(11-12): 2447-2473.

Maldonado, M.T. and Price, N.M., 2000. Nitrate regulation of Fe reduction and transport by Fe-limited *Thalassiosira oceanica*. Limnol. Oceanogr., 45(4): 814-826.

Maldonado, M.T. and Price, N.M., 2001. Reduction and transport of organically bound iron by *Thalassiosira oceanica* (Bacillariophyceae). J. Phycol., 37(2): 298-309.

Martin, J.H., 1990. Glacial-interglacial CO_2 change: the iron hypothesis. Paleoceanography, 5: 1-13.

Martin, J.H., Coale, K.H., Johnson, K.S., Fitzwater, S.E., Gordon, R.M., Tanner, S.J., Hunter, C.N., Elrod, V.A., Nowicki, J.L., Coley, T.L., Barber, R.T., Lindley, S., Watson, A.J., Vanscoy, K., Law, C.S., Liddicoat, M.I., Ling, R., Stanton, T., Stockel, J., Collins, C., Anderson, A., Bidigare, R., Ondrusek, M., Latasa, M., Millero, F.J., Lee, K., Yao, W., Zhang, J.Z., Friederich, G., Sakamoto, C., Chavez, F., Buck, K., Kolber, Z., Greene, R., Falkowski, P., Chisholm, S.W., Hoge, F., Swift, R., Yungel, J., Turner, S., Nightingale, P., Hatton, A., Liss, P. and Tindale, N.W., 1994. Testing the iron hypothesis in ecosystems of the equatorial Pacific Ocean. Nature, 371(6493): 123-129.

Martin, J.H. and Fitzwater, S.E., 1988. Iron-deficiency limits phytoplankton growth in the northeast Pacific subarctic. Nature, 331(6154): 341-343.

Martin, J.H. and Gordon, R.M., 1988. Northeast Pacific iron distributions in relation to phytoplankton productivity. Deep Sea Res. I, 35(2): 177-196.

Martin, J.H., Gordon, R.M. and Fitzwater, S.E., 1990. Iron in Antarctic waters. Nature, 345(6271): 156-158.

Martinez, J.S., Carter-Franklin, J.N., Mann, E.L., Martin, J.D., Haygood, M.G. and Butler, A., 2003. Structure and membrane affinity of a suite of amphiphilic siderophores produced by a marine bacterium. Proc. Natl. Acad. Sci. U. S. A., 100(7): 3754-3759.

Martinez, J.S., Zhang, G.P., Holt, P.D., Jung, H.T., Carrano, C.J., Haygood, M.G. and Butler, A., 2000. Self-assembling amphiphilic siderophores from marine bacteria. Science, 287(5456): 1245-1247.

McCormack, P., Worsfold, P.J. and Gledhill, M., 2003. Separation and detection of siderophores produced by marine bacterioplankton using high-performance liquid chromatography with electrospray ionization mass spectrometry. Anal. Chem., 75(11): 2647-2652.

Miller, W.L. and Kester, D., 1994. Photochemical iron reduction and iron bioavailability in seawater. J. Mar. Res., 52: 325-343.

Miller, W.L. and Kester, D.R., 1994. Peroxide variations in the Sargasso sea. Mar. Chem., 48(1): 17-29.

Millero, F.J., 1988. Effect of ionic interactions on the oxidation of Fe(II) and Cu(II) in natural waters. Mar. Chem., 28: 1-18.

Millero, F.J., 1998. Solubility of Fe(III) in seawater. Earth. Planet. Sci. Let., 154(1-4): 323-329.

Millero, F.J. and Izaguirre, M., 1989. Effect of ionic-strength and ionic interactions on the oxidation of Fe(II). J. Solut. Chem., 18(6): 585-599.

Millero, F.J. and Sotolongo, S., 1989. The oxidation of Fe(II) with H_2O_2 in seawater. Geochim. Cosmochim. Acta, 53(8): 1867-1873.

Millero, F.J., Sotolongo, S. and Izaguirre, M., 1987. The oxidation-kinetics of Fe(II) in seawater. Geochim. Cosmochim. Acta, 51(4): 793-801.

Mills, M.M., Ridame, C., Davey, M., La Roche, J. and Geider, R.J., 2004. Iron and phosphorus co-limit nitrogen fixation in the eastern tropical North Atlantic. Nature, 429(6989): 292-294.

Mitchell, B.G., Brody, E.A., Holmhansen, O., McClain, C. and Bishop, J., 1991. Light limitation of phytoplankton biomass and macronutrient utilization in the Southern Ocean. Limnol. Oceanogr., 36(8): 1662-1677.

Moffett, J.W., 2001. Transformations among different forms of iron in the ocean. In: D.R. Turner and K.A. Hunter (Editors), The Biogeochemistry of Iron in Seawater. IUPAC series on analytical and physical chemistry of environmental systems. John Wiley & Sons, LTD, New York, pp. 343-372.

Moffett, J.W. and Zika, R.G., 1987. Reaction-kinetics of hydrogen-peroxide with copper and iron in seawater. Environ. Sci. Technol., 21(8): 804-810.

Morel, F.M.M., Hudson, R.J.M. and Price, N.M., 1991. Limitation of productivity by trace-metals in the sea. Limnol. Oceanogr., 36(8): 1742-1755.

Mulay, L.N. and Selwood, P.W., 1955. Hydrolysis of Fe^{3+}: magnetic and spectrophotometric studies on ferric perchlorate solutions. J. Am. Chem. Soc., 77: 2693-2701.

Nadtochenko, V.A. and Kiwi, J., 1998. Photolysis of $FeOH^{2+}$ and $FeCl^{2+}$ in aqueous solution. Photodissociation kinetics and quantum yields. Inorg. Chem., 37(20): 5233-5238.

Neale, P.J., Davis, R.F. and Cullen, J.J., 1998. Interactive effects of ozone depletion and vertical mixing on photosynthesis of Antarctic phytoplankton. Nature, 392(6676): 585-589.

Nelson, D.M. and Smith, W.O., 1991. Sverdrup revisited - critical depths, maximum chlorophyll levels, and the control of Southern Ocean productivity by the irradiance-mixing regime. Limnol. Oceanogr., 36(8): 1650-1661.

Nolting, R.F., Gerringa, L.J.A., Swagerman, M.J.W., Timmermans, K.R. and de Baar, H.J.W., 1998. Fe(III) speciation in the high nutrient, low chlorophyll Pacific region of the Southern Ocean. Mar. Chem., 62(3-4): 335-352.

O'Sullivan, D.W., Hanson, A.K., Miller, W.L. and Kester, D.R., 1991. Measurement of Fe(II) in surface-water of the equatorial Pacific. Limnol. Oceanogr., 36(8): 1727-1741.

Osburn, C.L., Zagarese, H.E., Morris, D.P., Hargreaves, B.R. and Cravero, W.E., 2001. Calculation of spectral weighting functions for the solar photobleaching of chromophoric dissolved organic matter in temperate lakes. Limnol. Oceanogr., 46(6): 1455-1467.

Osterberg, 1974. Origins of metals in biology. Nature, 249: 382-383.

Parker, C.A., 1954. Induced autoxidation of oxalate in relation to the photolysis of potassium ferrioxalate. Trans. Faraday Soc., 50: 1213.

Parker, C.A. and Hatchard, C.G., 1959. Photodecomposition of complex oxalates. Some preliminary experiments by flash photolysis. J. Phys. Chem, 63: 22.

Pehkonen, S.O., Siefert, R., Erel, Y., Webb, S. and Hoffmann, M.R., 1993. Photoreduction of iron oxyhydroxides in the presence of important atmospheric organic-compounds. Environ. Sci. Technol., 27(10): 2056-2062.

Petasne, R.G. and Zika, R.G., 1987. Fate of superoxide in coastal seawater. Nature, 325(6104): 516-518.

Plane, J.M.C., Zika, R.G., Zepp, R.G. and Burns, L.A., 1987. Photochemical modeling applied to natural waters. In: R.G. Zika and W.J. Cooper (Editors), Photochemistry of environmental aquatic systems. American Chemical Society Group, Washington D.C., pp. 250-267.

Popova, E.E., Ryabchenko, V.A., Fasham, M.J.R., 2000. Biological pump and vertical mixing in the Southern Ocean: their impact on atmospheric CO_2. Global Biogeochem. Cycles, 14: 477-498.

Powell, R.T. and Wilson-Finelli, A., 2003. Photochemical degradation of organic iron complexing ligands in seawater. Aquat. Sci., 65(4): 367-374.

Price, N.M. and Morel, F.M.M., 1998. Biological cycling of iron in the ocean, Metal Ions in Biological Systems, Vol 35, pp. 1-36.

Rich, H.W. and Morel, F.M.M., 1990. Availability of well-defined iron colloids to the marine diatom *Thalassiosira weissflogii*. Limnol. Oceanogr., 35(3): 652-662.

Ridgwell, A.J., 2002. Dust in the Earth system: the biogeochemical linking of land, air and sea. Philosophical Transactions of the Royal Society of London Series a-Mathematical Physical and Engineering Sciences, 360(1801): 2905-2924.

Ridgwell, A.J. and Watson, A.J., 2002. Feedback between aeolian dust, climate, and atmospheric CO2 in glacial time. Paleoceanography, 17(4).

Rose, A.L. and Waite, T.D., 2002. Kinetic model for Fe(II) oxidation in seawater in the absence and presence of natural organic matter. Environ. Sci. Technol., 36(3): 433-444.

Ross, A.B. and Neta, P., 1982. Rate constants for reactions of aliphatic carbon-centered radicals in aqueous solution. *Natl. Stand. Ref. Data Ser.*, NSRDS-NBS-70: U.S. National Bureau of Standards.

Rue, E.L. and Bruland, K.W., 1995. Complexation of iron(III) by natural organic-ligands in the central north Pacific as determined by a new competitive ligand equilibration adsorptive cathodic stripping voltammetric method. Mar. Chem., 50(1-4): 117-138.

Rue, E.L. and Bruland, K.W., 1997. The role of organic complexation on ambient iron chemistry in the equatorial Pacific Ocean and the response of a mesoscale iron addition experiment. Limnol. Oceanogr., 42(5): 901-910.

Rueter, J.G. and Ades, D.R., 1987. The role of iron nutrition in photosynthesis and nitrogen assimilation in *Scenedesmus quadricauda* (Chlorophyceae). J. Phycol., 23(3): 452-457.

Santana-Casiano, J.M., Gonzalez-Davila, M. and Millero, F.J., 2004. The oxidation of Fe(II) in NaCl-HCO_3- and seawater solutions in the presence of phthalate and salicylate ions: a kinetic model. Mar. Chem., 85(1-2): 27-40.

Santana-Casiano, J.M., Gonzalez-Davila, M., Rodriguez, M.J. and Millero, F.J., 2000. The effect of organic compounds in the oxidation kinetics of Fe(II). Mar. Chem., 70(1-3): 211-222.

Saydam, A.C. and Senyuva, H.Z., 2002. Deserts: Can they be the potential suppliers of bioavailable iron? Geophys. Res. Lett., 29(11).

Schofield, O., Kroon, B.M.A., Prezelin, B.B., 1995. Impact of ultraviolet-B radiation on photosystem II activity and its relation to the inhibition of carbon fixation rates for Antarctic ice algea communities. J. Phycol., 31: 703-715.

Schwertmann, U. and Fischer, W.R., 1973. Natural amorphous ferric hydroxide. Geoderma, 10: 237-247.

Schwertmann, U. and Taylor, R.M., 1972. The transformationof lepidocrocite to goethite. Clays Clay Miner., 20: 151-158.

Schwertmann, U. and Thalmann, H., 1976. The influence of [FeII], [Si], and pH on the formation of lepidocrocite and ferrihydrite during oxidation of aqueous $FeCl_2$ solutions. Clay Miner., 11: 189-200.

Sedlak, D.L. and Hoigne, J., 1993. The role of copper and oxalate in the redox cycling of iron in atmospheric waters. Atmos. Environ., 27(14): 2173-2185.

Sedwick, P.N. and DiTullio, G.R., 1997. Regulation of algal blooms in Antarctic shelf waters by the release of iron from melting sea ice. Geophys. Res. Lett., 24(20): 2515-2518.

Shaked, Y., Erel, Y. and Sukenik, A., 2002. Phytoplankton-mediated redox cycle of iron in the epilimnion of Lake Kinneret. Environ. Sci. Technol., 36(3): 460-467.

Sherman, D.M. and Waite, T.D., 1985. Electronic-spectra of Fe^{3+} oxides and oxide hydroxides in the near IR to near UV. Am. Miner., 70(11-12): 1262-1269.

Siffert, C. and Sulzberger, B., 1991. Light-induced dissolution of hematite in the presence of oxalate - a case-study. Langmuir, 7(8): 1627-1634.

Singer, P.C., Stumm, W., 1969. Acidic Mine Drainage: The rate determining step. Science, 167: 1121-1123.

Smith, R.C., Prezelin, B.B., Baker, K.S., Bidigare, R.R., Boucher, N.P., Coley, T., Karentz, D., Macintyre, S., Matlick, H.A., Menzies, D., Ondrusek, M., Wan, Z. and Waters, K.J., 1992. Ozone depletion - ultraviolet radiation and phytoplankton biology in Antarctic waters. Science, 255(5047): 952-959.

Solomon, S., 1990. Progress towards a quantitative understanding of Antarctic ozone depletion. Nature, 347(6291): 347-354.

Soriadengg, S. and Horstmann, U., 1995. Ferrioxamine-B and ferrioxamine-E as iron sources for the marine diatom *Phaeodactylum tricornutum*. Mar. Ecol. Progr. Ser., 127(1-3): 269-277.

Sulzberger, B. and Laubscher, H., 1995. Photochemical reductive dissolution of lepidocrocite - effect of pH, Aquat. Chem. Advances in Chemistry Series, pp. 279-290.

Sulzberger, B. and Laubscher, H., 1995. Reactivity of various types of iron(III) (hydr)oxides towards light-induced dissolution. Mar. Chem., 50(1-4): 103-115.

Sulzberger, B., Schnoor, J.L., Giovanoli, R., Hering, J.G. and Zobrist, J., 1990. Biogeochemistry of iron in an acidic Lake. Aquat. Sci., 52(1): 56-74.

Sunda, W.G., 1997. Control of dissolved iron concentrations in the world ocean: A comment. Mar. Chem., 57(3-4): 169-172.

Sunda, W.G., 2001. Bioavailability and bioaccumulation of iron in the sea. In: D.R. Turner, Hunter, K.A. (Editor), The biogeochemistry of iron in seawater. John Wiley & sons, New York, pp. 41-84.

Sunda, W.G. and Huntsman, S.A., 1995. Iron uptake and growth limitation in oceanic and coastal phytoplankton. Mar. Chem., 50(1-4): 189-206.

Sunda, W.G. and Huntsman, S.A., 1997. Interrelated influence of iron, light and cell size on marine phytoplankton growth. Nature, 390(6658): 389-392.

Sung, W. and Morgan, J.J., 1980. Kinetics and product of ferrous iron oxidation in aqueous systems. Environ. Sci. Technol., 14(5): 561-568.

Takeda, S. and Kamatani, A., 1989. Photoreduction of Fe(III)-EDTA complex and its availability to the coastal diatom *Thalassiosira weissflogii*. Red Tides: Biol., Environ. Sci., Toxicol.: 349-352.

Tamura, H., Goto, K. and Nagayama, M., 1976. The effect of ferric hydroxide on the oxygenation of ferrous ions in neutral solutions. Corros. Sci., 16(4): 197-207.

Theis, T.L. and Singer, P.C., 1974. Complexation of iron(II) by organic matter and its effect on iron(II) oxygenation. Environ. Sci. Technol., 8(6): 569-573.

Timmermans, K.R., Stolte, W. and de Baar, H.J.W., 1994. Iron-mediated effects on nitrate reductase in marine-phytoplankton. Mar. Biol., 121(2): 389-396.

Tipping, E., Thompson, D.W. and Woof, C., 1989. Iron-oxide particulates formed by the oxygenation of natural and model lakewaters containing Fe(II). Archiv Fur Hydrobiologie, 115(1): 59-70.

Trick, C.G., 1989. Hydroxamate-siderophore production and utilization by marine eubacteria. Curr. Microbiol., 18: 375-378.

Trick, C.G., Anderson, R.J., Price, N.M., Gillam, A. and Harrison, P.J., 1983. Examination of hydroxamate-siderophore production by neritic eukaryotic marine phytoplankton. Mar. Biol., 75: 9-17.

Turner, D.R., Hunter, K.A. and de Baar, H.J.W., 2001. Introduction. In: D.R. Turner, Hunter, K.A. (Editor), The Biogeochemistry of Iron in Seawater. IUPAC series on analytical and physical chemistry of environmental systems. John Wiley & Sons, LTD., Chichester. New York. Weinheim. Brisbane. Singapore. Toronto, pp. 1-7.

Turner, S.M., Harvey, M.J., Law, C.S., Nightingale, P.D. and Liss, P.S., 2004. Iron-induced changes in oceanic sulfur biogeochemistry. Geophys. Res. Lett., 31(14).

van den Berg, C.M.G., 1995. Evidence for organic complexation of iron in seawater. Mar. Chem., 50(1-4): 139-157.

van Leeuwe, M.A., Scharek, R., de Baar, H.J.W., de Jong, J.T.M. and Goeyens, L., 1997. Iron enrichment experiments in the Southern Ocean: physiological responses of plankton communities. Deep Sea Res. II, 44: 189-207.

Voelker, B.M., Morel, F.M.M. and Sulzberger, B., 1997. Iron redox cycling in surface waters: Effects of humic substances and light. Environ. Sci. Technol., 31(4): 1004-1011.

Voelker, B.M. and Sedlak, D.L., 1995. Iron reduction by photoproduced superoxide in seawater. Mar. Chem., 50(1-4): 93-102.

Voelker, B.M. and Sulzberger, B., 1996. Effects of fulvic acid on Fe(II) oxidation by hydrogen peroxide. Environ. Sci. Technol., 30(4): 1106-1114.

Waite, D.T. and Morel, F.M.M., 1984. Photoreductive dissolution of colloidal iron oxides in natural waters. Environ. Sci. Technol., 18: 860-868.

Waite, T.D., 2001. Thermodynamics of the iron system in seawater. In: D.R. Turner and K.A. Hunter (Editors), The biogeochemistry of iron in seawater. IUPAC series on Analytical and Physical Chemistry of Environmental Systems. John Wiley & Sons, LTD, pp. 291-342.

Waite, T.D. and Morel, F.M.M., 1984. Ligand-exchange and fluorescence quenching studies of the fulvic acid-iron interaction - effects of pH and light. Anal. Chim. Acta, 162(AUG): 263-274.

Waite, T.D. and Morel, F.M.M., 1984. Photoreductive dissolution of colloidal iron-oxide - effect of citrate. J. Colloid Interface Sci., 102(1): 121-137.

Waite, T.D. and Szymczak, R., 1993. Particulate Iron Formation Dynamics in Surface Waters of the Eastern Caribbean. Journal of Geophysical Research-Oceans, 98(C2): 2371-2383.

Waite, T.D., Szymczak, R., Espey, Q.I. and Furnas, M.J., 1995. Diel variations in iron speciation in northern Australian shelf waters. Mar. Chem., 50(1-4): 79-91.

Wardman, P. and Candeias, L.P., 1996. Fenton chemistry: An introduction. Radiat. Res., 145(5): 523-531.

Weaver, R.S., Kirchman, D.L. and Hutchins, D.A., 2003. Utilization of iron/organic ligand complexes by marine bacterioplankton. Aquat. Microb. Ecol., 31(3): 227-239.

Weiss, J., 1935. Elektronenübergangsprozesse im Mechanismus von Oxidations- und Reduktionsreaktionen in Lösungen. Die Naturwissenschaften, 4: 64-69.

Wells, M.L. and Mayer, L.M., 1991. The photoconversion of colloidal iron oxyhydroxides in seawater. Deep Sea Res. I, 38(11): 1379-1395.

Wells, M.L., Mayer, L.M., Donard, O.F.X., Sierra, M.M.D. and Ackelson, S.G., 1991. The photolysis of colloidal iron in the oceans. Nature, 353(6341): 248-250.

Wells, M.L., Price, N.M. and Bruland, K.W., 1994. Iron limitation and the cyanobacterium *Synechococcus* in equatorial Pacific waters. Limnol. Oceanogr., 39(6): 1481-1486.

Wilhelm, S.W. and Trick, C.G., 1994. Iron-limited growth of cyanobacteria: multiple siderophore production is a common response. Limnol. Oceanogr., 39(8): 1979-1984.

Witter, A.E., Hutchins, D.A., Butler, A. and Luther, G.W., 2000. Determination of conditional stability constants and kinetic constants for strong model Fe-binding ligands in seawater. Mar. Chem., 69(1-2): 1-17.

Witter, A.E., Lewis, B.L. and Luther, G.W., 2000. Iron speciation in the Arabian Sea. Deep Sea Res. II, 47(7-8): 1517-1539.

Witter, A.E. and Luther, G.W., 1998. Variation in Fe-organic complexation with depth in the northwestern Atlantic Ocean as determined using a kinetic approach. Mar. Chem., 62(3-4): 241-258.

Wu, J.F. and Luther, G.W., 1995. Complexation of Fe(III) by natural organic-ligands in the northwest Atlantic Ocean by a competitive ligand equilibration method and a kinetic approach. Mar. Chem., 50(1-4): 159-177.

Yocis, B.H., Kieber, D.J. and Mopper, K., 2000. Photochemical production of hydrogen peroxide in Antarctic waters. Deep Sea Res. I, 47(6): 1077-1099.

Yoshida, T., Hayashi, K. and Ohmoto, H., 2002. Dissolution of iron hydroxides by marine bacterial siderophore. Chem. Geol., 184(1-2): 1-9.

Yung, Y.L., Lee, T., Wang, C.-H. and Shieh, Y.-T., 1996. Dust: a diagnostic of the hydrologic cycle during the last glacial maximum. Science, 271: 962-963.

Zhu, X., Prospero, J.M., Savoie, D.L., Millero, F.J., Zika, R.G. and Saltzman, E.S., 1993. Photoreduction of iron(III) in marine mineral aerosol solutions. J. Geophys. Res.-Atmos., 98(D5): 9039-9046.

Zhuang, G.S., Yi, Z., Duce, R.A. and Brown, P.R., 1992. Link between iron and sulfur cycles suggested by detection of Fe(II) in remote marine aerosols. Nature, 355(6360): 537-539.

Zuo, Y. and Hoigne, J., 1992. Formation of hydrogen peroxide and depletion of oxalic acid in atmospheric water by photolysis of iron(III)-oxalato complexes. Envir. Sci. Technol., 26: 1014-1022.

Zuo, Y.G., 1995. Kinetics of photochemical chemical cycling of iron coupled with organic-substances in cloud and fog droplets. Geochim. Cosmochim. Acta, 59(15): 3123-3130.

Chapter 2

The influence of solar ultraviolet radiation on the photochemical production of H_2O_2 in the equatorial Atlantic Ocean

Loes J.A. Gerringa, Micha J.A. Rijkenberg, Klaas R. Timmermans, Anita G.J. Buma

Abstract

Hydrogen peroxide (H_2O_2) was measured in marine surface waters of the eastern Atlantic Ocean between 25ºN and 25ºS. H_2O_2 concentrations decreased from 80 nM in the north to 20 nM in the south, in agreement with earlier observations. A diel cycle of H_2O_2 production as function of sunlight in surface waters was followed twice whilst the ship steamed southward. Around 23ºN a distinct diel cycle could be measured which correlated well with irradiance conditions.

The wavelength dependency of H_2O_2 formation was studied near the equator. For 16 hours water samples were incubated with wavelength bands of the solar spectrum, i.e. visible (VIS: 400-700 nm), VIS and ultraviolet A radiation (UVAR: 320-400 nm) and VIS, UVAR and ultraviolet B radiation (UVBR: 280-320 nm). A significant relationship was found between wavelength band and the production of H_2O_2. In addition, a clear positive relationship between intensity and production was found. UVAR was 6.5 times more efficient than VIS in producing 1 nM of H_2O_2, whereas UVBR was 228 times more efficient than VIS. When these data were weighted with respect to the energy of the solar spectrum at zenith hour, 28 % of the H_2O_2 was formed by VIS, 23% was formed by UVAR and 48 % was formed by UVBR. Considering the strong attenuation of UVBR in marine waters as compared with UVAR and VIS radiation, the role of UVAR deeper in the water column is recognized. Furthermore results of this research emphasize the importance of VIS radiation in the formation of H_2O_2.

1. Introduction

Hydrogen peroxide (H_2O_2) is an intermediate in the reduction of oxygen to water. It is a potential toxicant and it can affect the distribution and redox-chemistry of biologically active metals such as iron, copper and manganese. For example H_2O_2 is the dominant oxidation pathway of Fe(II) (Miller and Kester, 1994; Moffett and Zika, 1987).

H_2O_2 can be formed by photochemical reactions and (to a lesser extent) by biota (Hanson et al., 2001; Palenik and Morel, 1988; Palenik et al., 1987). It can be introduced to the marine environment by dry and wet deposition (Hanson et al., 2001; Kieber et al., 2001; Miller and Kester, 1994). The focus of the present study was on the photochemical origin of H_2O_2. Samples of natural surface and ground waters showed a rapid increase in H_2O_2 concentration after exposure to sunlight (Cooper and Zika, 1983). H_2O_2 is photochemically generated from organic constituents present in water. Humic materials are believed to be the primary agent producing the H_2O_2 (Cooper and Zika, 1983). Distinct diel variation of the H_2O_2 concentration was observed with highest concentrations in the late afternoon. The observations are consistent with patterns of H_2O_2 formation due to photo-oxidation of dissolved organic matter (Moore et al., 1993; Palenik and Morel, 1988; Zika et al., 1985). The H_2O_2 concentrations were not only related to light intensity, but also to wavelength (Plane et al., 1987). Plane et al. (1987) demonstrated that production occurs primarily between 300 and 400 nm. This wavelength dependence of H_2O_2 formation is related to the light absorbance of organic substances in the water (Cooper et al., 1988; Plane et al., 1987; Sikorski and Zika, 1993). The absorbance of organic substances is highest in the UVB region of the solar spectrum (280 - 320 nm), decreasing in the UVA region (320 - 400 nm) and lower at higher wavelengths (> 400 nm). The weighting function, relating wavelength band and H_2O_2 formation was assessed by Yocis et al. (2000).

Published data of H_2O_2 concentrations in the Atlantic Ocean are scarce (Miller and Kester, 1994; Obernosterer et al., 2001; Obernosterer, 2000; Weller and Schrems, 1993). Recently, diel cycles in H_2O_2 concentrations were reported by Yuan and Shiller (2001) in the western Central Atlantic Ocean. They observed a decrease of H_2O_2 concentrations with latitude from north to south.

In the present study we investigated factors affecting H_2O_2 formation in marine waters, such as solar irradiance and wavelength dependency. We measured surface H_2O_2 concentrations in the Eastern Atlantic, from 25° N to 25° S, encountering various water masses and irradiance conditions.

Furthermore, during the cruise two diel cycles were measured. Finally, water taken near the equator (2° N) was incubated on deck under different wavelength conditions during which H_2O_2 formation was followed.

2. Material and methods

Measurements were executed during a cruise from Bremerhaven (Germany) to Cape Town (South Africa) aboard RV Polarstern in October 2000 (Figure 1). Data on salinity, temperature, and the position of the ship were obtained from the "Polarstern" PODEV data
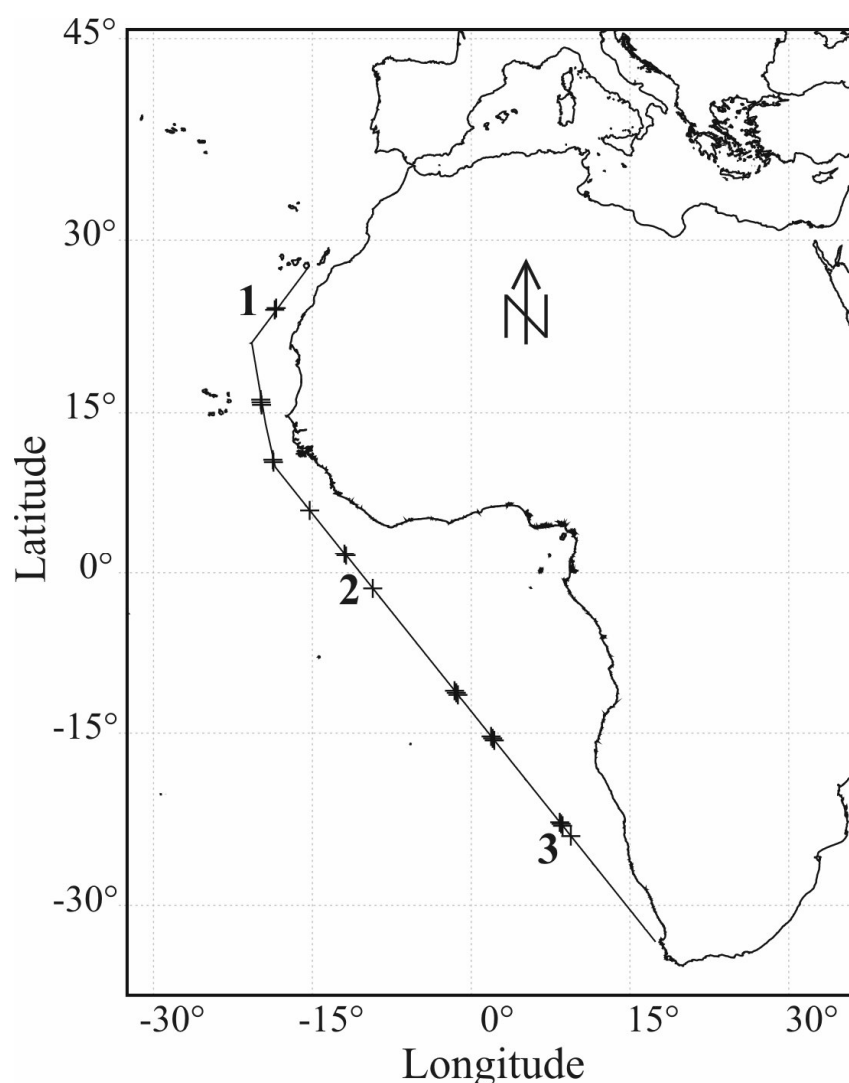
Figure 1. Cruise track of cruise ANT18/1 of the R.V. "Polarstern" from Bremerhaven (Germany) to Cape Town (South Africa). The positions of H_2O_2 measurements are indicated by crosses, the positions of the experiments by numbers.

acquisition system. Samples were taken underway by a FISH towed just under the sea surface, alongside the ship. The samples were filtered on-line through a 0.2 μm filter cartridge. Global radiation was measured by an artificially ventilated pyranometer (model CM11, Kipp & Zonen) mounted on the mast of the "Polarstern". It was fixed horizontally with respect to the ship. Rolling and pitching will have had no significant influence on averaged values, but on individual measurements. The values given are 1-min averages (Figure 2 and 3). Light measurements used for the deck incubations were measured every hour using a high accuracy UV-Visible spectroradiometer (model OL 752, Optronic
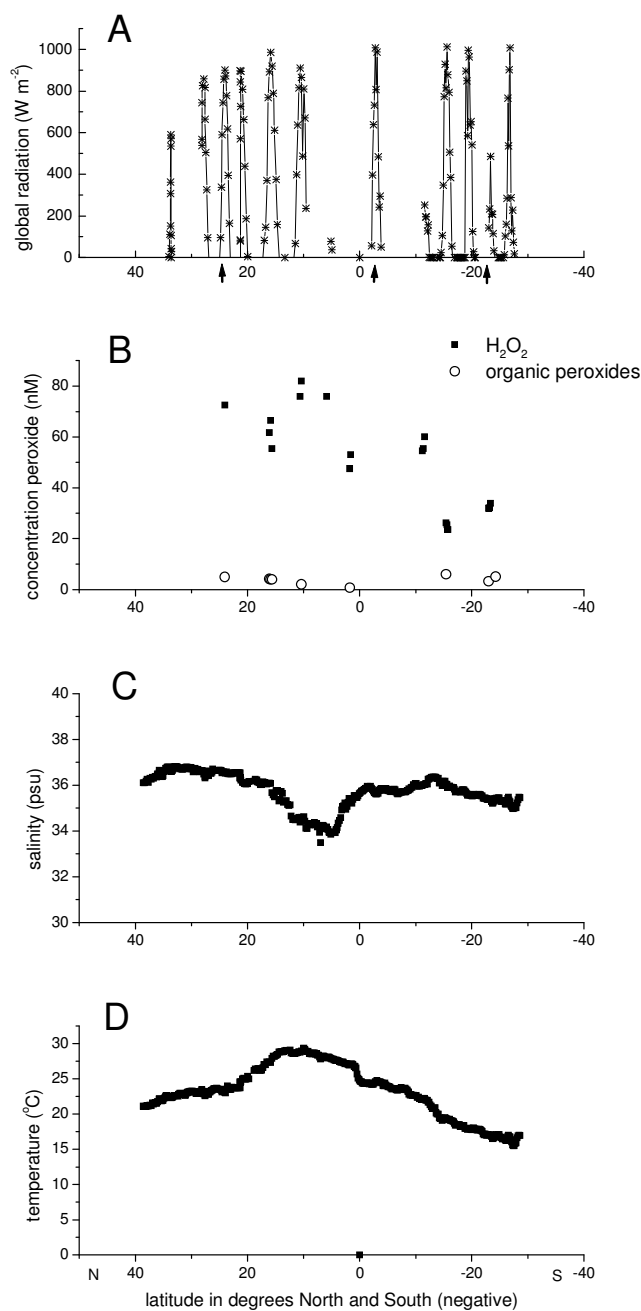
Figure 2. (A) Global solar radiation in W m^{-2}; (B) H$_2$O$_2$ (■) and organic peroxide (○) concentrations (all in nM) in sea surface waters; (C) salinity in psu; (D) temperature in °C against latitude. In (A) the three days on which experiments were executed (9, 15 and 20 October 2000) are indicated by arrows. Where no data are shown, no measurements were made.

Laboratories). The OL 752 system consisted of an Optics Head (OL 752-O-PMT) and an OL 752-C Controller. One measurement of the solar spectrum, 280-750 nm, took ~ 28 minutes.

VIS is defined as light between 400 and 700 nm, UVA between 320 and 400 nm, and UVB between 280 and 320 nm. Diel cycles of H_2O_2 formation were followed on 9 October near 23ºN 18ºW (1 in Figure 1) and on 20 October near 23ºS 8.5ºE (3 in Figure 1). Unfortunately, on 20 October the sky was cloudy, resulting in a global radiation at noon that was half of the global radiation at noon on 9 October.

A sample of 50 L of filtered seawater was taken on 14 October, near 2º N, 12º W (2 in Figure 1). The salinity of the water was 35.6 ppt. The water was stored in the dark at ambient seawater temperature (24°C) during the afternoon. After sunset, the water was sub-sampled in 2-L home-made polymethylmetacrylate (PMMA) bottles, which have a high transmission in the UV region (Steeneken et al., 1995). To assure minimal shading the bottles were, immediately after filling, put in UV transparent PMMA incubators on the highest deck of the ship. The bottles were kept at a constant ambient temperature of 24 °C using running seawater from the ship's pumping system. Two PMMA bottles packed in light-tight black plastic functioned as dark controls. Two PMMA bottles received the full solar spectrum (UVB,UVA and VIS), two PMMA bottles were screened by glass, which served as a UVB cut-off filter, receiving only UVA and VIS, two PMMA bottles were screened by UV-opaque PMMA, only permeable for VIS and thus serving as a UVB and UVA cut-off filter. Total irradiance was varied by aluminum neutral density gauze, painted black, causing a 50% reduction in the full solar spectrum. 80% light reduction was obtained by wrapping two bottles in black plastic with tiny (1mm) holes. Light reduction of these materials was measured before use. Sampling during the deck incubation started at 5:00 h UTC in the morning of 15 October and continued until 23:00 h UTC. Each bottle was sampled at least every two hours, and all light conditions were sampled at least once every hour. The dark bottles were only sampled three times during the day.

H_2O_2 was measured as fluorescence (Waters fluorometer, type 470) after enzyme-catalyzed dimerisation of (*p*-hydroxyphenyl)acetic acid (POHPAA) (Miller and Kester, 1988; Miller and Kester, 1994). The POHPAA (Merck, purified by recrystallization) stock solution (25 mM in milliQ) was kept at 4˚C. The peroxidase stock solution (horseradish, 10000 U/val, Merck; 3.6 mg in 100 ml 0.25 M TRIS, pH 8.8) was stored in 2 ml portions at -20˚C. A fluorometric reagent of POHPAA and peroxidase was prepared daily in 0.25 M TRIS (pH 8.8). Concentrations and enzyme activities in the samples were $5.1.10^{-6}$ M POHPAA and 0.153 units/ml (U/ml) peroxidase.

The fluorometric reagent was immediately added to the sample to fix the hydrogen peroxide. The samples (in triplicate) were stored at 4˚C and analysis was completed within 12 h. The fluorescence response is a combination of the signal of the hydrogen peroxide and the organic peroxides. To distinguish between these forms, 4 min before the addition of the

fluorometric reagent, catalase (65 U/ml) was added to the samples to remove the hydrogen peroxide. The resulting fluorescence signal represented the organic peroxides, whereas subtraction from the total signal resulted in the hydrogen peroxide concentrations. Corrections were made for the natural fluorescence of seawater (no reactants added to the seawater) and the fluorescence of catalase (only catalase added to the seawater).

The precision of the method was 3% (st dev after 15 analyses of the same sample). Its detection limit was smaller than 2 nM (three times the standard deviation of open ocean water blank). The H_2O_2 standard was checked by measuring the reaction with KI at 353 nm (Cotton and Dunford, 1973).

3. Results and discussion

3.1 Surface samples from the transect

The H_2O_2 concentrations in the surface samples decreased from 70-80 nM at 25ºN to 20-30 nM at 25ºS in samples taken at noon (Fig 2B). Obernosterer (2000) found surface values between 125 and 50 nM in the subtropical northern Atlantic Ocean in 1996. In 1992, Weller and Schrems (1993) measured concentrations from 150 nM at 30ºN to 100 nM at 30ºS over approximately the same cruise track as shown in Figure 1. A decrease from north to south was also observed by Yuan and Shiller (2001) in the central and southern Atlantic Ocean. They suggest that this latitude dependence is due to differences in precipitation. Rain is a well-known source of H_2O_2 in oceans (Hanson et al., 2001; Miller and Kester, 1988; Miller and Kester, 1994; Weller and Schrems, 1993; Yuan and Shiller, 2000).

Organic peroxides were measured irregularly; they varied between 1 and 6 nM (Figure 2B). To our knowledge no other data on organic peroxides in the Atlantic Ocean have been published, making comparison impossible.

In the Northern Hemisphere the H_2O_2 concentrations did show a clear positive relationship with the global radiation (Figure 3). A decrease in H_2O_2 concentrations, seen the night before, was followed by a sharp increase of more than 30 nM H_2O_2 with increasing radiation. Obernosterer et al. (2001) found diel variations of 42 nM in the northern subtropical Atlantic Ocean, whereas Yuan and Shiller (2001) found a variation of 25 nM in the central and southern Atlantic Ocean. A slight decrease in concentration in our data occurred after sunset on 9 October (Figure 3). Johnson et al. (1989) observed such a slow decrease of peroxide concentrations with time and with depth in the western Mediterranean Sea, where they used H_2O_2 as a tracer for vertical advection. Johnson et al. (1989) calculated a decay rate of 3.8 nM h^{-1} during darkness. The decrease in the present data in Figure 3 for
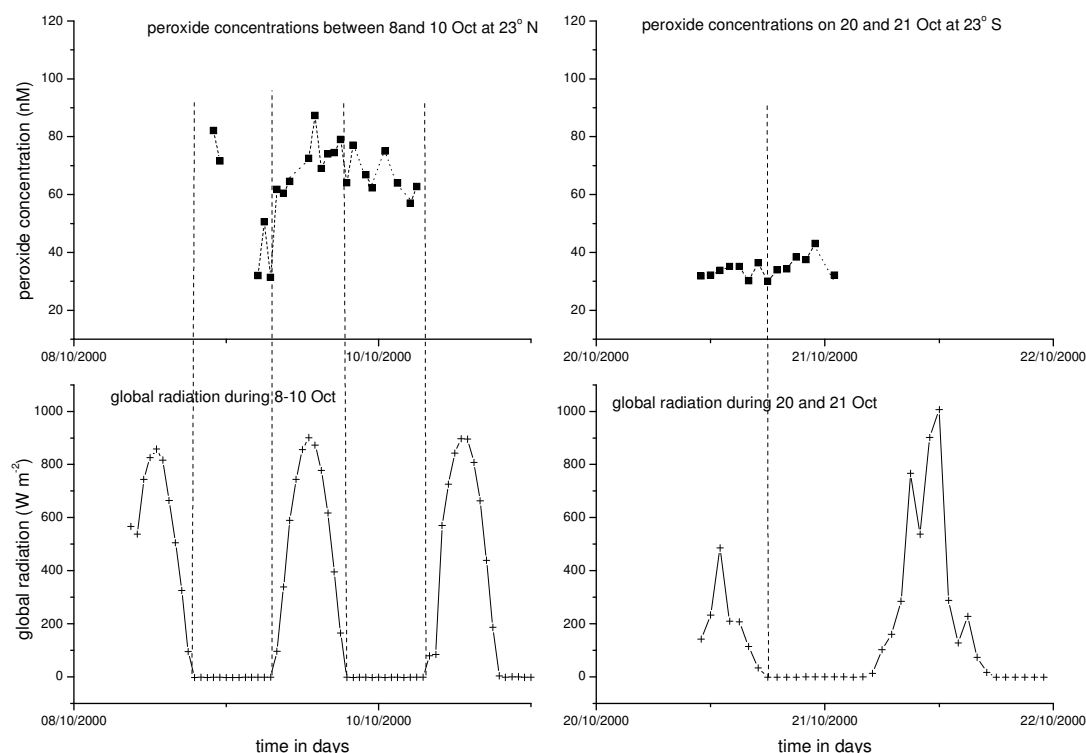
Figure 3. H$_2$O$_2$ concentrations (nM) and global solar radiation (W m^{-2}) of two diel cycles between 8 and 10 October 2000 at 23° N, and around 20 and 21 October 2000 at 23° S.

the Northern Hemisphere, measured from the slope through the middle of the data points, would give a rate of 1 nM h^{-1}. Johnson et al. (1989) did not observe a decline in concentration until after sunset as is also the case in our data. This is especially the case for seawater compared to a relatively rapid decrease observed in fresh water (Cooper and Lean, 1989).

The second diel cycle observation in the Southern Hemisphere gave a different result (Figure 3). A potential diel variation of 5-10 nM in H$_2$O$_2$ concentration disappeared in the noise of the measurements during the day and the following night. Since the global radiation was lower due to clouds, a lower production of H$_2$O$_2$ was expected. In order to check whether the difference in H$_2$O$_2$ production could be explained by the difference in the solar intensity a linear relationship between H$_2$O$_2$ production and the intensity of the global radiation of 9 and 20 October was calculated. The slope of the linear relation in the data of 9 October was 2.7 times higher than that of 20 October. Thus the lower magnitude in the diel cycle must have had an additional cause, most likely a lower concentration in organic matter in the Southern hemisphere sampling station (Scully et al., 1996). Both the northern and the southern experiments were performed in subtropical gyres, which presumably have relatively nutrient-

poor surface waters (Antoine et al., 1996; Field et al., 1998). The northern experiment was in warmer more saline waters (S=36.5, T=23.1ºC versus S=35.4, T=16.2ºC, Fig 2). Both locations are relatively close to deserts, known to release dust into the adjacent ocean. Both positions are close to a zone of coastal upwelling (Krauss, 1996; Shannon and Nelson, 1996). However, the northern position is closer to the coast and it is thus more likely to receive organic-rich water from the coastal upwelling. Since the formation of H_2O_2 results principally from the excitation of humic substances (Cooper et al., 1988; Scully et al., 1996) differences in H_2O_2 can be expected from differences in water characteristics such as content of organic material. Moore et al. (1993) related peroxide production with organic matter fluorescence in the Eastern Caribbean. Fluorescence was measured continuously aboard the "Polarstern", but values were very low and had the same order of magnitude for both regions. No rain fell during the cruise, giving no additional explanation for the relatively high diel cycle of H_2O_2 at the northern position or for the decrease of H_2O_2 concentrations from north to south in this part of the Atlantic Ocean.

3.2 Deck incubations

The results of the deck incubations showed a clear relationship between H_2O_2 concentration and the wavelength and cumulative dose of sunlight (Figure 4 and 5). More H_2O_2 was produced with decreasing wavelength (Figure 5A). Even when only VIS was allowed through the bottles, H_2O_2 concentrations increased during the day compared to the dark control bottles. The net H_2O_2 production rate at noon was 7 nM h^{-1} in the bottles with the full solar spectrum, 4 nM h^{-1} in the bottles without UVB and 2 nM h^{-1} in the bottles in which only VIS was allowed. In the dark control bottles 0.4 nM h^{-1} H_2O_2 formed. Taking into account that 88% of the energy of the solar spectrum consisted of VIS, 11% consisted of UVA, and less than 1 % of UVB, the relationship between wavelength and H_2O_2 was much stronger than the production rates show.

A net production rate under the full solar spectrum of 7 nM h^{-1} compares well with other studies. Yuan and Shiller (2001) found 8.3 nM h^{-1} at local noon in the central Atlantic Ocean. Obernosterer (2000) found a net production of 5.5 nM h^{-1} in the northern subtropical region of the Atlantic Ocean. Yocis et al. (2000) measured 4.5 nM h^{-1} in Antarctic waters and attributed this relatively low production to the high latitude, lower temperatures and lower UV irradiances in polar waters.

In order to calculate the wavelength dependency of the net H_2O_2 production, by UVA, the concentrations of H_2O_2 formed under the full solar spectrum were subtracted from those
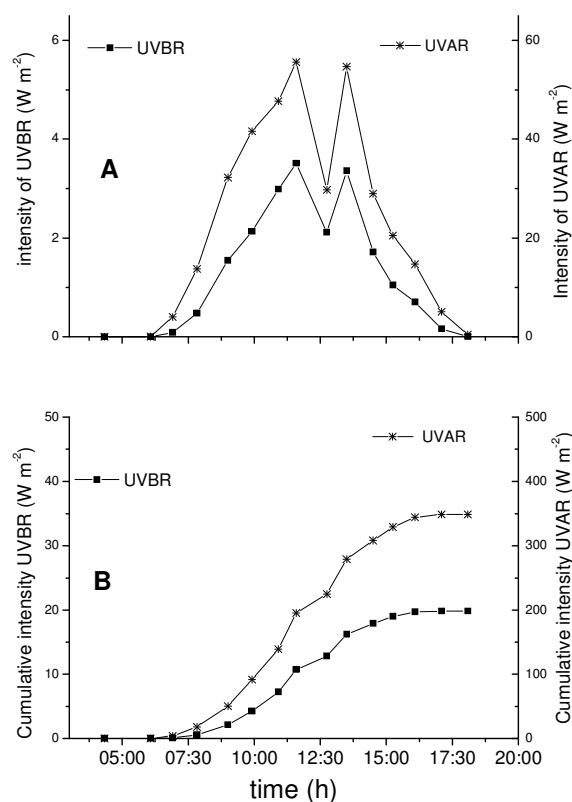
Figure 4. (A) UVA and UVB (W m^{-2}) of the solar spectrum of 15 October 2000 against time (UTC); (B) the cumulative energies for UVA and UVB against time (UTC).

formed under UVA and VIS. By subtracting concentrations formed under UVA and VIS from those under VIS we obtained the production caused by UVA.

The light intensities of the UVB, UVAR and the VIS portion of the solar spectrum were fitted into a model in order to explain the increases in H_2O_2. It was assumed that the relation between H_2O_2 production and light intensity is linear Cooper et al. (1994). It was assumed that the increase in peroxide concentration C at time t_{x+1} was due to the energy of the incoming light E between t_x and t_{x+1} multiplied by a factor L, according to:

$$C_{x+1} = C_x + \frac{(E_x + E_{x+1})}{2} \cdot (t_x - t_{x+1}) \cdot L \qquad (1)$$

L (nM min^{-1} W^{-1} m^2) was found by minimising the root mean square (RSQ) of the differences between measured and calculated concentrations. To account for the oxidation of peroxides, a

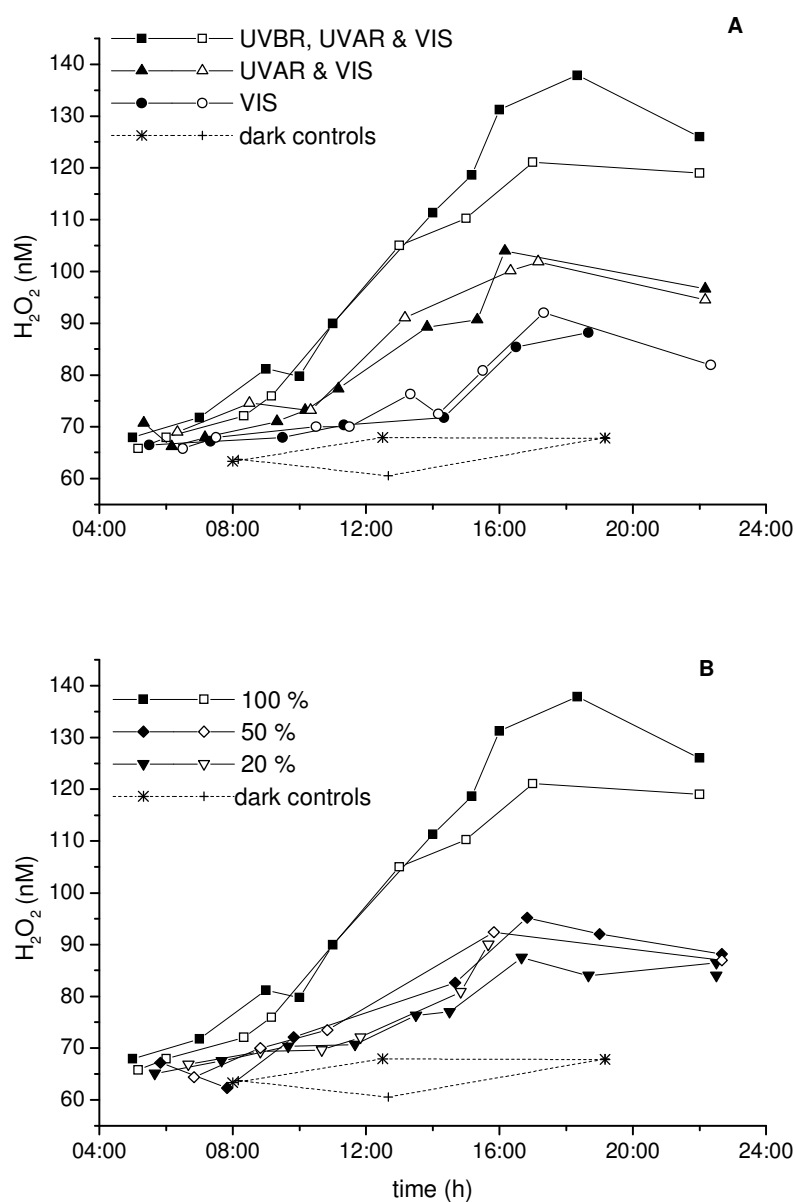**Figure 5.** Peroxide concentrations (nM) in the incubated bottles against time (UTC). Two bottles per light condition were used, distinguished by filled and open symbols. (A) Peroxide production related to wavelength of the incoming light. (B) peroxide production related to light intensity. In both figures the data of the dark control bottles are presented. 100% light intensity in (B) is similar to the data of UVBR, UVA and VIS in (A).

Table 1. The factor L indicating the relation between light intensity (W m^{-2}) and peroxide increase (nM min^{-1}). L was obtained by fitting the data in equation (1). The obtained root mean square of the differences between measured and calculated concentrations (RSQ C_{x+1}-C_x) are given.

Experimental conditions	Factor L $*10^{-3}$ (nM min^{-1}. W^{-1}m^2)	RSQ(C_{x+1},C_x)
20% of full spectrum	0.112	0.76
50% of full spectrum	0.175	1.46
100% of full spectrum	0.347	1.77
VIS	0.121	1.2
UVA	0.785	1.29
UVB	27.5	2

loss function was included in the model, assuming dC/dt = LE-KC. However, this loss factor (K) did not improve the model and was left out.

A 50% light reduction indeed gives half of the peroxide production, a reduction to 20% of the original light causes the production to decrease to 30 % compared to full light conditions (Figure 5B, Table 1). This discrepancy between 20 and 30% is difficult to explain. The light reduction to 20% by the plastic was valid for the entire solar spectrum, independent of wavelength.

The importance of UVB for production of H$_2$O$_2$ is evident, confirming the results of Cooper et al. (1994). This radiation is 227 times more efficient for the production of H$_2$O$_2$ than VIS and 35 times more efficient than UVA (Table 1). The result of Yocis et al. (2000) showed a comparable ratio in the UVB-UVA region, demonstrating a factor 100 in the relationship between wavelength and peroxide production for the wavelengths at 290 and at 410 nm. However, some care must be taken in directly comparing the results from Yocis et al. (2000) and our results. We did not incorporate wavelength-related differences in absorption into our results.

The energy distribution of the solar spectrum at noon on 14 October near the equator consisted of 88% of VIS, 11.4 % of UVA and 0.65 % of UVR (280-700 nm: 391 W m^{-2}, 400-700 nm: 346 W m^{-2}, 320-400 nm: 43 W m^{-2}, 280-320 nm: 2.8 W m^{-2}). Considering the contribution of the energies in the solar spectrum and using the L factors from Table 1, we

obtained a H_2O_2 production rate at noon of which 28 % originated from the VIS region, 24 % from UVA and 48% from UVB.

UVA penetrates to greater depths than UVB, so the role of UVA may become increasingly important at greater water depths (Obernosterer, 2000; Scully et al., 1996; Yocis et al., 2000). The decrease with depth found paralleled decrease in UV penetration. However, the data from our study showed an important contribution of VIS to H_2O_2 formation as well. This was also concluded by Sikorski and Zika (1993). They constructed a model in which the optical properties of light in water play an important role. They found that the attenuation of light was very sensitive to the solar angel of incident light and that this effect has a large wavelength dependency. They concluded that due to these optical properties of the solar spectrum, the visible part of the irradiance penetrates much deeper into the water column compared to the UV part of the spectrum than was thought before. They therefore concluded that part of the solar spectrum above 400 nm caused a significant production of hydrogen peroxides, especially at larger depth and at smaller zenith angles.

Acknowledgements

References

Antoine, D., Andre, J.M. and Morel, A., 1996. Oceanic primary production.2. Estimation at global scale from satellite (coastal zone color scanner) chlorophyll. Global Biogeochem. Cycles, 10(1): 57-69.

Cooper, W.J. and Lean, D.R.S., 1989. Hydrogen peroxide concentration in a northern lake - photochemical formation and diel variability. Environ. Sci. Technol., 23(11): 1425-1428.

Cooper, W.J., Shao, C., Lean, D.R.S., Gordon, A.S. and Scully, F.E., 1994. Factors affecting the distribution of H_2O_2 in surface waters. In: L.A. Baker (Editor), Environmental chemistry in lakes and reservoirs. Adv. Chem. Ser. 237, ACS.

Cooper, W.J. and Zika, R.G., 1983. Photochemical formation of hydrogen-peroxide in surface and ground waters exposed to sunlight. Science, 220(4598): 711-712.

Cooper, W.J., Zika, R.G., Petasne, R.G. and Plane, J.M.C., 1988. Photochemical formation of H_2O_2 in natural waters exposed to sunlight. Environ. Sci. Technol., 22(10): 1156-1160.

Cotton, M.L. and Dunford, H.B., 1973. Studies on horseradish peroxidase. XI. On the nature of compounds I and II as determined from the kinetics of oxidation of ferrocyanide. Can. J. Chem., 51: 582-587.

Field, C.B., Behrenfeld, M.J., Randerson, J.T. and Falkowski, P., 1998. Primary production of the biosphere: Integrating terrestrial and oceanic components. Science, 281(5374): 237-240.

Hanson, A.K., Tindale, N.W. and Abdel-Moati, M.A.R., 2001. An equatorial Pacific rain event: influence on the distribution of iron and hydrogen peroxide in surface waters. Mar. Chem., 75(1-2): 69-88.

Johnson, K.S., Willason, S.W., Wiesenburg, D.A., Lohrenz, S.E. and Arnone, R.A., 1989. Hydrogen peroxide in the western Mediterranean Sea - a tracer for vertical advection. Deep Sea Res. I, 36(2): 241-254.

Kieber, R.J., Cooper, W.J., Willey, J.D. and Avery, G.B., 2001. Hydrogen peroxide at the Bermuda Atlantic Time Series Station. Part 1: Temporal variability of atmospheric hydrogen peroxide and its influence on seawater concentrations. J. Atmos. Chem., 39(1): 1-13.

Krauss, W., 1996. Comments on the development of our knowledge of the general circulation of the North Atlantic Ocean. In: W. Krauss (Editor), The warm water sphere of the North Atlantic Ocean. Borntrager, Berlin, pp. 1-32.

Miller, W.L. and Kester, D.R., 1988. Hydrogen peroxide measurement in seawater by (para-hydroxyphenyl)acetic acid dimerization. Anal. Chem., 60(24): 2711-2715.

Miller, W.L. and Kester, D.R., 1994. Peroxide variations in the Sargasso sea. Mar. Chem., 48(1): 17-29.

Moffett, J.W. and Zika, R.G., 1987. Reaction-kinetics of hydrogen-peroxide with copper and iron in seawater. Environ. Sci. Technol., 21(8): 804-810.

Moore, C.A., Farmer, C.T. and Zika, R.G., 1993. Influence of the Orinoco river on hydrogen-peroxide distribution and production in the eastern Caribbean. J. Geophys. Res.-Oceans, 98(C2): 2289-2298.

Obernosterer, I., Ruardij, P. and Herndl, G.J., 2001. Spatial and diurnal dynamics of dissolved organic matter (DOM) fluorescence and H_2O_2 and the photochemical oxygen demand of surface water DOM across the subtropical Atlantic Ocean. Limnol. Oceanogr., 46(3): 632-643.

Obernosterer, I.B., 2000. Photochemical transformations of dissolved organic matter and its subsequent utilization by marine bacterioplankton. PhD Thesis, University of Groningen, The Netherlands, 133 pp.

Palenik, B. and Morel, F.M.M., 1988. Dark production of H_2O_2 in the Sargasso sea. Limnol. Oceanogr., 33(6): 1606-1611.

Palenik, B., Zafiriou, O.C. and Morel, F.M.M., 1987. Hydrogen-peroxide production by a marine phytoplankter. Limnol. Oceanogr., 32(6): 1365-1369.

Plane, J.M.C., Zika, R.G., Zepp, R.G. and Burns, L.A., 1987. Photochemical modeling applied to natural waters. In: R.G. Zika and W.J. Cooper (Editors), Photochemistry of environmental aquatic systems. American Chemical Society Group, Washington D.C., pp. 250-267.

Scully, N.M., McQueen, D.J., Lean, D.R.S. and Cooper, W.J., 1996. Hydrogen peroxide formation: The interaction of ultraviolet radiation and dissolved organic carbon in lake waters along a 43-75 degrees N gradient. Limnol. Oceanogr., 41(3): 540-548.

Shannon, L.V. and Nelson, G., 1996. The Benguela: Large scale features and processes and system variability. In: G. Wever, W.H. Berger, G. Siedler and D.J. Webb (Editors), The South Atlantic. Springer Verlag, pp. 163-210.

Sikorski, R.J. and Zika, R.G., 1993. Modeling mixed-layer photochemistry of H_2O_2 - optical and chemical modeling of production. J. Geophys. Res.-Oceans, 98(C2): 2315-2328.

Steeneken, S.F., Buma, A.G.J. and Gieskes, W.W.C., 1995. Changes in transmission characteristics of polymethylmethacrylate and cellulose-(III) acetate during exposure to ultraviolet-light. Photochem. Photobiol., 61(3): 276-280.

Weller, R. and Schrems, O., 1993. H_2O_2 in the marine troposphere and seawater of the Atlantic Ocean (48-degrees-N-63-degrees-S). Geophys. Res. Lett., 20(2): 125-128.

Yocis, B.H., Kieber, D.J. and Mopper, K., 2000. Photochemical production of hydrogen peroxide in Antarctic waters. Deep Sea Res. I, 47(6): 1077-1099.

Yuan, J.C. and Shiller, A.M., 2000. The variation of hydrogen peroxide in rainwater over the South and Central Atlantic Ocean. Atmos. Environ., 34(23): 3973-3980.

Yuan, J.C. and Shiller, A.M., 2001. The distribution of hydrogen peroxide in the Southern and central Atlantic Ocean. Deep Sea Res. II, 48(13): 2947-2970.

Zika, R.G., Saltzman, E.S. and Cooper, W.J., 1985. Hydrogen-peroxide concentrations in the Peru upwelling area. Mar. Chem., 17(3): 265-275.

Chapter 3

The influence of UV irradiation on the photoreduction of iron in the Southern Ocean

Micha J.A. Rijkenberg, Astrid C. Fischer, Koos J. Kroon, Loes, J.A. Gerringa, Klaas R. Timmermans, Bert Th. Wolterbeek, Hein J.W. de Baar

Abstract

An iron enrichment experiment, EisenEx, was performed in the Atlantic sector of the Southern Ocean during the Antarctic spring of 2000. Deck-incubations of open ocean water were performed to investigate the influence of ultraviolet B (UVB: 280-315 nm) and ultraviolet A (UVA: 315-400 nm) on the speciation of iron in seawater, using an addition of the radio-isotopes ^{59}Fe(III) (1.25 nM) or ^{55}Fe(III) (0.5 nM). Seawater was sampled inside and outside the iron enriched region. The radio-isotopic Fe(II) concentration was monitored during daylight under three different light conditions: the full solar spectrum (total), total minus UVB and total minus UVB + UVA. A distinct diel cycle was observed with a clear distinction between the three different light regimes. A clear linear relationship was found for the concentration of radio-isotopic Fe(II) versus irradiance. UVB produced most of the Fe(II) followed by UVA and visible light (VIS: 400-700 nm), respectively. UVB produced 4.89 and 0.69 pM m^2 W^{-1} radio-isotopic Fe(II) followed by UVA with 0.33 and 0.10 pM m^2 W^{-1} radio-isotopic Fe(II) and VIS with 0.04 and 0.03 pM m^2 W^{-1} radio-isotopic Fe(II).

1. Introduction

Phytoplankton growth in the Southern Ocean, known as a High Nutrient Low Chlorophyll (HNLC) region, is limited strongly by iron availability (de Baar et al., 1990; Martin et al., 1990) and light (Mitchell et al., 1991; Nelson and Smith, 1991). In addition, the phytoplankton have to deal with increasing levels of UVB radiation in spring, caused by reduction in stratospheric ozone concentration over the Antarctic (Frederick and Snell, 1988; Solomon, 1990).

It has been established that UVB can penetrate to 60 m depth in the Southern Ocean during the spring ozone-depletion cycle (Smith et al., 1992). Biological effects of enhanced UVB, detected to maximum depths of 20-30 m (Karentz and Lutze, 1990; Smith et al., 1992), negatively affect the marine Antarctic primary producers. It has been demonstrated that

enhanced UVB increases photoinhibition (Neale et al., 1998), by decreasing photosystem II efficiency (Schofield, 1995), and modifying the RUBISCO pool (Lesser et al., 1996). Also much information is available on UVB-related accumulation of DNA damage, as demonstrated by the formation of cyclobutane pyrimidine dimers (CPD) in marine phytoplankton (Buma et al., 1996; Buma et al., 2001). However, the negative effects of UVB radiation on primary production may be outweighed by its potential positive effect of releasing sequestered Fe(III) and increasing the Fe(II) concentration in iron limited environments.

Iron(III) has a very low solubility in seawater (Millero, 1998; Liu and Millero, 2002) and rapidly becomes hydrolyzed into various iron(III) oxyhydroxides. 99% of the iron in the ocean is organically complexed (van den Berg, 1995) increasing the solubility of iron (Kuma et al., 1996). Iron(III) is the dominant redox species in natural oxygenated waters, while iron(II), although better soluble at seawater pH, becomes rapidly oxidized by O_2 and H_2O_2 (Millero et al., 1987; Millero and Izaguirre, 1989; Millero and Sotolongo, 1989; King et al., 1991; King et al., 1995; King, 1998).

The redox-cycle of iron initiated by photochemical processes is mentioned as an important mechanism by which (colloidal) iron is converted in more reactive iron species (defined by the method applied) resulting in a higher bioavailability to phytoplankton (Wells and Mayer, 1991; Johnson et al., 1994; Miller and Kester, 1994). Furthermore, Fe(II) is expected to be a bioavailable species (Takeda and Kamatani, 1989).

Much evidence exists that light is responsible for photo-reduction of iron in seawater (Hong and Kester, 1986; O'Sullivan et al., 1991; Johnson et al., 1994). For example, Rich and Morel (1990) have shown that light with wavelengths less then 560 nm can photo-reduce iron. Correspondingly, Wells et al. (1991) have observed increasing lability of colloidal iron in seawater, with a spectral dependency that generally increases with decreasing wavelength. Furthermore, Waite et al. (1995) have found that the concentration of Fe(II) can be strongly related to the light intensity. Kuma et al. (1992) investigated the increase in photochemical reduction of Fe(III) in the presence of hydrocarboxylic acids under UV irradiance, e.g. hydrolytic products of phytoplankton as glucuronic acid (Parsons, 1961). Glucuronic acid is able to aid the photo-reduction of Fe(III) in sunlight.

Photoreduction was the most likely candidate mechanism to explain the high Fe(II) concentrations during the iron enrichment experiment SOIREE. Suggested maximal photoreduction rates at 20 m depth were as high as 370 pM hr^{-1}, despite cloudy skies (Croot et al., 2001). The present study investigates the role of UVB and UVA in driving the Fe redox-cycle during the *in situ* iron enrichment experiment EisenEx (Gervais et al., 2002) in the Southern Ocean. A combination of iron isotopes and ferrozine preloaded C-18 SepPak cartridges was used to detect very small quantities of iron(II) (King et al., 1991; Fischer et al., 2004).

2. Experimental

2.1 Experiments

Surface seawater (pH = 7.94, 4ºC) was pumped into an over-pressurized class 100 clean air container using a Teflon diaphragm pump (Almatec A-15, Germany) driven by a compressor (Jun-Air, Denmark, model 600-4B) connected via acid-washed braided PVC tubing to a torpedo towed at approximately 5 m alongside the ship. The seawater was filtered in-line by a (Sartorius Sartobran filter capsule 5231307H8) with a cut-off of 0.2 μm.

Seawater was sampled inside and outside the iron enriched patch. The iron enriched patch was situated in a cyclonic eddy of approximately 150 km diameter, separated from the Antarctic Polar Front (APF) by detachment of a northward protruding meander. Due to its origin, the eddy contained in its centre reasonably high concentrations of macro-nutrients ($[Si] = 14$ μM, $[NO_3] = 23$ μM, $[PO_4] = 1.65$ μM, as measured during the North-South transect (Hartmann et al., 2001)) typical of the southern APF side (Strass et al., 2001).

The seawater for experiment I was sampled inside the iron enriched region at ~ 47°59'08 S, and 20°50'65 E, 11 November 2000 and contained a concentration of 3.83 nM dissolved iron. ^{59}Fe(III)Cl$_3$ (Isotope Products Laboratory, BLASEG GmbH, Waldburg, Germany; half-life of 44.5 days, emitting both β (0.5 and 1.6 MeV) and γ- rays (1.1 and 1.2 MeV)) in 0.1 M HCl was added to a concentration of 1.25 nM to the seawater. It was incubated under sunny conditions (detailed information about irradiance can be found in Figure 2).

Seawater for experiment II was sampled outside the iron enriched patch but within the eddy region at ~ 47°42'79 S and 21°03'22 E, 25 November 2000 and contained 0.852 nM dissolved iron. ^{55}Fe(III)Cl$_3$ (Isotope Products Laboratory, BLASEG GmbH, Waldburg, Germany; half-life of 2.7 years, ^{55}Fe decays via electron capture emitting röntgen radiation with an energy of 4.7 KeV) in 0.1 M HCl was added to this sample at a concentration of 0.5 nM. This seawater was incubated under cloudy conditions (detailed information about irradiance can be found in Figure 2).

For both experiments sampling started in the dark, 1:45 am local time. Experiment I had to be stopped before dark because of a storm. Experiment II ended in the dark, 21:45 local time.

The choice of the concentrations of radio-isotopic iron used in the experiments was based on the detection limit of the gamma counter (3x3 Scionix NaI(Ti) crystal with a Tracor
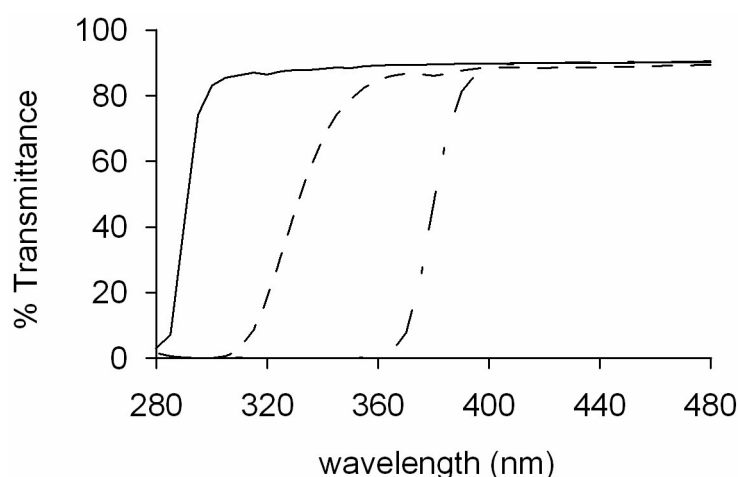
Figure 1. Transmittance spectra for UV transparent PMMA (—), the glass filter (- - -), and UV-opaque PMMA (— - —) in % transmittance.

Northern TN-7200 Pulse Height Analyser) on board of the ship and the liquid scintillation counter (Packard Tri-carb 2750 TR/LL liquid scintillation counter). For experiment I the isotope ^{59}Fe was used, thereby allowing measurement of the samples of the first experiment on board of the ship. For the second experiment, II, the isotope ^{55}Fe was used which made it possible to use a lower concentration Fe. These samples were measured after the cruise at the Interfaculty Reactor Institute, Delft University of Technology, The Netherlands.

The incubations were performed using acid cleaned 2 liter polymethylmethacrylate (PMMA) bottles and PMMA incubators (Steeneken et al., 1995). PMMA has a 50% light cut-off at 290 nm (Figure 1). The light conditions were accomplished using a glass filter with a 50% cut-off at 330 nm and a UV-opaque PMMA filter with a 50% cut-off at 380 nm (Figure 1). The wavelength regions as mentioned in this paper are defined by the experimental set-up. Consequently, UVB is the wavelength region 290-330 nm, UVA is 330-380 nm and VIS is 380-700 nm (Figure 1), although the definitions, as proposed by ISO International Standard (ISO/CD 21348), are UVB 280-315 nm, UVA 315-400 nm and VIS 400-700 nm.

The bottles were pre-equilibrated overnight with seawater. The incubation bottles were kept at a constant ambient temperature of 4°C using running seawater from the ship's pumping system.

2.2 Sampling and measurements

For the determination of Fe(II) concentrations an extracting column method described by King et al. (1991) modified by Fischer et al. (submitted) was used. In short, a SepPak®️ C-18 cartridge was preloaded with ferrozine (Acros). Samples were taken directly online from the PMMA bottles. Tygon tubing was connected to the PMMA bottle and with a

peristaltic pump 40 ml sample was pumped in 15 minutes (flow-rate of 2.7 ml min^{-1}) over the ferrozine loaded C-18 SepPak$^{®}$ cartridge (Waters). The Fe(II) fraction was retained as Fe(ferrozine)$_3$ complexes on the column.

The Fe(ferrozine)$_3$ complex was eluted from the C-18 SepPak$^{®}$ with 10 ml methanol (Baker, analytical grade) after rinsing the column with 5 ml 0.1 M NaCl (Baker, analytical grade)-0.005 M NaHCO$_3$ (Baker, analytical grade) (pH = 8) to remove the sea salts and make the samples ready for measurement.

2.3 Light measurements

UVB and UVA were measured by a non-scanning diode array spectroradiometer developed at the "Alfred Wegener Institute für Polar und Meeresforschung" (AWI) in Bremerhaven (Groß et al., 2001; Hanken and Tueg, 2002). The non-scanning diode array spectroradiometer was situated at the observatory deck above the bridge. VIS was measured using a LI-COR 192SA cosine quantum sensor. The LI-COR was situated near the experimental set up on the helicopter deck. Both instruments were calibrated separately.

2.4 Absorption spectra

Seawater samples were taken before the addition of radio-isotopic iron and frozen at -20°C. Prior to measurement the seawater samples were thawed at 4°C and left to warm up to room temperature. The samples were kept in a light tight bag throughout. The absorption spectra were taken using a Cary 300 UV-VIS double beam spectrophotometer (Varian) and a 10 cm quartz cuvet. 18.2 MΩ nanopure water was used as blank.

3. Results and discussion

3.1 Radio-isotopic Fe speciation

The concentration of dissolved iron was higher than the concentration of dissolved organic ligands (Table 1) in the seawater sampled inside the patch (Exp. I, 11th of November) (Boye et al., in press). This resulted in the saturation of the assemblage of organic Fe complexing ligands with iron. Considering the solubility of Fe(III) oxyhydroxides, which is 0.07 nM in seawater of 4°C (pH = 8, S = 36) (Liu and Millero, 1999), addition of radio-isotopic Fe(III) in concentrations above the solubility of Fe(III) oxyhydroxides resulted in the

Table 1. Data on the organic complexation of Fe (Boye, in preparation; Boye et al., in press) resembling the seawater as used during experiment I and II.

date	Out-/inside Fe enriched patch	Depth (m)	Dissolved [L] (nM)	Log K'	Dissolved [Fe] (nM)
11 November	Inside	20	1.61	22.34	2.62
25 November	Outside	50	0.86	21.74	0.11

formation of amorphous iron hydroxides. The difference in the concentration dissolved iron determined by Boye et al. (in press) (Table 1) and the seawater sample of experiment I is caused by variation of the dissolved Fe concentration in time and space within the iron enriched patch.

Complexation characteristics of the seawater sample used for experiment II (outside the iron enriched patch) were taken from data of 25 November (Boye, in preparation). The dissolved Fe concentration was 0.11 nM, much lower than the concentration iron of the seawater used in experiment II (0.85 nM). Comparing the concentration of dissolved ligands, 0.86 nM, with the concentration dissolved Fe of 0.85 nM led us to assume that the added radio-isotopic Fe(III) mainly formed amorphous iron hydroxides.

The time between the addition of the radio-isotopic iron and the first sampling in the dark was between 1.5 and 2 hours, sufficient time for the inorganic radio-isotopic iron to reach a steady state in the formation of amorphous iron hydroxides. Laboratory experiments in seawater show that with an addition of Fe(III) to seawater (50 nM) the formation of amorphous iron hydroxides reaches a steady state within 1.5 hours (see Chapter 5).

The radio-isotopic Fe could not reach equilibrium with "cold" (non-radioactive) Fe in the organic complexes before the first sampling time in the dark. Since the conditional stability constant of the assemblage of dissolved organic complexes is high (K' = 10^{22}, Table 1), the exchange between "cold" and radio-isotopic iron on the organic complex is depending on the dissociation rate constant (k_d) of the complex. Dissociation rate constants in the Northwest Atlantic and the Arabian sea for FeL complexes vary by a factor of 400 and range in value between 0.10 and 39.2 x 10^{-6} s^{-1} (Witter et al., 2000). Using the average of the values reported by (Witter et al., 2000), a value of k_d = 6.5 x 10^{-6} ± 10 x 10^{-6} s^{-1}, the half-life of dissolved inorganic iron (Fe') in seawater (Witter et al., 2000) can be calculated using the formula:

$$t_{1/2} = \frac{0.693}{k_d} \qquad (1)$$

T$_{1/2}$ is then 29.6 hours.

Assuming that all dissolved inorganic iron (radio-isotopic Fe and "cold" Fe) is equally available for exchange with ligand sites, it is the proportion of inorganic radio-isotopic Fe compared to inorganic "cold" Fe determining the increase of radio-isotopic FeL. The increase of radio-isotopic FeL in experiment I would then be $2.7 \cdot 10^{-6}$ nM s^{-1} ^{59}FeL and in experiment II $2.8 \cdot 10^{-6}$ nM s^{-1} ^{55}FeL.

It's not sure whether the radio-isotopic Fe(II) formed during the experiments originates from dissolved inorganic Fe, organically complexed iron or from both Fe species. Barbeau et al. (2001) observed photochemical reactions resulting in Fe(II) production involving Fe(III) bound to marine siderophores. Although certain siderophores may be photo-degradable (Barbeau et al., 2003), none of the depth profiles of Fe chelators reported thus far (Gledhill and van den Berg, 1994; Rue and Bruland, 1995; Wu and Luther, 1995) exhibited shallow mixed layer minima or any other features which would suggest a surface/photochemical sink (Moffett, 2001). It is known that inorganic Fe oxyhydroxides; e.g. ferrihydrite, goethite, lepidocrocite, hematite and amorphous iron hydroxides (Waite and Morel, 1984a; Wells and Mayer, 1991; Sulzberger and Laubscher, 1995) are photoreactive and participating in photolytic electron reactions with organic electron donors such as carboxylic acids, thiols, and alcohols (Stramel and Thomas, 1986; Waite et al., 1986; Cunningham et al., 1988; Siffert and Sulzberger, 1991). The nature of these organic molecules in the open ocean is not known, but they can be dissolved humic matter containing Fe binding functional groups, the remains of cell lysis or siderophores.

Processes resulting in the reduction of the added radio-isotopic Fe which formed amorphous iron hydroxides containing organic electron donors were probably direct ligand-to-metal charge transfer (Waite and Morel, 1984b) and reduction by secondary photolysis products as the photo-produced superoxide radical (Voelker and Sedlak, 1995).

3.2 The diel cycle of Fe(II) production

A distinct diel cycle of Fe(II) production was obtained in open Antarctic ocean water for both experiments (Figure 2 a, b). The concentration Fe(II) is strongly dependent on light intensity with the maximum concentration observed at peak light intensity. The diel cycle, although clearly present under all spectral conditions, was more pronounced when UVB and UVA were included in the offered light spectrum. These findings are in line with those of Emmenegger et al. (2001) for Swiss mountain lake waters. Diel cycles showing the photoreactivity of iron in seawater (Hong and Kester, 1986; Waite et al., 1995), in mineral particles suspended in the atmosphere (Zhu et al., 1997) and in lakes and streams (McMahon, 1969; Kimball et al., 1992; Emmenegger et al., 2001) have been observed before. No studies
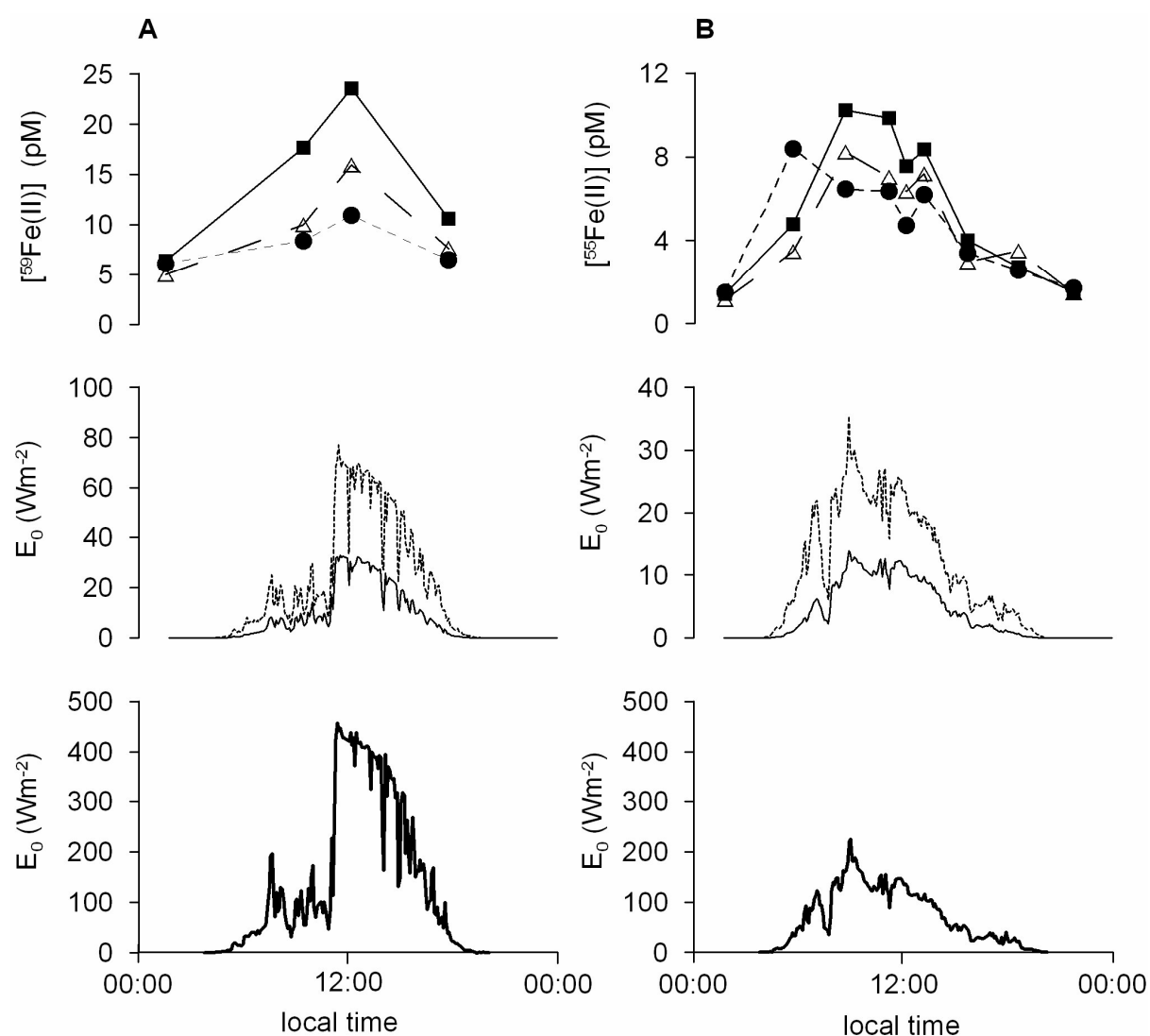
Figure 2. The diel cycle for the concentration radio-isotopic Fe(II) (pM) under three different light conditions, UVB+UVA+VIS (■), UVA+VIS (Δ) and VIS (●) and the light intensities (W m^{-2}) of UVB (x10) (—), UVA (…) and VIS (–). (A) experiment I, (B) experiment II. Experiment I, sunrise was at ~ 5:05 am and sunset at ~ 19:25 local time, 12th of November 2000. Experiment II, sunrise was at ~ 4:45 am and sunset at ~ 20:05 local time, 26th of November 2000.

have been performed using different wavelength ranges to study the result of natural UVB and UVA irradiance on the diel cycle of Fe(II) production in open oceanic waters.

3.3 The linear relationship between the radio-isotopic Fe(II) concentration and irradiance

A clear linear relationship consisted between Fe(II) concentrations and the light intensities of the different light spectra offered (Figure 3 a, b and c) although, the data points

54
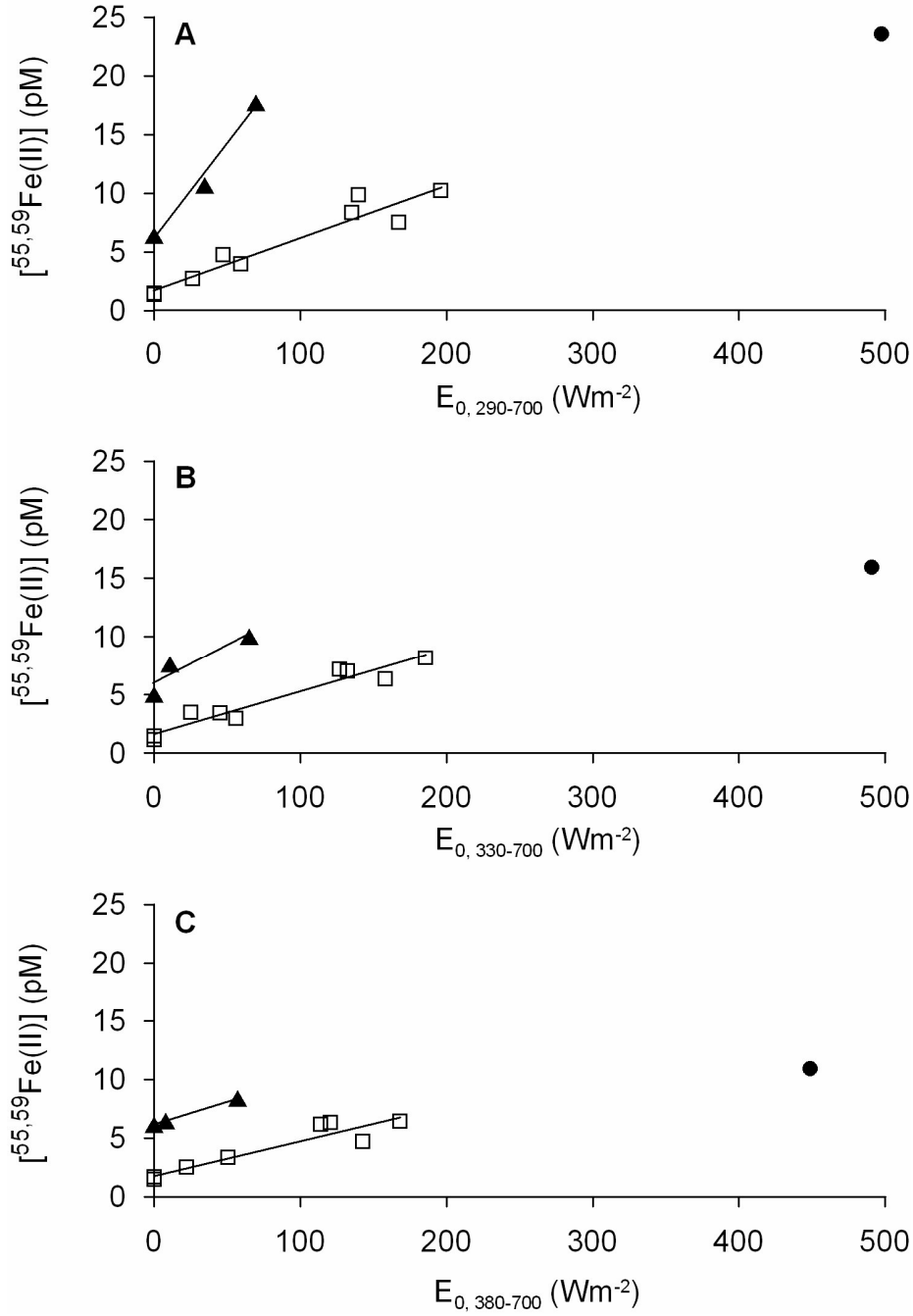
Figure 3. The concentration ^{59}Fe(II) (pM) for experiment I ($\triangle$), experiment I zenith hour ($\bullet$) and the concentration ^{55}Fe(II) (pM) for experiment II ($\square$) versus irradiance (W m^{-2}): (A) the radio-isotopic Fe(II) concentration due to UVB+UVA+VIS versus the irradiance between 290-700 nm (Exp. I: y = 0.16 x + 5.93, R^2_I = 0.981; Exp. II: y = 0.045 x + 1.78, R^2_{II} = 0.919), (b.) the radio-isotopic Fe(II) concentration due to UVA+VIS versus the irradiance between 330-700 nm (Exp. I: y = 0.066 x + 5.88, R^2_I = 0.850; Exp. II: y = 0.036 x + 1.68, R^2_{II} = 0.929), and (c.) the Fe(II) concentration due to VIS versus the irradiance between 380-700 nm (Exp. I: y = 0.039 x + 6.16, R^2_I = 1.00; Exp. II: y = 0.029 x + 1.86, R^2_{II} = 0.873).

at Zenith hour of experiment I do not fit this linear relationship. Several reasons are proposed to explain the non-linearity at that high light intensity. It could be caused by a counter reaction, e.g. increasing hydrogen peroxide levels, due to the sudden transition from low-light to high-light conditions before noon, or by a limiting reactant.

The concentration Fe(II) as determined is the result of competing kinetics of reduction and oxidation. Light is, directly or indirectly, important for the reduction of Fe. A photo-induced increase in the concentration of hydrogen peroxide would cause an increase in the oxidation rate causing thus a net decrease in Fe(II) production. The last data-points of the three light conditions of experiment I clearly fit the linear relationship (Figure 3 a, b, c). This suggests that the hydrogen peroxide concentration decreases with decreasing irradiance. However, although photochemical production rates of H_2O_2 determined in the Atlantic Ocean and Antarctic waters ranged between 2.1 and 9.6 nM h^{-1} (Obernosterer, 2000; Yocis et al., 2000; Yuan and Shiller, 2001; Gerringa et al., 2004 and Chapter 2), H_2O_2 concentrations will not decrease until after sunset (Plane et al., 1987; Johnson et al., 1989). Furthermore, the linearity of the Fe(II) concentrations versus the irradiance itself seems to predict that the oxidation process remains constant during the experiments.

The sudden transition from low-light to high-light conditions, 1 hour before noon (Figure 2 a), cannot explain the lower than expected Fe(II) concentration with regard to the linear relation between concentration Fe(II) and irradiance. A laboratory experiment showed an initial photo-production rate of Fe(II) of 1.83 nM s^{-1}. This photo-production rate resulted from an addition of 10 nM Fe(III), 12 hours before the start of the experiment, forming amorphous iron hydroxides in Southern Ocean seawater (pH = 8, 4°C, 0.352 W/m^2 UVB, 2.15 W/m^2 UVA and 1.93 W/m^2 VIS). This rate of Fe(II) production in combination with a half-life of ~ 90 minutes for the oxidation of Fe(II) (pH of 8, ~ 4°C) (Croot and Laan, 2002) reveals that an hour is enough time for the Fe redox cycle to adapt to higher light conditions.

Another explanation is a limited amount of a chromophoric iron species. Fe photoreduction, during a diel cycle, limited by available chromophoric iron species has been observed before in an acidic stream (Kimball et al., 1992). Similarly, Wells and Mayer (1991) found that the photoconversion rates diminished with continued irradiation when ferrihydrite was irradiated. Waite and Morel (1984c) found the same decrease in the photodissolution rate of lepidocrocite, even with an excess of the chromophore citrate indicating that other factors than organic chromophores influenced this process. Wells and Mayer (1991) suggested a number of possible reasons for the decreasing photolysis rate with time: i) photolysis could become inhibited if residues from the photo-oxidation of chromophores accumulated on colloid surfaces over time, thereby influencing active sites against further photoreaction, ii) the retention of photoreduced Fe(II) at the surface, or the rapid resorption of the re-oxidized Fe(III) species back onto the original surface. In either case, a shell of rapid-cycling Fe might
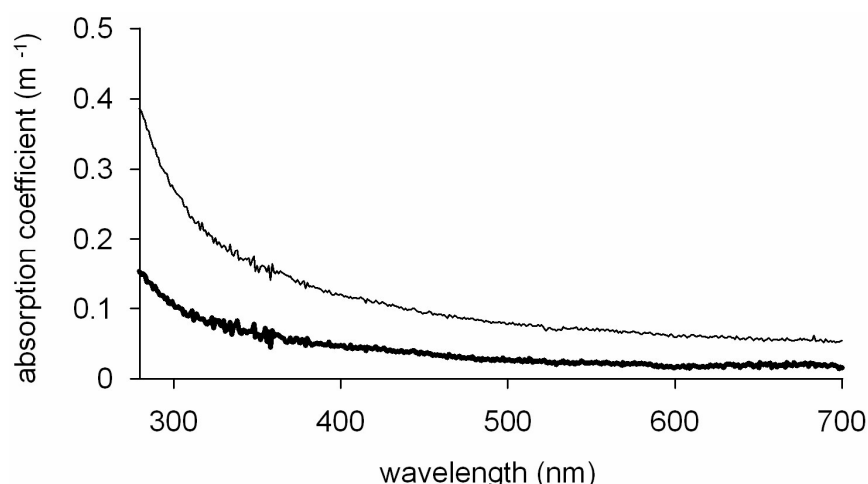
Figure 4. Absorption spectra of the seawater used for experiment I (——) and experiment II (━━).

form on the oxyhydroxide surface upon prolonged photolysis, iii) progressive photochemical alterations of the oxyhydroxide surface would decrease its charge trapping efficiency. Possibly that these processes limit the amount of available chromophoric iron species for photoreduction. Furthermore, indirect photo-induced reduction of Fe could be limited by a limited superoxide production due to low concentrations of CDOM (Micinski et al., 1993) in the Southern Ocean seawater. The CDOM concentrations, shown as absorption coefficients at 375 nm, are 0.14 m^{-1} for the seawater (inside patch) used in experiment I and 0.05 m^{-1} for the seawater (outside patch) used in experiment II (Figure 4). The absorption coefficients fall within the low range (0.05-0.3 m^{-1} at 375 nm) found for oceanic waters (Bricaud et al., 1981). Possibly a concentration CDOM as low as found in the Southern Ocean seawater used for these experiments limits the formation of photo-produced superoxide. If the direct and/or indirect photoreduction of the Fe is limited by the presence of chromophoric Fe species and/or the Fe reducing superoxide, it results in a concentration Fe(II) at noon which is non-linear with regard to the linear relation between concentration Fe(II) and irradiance.

3.4 Wavelength range dependent photoreduction of Fe

The quantum yield of the Fe(II) production (mole product/ mole photons absorbed) could not be determined because we have no knowledge of the nature, concentrations and molar absorption coefficients of the reactive Fe(III) species. So, to investigate the influence of UVB, UVA and VIS wavelength regions on the photoreduction of iron, the difference in Fe(II) concentration for each sample point in time between the data resulting from incubations receiving different wavelength regions was determined, according to:

$$\Delta[Fe(II)]_{UVB} = [Fe(II)]_{UVB+UVA+VIS} - [Fe(II)]_{UVA+VIS} \qquad (2)$$

$$\Delta[Fe(II)]_{UVA} = [Fe(II)]_{UVA+VIS} - [Fe(II)]_{VIS} \qquad (3)$$

$$\Delta[Fe(II)]_{VIS} = [Fe(II)]_{VIS} - [Fe(II)]_{VIS,\text{ first point in the dark}} \qquad (4)$$

and displayed against the irradiance of the responsible wavelength region (Figure 5 a, b, c). This treatment of the data resulted in some negative values for the difference in radio-isotopic Fe(II) concentration between two different light treatments (Figure 5 a, b, c). These negative values are generated by variation in the radio-isotopic Fe(II) concentration possibly caused by differences in Fe speciation between the three light treatments and by variation in the analytical method. For example, the first point sampled in the dark, a condition similar for the three light treatments, resulted in an average radio-isotopic Fe(II) concentration of 5.85 ± 0.74 pM for experiment I and 1.36 ± 0.18 pM for experiment II.

There are a number of possible reasons why the photo-production of Fe(II) per Wm^{-2} in experiment I was higher than in experiment II (Figure 5, a, b, c, Table 2). Firstly, the concentration radio-isotopic iron was higher in experiment I possibly resulting in a higher concentration of photo-reactive iron. Secondly, the CDOM concentration in experiment I (inside the iron enriched patch) was higher than in the seawater of experiment II (outside the iron enriched patch). CDOM plays a central and yet poorly understood role in the light-induced production of Fe(II) in surface waters (Emmenegger et al., 2001), either by providing photo-sensitive iron binding organic compounds to form photo-reactive iron complexes (Kuma, 1992) or by acting as a source of superoxide (Micinski et al., 1993). Micinski et al. (1993) found that the production of superoxide is proportional to the absorption coefficient at 300 nm of seawater containing terrestrially derived coloured organic matter. The absorbance of the seawater at 300 nm used in Experiment I was 2.6 times the absorbance of the seawater at 300 nm in experiment II (Figure 4). This implies that, when applied to total oceanic CDOM, more superoxide was produced in experiment I, reducing more Fe.

Table 2. The capability of UVB, UVA and VIS to photo-produce radio-isotopic Fe(II) (pM ^{55,59}Fe(II)/ Wm^{-2}).

Light range	Experiment I		Experiment II	
	pM ^{59}Fe(II)/ Wm^{-2}	R^2	pM ^{55}Fe(II)/ Wm^{-2}	R^2
UVB	4.89	0.999	0.69	0.505
UVA	0.33	0.770	0.10	0.689
VIS	0.04	0.844	0.03	0.873
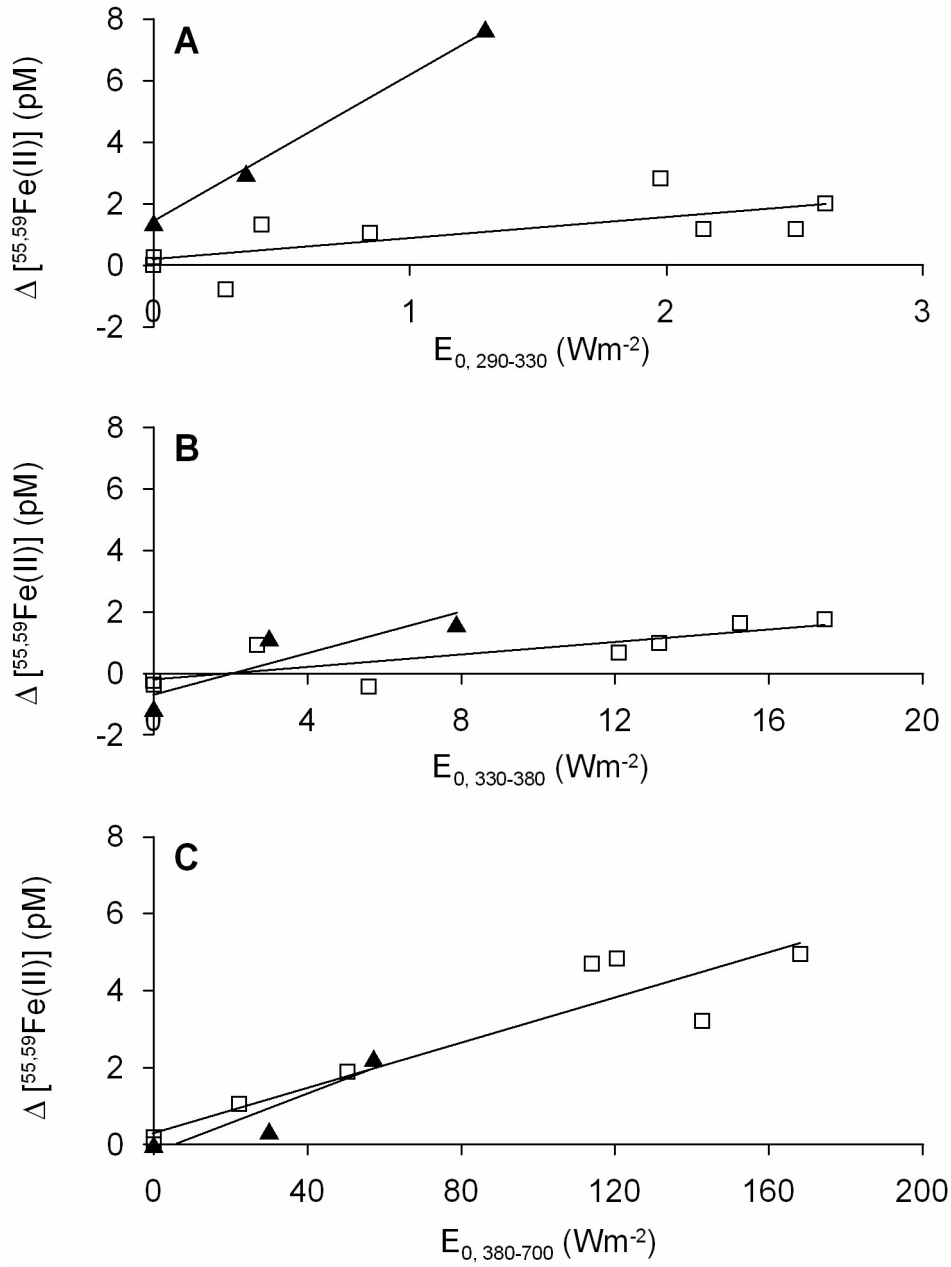
Figure 5. The concentration radio-isotopic Fe(II) (pM) produced due to UVB, UVA and VIS versus irradiance (W m^{-2}), during experiment I ($\triangle$) and experiment II ($\square$): (A) $\Delta[^{55,59}Fe(II)]_{UVB}$ ($[^{55,59}Fe(II)]_{UVB+UVA+VIS} - [^{55,59}Fe(II)]_{UVA+VIS}$) versus UVB irradiance (Exp. I: y = 4.89 x + 1.32, R^2_I = 0.999; Exp. II: y = 0.69 x + 0.18, R^2_{II} = 0.505), (B) $\Delta[^{55,59}Fe(II)]_{UVA}$ ($[^{55,59}Fe(II)]_{UVA+VIS} - [^{55,59}Fe(II)]_{VIS}$) versus UVA irradiance (Exp. I: y = 0.33 x − 0.63, R^2_I = 0.770; Exp. II: y = 0.10 x − 0.23, R^2_{II} = 0.689), and (C) $\Delta[^{55,59}Fe(II)]_{VIS}$ ($[^{55,59}Fe(II)]_{VIS} - [^{55,59}Fe(II)]_{VIS, \text{first point in the dark}}$) versus VIS irradiance (Exp. I: y = 0.04 x − 0.26, R^2_I = 0.844; Exp. II y = 0.03 x + 0.35, R^2_{II} = 0.873).

4. Summary and conclusions

Incubations of open ocean seawater showed a distinct diel cycle in iron photoreduction under the three different light conditions. Fe(II) production was highest for the incubation receiving the full solar spectrum, followed by the full solar spectrum minus UVB and the full solar spectrum minus UVB and UVA respectively. UVB is clearly responsible for the highest concentrations of Fe(II).

These results indicate that UV has a very important role in the chemical speciation of iron in seawater. Wells and Mayer (1991), Johnson et al. (1994) and Miller and Kester (1994) already reported that the redox-cycle of iron induced by light formed a more reactive species of iron.

Our experiments show that the UV part of the solar spectrum plays a major role in the photoreduction of iron, suggesting that any increases in UV could induce the formation of Fe(II) resulting after oxidation in a more reactive iron species. In turn this will increase the retention time and the bioavailability of iron in the euphotic zone during springtime when the Southern Ocean is subject to ozone depletion. This might be especially important when fresh iron is added in large quantities to the ocean, e.g. during a dust event. Moreover, it might influence the reactions taking place after an artificial iron enrichment experiment as EisenEx.

Acknowledgements

References

Barbeau, K., Rue, E.L., Bruland, K.W. and Butler, A., 2001. Photochemical cycling of iron in the surface ocean mediated by microbial iron(III)-binding ligands. Nature, 413(6854): 409-413.

Barbeau, K., Rue, E.L., Trick, C.G., Bruland, K.T. and Butler, A., 2003. Photochemical reactivity of siderophores produced by marine heterotrophic bacteria and cyanobacteria based on characteristic Fe(III) binding groups. Limnol. Oceanogr., 48(3): 1069-1078.

Boye, M., in preparation. Colloidal iron accounts for a significant portion of dissolved organic iron-complexes in the Southern Ocean.

Boye, M., Nishioka, J., Croot, P.L., Laan, P., Timmermans, K.R. and de Baar, H.J.W., in press. Major deviations of iron complexation during 22 days of a mesoscale iron enrichment in the open Southern Ocean. Mar. Chem.

Bricaud, A., Morel, A. and Prieur, L., 1981. Absorption by dissolved organic matter of the sea (yellow substance) in the UV and visible domains. Limnol. Oceanogr, 26(1): 43-53.

Buma, A.G.J., de Boer, M.K. and Boelen, P., 2001. Depth distributions of DNA damage in Antarctic marine phyto- and bacterioplankton exposed to summertime UV radiation. J. Phycol., 37(2): 200-208.

Buma, A.G.J., van Hannen, E.J., Veldhuis, M.J.W. and Gieskes, W.W.C., 1996. UV-B induces DNA damage and DNA synthesis delay in the marine diatom *Cyclotella* sp. Sci. Mar., 60: 101-106.

Croot, P.L., Bowie, A.R., Frew, R.D., Maldonado, M.T., Hall, J.A., Safi, K.A., la Roche, J., Boyd, P.W. and Law, C.S., 2001. Retention of dissolved iron and Fe-II in an iron induced Southern Ocean phytoplankton bloom. Geophys. Res. Lett., 28(18): 3425-3428.

Croot, P.L. and Laan, P., 2002. Continuous shipboard determination of Fe(II) in polar waters using flow injection analysis with chemiluminescence detection. Anal. Chim. Acta, 466(2): 261-273.

Cunningham, K.M., Goldberg, M.C. and Weiner, E.R., 1988. Mechanisms for aquaeos photolysis of adsorbed benzoate, oxalate, and succinate on iron oxyhydroxide (goethite) surfaces. Environ. Sci. Technol., 22(9): 1090-1097.

de Baar, H.J.W., Buma, A.G.J., Nolting, R.F., Cadee, G.C., Jacques, G. and Treguer, P.J., 1990. On iron limitation of the Southern Ocean - experimental- observations in the Weddell and Scotia seas. Mar. Ecol. Progr. Ser., 65(2): 105-122.

Emmenegger, L., Schonenberger, R.R., Sigg, L. and Sulzberger, B., 2001. Light-induced redox cycling of iron in circumneutral lakes. Limnol. Oceanogr., 46(1): 49-61.

Fischer, A.C., Wolterbeek, H.T., Kroon, J.J., Gerringa, L.J.A. and van Elteren, J.T., submitted. The use of radio-isotopes to study the kinetics of iron speciation in seawater.

Frederick, J.E. and Snell, H.E., 1988. Ultraviolet-radiation levels during the Antarctic spring. Science, 241(4864): 438-440.

Gerringa, L.J.A., Rijkenberg, M.J.A., Timmermans, K.R. and Buma, A.G.J., 2004. The influence of solar ultraviolet radiation on the photochemical production of H_2O_2 in the equatorial Atlantic Ocean. J. Sea Res., 51(1): 3-10.

Gervais, F., Riebesell, U. and Gorbunov, M.Y., 2002. Changes in primary productivity and chlorophyll a in response to iron fertilization in the Southern Polar Frontal Zone. Limnol. Oceanogr., 47(5): 1324-1335.

Gledhill, M. and van den Berg, C.M.G., 1994. Determination of complexation of iron(III) with natural organic complexing ligands in seawater using cathodic stripping voltammetry. Mar. Chem., 47(1): 41-54.

Groß, C., Tüg, H. and Schrems, O., 2001. Three Years Spectral Resolved UV-Measurements at Koldewey-Station (1997 - 1999). Memoirs of National Institute of Polar Research, 54(113-123).

Hanken, T. and Tueg, H., 2002. Development of a multichannel UV-spectroradiometer for field measurements. Environ. Sci. Pol. Res., 4(35-39).

Hartmann, C., Richter, K.-U. and Harms, C., 2001. Distribution of nutrients during the iron experiment. Report on Polar and Marine Research., 400: 186-190.

Hong, H. and Kester, D.R., 1986. Redox state of iron in the offshore waters of Peru. Limnol. Oceanogr., 31: 512-524.

Johnson, K.S., Coale, K.H., Elrod, V.A. and Tindale, N.W., 1994. Iron photochemistry in seawater from the equatorial Pacific. Mar. Chem., 46(4): 319-334.

Johnson, K.S., Willason, S.W., Wiesenburg, D.A., Lohrenz, S.E. and Arnone, R.A., 1989. Hydrogen peroxide in the western Mediterranean Sea - a tracer for vertical advection. Deep Sea Res. I, 36(2): 241-254.

Karentz, D. and Lutze, L.H., 1990. Evaluation of biologically harmful ultraviolet-radiation in Antarctica with a biological dosimeter designed for aquatic environments. Limnol. Oceanogr., 35(3): 549-561.

Kimball, B.A., McKnight, D.M., Wetherbee, G.A. and Harnish, R.A., 1992. Mechanisms of iron photoreduction in a metal-rich, acidic stream (St-Kevin Gulch, Colorado, USA). Chem. Geol., 96(1-2): 227-239.

King, D.W., 1998. Role of carbonate speciation on the oxidation rate of Fe(II) in aquatic systems. Environ. Sci. Technol., 32(19): 2997-3003.

King, D.W., Lin, J. and Kester, D.R., 1991. Spectrophotometric determination of iron(II) in seawater at nanomolar concentrations. Anal. Chim. Acta, 247(1): 125-132.

King, D.W., Lounsbury, H.A. and Millero, F.J., 1995. Rates and mechanism of Fe(II) oxidation at nanomolar total iron concentrations. Environ. Sci. Technol., 29(3): 818-824.

Kuma, K., Nakabayashi, S., Suzuki, Y., Kudo, I. and Matsunaga, K., 1992. Photo-reduction of Fe (III) by dissolved organic-substances and existence of Fe (II) in seawater during spring blooms. Mar. Chem., 37(1-2): 15-27.

Kuma, K., Nakabayashi, S., Suzuki, Y., Kudo, I., Matsunaga, K., 1992. Photo-reduction of Fe(II) by dissolved organic substances and existence of Fe(II) in seawater during spring blooms. Mar. Chem., 37: 15-27.

Kuma, K., Nishioka, J. and Matsunaga, K., 1996. Controls on iron(III) hydroxide solubility in seawater: The influence of pH and natural organic chelators. Limnol. Oceanogr., 41(3): 396-407.

Lesser, M.P., Neale, P.J. and Cullen, J.J., 1996. Acclimation of Antarctic phytoplankton to ultraviolet radiation: Ultraviolet-absorbing compounds and carbon fixation. Mol. Mar. Biol. Biotechnol., 5(4): 314-325.

Liu, X.W. and Millero, F.J., 1999. The solubility of iron hydroxide in sodium chloride solutions. Geochim. Cosmochim. Acta, 63(19-20): 3487-3497.

Liu, X.W. and Millero, F.J., 2002. The solubility of iron in seawater. Mar. Chem., 77(1): 43-54.

Martin, J.H., Gordon, R.M. and Fitzwater, S.E., 1990. Iron in Antarctic waters. Nature, 345(6271): 156-158.

McMahon, J.W., 1969. The annual and diurnal variation in the vertical distribution of acid-soluble ferrous and total iron in a small dimictic lake. Limnol. Oceanogr., 14: 357-367.

Micinski, E., Ball, L.A. and Zafiriou, O.C., 1993. Photochemical oxygen activation - superoxide radical detection and production-rates in the eastern Caribbean. J. Geophys. Res.-Oceans, 98(C2): 2299-2306.

Miller, W.L. and Kester, D., 1994. Photochemical iron reduction and iron bioavailability in seawater. J. Mar. Res., 52: 325-343.

Millero, F.J., 1998. Solubility of Fe(III) in seawater. Earth. Planet. Sci. Let., 154(1-4): 323-329.

Millero, F.J. and Izaguirre, M., 1989. Effect of ionic-strength and ionic interactions on the oxidation of Fe(II). J. Solut. Chem., 18(6): 585-599.

Millero, F.J. and Sotolongo, S., 1989. The oxidation of Fe(II) with H_2O_2 in seawater. Geochim. Cosmochim. Acta, 53(8): 1867-1873.

Millero, F.J., Sotolongo, S. and Izaguirre, M., 1987. The oxidation-kinetics of Fe(II) in seawater. Geochim. Cosmochim. Acta, 51(4): 793-801.

Mitchell, B.G., Brody, E.A., Holmhansen, O., McClain, C. and Bishop, J., 1991. Light limitation of phytoplankton biomass and macronutrient utilization in the Southern Ocean. Limnol. Oceanogr., 36(8): 1662-1677.

Moffett, J.W., 2001. Transformations among different forms of iron in the ocean. In: D.R. Turner and K.A. Hunter (Editors), The Biogeochemistry of Iron in Seawater. IUPAC series on analytical and physical chemistry of environmental systems. John Wiley & Sons, LTD, New York, pp. 343-372.

Neale, P.J., Davis, R.F. and Cullen, J.J., 1998. Interactive effects of ozone depletion and vertical mixing on photosynthesis of Antarctic phytoplankton. Nature, 392(6676): 585-589.

Nelson, D.M. and Smith, W.O., 1991. Sverdrup revisited - critical depths, maximum chlorophyll levels, and the control of Southern Ocean productivity by the irradiance-mixing regime. Limnol. Oceanogr., 36(8): 1650-1661.

O'Sullivan, D.W., Hanson, A.K., Miller, W.L. and Kester, D.R., 1991. Measurement of Fe(II) in surface-water of the equatorial Pacific. Limnol. Oceanogr., 36(8): 1727-1741.

Obernosterer, I.B., 2000. Photochemical transformations of dissolved organic matter and its subsequent utilization by marine bacterioplankton. PhD Thesis, University of Groningen, The Netherlands, 133 pp.

Parsons, T.R., Stephens, K., Strickland, J.D.H., 1961. On the chemical composition of eleven species of marine phytoplankters. J. Fish. Res. Board Chan, 18: 1001-1016.

Plane, J.M.C., Zika, R.G., Zepp, R.G. and Burns, L.A., 1987. Photochemical modeling applied to natural waters. In: R.G. Zika and W.J. Cooper (Editors), Photochemistry of environmental aquatic systems. American Chemical Society Group, Washington D.C., pp. 250-267.

Rich, H.W. and Morel, F.M.M., 1990. Availability of well-defined iron colloids to the marine diatom *Thalassiosira weissflogii*. Limnol. Oceanogr., 35(3): 652-662.

Rue, E.L. and Bruland, K.W., 1995. Complexation of iron(III) by natural organic-ligands in the central north Pacific as determined by a new competitive ligand equilibration adsorptive cathodic stripping voltammetric method. Mar. Chem., 50(1-4): 117-138.

Schofield, O., Kroon, B.M.A., Prezelin, B.B., 1995. Impact of ultraviolet-B radiation on photosystem II activity and its relation to the inhibition of carbon fixation rates for Antarctic ice algea communities. J. Phycol., 31: 703-715.

Siffert, C. and Sulzberger, B., 1991. Light-induced dissolution of hematite in the presence of oxalate - a case-study. Langmuir, 7(8): 1627-1634.

Smith, R.C., Prezelin, B.B., Baker, K.S., Bidigare, R.R., Boucher, N.P., Coley, T., Karentz, D., Macintyre, S., Matlick, H.A., Menzies, D., Ondrusek, M., Wan, Z. and Waters, K.J., 1992.

Ozone depletion - ultraviolet radiation and phytoplankton biology in Antarctic waters. Science, 255(5047): 952-959.

Solomon, S., 1990. Progress towards a quantitative understanding of Antarctic ozone depletion. Nature, 347(6291): 347-354.

Steeneken, S.F., Buma, A.G.J. and Gieskes, W.W.C., 1995. Changes in transmission characteristics of polymethylmethacrylate and cellulose-(III) acetate during exposure to ultraviolet-light. Photochem. Photobiol., 61(3): 276-280.

Stramel, R.D. and Thomas, J.K., 1986. Photochemistry of iron-oxide colloids. J. Colloid Interface Sci., 110(1): 121-129.

Strass, V.H., Leach, H., Cisewski, B., Gonzalez, S., Post, J., da Silva Duarte, V. and Trumm, F., 2001. The physical setting of the Southern Ocean iron fertilisation experiment. Reports on Polar and Marine Research, 400: 94-130.

Sulzberger, B. and Laubscher, H., 1995. Reactivity of various types of iron(III) (hydr)oxides towards light-induced dissolution. Mar. Chem., 50(1-4): 103-115.

Takeda, S. and Kamatani, A., 1989. Photoreduction of Fe(III)-EDTA complex and its availability to the coastal diatom *Thalassiosira weissflogii*. Red Tides: Biol., Environ. Sci., Toxicol.: 349-352.

van den Berg, C.M.G., 1995. Evidence for organic complexation of iron in seawater. Mar. Chem., 50(1-4): 139-157.

Voelker, B.M. and Sedlak, D.L., 1995. Iron reduction by photoproduced superoxide in seawater. Mar. Chem., 50(1-4): 93-102.

Waite, D.T. and Morel, F.M.M., 1984a. Photoreductive dissolution of colloidal iron oxides in natural waters. Environ. Sci. Technol., 18: 860-868.

Waite, T.D. and Morel, F.M.M., 1984b. Ligand-exchange and fluorescence quenching studies of the fulvic acid-iron interaction - effects of pH and light. Anal. Chim. Acta, 162(AUG): 263-274.

Waite, T.D. and Morel, F.M.M., 1984c. Photoreductive dissolution of colloidal iron-oxide - effect of citrate. J. Colloid Interface Sci., 102(1): 121-137.

Waite, T.D., Szymczak, R., Espey, Q.I. and Furnas, M.J., 1995. Diel variations in iron speciation in northern Australian shelf waters. Mar. Chem., 50(1-4): 79-91.

Waite, T.D., Torikov, A. and Smith, J.D., 1986. Photoassisted dissolution of colloidal iron-oxides by thiol- containing compounds.1. Dissolution of hematite (alpha-Fe_2O_3). J. Colloid Interface Sci., 112(2): 412-420.

Wells, M.L. and Mayer, L.M., 1991. The photoconversion of colloidal iron oxyhydroxides in seawater. Deep Sea Res. I, 38(11): 1379-1395.

Wells, M.L., Mayer, L.M., Donard, O.F.X., Sierra, M.M.D. and Ackelson, S.G., 1991. The photolysis of colloidal iron in the oceans. Nature, 353(6341): 248-250.

Witter, A.E., Hutchins, D.A., Butler, A. and Luther, G.W., 2000. Determination of conditional stability constants and kinetic constants for strong model Fe-binding ligands in seawater. Mar. Chem., 69(1-2): 1-17.

Witter, A.E., Lewis, B.L. and Luther, G.W., 2000. Iron speciation in the Arabian Sea. Deep Sea Res. II, 47(7-8): 1517-1539.

Wu, J.F. and Luther, G.W., 1995. Complexation of Fe(III) by natural organic-ligands in the northwest Atlantic Ocean by a competitive ligand equilibration method and a kinetic approach. Mar. Chem., 50(1-4): 159-177.

Yocis, B.H., Kieber, D.J. and Mopper, K., 2000. Photochemical production of hydrogen peroxide in Antarctic waters. Deep Sea Res. I, 47(6): 1077-1099.

Yuan, J.C. and Shiller, A.M., 2001. The distribution of hydrogen peroxide in the Southern and central Atlantic Ocean. Deep Sea Res. II, 48(13): 2947-2970.

Zhu, X.R., Prospero, J.M. and Millero, F.J., 1997. Diel variability of soluble Fe(II) and soluble total Fe in North African dust in the trade winds at Barbados. J. Geophys. Res.-Atmos., 102(D17): 21297-21305.

Chapter 4

UVA variability overrules UVB ozone depletion effects on the photoreduction of iron in the Southern Ocean

Micha, J.A. Rijkenberg, Loes J.A. Gerringa, Patrick J. Neale, Klaas R. Timmermans, Anita G.J. Buma, Hein J.W. de Baar

Abstract

A spectral weighting function describing the wavelength dependency of the photo-production of Fe(II) in Antarctic seawater was established. The strong wavelength-dependent photo-production of Fe(II) from amorphous ferric hydroxides can be described as an exponential function: $\varepsilon(\lambda) = 3.57 \cdot 10^3 \cdot e^{-0.02(\lambda-300)}$. Solar spectra recorded during the 2000 Antarctic ozone depletion season were used to demonstrate that daily and seasonal variability of the ultraviolet A (UVA: 315-400 nm) and the visible part of the light spectrum (VIS: 400-700 nm) dominates Fe(II) production rates in surface waters (respectively >60% and about 30%) and in the water column. Although ultraviolet B (UVB: 280-315 nm) is the most effective wavelength region for Fe(II) photo-production, the impact of UVB was small due to the relatively low flux of UVB into the ocean surface waters. However, the impact of UVB did indeed increase significantly from 3.54 to 6.15 % during the austral ozone minimum.

1. Introduction

The Southern Ocean plays an important role in controlling the CO_2 concentration in the atmosphere (Hoppema et al., 1999). Here biological fixation of CO_2 by phytoplankton in surface waters exceeds the expected outgassing of CO_2-rich upwelling waters (de Baar and Boyd, 2000). However, extremely low iron (Fe) concentrations (de Baar et al., 1990; Martin et al., 1990) in concert with factors such as light and grazing (de Baar et al., 1999; de Baar and Boyd, 2000) regulate primary production, species composition (Buma et al., 1991) and carbon cycling within Southern Ocean planktonic communities. Various lines of evidence stress the great importance of the Fe(II) versus Fe(III) colloids oxidation/photoreduction cycle as the key process for keeping Fe available for uptake by plankton cells (Wells et al., 1991; Johnson et al., 1994).

Effects of spectral changes on biological or chemical processes can be predicted by a spectral weighting function (Neale et al., 1998), a set of coefficients that, by multiplication

with the energy of a discrete wavelength reveals its biological or chemical effect (here photo-production of Fe(II)). Natural variations and anthropogenic perturbations of incoming solar irradiance (most importantly in the UV spectrum) play an important role in the plankton ecosystem of the Southern Ocean, as already shown using weighting functions for inhibition of photosynthesis (Neale et al., 1998) and DNA damage (Karentz, 1994).

In this study we established a spectral weighting function for Fe(II) photo-production in the Southern Ocean. This allows prediction of the impact on Fe(II) photoreduction of natural variability of irradiance, as well as the anthropogenic effect of increased levels of UVB due to springtime stratospheric ozone depletion. Freshly formed colloidal iron was the substrate, serving as the best possible simulation of colloidal iron formed upon an aeolian wet deposition dust event (Hanson et al., 2001; Jickells and Spokes, 2001), after the supply of iron by melting sea-ice (Sedwick and DiTullio, 1997) or during an *in situ* Fe enrichment experiment (Nishioka et al., in press).

2. Experimental procedures

2.1 Experimental

Southern Ocean surface seawater (44ºS 20º E, 30th November 2000) (0.2 μm filtered) for the irradiation experiments was collected in an acid-cleaned tank (1 m^3) by means of an acid-washed braided PVS tubing attached to a torpedo towed alongside the ship (Polarstern, ANTXVIII/2). The tank was stored at room temperature for about a year.

The 1 liter, UV transparent, polymethylmetacrylate (PMMA) bottles were pre-equilibrated with Southern Ocean seawater containing 10 nM Fe(III) (ammonium Fe(III) sulfate, Baker Analyzed, reagent grade). For each optical treatment a new PMMA bottle was prepared. The experiments were performed in a temperature controlled (4°C) class 100 clean container. The pH of the samples was 8.053 ± 0.051. The seawater was stirred with a Teflon stirring bean.

2.2 Fe in Southern Ocean seawater

Fresh colloidal iron was prepared by the addition of 10 nM Fe(III) to the seawater followed by overnight equilibration (12 hours, 4°C). Measurement of Fe, labile to 2-(2-Thiazolylazo)-p-cresol (Croot and Johansson, 2000), after a 50 nM Fe(III) addition showed that Fe colloid formation reached equilibrium within 2-3 hours.

The seawater contained 1.1 nM dissolved Fe and 1.75 ± 0.28 equivalents of nM Fe of natural ligands with a conditional stability constant of $10^{21.75} \pm 10^{0.34}$. The excellent linear relationship between the initial Fe(II) photo-production rate and the addition of three different

concentrations Fe(III) in the range 10-20 nM (R^2 = 0.999) showed that aging of Fe colloids did not play a substantial role in the Fe(II) photo-production. The inability to destruct the Fe binding ligands with UV suggested that the natural ligands in the seawater were hardly photoreactive.

2.3 Light

Philips UVB (TL-12), UVA (TL' 40W/05), VIS (TL'D 36W/33) lamps and 7 Schott optical cut-off filters (WG280, WG295, WG305, WG320, WG335, WG345 and WG360 nm) were used to create different optical treatments. Spectral conditions were measured for every treatment using a MACAM Spectroradiometer SR9910 with a spherical 4π sensor (280-700 nm). To prevent focussing effects during the experiments and measurement of the irradiance spectra (from inside a PMMA bottle) all sides of the box-shaped PMMA bottle, except the top, were covered with black plastic.

PMMA bottles without a Schott filter received traces of wavelengths <280 nm (UVC). Using a spectrum (270-400 nm) of a Philips UVB (TL-12) lamp the spectra between 270 and 280 nm were reconstructed.

2.4 Weighting function

For each of the eight spectral treatments an exposure versus response curve was determined based on four different irradiance levels, each by measuring the concentration Fe(II) over time.

The initial Fe(II) photo-production rates (d[Fe(II)]/dt at t = 0, upon turning on the lights) were used to construct the weighting function. To establish the weighting function, weights were optimized to obtain the best fit with measured Fe(II) photo-production using the equation:

$$\frac{\partial Fe(II)}{\partial t} = \sum \varepsilon(\lambda)E(\lambda)\Delta\lambda, \tag{1}$$

where λ is the wavelength (nm), $\varepsilon(\lambda)$ is the weight (M m J^{-1}), i.e. effectiveness in photo-production of Fe(II), at λ, and $E(\lambda)$ is the measured spectral irradiance (W m^{-2}) at λ.

The spectral weighting function was determined by using iterative non-linear regression (Marquardt method as implemented in the SAS NLIN procedure) to compute the best-fit parameters of an equation describing the wavelength dependence of $\varepsilon(\lambda)$ over the range 270 to 700 nm:

$$\varepsilon(\lambda) = W_{300} \cdot e^{-S_w(\lambda-300)}, \qquad\qquad (2)$$

where W_{300} is the weight at 300 nm (a reference wavelength) and S_w is the slope of the exponential function. The choice of a single slope exponential equation for the weighting function is general to a wide variety of chemical and biological effects ((Neale, 2000).

2.5 Iron(II) analysis

Concentrations of Fe(II) were followed using an automated flow injection analysis system employing a luminol-based chemiluminescence detection of Fe(II) (King et al., 1995). An alkaline luminol solution (50 μM luminol in 0.5 M NH$_3$ (suprapur, Merck) and 0.1 M HCl (suprapur, Merck)) is mixed with the sample in a flow cell in front of a Hamamatsu HC135 photon counter. At pH 10, Fe(II) is rapidly oxidized by oxygen on a millisecond time scale causing the oxidation of luminol, producing blue light (Xiao et al., 2002). Every 93 seconds a sample was transported in-line from the PMMA bottle into the flow cell using an 18.2 MΩ nanopure water carrier. The complete analysis system, reagents and tubing, were kept in the dark.

Calibration was performed by standard addition to the sample matrix. The 0.01 M Fe(II) stock was prepared monthly by dissolving ferrous ammonium sulfate hexahydrate ($Fe^{(II)}(NH_4SO_4)_2 \cdot 6H_2O$, Baker Analyzed, reagent grade) in 0.012 M 3xQD HCl. Working solutions were prepared daily. All Fe(II) stock solutions were refrigerated in the dark at 4°C if not in use.

The time delay between Fe(II) addition and measurement caused oxidation. This oxidation was accounted for by extrapolating the data back to time zero because Fe(II) oxidation in seawater approximates pseudo-first-order kinetics.

2.6 Attenuation coefficients, solar spectra and ozone concentration

An attenuation spectrum determined in the Southern Ocean near Palmer station (data available at: www.lifesci.ucsb.edu/eemb/labs/prezelin/Public_datasets.html) (Boucher and Prezelin, 1996), the Beer-Lambert law and the weighting function were used to describe Fe redox cycling in the watercolumn. Solar spectra and ozone concentrations for Palmer Station were recorded by respectively the NSF Polar Programs UV Monitoring Network and the Total Ozone Mapping Spectrometer, NASA.

3. Results and discussion

The spectral weighting function for the photo-production of Fe(II) from amorphous iron hydroxides showed the strongest Fe(II) production at the shortest wavelengths (UVB), the weight decreases about 2% for each nm increase in wavelength ($R^2 = 0.92$, $P < 0.0001$) (Figure 1A):

$$\varepsilon(\lambda) = 3.57 \cdot 10^3 \cdot e^{-0.02(\lambda - 300)}, \tag{3}$$

Upon application of the weighting function to a single solar spectrum collected in the morning (08.01 local time) under ozone repleted conditions near Palmer station, Antarctica
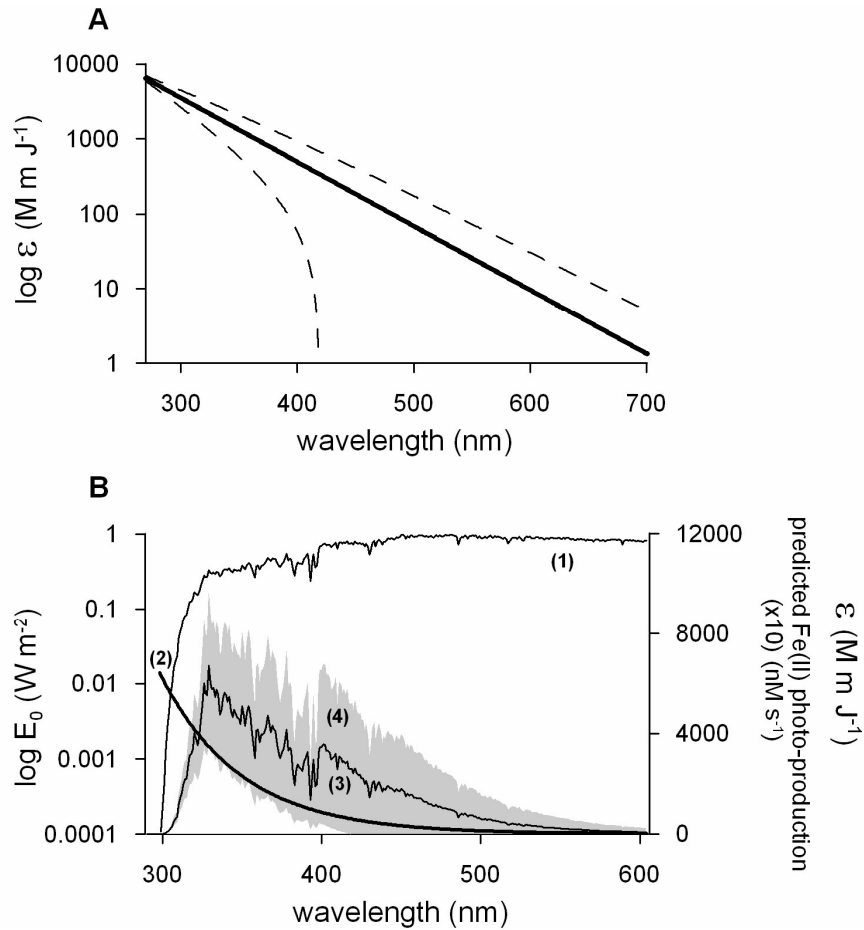
Figure 1. (A) The spectral weighting function (log ε scale) for the photoreduction of Fe in Southern Ocean seawater. The upper and lower lines represent the 95% confidence interval. (B) The solar spectrum (1) (log E scale (W m^{-2})), recorded on 22 Nov. 2000 (12:00 GMT) under ozone repleted conditions (370.4 DU), the weighting function (2) (ε (M m J^{-1})) and the resulting predicted Fe(II) photo-production (3) ((x10) nM s^{-1}) with its 95% confidence interval (4) (light grey).

(64.8ºS, 64.1ºW), the strong contribution of UVA (62%) to total solar radiation induced Fe(II) production was revealed (Figure 1B). Despite exhibiting very low weights, the visible part of the spectrum (VIS) was found to play a significant role (36%) (Figure 1B). The contribution of UVB to Fe redox cycling was small (2.4%). The predicted maximum of the Fe(II) photo-production rate occurred between 325 and 345 nm, at the shorter UVA wavelengths.
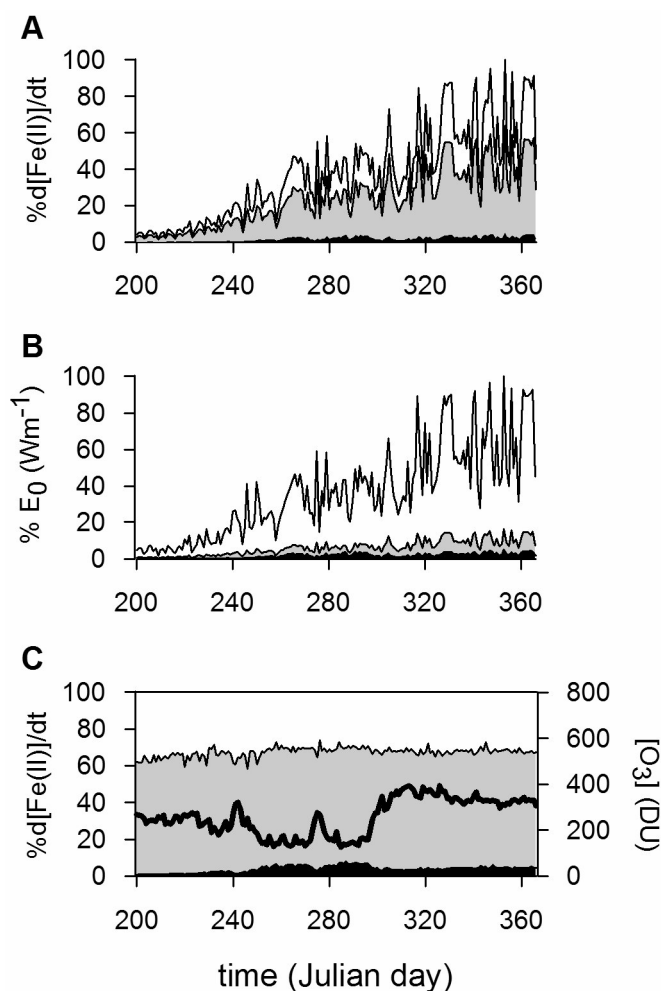
Figure 2. (A) Relative Fe(II) photo-production rates in the surface ocean as a result of UVB (black), UVA (grey) and VIS (clear) exposure, using solar spectra from 18 July until 31 Dec. 2000 (16:00 GMT). Values were taken as percentage of the highest value for the Fe(II) photo-production rate. (B) The relative intensities of incident UVB (x10) (black), UVA (grey) and VIS (clear) at the sea surface. Values were taken as percentage of the highest measured value for the light intensity. (C) The predicted relative Fe(II) photo-production rate as a result of UVB (black), UVA (grey) and VIS (clear) and the concentration ozone in Dobson Units (DU) (black line). The Fe(II) photo-production rates are relative to the Fe(II) photo-production rate due to total irradiance each day.

When assessing the role of the three major wavelength bands on Fe(II) photo-production throughout the major phytoplankton growth season (spring and summer), a large day-to-day variability was observed (Figure 2A). Yet on any given day, UVA was found to play the predominant role at a very steady 60%, followed by VIS at a quite uniform 35% (Figure 2C). In contrast, unweighted solar energy is primarily in the VIS band (83%) followed by UVA (16%) and UVB (0.3%) (Figure 2B). With the progression of the growth season the total Fe(II) photo-production at midday doubled from early-spring until early-summer.

Stratospheric ozone depletion in the austral spring results in significantly increased levels of UVB as well as spectral shifts in favor of the shorter UVB wavelengths. Under ozone depleted conditions the application of the weighting function continued to predict a major contribution of UVA of 63% of the total Fe(II) photo-production rate followed by VIS, 31% (Figure 2C). Temporal decreases in ozone (between day 250 and 300, Figure 2C) coincided with an increase in UVB mediated Fe(II) photo-production (>6%). After the ozone repletion (after appr. day 301) UVB related Fe(II) photoproduction rates exceeded those in
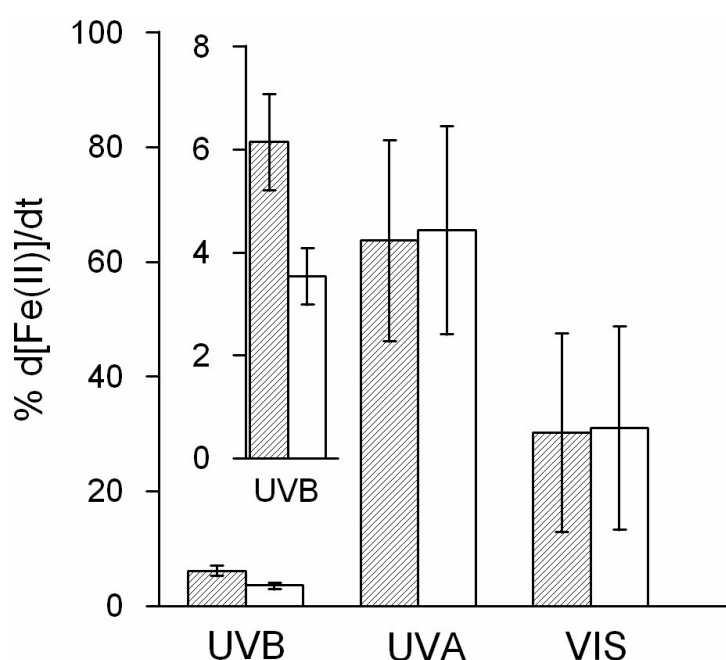
Figure 3. The wavelength band dependent Fe(II) photo-production as percentage of the photo-production due to the total spectrum (280-605 nm) at 23 Sept. 2000 (16:00 GMT) (145.1 DU) (hatched) and 9 Nov. 2000 (16:00 GMT) (389.9 DU) (non-hatched). Incident UVB increased from 0.40% to 0.68% of solar irradiance. Insert: The difference in Fe(II) photoproduction rate due to UVB is significant (3.54% to 6.15%) and due to ozone depletion on 23 Sept. The uncertainty is given as the standard error derived from the weighting function.
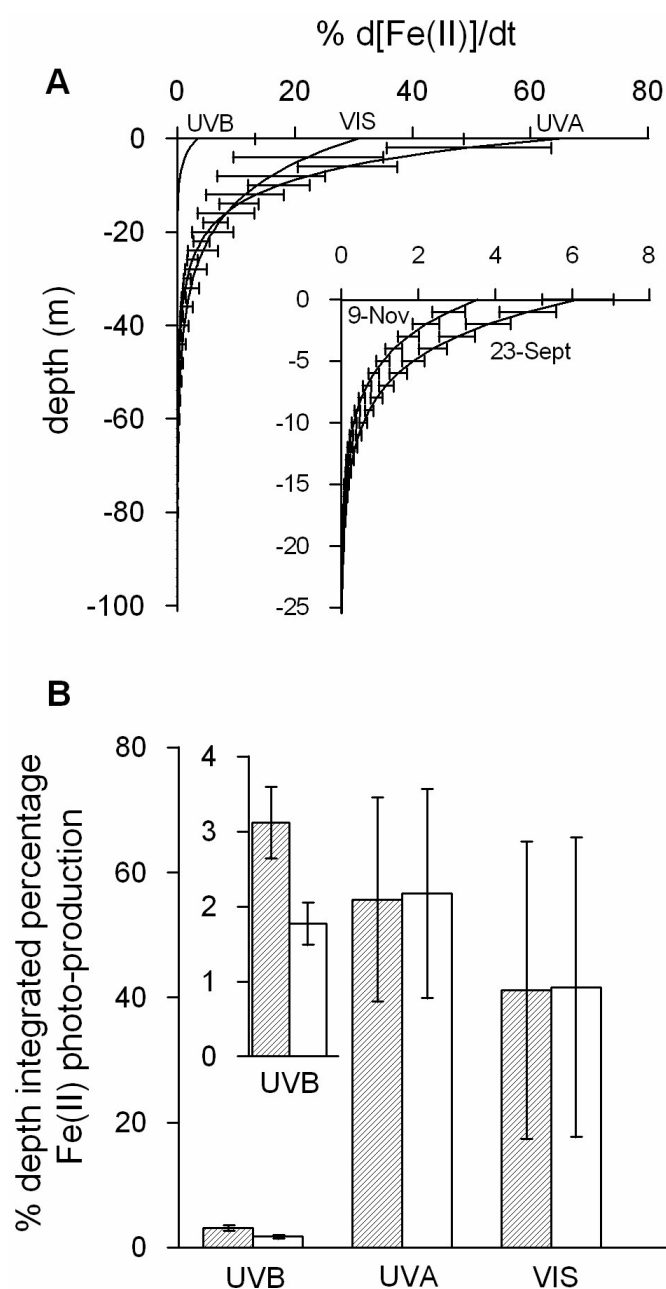
Figure 4. (A) The relative Fe(II) photo-production rate due to natural UVB, UVA and VIS exposures (9 Nov. 2000, 16:00 GMT) with depth. Insert: The relative Fe(II) photo-production rate due to UVB at 23 Sept. 2000 (16:00 GMT) (145.1 DU) and at 9 Nov. 2000 (389.9 DU) with depth. Values are expressed as relative to the total irradiance at the surface. (B) The percentage depth integrated Fe(II) photo-production due to UVB, UVA and VIS for 23 Sept. (hatched) and 9 Nov. (non-hatched). Insert: The significant difference in depth integrated Fe(II) photo-production due to enhanced UVB during ozone depletion. The uncertainties are given as standard errors derived from both the weighting function and the attenuation coefficients.

the pre-ozone depleted period due to the higher solar zenith angle. This is further shown by application of the weighting function to two individual spectra recorded at Palmer station under ozone depleted and ozone repleted conditions respectively (Figure 3). Natural variations of the UVA and VIS effect on Fe photoreduction in surface waters, due to changing weather conditions, solar zenith angle etc., largely dwarf the significant (3.54% versus 6.15%) but much smaller variations in UVB effect due to ozone depletion (Figure 3).

Fe redox cycling as function of depth is shown in Figure 4A. Both natural and enhanced UVB were found to play a minor role in the upper 10 m water column for Fe(II) photoproduction (Figure 4A). Instead UVA and VIS were shown to be the most important wavelength regions within the water column. Because VIS penetrates deeper into the euphotic zone (1% Fe(II) photoproduction at 57 m depth) as compared to both UVB (1% Fe(II) photoproduction at 19 m depth) and UVA (1% Fe(II) photoproduction at 39 m depth), the VIS became more important with depth. Where Fe chemistry and bio-availability are affected by the Fe redox-cycle, UVA and VIS play an equally important role (Figure 4B) in contributing to depth integrated Fe(II) photoproduction.

Sea ice causes strong attenuation of the solar spectrum, in the quantitative and the qualitative sense. As described UVB transmission through sea ice is highly variable (Prezelin et al., 1998), fluctuating between <0.5% and 9% of incident UVB, as it depends on many characteristics such as ice thickness, snow cover, turbidity or brine inclusions. These characteristics also cause a large variability in UVB/UVA/PAR ratios. As a result, ice cover will have a large impact on Fe redox cycling in the water column below. When spectral attenuation characteristics of sea ice are known however, our spectral weighting function will allow for the determination of under ice Fe photoreduction.

Our novel weighting function clearly shows that the UVA and the VIS govern the Fe photoreduction in Southern Ocean waters, in all seasons and at all depths. This function is now applicable in ecosystem models, in conjunction with suitable observed or modeled light spectra in open water and under the ice. Finally the natural day-to-day variability of UVA and VIS, completely overrides the enhanced UVB due to ozone depletion in the austral spring. Throughout the year, and even under ozone depleted conditions, the role of UVB in the photo induced redox cycle of iron is minor.

Acknowledgements

References

Boucher, N.P. and Prezelin, B.B., 1996. Spectral modeling of UV inhibition of in situ Antarctic primary production using a field-derived biological weighting function. Photochemistry and Photobiology, 64(3): 407-418.

Buma, A.G.J., de Baar, H.J.W., Nolting, R.F. and van Bennekom, A.J., 1991. Metal enrichment experiments in the Weddell-Scotia Seas - effects of iron and manganese on various plankton communities. Limnol. Oceanogr., 36(8): 1865-1878.

Croot, P.L. and Johansson, M., 2000. Determination of iron speciation by cathodic stripping voltammetry in seawater using the competing ligand 2-(2- thiazolylazo)-p-cresol (TAC). Electroanalysis, 12(8): 565-576.

de Baar, H.J.W. and Boyd, P.W., 2000. The role of iron in plankton ecology and carbon dioxide transfer of the global oceans. In: R.B. Hanson, H.W. Ducklow and J.G. Field (Editors), The dynamic ocean carbon cycle; A midterm synthesis of the joint global ocean flux study. University Press Cambridge, Cambridge.

de Baar, H.J.W., Buma, A.G.J., Nolting, R.F., Cadee, G.C., Jacques, G. and Treguer, P.J., 1990. On iron limitation of the Southern Ocean - experimental- observations in the Weddell and Scotia seas. Mar. Ecol. Progr. Ser., 65(2): 105-122.

de Baar, H.J.W., de Jong, J.T.M., Nolting, R.F., Timmermans, K.R., van Leeuwe, M.A., Bathmann, U., van der Loeff, M.R. and Sildam, J., 1999. Low dissolved Fe and the absence of diatom blooms in remote Pacific waters of the Southern Ocean. Mar. Chem., 66(1-2): 1-34.

Hanson, A.K., Tindale, N.W. and Abdel-Moati, M.A.R., 2001. An equatorial Pacific rain event: influence on the distribution of iron and hydrogen peroxide in surface waters. Mar. Chem., 75(1-2): 69-88.

Hoppema, M., Fahrbach, E., Stoll, M.H.C. and de Baar, H.J.W., 1999. Annual uptake of atmospheric CO_2 by the Weddell Sea derived from a surface layer balance, including estimations of entrainment and new production. J. Mar. Syst., 19(4): 219-233.

Jickells, T.D. and Spokes, L.J., 2001. Atmospheric iron inputs to the oceans. In: D.R. Turner and K.A. Hunter (Editors), The biogeochemistry of iron in seawater. IUPAC series on analytical and physical chemistry of environmental systems. John Wiley & Sons, LTD, New York, pp. 85-122.

Johnson, K.S., Coale, K.H., Elrod, V.A. and Tindale, N.W., 1994. Iron photochemistry in seawater from the equatorial Pacific. Mar. Chem., 46(4): 319-334.

Karentz, D., 1994. Considerations for Evaluating Ultraviolet Radiation-Induced Genetic-Damage Relative to Antarctic Ozone Depletion. Environmental Health Perspectives, 102: 61-63.

King, D.W., Lounsbury, H.A. and Millero, F.J., 1995. Rates and mechanism of Fe(II) oxidation at nanomolar total iron concentrations. Environ. Sci. Technol., 29(3): 818-824.

Martin, J.H., Gordon, R.M. and Fitzwater, S.E., 1990. Iron in Antarctic waters. Nature, 345(6271): 156-158.

Neale, P.J., Cullen, J.J. and Davis, R.F., 1998. Inhibition of marine photosynthesis by ultraviolet radiation: Variable sensitivity of phytoplankton in the Weddell-Scotia Confluence during the austral spring. Limnology and Oceanography, 43(3): 433-448.

Neale, P.J., Davis, R.F. and Cullen, J.J., 1998. Interactive effects of ozone depletion and vertical mixing on photosynthesis of Antarctic phytoplankton. Nature, 392(6676): 585-589.

Neale, P.J., Kieber, D.J., 2000. Assessing biological and chemical weighting functions. In: R.E. Hester, Harrison, R.M. (Editor), Causes and Environmental Implications of Increased UV-B Radiation. Royal Society of Chemistry, Cambridge, U.K., pp. 61-83.

Nishioka, J., Takeda, S., de Baar, H.J.W., Laan, P., Croot, P.L., Boye, M. and Timmermans, K.R., in press. Change in the concentrations of iron in different size fractions during an iron fertilization experiment in the Southern Ocean, EisenEx study. Mar. Chem.

Prezelin, B.B., Moline, M.A. and Matlick, H.A., 1998. Icecolors 93: spectral UV radiation effects on Antarctic frazil ice algae. Ant. Res. Ser., 73: 45-83.

Sedwick, P.N. and DiTullio, G.R., 1997. Regulation of algal blooms in Antarctic shelf waters by the release of iron from melting sea ice. Geophys. Res. Lett., 24(20): 2515-2518.

Wells, M.L., Mayer, L.M., Donard, O.F.X., Sierra, M.M.D. and Ackelson, S.G., 1991. The photolysis of colloidal iron in the oceans. Nature, 353(6341): 248-250.

Xiao, C.B., Palmer, D.A., Wesolowski, D.J., Lovitz, S.B. and King, D.W., 2002. Carbon dioxide effects on luminol and 1,10-phenanthroline chemiluminescence. Anal. Chem., 74(9): 2210-2216.

Chapter 5

Individual ligands have different effects on the photoreduction of iron in natural seawater of the Southern Ocean

Micha J.A. Rijkenberg, Loes J.A. Gerringa, Vicky E. Carolus, Ilona Velzeboer, Hein J.W. de Baar

Abstract

The influence of five Fe-binding model ligands (phaeophytin, ferrichrome, desferrioxamine B (DFOB), inositol hexaphosphate (phytic acid) and protoporphyrin IX (PPIX)) on the photo-induced redox speciation of Fe in Southern Ocean seawater was investigated. Phaeophytin and ferrichrome did not clearly affect the Fe photochemistry. The model ligands DFOB, phytic acid and PPIX all showed, although different and based on different mechanisms, an effect on the photoproduction of Fe(II). The DFOB decreased the photoreducible Fe fraction and prevented the formation of newly photoreducible Fe by binding the re-oxidized Fe(III) resulting in a lower Fe(II) steady state during irradiance. Addition of phytic acid led to higher concentrations of photoproduced Fe(II) compared to the control. Furthermore, an increasing phytic acid concentration coincided linearly with increasing maximum photoproduced Fe(II) concentrations, presumably due to influencing the aggregation of Fe(III) and increasing the photoreducible Fe fraction. In seawater, the PPIX does not bind Fe(III) but Fe(II). Subsequently, PPIX acted as a photosensitizing catalytic producer of superoxide, thus increasing the dark reduction of Fe(III) to Fe(II). Yet, the presence of PPIX decreased the overall concentration of free Fe(II).

1. Introduction

Iron, Fe, is an important trace metal required in essential biochemical systems necessary to provide cells with the energy and biological components for growth and multiplication (Harrison and Morel, 1986; Rueter and Ades, 1987; Raven, 1990; Rueter et al., 1990; Greene et al., 1991; Geider and la Roche, 1994). Well known Fe-requiring cellular processes include photosynthesis and nitrogen fixation (Rueter and Ades, 1987; Geider et al., 1993). Iron is one of the important factors limiting primary production in large oceanic areas such as the Northeast Pacific, the Equatorial Pacific and the Southern Ocean. These areas are known as high-nutrient low-chlorophyll (HNLC) areas, because major nutrients such as phosphate, nitrate and silicate cannot be fully utilized by phytoplankton (Martin and Fitzwater, 1988; de Baar et al., 1990; Martin et al., 1990; Martin et al., 1994). Although the

concentrations of Fe are higher in coastal regions, the higher cellular demand by coastal phytoplankton (Sunda et al., 1991), and the lack of bioavailable chemical Fe species, can also lead to limitation of primary production in the coastal environment (Hutchins and Bruland, 1998; Bruland et al., 2001; Strzepek and Harrison, 2004).

The chemistry of Fe in seawater is very complex. The Fe(III) and its hydrolysis products have very low solubility products resulting in a tendency to form particulate iron oxyhydroxides (Millero, 1998; Liu and Millero, 1999; Moffett, 2001; Waite, 2001; Liu and Millero, 2002). Organic complexation of Fe(III) in seawater increases the overall Fe solubility (Kuma et al., 1996; Johnson et al., 1997). Although organic Fe(III)-binding ligands are often found in excess over the dissolved Fe pool (Boye et al., 2001) it does not prevent the existence of a colloidal Fe pool within the operational defined "dissolved" Fe fraction (all Fe passing through a 0.2 μm filter). Nishioka et al. (in press) distinguished the Fe pools by operational size discrimination among others in a particulate Fe (> 0.2 μm), and a fine colloidal Fe pool (200 kDa-0.2 μm), and showed the importance of these Fe fractions in the Southern Ocean polar front between South Africa and Antarctica.

The Fe(II), although better soluble in seawater, becomes rapidly oxidized by O_2 and H_2O_2 (Millero et al., 1987; Millero and Sotolongo, 1989; King et al., 1995). Remarkably, significant and stable concentrations of Fe(II) have been determined in the Northeast Atlantic (Boye et al., 2003), the East-equatorial Atlantic (Bowie et al., 2002) and during a Southern Ocean Fe enrichment experiment (Croot et al., 2001).

Redox reactions and speciation are shown to be important for the bioavailability of Fe for phytoplankton. The Fe(II) is assumed to be an Fe fraction suitable for biological uptake (Anderson and Morel, 1980; Anderson and Morel, 1982; Takeda and Kamatani, 1989; Maldonado and Price, 2001). Furthermore, the Fe redox cycle initiated by photochemical processes is mentioned as an important mechanism by which (colloidal) Fe is converted in more reactive species (defined by the method applied) resulting in a higher bioavailability to phytoplankton (Wells and Mayer, 1991; Johnson et al., 1994; Miller and Kester, 1994).

Organic complexation can influence the redox speciation of Fe in seawater. Extensive literature on the influence of organic complexation of Fe on the oxidation kinetics is available (Theis and Singer, 1974; Millero et al., 1987; Voelker et al., 1997; Santana-Casiano et al., 2000; Moffett, 2001; Rose and Waite, 2002; Santana-Casiano et al., 2004). Organic compounds can also induce photoreductive dissolution of Fe from colloidal material (Waite and Morel, 1984; Waite et al., 1986; Waite and Torikov, 1987; Siffert and Sulzberger, 1991; Pehkonen et al., 1993; Pehkonen et al., 1995; Sulzberger and Laubscher, 1995). Barbeau et al. (2001) have shown the photolysis of marine Fe(III)-siderophore complexes. The latter high affinity Fe(III)-binding ligands secreted by e.g. marine bacteria to scavenge and transport Fe (Trick, 1989; Wilhelm and Trick, 1994; Granger and Price, 1999), may lead to the formation of lower-affinity Fe(III) ligands and the reduction of Fe(III) to Fe(II). The

ability of the Fe(III)-siderophore complex to be photoreduced was found to be strongly dependent on the Fe-binding functional group (Barbeau et al., 2003).

The identity, origin, and chemical characteristics of the assemblage of organic Fe-binding ligands in the oceans are largely unknown. Despite differences in location and the method used, a remarkably similar picture has emerged for the conditional stability constants of Fe ligand complexes, ranging between 10^{18} and 10^{23}, and measured in the North Atlantic (Gledhill and van den Berg, 1994; Wu and Luther, 1995; Witter and Luther, 1998), the North Sea (Gledhill et al., 1998), the Mediterranean Sea (van den Berg, 1995), the Arabian Sea (Witter et al., 2000), the North Central and equatorial Pacific Ocean (Rue and Bruland, 1995; Rue and Bruland, 1997) and the Southern Ocean (Nolting et al., 1998; Boye et al., 2001; Boye, in press). Witter et al. (2000) conclude from comparisons between formation and dissociation rate constants of model ligands and field samples that most unknown ligands in seawater could originate from porphyrin and siderophore-like compounds. Macrellis et al. (2001) isolated organic Fe-binding ligands with hydroxamate and catecholate Fe-binding functional groups from the central California coastal upwelling system. Recently, Gledhill et al. (2004) detected 7 siderophore type compounds in coastal and near shore environments among which one was identified as DFOB (McCormack et al., 2003).

In the present study, the influence of Fe binding ligands on the redox speciation of Fe in Southern Ocean seawater was investigated. The choice of model ligands to be investigated was based on their possible natural occurrence. Inspired by the article of Witter et al. (2000), three Fe-chelating moieties were studied including: tetrapyrrole ligands (phaeophytin and PPIX), terrestrial and marine hydroxamate siderophores (ferrichrome and DFOB) and the terrestrial Fe-complexing storage ligand inositol hexaphosphate (phytic acid). The tetrapyrrole ligands were chosen to represent Fe-binding ligands derived from pigments such as chlorophyll-*a* released in the seawater upon cell lysis. Ferrichrome and DFOB (trihydroxamates from terrestrial microorganisms) were chosen to represent the structural types of siderophores that could be present in seawater (Macrellis et al., 2001; Martinez et al., 2001; Gledhill et al., 2004). DFOB is very similar to the siderophore desferrioxamine G produced by a marine bacterium belonging to the genus *Vibrio* (Martinez et al., 2001) and is found in coastal seawater (Gledhill et al., 2004). Furthermore, DFOB is widely used in experiments causing massive reduction in iron uptake (Wells et al., 1994; Wells, 1999) and phytoplankton growth in offshore and near shore waters (Wells et al., 1994; Hutchins et al., 1999). It is not known how DFOB influences the photoreducible Fe pool. Phytic acid is an organic phosphorous, metal-complexing (including Fe), storage compound abundant in seeds of terrestrial plants and has also been used as a terrestrial biomarker in coastal environments (Suzumura and Kamatani, 1995).

2. Materials and methods

2.1 Seawater

Clean Southern Ocean surface seawater (44ºS 20º E, 30 November, 2000) was pumped into an over-pressurized class 100 clean air container using a Teflon diaphragm pump (Almatec A-15, Germany) driven by a compressor (Jun-Air, Denmark, model 600-4B) connected via acid-washed braided PVC tubing to a torpedo towed at approximately 5 m alongside the ship (Polarstern, ANTXVIII/2). The seawater was filtered in-line by a filter (Sartorius Sartobran filter capsule 5231307H8) with a cut-off of 0.2 μm. Upon return to the institute the tank was stored at room temperature. The Southern Ocean seawater contained 1.1 nM dissolved Fe and 1.75 ± 0.28 equivalents of nM Fe of natural ligands with a conditional stability constant (log K') of 21.75 ± 0.34 (given errors show the 95% confidence interval). The DOC concentration was 86.8 ± 1.13 μM C (given error is the standard deviation).

Artificial seawater was prepared using $CaCl_2\cdot 2H_2O$ (8.9 10^{-3} M, Baker Analyzed), $MgCl_2\cdot 6H_2O$ (4.6 10^{-2} M, Baker Analyzed), NaCl (0.53 M, Merck (Gr for analysis)) and $NaHCO_3$ (2.5 10^{-3} M, Baker Analyzed) in 18.2 Milli-Ω nanopure water (MQ). The artificial seawater had an ionic strength of 0.7 and a pH of 8.01 (Metrohm 713 pH meter). The Fe concentration was 100 nM.

2.2 Reagents

All solutions were prepared using MQ. Chemicals, except for phaeophytin and ferrichrome (see below), which were used as received. Three times quartz distilled (3xQD) HCl was prepared for use in iron stock solutions. A 20 μM Fe(III) stock solution was made with ammonium Fe(III) sulfate ($NH_4Fe^{(III)}(SO_4)_2\cdot 12H_2O$, Baker Analyzed, reagent grade) in 0.012 M 3xQD HCl. A 5.9 10^{-5} M PPIX (disodium salt) (Aldrich Chem.) stock solution, a 2.4 10^{-5} M DFOB (Novartis) stock solution and a 8.7 10^{-5} M phytic acid (Aldrich Chem.) stock solution were used without further purification.

Phaeophytin (Sigma) and ferrichrome (from *Ustilago sphaerogena*) (Sigma) were deferrated using a method described by Witter et al. (2000). One milligram of chlorophyll-*a* (from spinach) and ferrichrome were first diluted in 1 ml of 90% acetone / 10% MQ water. This solution was further diluted to 10 ml in MQ and acidified to pH 3.0 with 6 M HCl (3xQD). Magnesium was removed from chlorophyll-*a* by passing the acidified ligand through an 8-cm column of XAD-16 resin (Sigma). The XAD-16 resin had been cleaned previously by vacuum extraction in methanol (3xQD). The organic loaded column was eluted with

methanol (3xQD), followed by a washing step with 3xQD methanol:chloroform (1:1) to liberate any remaining ligand. The methanol and chloroform fractions were removed by evaporation and the collected ligand (phaeophytin, ferrichrome) was resuspended in MQ.

2.3 Light

Philips ultraviolet B (UVB: 280-315 nm) (TL-12), ultraviolet A (UVA: 315-400 nm) (TL' 40W/05) and visible light (VIS: 400-700 nm) (TL'D 36W/33) lamps were used to simulate the solar spectrum in the experiments. Spectral conditions were measured using a MACAM Spectroradiometer SR9910 with a small spherical 4π sensor. All sides of the rectangular UV transparent polymethylmetacrylate (PMMA) bottle (Steeneken et al., 1995), except the top, were covered with black plastic to prevent focussing effects. Spectra were recorded from 280-700 nm.

2.4 Fe colloid formation

An acid cleaned Teflon bottle was equilibrated overnight with natural seawater containing 50 nM Fe(III). The Fe colloid formation was visualized in an experiment where Fe, labile with respect to 10 μM 2-(2-Thiazolylazo)-p-cresol (TAC) (labile Fe), was measured as function of time after the addition of 50 nM Fe(III) to 1 liter of natural seawater. The experiment was performed at 15°C in the dark. Samples (15 ml) were taken in time and immediately measured for Fe able to be bound by TAC using Cathodic Stripping Voltammetry (CSV) (see below).

2.5 Photoreduction of Fe with and without different organic Fe binding ligands

All experiments were performed in an over-pressurized class 100 clean air, temperature controlled container laboratory using a temperature of 4ºC. Prior to use, the 1 liter, PMMA bottles were equilibrated with natural seawater containing the same concentration Fe(III) and ligand as used during the experiments. Equilibration occurred in the dark under the same conditions as the experiments.

An experiment typically started with measuring the background concentration Fe(II) in the dark, after which the lamps were switched on. During 60-90 minutes the concentration of Fe(II) was followed. Next, the oxidation of Fe(II) was followed for 30 minutes after turning off the light. The seawater solution was continuously stirred using a Teflon stirring bean.

Investigation of the photoreducibility of amorphous Fe hydroxides was performed in artificial seawater. The Fe(II) photoproduction of amorphous Fe hydroxides was investigated

using a blank (100 nM Fe(III) present but no Fe addition) and an addition of 20 nM Fe(III) (both after overnight equilibration), and a fresh addition of 20 nM Fe(III). The optical spectrum used for the experiments contained UVB (1.82 Wm^{-2}), UVA (4.08 Wm^{-2}) and VIS (13.16 Wm^{-2}).

One experiment series was performed with increasing concentrations of Fe(III), additions of 11, 15 and 20 nM Fe to natural seawater. The optical spectrum used for these experiments contained UVB (0.91 Wm^{-2}), UVA (2.57 Wm^{-2}) and VIS (2.77 Wm^{-2}).

The influence of different ligands on the photo-induced redox speciation of Fe in natural seawater was studied in separate experiments by addition of 10 nM Fe(III) and 20 nM of the ligands PPIX, phytic acid and DFOB. Phaeophytin and ferrichrome were added in excess to 500 ml of Southern Ocean seawater (0.2 μm filtered, pH 8.07 (Metrohm 713 pH meter)) containing 10 nM Fe(III). Additional experiments with increasing concentrations of DFOB, phytic acid and PPIX were performed in 500 ml Southern Ocean seawater to which 100 nM Fe(III) was added. The addition of ligand always preceded the addition of the Fe. The optical spectrum used for these experiments contained UVB (1.25 Wm^{-2}), UVA (3.72 Wm^{-2}) and VIS (3.24 Wm^{-2}).

2.6 UV-digestion

The UV digestion was performed using a UV emitting 15 W low pressure mercury vapour lamp (Glasco Ultraviolet Systems) emitting radiation with maxima at 254 and 185 nm. The seawater was incubated in acid-cleaned quartz tubes at a distance of 3 cm from the lamp for 8 hours. The whole set up was placed in a fume hood to remove the produced UV absorbing ozone (O_3).

2.7 Iron(II) analysis

Concentrations of Fe(II) were measured inline using an automated flow injection analysis system employing a luminol-based chemiluminescence detection of Fe(II) (Seitz and Hercules, 1972; King et al., 1995; O'Sullivan et al., 1995). An alkaline luminol solution is mixed with the sample in a spiral shaped flow cell in front of a Hamamatsu HC135 photon counter. At pH 10, Fe(II) is rapidly oxidized by oxygen on a millisecond time scale causing the oxidation of luminol and producing blue light (Xiao et al., 2002).

Samples were transported in-line from the PMMA bottle to a sample loop. Then, by introducing it in MQ, the sample was transported into the flow cell every 93 seconds.

The complete analysis system was built inside a light-tight wooden box. The luminol reagent and the carrier were kept in light-tight bags (as used for storage of photographic

films). The tubing was covered by aluminum foil and the tubing of the peristaltic pump was shaded by black plastic.

The alkaline luminol solution was prepared weekly with 15 mM 5-amino-2,3-dihyfro-1,4-phthal-azinedione (Luminol) (SIGMA) in 20 mM Na_2CO_3. The 50 µM luminol reagent solution was made in 0.5 M NH_3 (suprapur, Merck) and 0.1 M HCl (suprapur, Merck). The luminol reagent solution was stored in the dark for at least 24 hours before use, to ensure that the reagent properties had stabilized. A 0.01 M Fe(II) stock was prepared monthly by dissolving ferrous ammonium sulfate hexahydrate ($Fe^{(II)}(NH_4SO_4)_2 \cdot 6H_2O$) (Baker Analyzed, reagent grade) in 0.012 M (3xQD) HCl. Working solutions were prepared daily just before use. All Fe(II) stock solutions were refrigerated in the dark at 4°C when not in use.

Calibration was performed by the standard addition of known concentrations of Fe(II) to the sample matrix. The time delay between Fe(II) addition and the actual measurement caused an oxidation effect. This oxidation effect was accounted for by extrapolating the data back to time zero using the fact that Fe(II) oxidation in seawater very closely approximates pseudo-first-order kinetics.

2.8 Fe(III) analysis

Dissolved iron, defined as the Fe fraction passing a 0.2 µm filter, was determined using flow injection analysis with luminol chemiluminescence and H_2O_2 (de Jong et al., 1998).

2.9 CLE-ACSV

Determination of the organic speciation of iron was performed using CLE-ACSV. The 2-(2-Thiazolylazo)-p-cresol (TAC) (Aldrich, used as received) reagent was used as competing ligand (Croot and Johansson, 2000). All solutions were prepared using 18.2 MΩ nanopure water. The equipment consisted of a µAutolab voltammeter (Ecochemie, Netherlands), a static mercury drop electrode (Metrohm Model VA663), a double-junction Ag/saturated AgCl reference electrode with a salt bridge containing 3 M HCl and a counter electrode of glassy carbon. The titration was performed using 0.01 M stock solution of TAC in 3x quartz distilled (QD) methanol, 1 M boric acid (Suprapur, Merck) in 0.3 M ammonia (Suprapur, Merck) (extra cleaning by the addition of TAC after which TAC and Fe(TAC)$_2$ was removed with a C18 SepPak column) to buffer the samples to a pH of 8.05 and a 10^{-6} M Fe(III) stock solution acidified with 0.012 M HCl (3xQD). Aliquots of 15 ml were spiked with Fe(III) until final concentrations between 0 and 20 nM and allowed to equilibrate overnight (> 15 hours) with 5 mM borate buffer and 10 µM TAC. The concentration Fe(TAC)$_2$ in the samples were measured using the following procedure: i) removal of oxygen

from the samples for 200 seconds with dry nitrogen gas, a fresh Hg drop was formed at the end of the purging step, ii) a deposition potential of –0.40 V was applied for 30-60 seconds according to the sample measured, the solution was stirred to facilitate the adsorption of the $Fe(TAC)_2$ to the Hg drop, iii) at the end of the adsorption period the stirrer was stopped and the potential was scanned using the differential pulse method from -0.40 to -0.90 V at 19.5 mV s^{-1} and the stripping current from the adsorbed $Fe(TAC)_2$ recorded.

The ligand concentration and the conditional stability constant were calculated using the non-linear fit of the Langmuir isotherm (Gerringa et al., 1995).

2.10 Hydrogen peroxide analysis

Hydrogen peroxide (H_2O_2) was measured as fluorescence (Waters fluorometer, type 470) after enzyme-catalyzed dimerisation of (*p*-hydroxyphenyl) acetic acid (POHPAA) (Miller and Kester, 1988; Miller and Kester, 1994). The exact method used to analyze hydrogen peroxide is described in (Gerringa et al., 2004).

2.11 Binding of Fe(III) and Fe(II) by PPIX

To investigate binding of Fe(III) by PPIX, a fixed concentration of Fe (15 nM) was titrated with PPIX. Aliquots of 15 ml seawater containing 5 mM borate buffer and 10 μM TAC were spiked with PPIX up to final concentrations between 0 and 125 nM and allowed to equilibrate overnight (> 15 hours). The concentration $Fe(TAC)_2$ in the samples was measured using the procedure as described above (CLE-ACSV).

To investigate the binding of Fe(II) by PPIX the disappearance of Fe(II) due to different concentrations of PPIX was compared with the disappearance of Fe(II) by oxidation alone (Figure 1A). The experiments were performed in an over-pressurized class 100 clean air, temperature-controlled container laboratory using a temperature of 15ºC. The Fe(II) (1.0 10^{-7} M stock solution in 0.012 M 3xQD HCl) and PPIX (2.58 10^{-5} M stock solution in MQ) were added to Southern Ocean seawater in a 25 ml volumetric flask by pipetting it at different dry spots in the neck of the flask. By swirling the flask Fe(II) and PPIX were added to the seawater at exactly the same time. This experiment was performed with 1 nM Fe(II) and increasing concentrations of PPIX (25, 50, and 100 nM). Fe(II) oxidation in the Fe(II) standard was controlled for by additions of 1 nM Fe(II) to the seawater. The concentration of Fe(II) of the standard solution as used during the experiment decreased with 0.064 nM h^{-1} (R^2 = 0.98). This decrease in the concentration of Fe(II) was corrected for by calculating the concentration of Fe(II) that we added to the seawater as a function of time. The results (the oxidation of Fe(II) and binding of Fe(II) by PPIX as function of time between t = 0 and t = ~600 s) were mathematically described using:

$$[Fe(II)] = a + be^{c \cdot t} \tag{1}$$

The Fe(II) concentration was calculated as a function of time between t= 0 and t=115 seconds after the addition of 1 nM Fe(II) to the seawater with and without the addition of PPIX. The reactions with Fe(II) taking place in seawater containing PPIX can be described by the binding of Fe(II) by PPIX:

$$[Fe(II)] + [PPIX] \xrightarrow{k_{Fe(II)PPIX}} [Fe(II)PPIX] \tag{2}$$
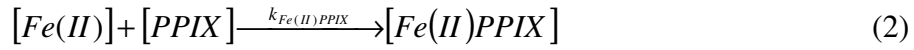
and the parallel (hence competing) oxidation reaction of Fe(II),

$$[Fe(II)] \xrightarrow{k_{ox}} [Fe(III)] \tag{3}$$

We assumed that no reduction of Fe(III) would take place during our experiments and that the dissociation of the [Fe(II)PPIX] complex is much slower then the reverse association of Fe(II) to PPIX. Pseudo first order kinetics was assumed for oxidation as well as the combination of oxidation and binding of Fe(II) by PPIX (excess of PPIX and oxidants). Integration (assuming that $[Fe(II)] = [Fe(II)_0]$ at t=0) of the differential equations for the reactions with Fe(II) in seawater containing PPIX:

$$\frac{d[Fe(II)]}{dt} = -k_{Fe(II)PPIX} \cdot [Fe(II)] \cdot [PPIX] - k_{ox} \cdot [Fe(II)] \tag{4}$$

$$\frac{d[Fe(II)]}{dt} = -\left(k_{Fe(II)PPIX} \cdot [PPIX] + k_{ox}\right) \cdot [Fe(II)] \tag{5}$$

$$\frac{d[Fe(II)]}{dt} = -\left(k_{overall}\right) \cdot [Fe(II)], \tag{6}$$

and for seawater without PPIX:

$$\frac{d[Fe(II)]}{dt} = -k_{ox} \cdot [Fe(II)], \tag{7}$$

resulted in a linear relationship between the natural logarithm of the concentration Fe(II) with time (Figure 1B).

The rate constant for the binding of Fe(II) by PPIX depending on the PPIX concentration was calculated by subtracting the rate constant of the oxidation of Fe(II) without PPIX from the rate constant for the combination of oxidation and binding in the presence of PPIX (6).

$$k_{Fe(II)PPIX} \cdot [PPIX] = k_{overall} - k_{ox} \qquad (8)$$

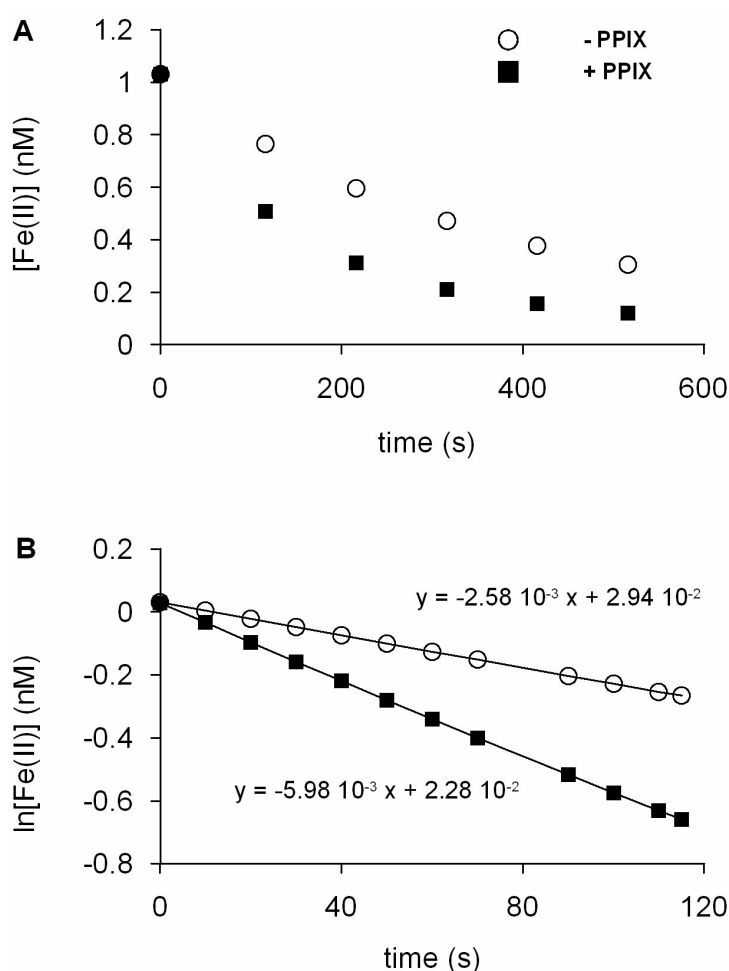**Figure 1.** (A) The concentration of Fe(II) decreasing with time due to oxidation (1 nM Fe(II)) without the addition of PPIX and due to the combination of oxidation and binding by PPIX (1 nM Fe(II), 50 nM PPIX). (B) The plot of the natural logarithm of the concentration Fe(II) versus time for the oxidation (1 nM Fe(II)) without the addition of PPIX and for the combination of oxidation and binding by PPIX (1 nM Fe(II), 50 nM PPIX).

3. Results and discussion

3.1 Inorganic Fe photoreduction

To understand the influence of organic Fe-binding ligands on the photo-induced Fe redox speciation in seawater it is necessary to know how the photo-induced Fe redox processes act in the absence of ligands. Little is known about the crystalline forms of the Fe species formed upon the addition of a low concentration of Fe(III) to seawater. Based on model studies (Moffett, 2001) suggested that in aqueous alkaline media Fe(III) polymerizes into amorphous Fe(III) hydroxides. With aging, these solids lose water and develop crystalline structures leading to two principal products, an amorphous solid, ferrihydrite (Fe_5-$OH_8 \cdot 4H_2O$) (Schwertmann and Thalmann, 1976), and a more crystalline form lepidocrocite (γ-FeOOH) (Tipping et al., 1989). Ultimately these oxyhydroxide minerals will lose more water with ageing, and turn into more refractory minerals as hematite (α-Fe_2O_3) and goethite (α-FeOOH) (Schwertmann and Taylor, 1972; Schwertmann and Fischer, 1973; Cornell and Schwertmann, 1996). Addition of Fe to seawater probably results in formation of amorphous iron hydroxides called marine ferrihydrite (Wells and Trick, 2004). The formation of Fe colloids (after a 50 nM Fe(III) addition to seawater) is fast and reaches equilibrium within 1.5-2 hours (Figure 2) as shown by the decrease in Fe concentration able to be bound to TAC (labile Fe).
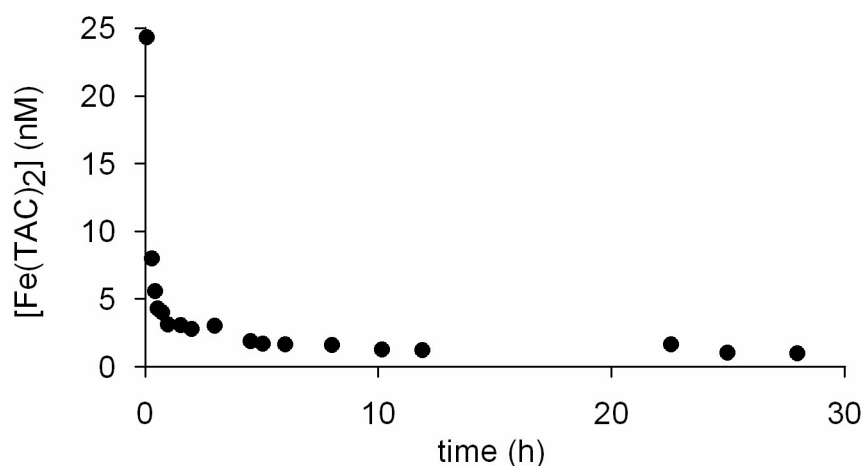

Figure 2. The Fe colloid formation after the addition of 50 nM Fe(III) from an acidified stock solution to seawater. The formation of amorphous iron hydroxides was visualized by measuring the concentration of labile Fe with the Fe-binding ligand TAC using CLE-ACSV.

The mechanisms for photoredox reactions occurring at the interface of Fe(III) solids involve a combination of charge-transfer bands in surficial complexes and in the solid itself (Waite and Morel, 1984; Siffert and Sulzberger, 1991; Faust, 1994). To determine if the resulting amorphous iron hydroxides contain a photo-reducible Fe fraction independent of organic constituents we added Fe(III) to artificial seawater. The production of Fe(II) showed that fresh colloidal material contains a photoreducible Fe fraction (Figure 3). Waite and Morel (1984) detected photoreduced Fe from amorphous Fe hydroxides and proposed that hydroxylated ferric surface species are the primary chromophore. The observation that Fe(II) was only detected at a pH 6.5 and not at a pH 8 was explained by the stronger hydrolization of the Fe(III) surface complexes at a pH 8 (Waite and Morel, 1984). This explanation was confirmed by the observation that the photoproduced concentration of Fe(II) decreased with increasing time period that Fe hydrolization and Fe colloid formation was allowed. More Fe(II) was photoproduced when 20 nM Fe(III) was added to the artificial seawater immediately before measurement compared to a 20 nM Fe(III) addition followed by an 18 hours equilibration time (Figure 3, Table 1).
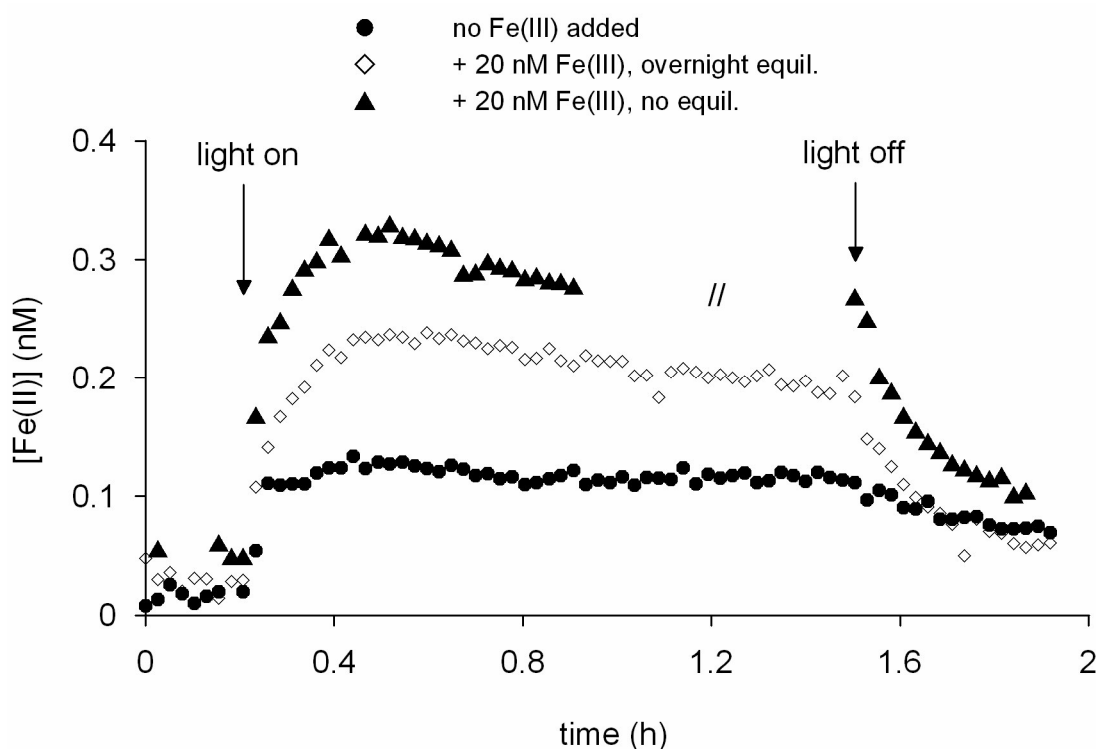

Figure 3. The Fe(II) production in artificial seawater. The photoproduction of Fe(II) is shown for artificial seawater without an Fe(III) addition, with an addition of 20 nM Fe(III) equilibrated overnight and with a fresh addition of 20 nM Fe(III).

Table 1. Experimental characteristics as the concentration InEqDark Fe(II), InPrRate Fe(II), the concentration Max Fe(II), Ox Fe(II), and the concentration FinEqDark Fe(II) for the experiments with artificial seawater. Standard errors are given for InEqDark Fe(II), Max Fe(II) and FinEqDark Fe(II).

Artificial SW	No Fe added	Overnight equil. Fe	Freshly added Fe
Fe added (nM)	-	20	20
InEqDark Fe(II) (nM)	0.016 ± 0.0058	0.026 ± 0.0067	0.054 ± 0.0055
InPrRate Fe(II) (nM/h)	1.49	2.92	5.14
Max Fe(II) (nM)	0.13 ± 0.0036	0.23 ± 0.0028	0.32 ± 0.0043
Ox Fe(II) (nM/h)	0.20	1.03	1.61
FinEqDark Fe(II) (nM)	0.064 ± 0.0039	0.054 ± 0.0054	0.101 ± 0.0045
MaxProd Fe(II) (nM)	0.11	0.21	0.27
Net dark reduction (norm) (nM/h$_{irradiance}$)	0.037	0.023	0.063

Several characteristics in the pattern of Fe(II) concentration versus time were used to interpret the photochemical experiments. The Fe(II) concentration versus time, typically resulting from an addition of 100 nM Fe(III) to Southern Ocean seawater, is shown in Figure 4. The concentration of Fe(II) in the dark, prior to the irradiance treatment, was constant (Initial Equilibrium in the Dark of the concentration Fe(II), InEqDark Fe(II)) (Figure 4, section A). The concentration of Fe(II) in oxic seawater is always the result of a dynamic cycle of oxidation and reduction. In the dark other processes than photo(induced) reduction of Fe(III) are responsible for InEqDark Fe(II) such as thermal reduction (Hudson et al., 1992; Pullin and Cabaniss, 2003), the reduction of Fe by superoxide (Voelker and Sedlak, 1995; Voelker et al., 1997), or enzymatic Fe reduction (Maldonado and Price, 2000). Although we cannot guarantee total sterile conditions, we assume the role of external or internal bacterial enzymes was negligible or non-existent in our 0.2 μm filtered seawater.

The irradiance treatment resulted in a rapid increase of the concentration of Fe(II). There are several photo(induced) reduction mechanisms, that could be responsible for this increase: i) the photo-reduction of inorganic Fe oxyhydroxides (Wells and Mayer, 1991), ii) a ligand metal charge transfer (LMCT) reaction where an organic molecule is oxidized and Fe is reduced (Kuma et al., 1995), and iii) photo-induced reduction of Fe via the oxygen radical superoxide (O_2^-) (Voelker and Sedlak, 1995). The initial Fe(II) photoproduction rate (Initial photoProduction Rate of Fe(II), InPrRate Fe(II)) was used in the comparison of the different photochemical experiments (Figure 4, section B). This InPrRate Fe(II) was calculated by modeling the concentration InEqDark Fe(II) and the increase in the Fe(II) concentration during the first half hour of the irradiance treatment. The intercept of both lines, the exact time at which the irradiance treatment started, filled in the derivative of the previously modeled function resulted in a value for InPrRate Fe(II).
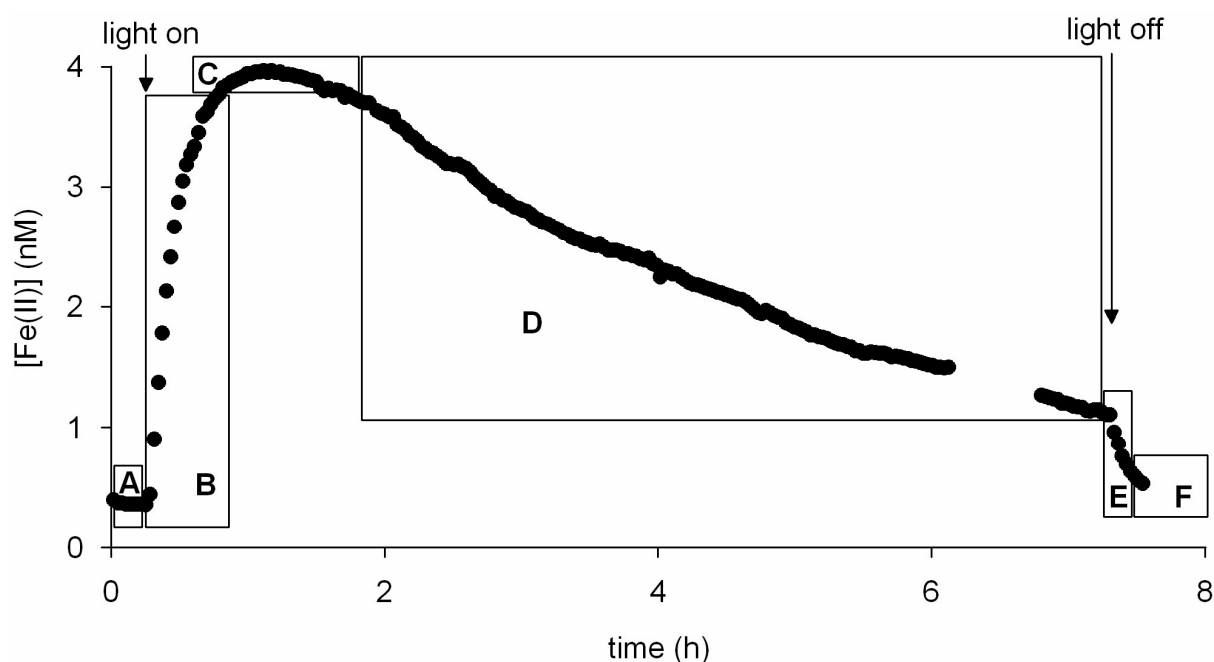
Figure 4. The concentration of Fe(II) as a result of the irradiation of colloidal Fe as produced due to a 100 nM Fe(III) addition to Southern Ocean seawater. The typical characteristics used to compare the photochemical experiments were: A the constant concentration of Fe(II) in the dark before illumination (InEqDark Fe(II)): B the rapid increase of Fe(II) after turning on the light with an initial Fe(II) photo-production rate upon irradiance (InPrRate Fe(II)): C the decrease in the rate of Fe(II) photo-production reaching a maximum Fe(II) concentration (Max Fe(II)): this followed by D the decrease of the concentration Fe(II) during irradiance towards an equilibrium (EqLight Fe(II)): and E turning off the light resulted in a sharp decline due to the oxidation of Fe(II) to Fe(III) (Ox Fe(II)): resulting in F equilibrium of the Fe(II) concentration (FinEqDark Fe(II)).

The Fe(II) photo-production rate decreased, after which a maximum was reached (Maximum Fe(II) concentration, Max Fe(II)) (Figure 4, section C). This maximal photo-produced Fe(II) concentration was calculated by subtracting of the initial Fe(II) equilibrium in the dark from the Fe(II) maximum (Maximum Produced Fe(II) concentration, MaxProd Fe(II)). After having reached this maximum the concentration of Fe(II) decreased slowly and reached an equilibrium (Equilibrium in the Light of the concentration Fe(II), EqLight Fe(II)) (Figure 4, section D). A rapid increase to a maximum followed by a slow decrease in the Fe(II) concentration, has been reported before. Wells and Mayer (1991) found that the photo-conversion rates diminished with continued irradiation when ferrihydrite was irradiated. In addition Waite and Morel (1984) have shown that the addition of excess amounts of the chromophore citrate did not influence this effect. Emmenegger et al. (2001) found similar behavior of the concentration of Fe(II) with time after UV digestion of Swiss lake water destroying the organic material, thereby confirming that the observed pattern is typical for colloidal Fe and independent of Fe complexing organic chromophoric molecules

(Waite and Morel, 1984). Wells and Mayer (1991) suggested several possible reasons for the decreasing photoreduction rate with time, among which: i) photoreduction becomes inhibited if residues from the photo-oxidation of chromophores accumulated on colloid surfaces over time, shielding active sites from further photoreaction, ii) the retention of photoreduced Fe(II) at the surface, or the rapid resorption of the re-oxidized Fe(III) species back onto the original surface. In either case, a shell of rapid-cycling labile Fe might form on the oxyhydroxide surface upon prolonged photolysis, iii) progressive photochemical alterations of the oxyhydroxide surface would decrease its charge trapping efficiency, resulting in more charge migration into the crystal lattice.

Organic ligands could influence the photoproduction of Fe(II) in several ways: i) by photoinduced Fe reduction via a LMCT reaction, ii) by decreasing the inorganic Fe concentration and subsequently decreasing the formation of Fe colloids, iii) by modification of the colloid surface due to binding or adsorption to surface iron, or iv) by influencing the overall structure of the iron colloids due to the precipitation of Fe(III)-organic solids.

The main process remaining, in the post illumination period, is the oxidation of Fe(II) to Fe(III) by O_2 and H_2O_2 (Oxidation of Fe(II), Ox Fe(II)) (Millero et al., 1987; Millero and Sotolongo, 1989; King et al., 1995) (Figure 4, section E). Organic ligands may inhibit (Theis and Singer, 1974), accelerate or decelerate (Santana-Casiano et al., 2000; Santana-Casiano et al., 2004) this Fe(II) oxidation.

The rapid oxidation of Fe(II) in the dark resulted in an equilibrium of the Fe(II) concentration in the dark (Final Equilibrium in the Dark of the concentration Fe(II), FinEqDark Fe(II)) (Figure 4, section F). The concentration FinEqDark Fe(II) is depending on both the oxidation as well as the thermal reduction of Fe in the dark. The concentration FinEqDark Fe(II) was often higher than the concentration InEqDark Fe(II), probably caused by the photo-induced production of superoxide leading to the reduction of Fe(III) in the dark (Voelker and Sedlak, 1995; Emmenegger et al., 2001). The concentration FinEqDark Fe(II) is reported as the final Fe(II) equilibrium in the dark minus the initial Fe(II) equilibrium in the dark. This is normalized to 1 hour of irradiance because photo-induced superoxide production could be responsible for Fe(III) reduction in the dark.

Increasing concentrations of Fe(III) were added to the Southern Ocean seawater to investigate how the possibly increasing photo-reducible Fe fraction influences the defined photochemical characteristics (Figure 5). Addition of Fe(III) indeed led to an increase in photoreducible Fe. The concentration InEqDark Fe(II), FinEqDark Fe(II), InPrRate Fe(II) and the MaxProd Fe(II) showed a linear increase with the addition of increasing concentrations Fe(III) (Figure 6, Table 2). The excellent linear relationship between the added Fe(III) concentration and the experimental characteristics as InPrRate Fe(II) and Max
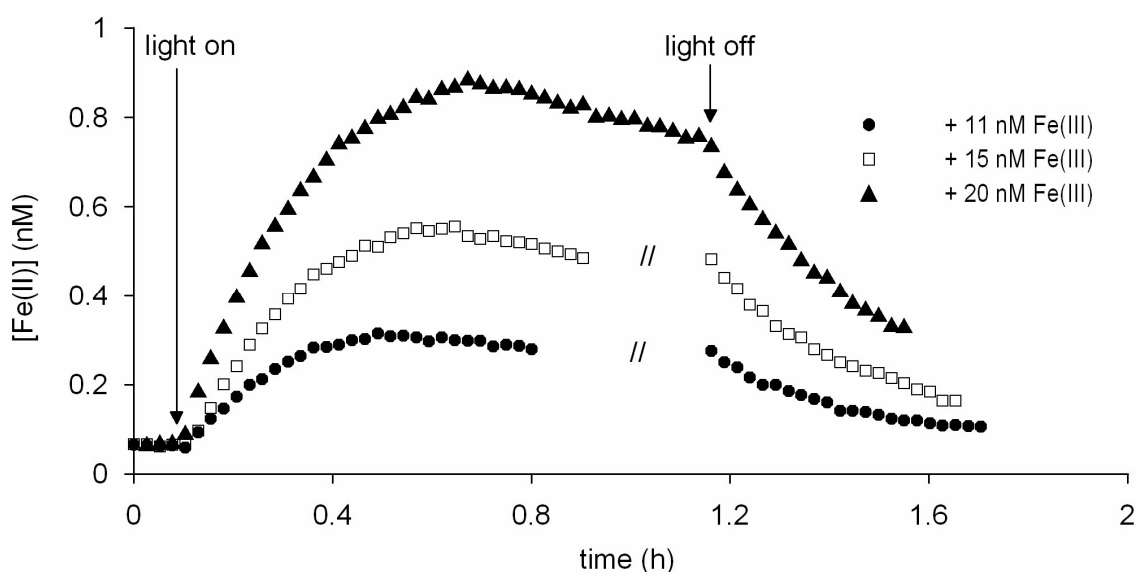
Figure 5. The concentration of Fe(II) as a result of the irradiation of colloidal Fe produced from a 11, 15 and 20 nM Fe(III) addition to Southern Ocean seawater.
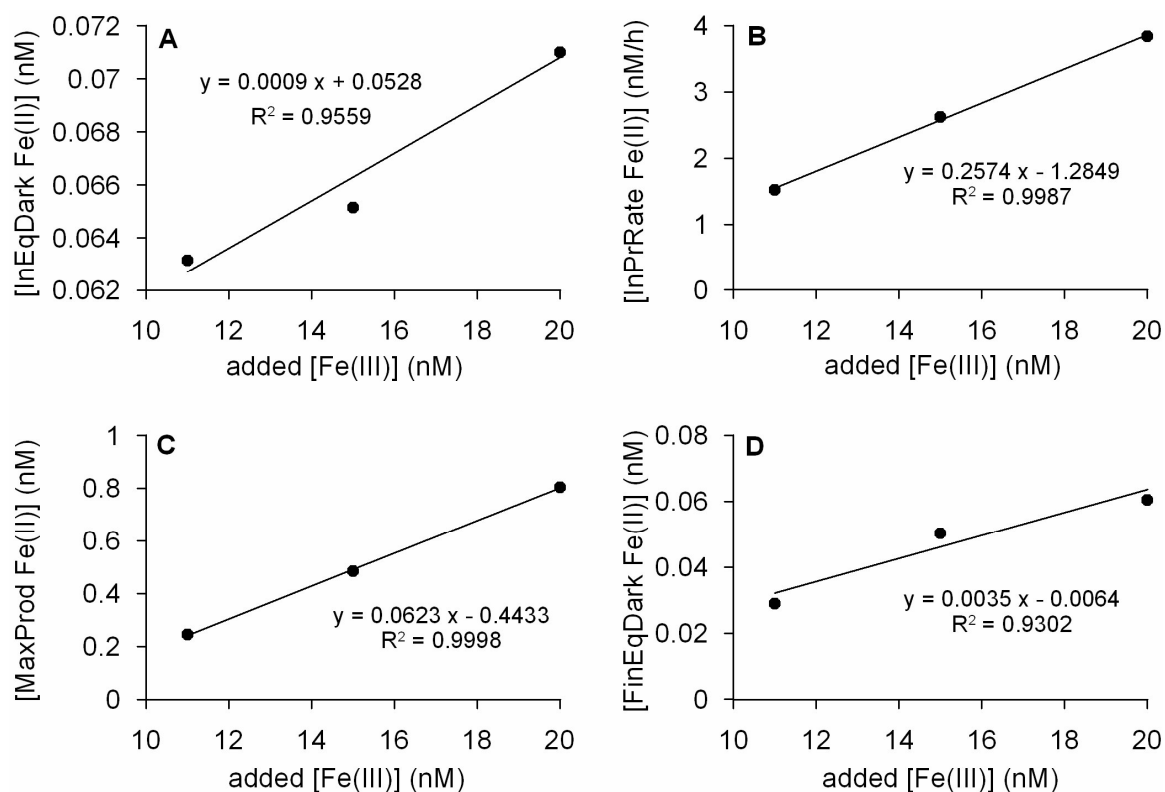

Figure 6. The linear relationship between the added concentration Fe(III) added and A) the concentration InEqDark Fe(II), B) the InPrRate Fe(II), C) the concentration MaxProd Fe(II), and D) the concentration FinEqDark Fe(II) which is normalized to 1 hour of irradiance in Southern Ocean seawater.

Fe(II) showed that aging of the colloids is slow and did not change the results within the experimental time frame (one day). Moreover, assuming that i) the solubility product of Fe stayed the same and thus that the concentration free Fe^{3+} and its truly soluble hydrolysis products did not increase, and ii) the concentration of organically complexed Fe did not change upon Fe(III) addition, we conclude that the increasing concentration of colloidal amorphous Fe hydroxides was responsible for the increasing InPrRate Fe(II) and the MaxProd Fe(II). This conclusion was confirmed by the photostability of the organic Fe-complexing ligands. The concentration of the assemblage of organic Fe binding ligands in the Southern Ocean seawater did not change significantly, from 1.75 ± 0.28 eq nM Fe of ligands to 1.74 ± 0.17 eq nM Fe of ligands, after 8 hours of UV digestion.

Table 2. Experimental characteristics as the concentration InEqDark Fe(II), InPrRate Fe(II), the concentration Max Fe(II), Ox Fe(II), and the concentration FinEqDark Fe(II) for increasing concentrations Fe(III) added to Southern Ocean seawater. Standard errors are given for InEqDark Fe(II), Max Fe(II) and FinEqDark Fe(II).

	Southern Ocean SW	Southern Ocean SW	Southern Ocean SW
Fe added (nM)	11	15	20
InEqDark Fe(II) (nM)	0.063 ± 0.0024	0.065 ± 0.0023	0.071 ± 0.0027
InPrRate Fe(II) (nM/h)	1.52	2.62	3.84
Max Fe(II) (nM)	0.31 ± 0.0048	0.55 ± 0.0038	0.86 ± 0.008
Ox Fe(II) (nM/h)	0.78	1.35	1.78
FinEqDark Fe(II) (nM)	0.084 ± 0.0046	0.11 ± 0.011	0.14 ± 0.027
MaxProd Fe(II) (nM)	0.25	0.49	0.81
Net dark reduction (norm) (nM/$h_{irradiance}$)	0.029	0.050	0.061

3.2 The influence of organic model ligands on the photochemistry of Fe in seawater

From the five model ligands only DFOB and PPIX clearly affected the redox speciation of Fe in seawater (Figure 7 and Table 3) The effect of phaeophytin, ferrichrome and phytic acid were less pronounced. The InPrRate Fe(II) decreased as follows: PPIX (4.48 nM/h) > no ligand ≥ phytic acid > phaeophytin ≥ DFOB > ferrichrome (2.71 nM/h) (Table 3). Remarkably, the overall production of Fe(II) was found to be lower with PPIX than measured for seawater containing the other ligands, although the InPrRate Fe(II) was clearly the highest for seawater containing PPIX. The influence of DFOB, PPIX and phytic acid on the photo-induced redox chemistry of Fe was therefore studied in more detail.
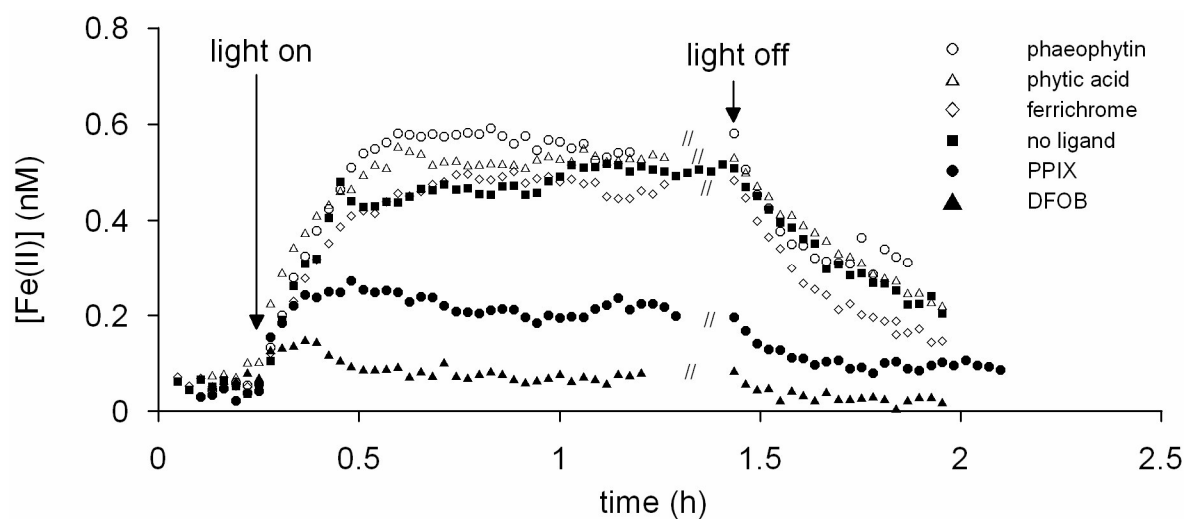
Figure 7. The photoproduction of Fe(II) after a 10 nM Fe(III) addition to Southern Ocean seawater in the presence of PPIX (20 nM), phytic acid (20 nM), DFOB (20 nM), ferrichrome (excess), phaeophytin (excess) and without an Fe binding ligand.

Table 3. Experimental characteristics as the concentration InEqDark Fe(II), InPrRate Fe(II), the concentration Max Fe(II), Ox Fe(II), and the concentration FinEqDark Fe(II) for different model Fe-binding ligands added to Southern Ocean seawater before addition of 10 nM Fe(III). Standard errors are given for InEqDark Fe(II), Max Fe(II) and FinEqDark Fe(II).

	No ligand	PPIX	Phytic acid	DFOB	phaeophytin	ferrichrome
Ligand added (nM)	-	20	20	20	20	20
Fe added (nM)	10	10	10	10	10	10
InEqDark Fe(II) (nM)	0.05 ± 0.01	0.04 ± 0.01	0.08 ± 0.003	0.07 ± 0.01	0.05 ± 0.01	0.06 ± 0.01
InPrRate Fe(II) (nM/h)	3.81	4.48	3.64	3.13	3.29	2.71
Max Fe(II) (nM)	0.48 ± 0.03	0.25 ± 0.01	0.53 ± 0.01	0.15 ± 0.003	0.58 ± 0.005	0.49 ± 0.008
Ox Fe(II) (nM/h)	1.10	1.28	0.89	0.91	2.63	1.77
FinEqDark Fe(II) (nM)	-	0.095 ± 0.002	-	-	0.29 ± 0.007	0.13 ± 0.008
MaxProd Fe(II) (nM)	0.43	0.22	0.45	0.08	0.53	0.43
Net dark reduction (norm) (nM/h$_{irradiance}$)	-	0.055	-	-	0.25	0.068

3.3 DFOB

The Fe complexed by DFOB is completely photo-stable irrespective of the wavelength of irradiance (Kunkely and Vogler, 2001). Although the long-wavelength absorption (426 nm) of DFOB is of the ligand to metal charge transfer (LMCT) type (Monzyk and Crumbliss, 1982) the LMCT excitation is not associated with any photo-activity. According to Kunkely and Vogler (2001) the DFOB ligand prevents a rapid decay to redox products and thus facilitates an efficient back electron transfer which leads to a complete regeneration of DFOB. However, it has been reported that a compound such as oxalate is able to induce the photoreduction of Fe(III) complexed by DFOB and the subsequent release of Fe(II) by an outer-sphere charge transfer excitation upon irradiance with UVB, leaving DFOB intact (Kunkely and Vogler, 2001).

We performed a series of experiments with increasing concentrations DFOB to investigate its influence on the photoproduction of Fe(II) (Figure 8 A, B). The concentrations of Fe(II), produced upon irradiance of seawater containing Fe and DFOB, were low compared to the same solution without DFOB (Figure 8 A). The concentration MaxProd Fe(II) in seawater containing DFOB was $7.5 \pm 1.4\%$ (n=5) of that without DFOB addition (Table 4). Remarkably, the addition of 65 nM DFOB resulted in a strong decrease in Fe(II) production compared to the same experiment performed without DFOB although 35 nM colloidal Fe(III) should still be present (Figure 8 B). This can only be explained when the assumption of 1 on 1 binding of Fe and DFOB (Rue and Bruland, 1995; Witter et al., 2000) is not valid under our experimental conditions, so consequently more Fe was bound to the added DFOB. This was further confirmed by the absence of any trend between both InPrRate Fe(II), the concentration MaxProd Fe(II) and the increasing concentration of DFOB (Table 4). The concentration MaxProd Fe(II) stayed around 0.21 ± 0.04 nM Fe(II) (n=5) and although a shift in InPrRate Fe(II) between the 80 and 95 nM DFOB addition caused a high standard deviation the values for InPrRate Fe(II) remained around 3.07 ± 0.96 nM Fe(II) h^{-1} (n=5) with increasing DFOB concentration (Table 4). Although DFOB is a very strong Fe chelator with reported conditional stability constants of $10^{21.6}$ (Witter et al., 2000) and $> 10^{23}$ (Rue and Bruland, 1995), constant non-negligible amounts of amorphous Fe oxyhydroxides apparently persisted, despite increasing concentrations of DFOB.

A clear negative trend between EqLight Fe(II) versus the increasing DFOB concentration was observed (Figure 9, Table 4). Two mechanisms could be responsible i) the overall photoreducible Fe fraction decreased with increasing DFOB concentration resulting in a decrease in EqLight Fe(II), or ii) recycled photoreducible Fe(III) resulting of the rapid oxidation of Fe(II) decreased as a result of the binding of the oxidized Fe(III) by DFOB. The binding of recycled photoreducible Fe(III) by DFOB is the main factor because we did not

see a decrease in the concentrations MaxProd Fe(II) or InPrRate Fe(II) with increasing concentrations of DFOB. This suggests that the increasing concentration of DFOB did not
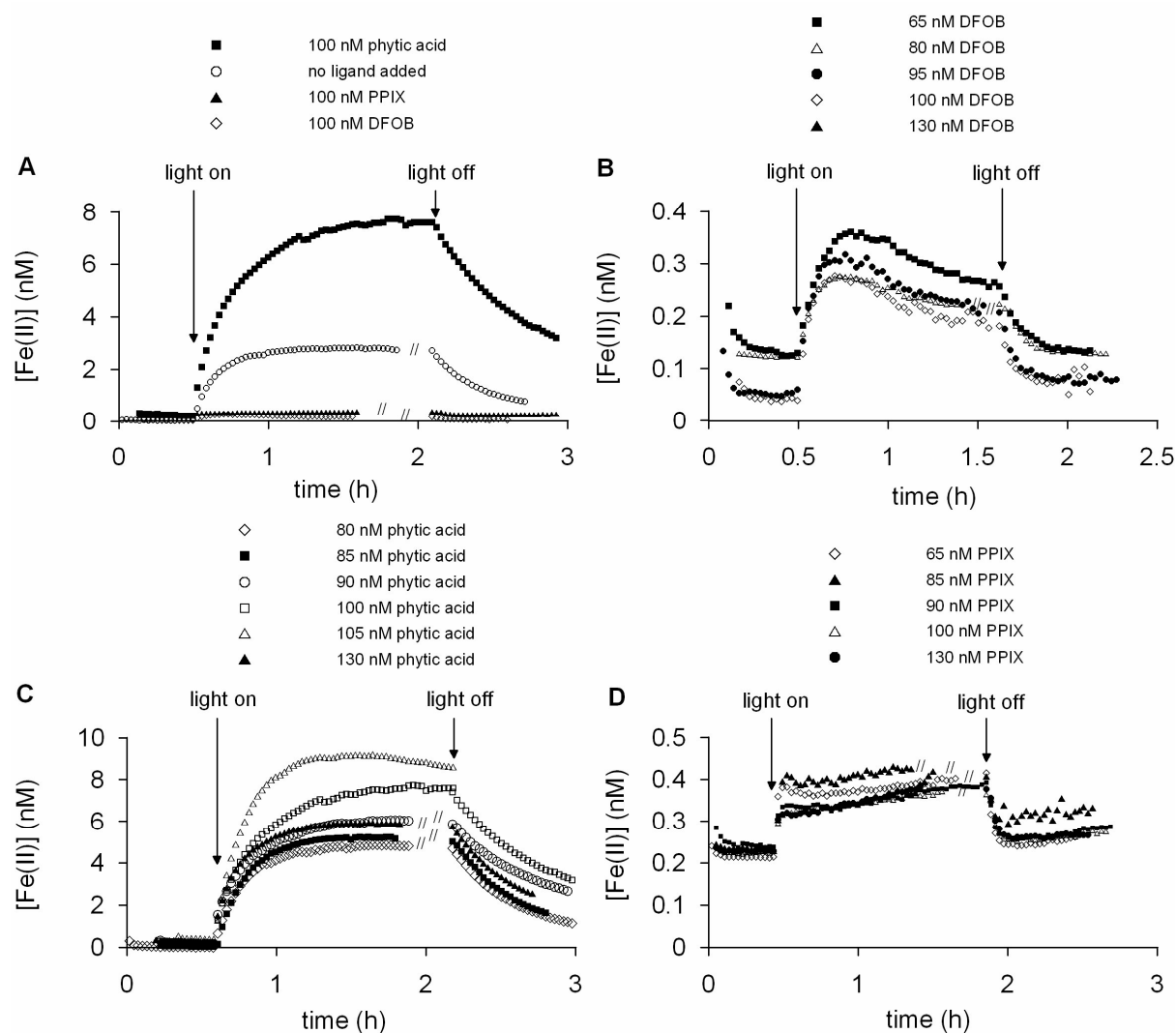
Figure 8. (A) The photoproduction of Fe(II) after a 100 nM Fe(III) addition to Southern Ocean seawater containing no ligand in comparison with the addition of 100 nM phytic acid, 100 nM PPIX and 100 nM DFOB. (B) The photoproduction of Fe(II) with increasing concentrations DFOB: 65 nM DFOB: 80 nM DFOB: 95 nM DFOB: 100 nM DFOB: and 130 nM DFOB. (C) The photoproduction of Fe(II) with increasing concentrations phytic acid: 80 nM phytic acid: 85 nM phytic acid: 90 nM phytic acid: 100 nM phytic acid: 105 nM phytic acid: and 130 nM phytic acid. (D) The photoproduction of Fe(II) with increasing concentrations PPIX: 65 nM PPIX: 85 nM PPIX: 90 nM PPIX: 100 nM PPIX: and 130 nM PPIX.
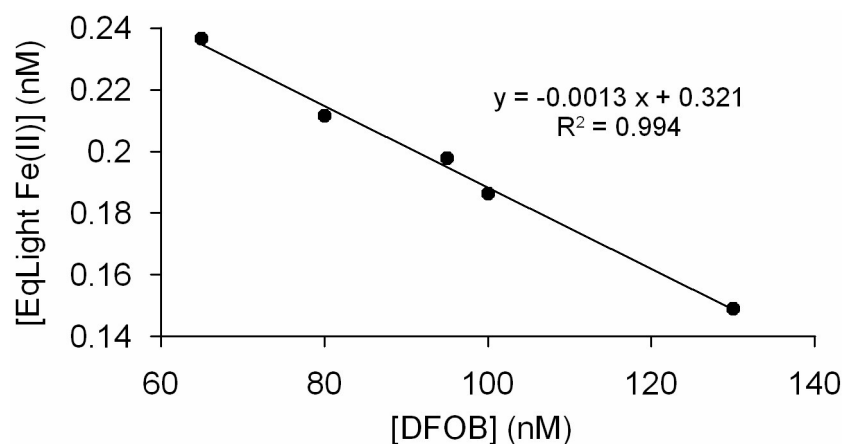
Figure 9. The concentration of EqLight Fe(II) for Southern Ocean seawater containing 100 nM Fe(III) and increasing concentrations DFOB.

Table 4. Experimental characteristics as the concentration InEqDark Fe(II), InPrRate Fe(II), the concentration Max Fe(II), Ox Fe(II), and the concentration FinEqDark Fe(II) for increasing concentrations DFOB added to Southern Ocean seawater. Standard errors are given for InEqDark Fe(II), Max Fe(II) and FinEqDark Fe(II).

|	No ligand	DFOB	DFOB	DFOB	DFOB	DFOB
Ligand added (nM)	-	65	80	95	100	130
Fe added (nM)	100	100	100	100	100	100
InEqDark Fe(II) (nM)	$0.042 \pm$ 0.0062	$0.132 \pm$ 0.0052	$0.123 \pm$ 0.0009	$0.0532 \pm$ 0.0034	$0.0422 \pm$ 0.0033	$0.0515 \pm$ 0.0036
InPrRate Fe(II) (nM/h)	17.87	2.07	2.04	3.97	3.96	3.29
Max Fe(II) (nM)	2.81 ± 0.011	$0.356 \pm$ 0.0038	$0.274 \pm$ 0.0027	$0.305 \pm$ 0.0074	$0.271 \pm$ 0.0043	$0.245 \pm$ 0.0012
Ox Fe(II) (nM/h)	4.52	1.13	1.03	1.70	1.77	1.89
FinEqDark Fe(II) (nM)	0.47 ± 0.012	$0.132 \pm$ 0.00145	$0.131 \pm$ 0.00061	$0.0792 \pm$ 0.0015	$0.0773 \pm$ 0.0041	$0.0862 \pm$ 0.0019
MaxProd Fe(II) (nM)	2.77	0.22	0.15	0.25	0.23	0.19
Net dark reduction (norm) (nM/h$_{irradiance}$)	0.31	$4.78 \ 10^{-5}$	0.0077	0.024	0.032	0.031

decrease the initial concentration of photoreducible Fe(III). The same mechanism could explain the negative trend between InEqDark Fe(II) versus the increasing concentration of DFOB (Table 4). This proposed mechanism is further confirmed by recent experiments

performed by Borer et al. (2005) who showed that siderophores such as DFOB accelerated the light-induced dissolution of iron(III) (hydr)oxides.

3.4 Phytic acid

Irradiance of Southern Ocean seawater containing 100 nM Fe(III) and concentrations phytic acid in the range of 80-130 nM resulted in higher concentrations of Fe(II) compared to the control (Figure 8 A, C). The similarity in the resulting Fe(II) production with time as compared with Figure 4 made us assume that we observed the reduction of Fe originating from a colloidal Fe pool (Wells and Mayer, 1991; Emmenegger et al., 2001). When the photoreducible colloidal Fe pool was only depending on the presence of free Fe or in case Fe-phytic acid is photoreactive we would expect to see a relation between InPrRate Fe(II) with increasing phytic acid concentration. Yet, no relationship between the InPrRate Fe(II) and the concentration of added phytic acid was found (Table 5). However, the concentration MaxProd Fe(II) clearly showed a linear relationship with the phytic acid concentration in the range 80-105 nM phytic acid (Figure 10). For every nM phytic acid added an increase in the concentration MaxProd Fe(II) of 0.16 nM (R^2 = 0.98) was observed. In contrast, the concentration of MaxProd Fe(II) as a result of a 130 nM phytic acid addition was found to be the same in two identical experiments and did not comply with the linear relationship (n=2).

The linear relationship between the concentration MaxProd Fe(II) and the concentration phytic acid could be explained by processes occurring when phytic acid and Fe were added to seawater. Upon the addition of 100 nM Fe(III) to Southern Ocean seawater containing phytic acid in concentrations ranging between 80 and 130 nM three processes are thought to occur: the hydrolysis and precipitation of Fe, forming colloids (Moffett, 2001), the binding and precipitation of Fe by phytic acid (Anderson, 1963), and the adsorption of phytic acid to the Fe containing aggregates (Ognalaga et al., 1994; Celi et al., 2003). The presence of six phosphate groups in the phytic acid molecules allowed different arrangements of the Fe and phytic acid molecules. The combination of these processes will result in undefined aggregates of Fe and phytic acid.

Anderson (1963) showed that precipitation of ferric phytic acid increased with a decreasing Fe to P ratio, with an increasing pH, and with increasing salinity. Moreover, phosphate can further disperse the already irregular surface of aggregates of amorphous Fe oxyhydroxides (Parfitt, 1989) and present a larger surface for interaction with the environment as for example for the photoproduction of Fe(II). If the same process occurs with phytic acid the aggregates will become more amorphous with an increasing concentration of phytic acid, thereby explaining the observation that more photo-reducible Fe is formed with increasing concentrations of phytic acid (Figure 10). The lower concentration of MaxProd Fe(II) observed after 130 nM phytic acid addition could be explained by the
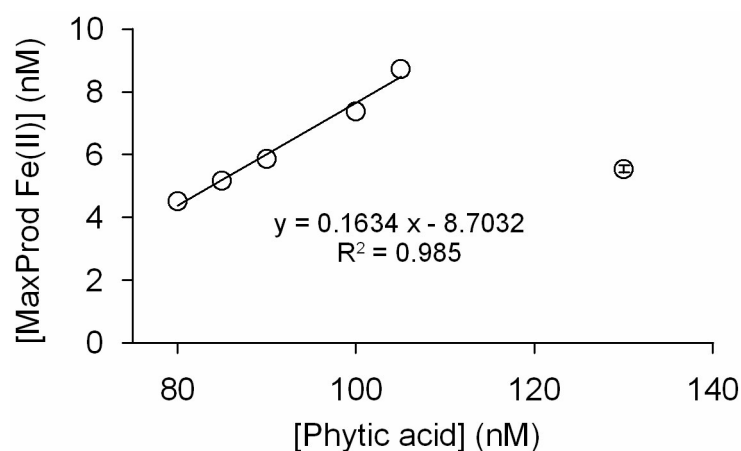
Figure 10. The concentration of MaxProd Fe(II) upon addition of 100 nM Fe(III) in Southern Ocean seawater, the latter containing increasing concentrations phytic acid. The photochemical experiment with 130 nM phytic acid was performed twice.

Table 5. Experimental characteristics as the concentration InEqDark Fe(II), InPrRate Fe(II), the concentration Max Fe(II), Ox Fe(II), and the concentration FinEqDark Fe(II) for increasing concentrations phytic acid (phytic) added to Southern Ocean seawater. Standard errors are given for InEqDark Fe(II), Max Fe(II) and FinEqDark Fe(II).

	phytic	phytic	phytic	phytic	phytic	phytic	phytic
Ligand added (nM)	80	85	90	100	105	130	130
Fe added (nM)	100	100	100	100	100	100	100
InEqDark Fe(II) (nM)	0.023 ± 0.0064	0.06 ± 0.0041	0.176 ± 0.0077	0.225 ± 0.0034	0.422 ± 0.0054	0.286 ± 0.0054	0.576 ± 0.0072
InPrRate Fe(II) (nM/h)	16.68	15.93	17.08	20.50	44.78	32.56	23.46
Max Fe(II) (nM)	4.54 ± 0.056	5.23 ± 0.023	6.05 ± 0.011	7.60 ± 0.004	9.15 ± 0.036	5.91 ± 0.012	6.05 ± 0.022
Ox Fe(II) (nM/h)	10.99	10.21	11.13	7.78	9.57	11.13	8.10
FinEqDark Fe(II) (nM)	0.64 ± 0.024	0.77 ± 0.054	1.72 ± 0.041	1.77 ± 0.055	-	1.48 ± 0.046	1.37 ± 0.079
MaxProd Fe(II) (nM)	4.52	5.17	5.87	7.37	8.72	5.62	5.47
Net dark reduction (norm) (nM/h$_{irradiance}$)	0.62	0.71	1.54	1.54	-	1.29	0.79

adsorption of the surplus phytic acid to the surface of the ferric phytic acid aggregates decreasing the available photoreducible Fe fraction.

Information on the complexation of Fe by phytic acid in seawater is limited to the conditional stability constant (log K'_{Fe3+L} = 22.3) and the Fe-phytic acid coordination (± 2:1) in seawater with a pH of 6.9 (Witter et al., 2000). Our study shows that phytic acid, until a certain concentration which is depending on the Fe concentration, will substantially increase the size of the photoreducible Fe fraction, probably via the formation of more amorphous ferric phytic acid aggregates.

3.5 Protoporphyrin IX

Addition of PPIX caused a dramatic decline in the produced concentration of Fe(II) in the Southern Ocean seawater (Figure 8 A, D). The different experimental characteristics did not show any relationship with the concentration of PPIX in seawater containing 100 nM Fe(III). This raised the question whether or not PPIX actually did bind Fe(III). To examine this we titrated Fe with increasing concentrations of PPIX using CLE-ACSV to detect TAC-labile Fe (Fe bound by TAC (10 µM) after > 12 hours equilibration) (Figure 11). Although Rue and Bruland (1995) and Witter et al. (2000) determined a log K' for PPIX (respectively 22.0 and 22.4), we did not find a substantial decrease in TAC-labile Fe with increasing PPIX concentration and therefore conclude that PPIX does not bind Fe(III). Nevertheless, because the effect of PPIX addition on the photoproduction of Fe(II) was demonstrated to be large (Figure 8 A, D), we investigated the possible role of PPIX in binding Fe(II).
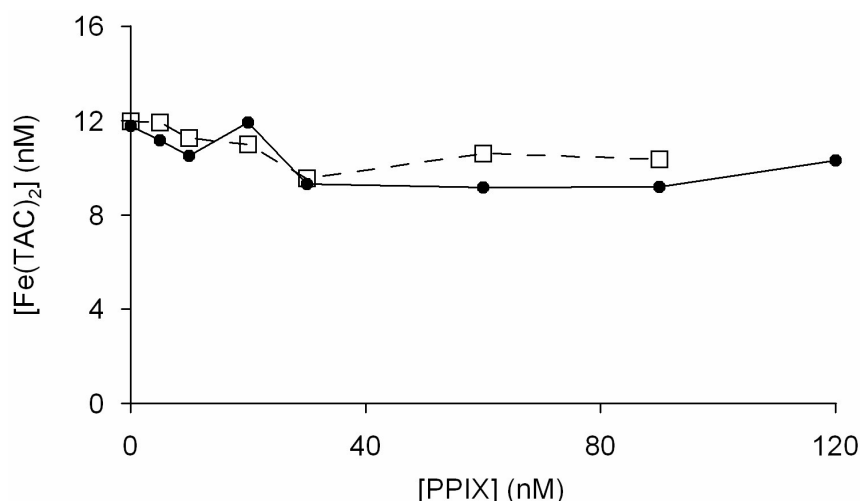

Figure 11. The binding of Fe(III) to PPIX as visualized by a titration of Fe(III) with PPIX using CLE-ACSV with the competing ligand TAC. The experiment was performed twice.

In a series of experiments we compared the removal of Fe(II) due to different concentrations of PPIX (eq. 4) with the disappearance of Fe(II) by oxidation alone (eq. 7) (Figure 1). From this we calculated the rate constant of the binding of Fe(II) by PPIX for concentrations of PPIX between 25 and 100 nM (eq. 8) (Figure 12). The Fe(II) was bound by PPIX with a rate constant ($k_{Fe(II)PPIX}$) of $3.0 \times 10^{-3} \pm 9.7 \times 10^{-4}$ s^{-1} (n=2) for 25 nM PPIX, $4.5 \times 10^{-3} \pm 9.8 \times 10^{-4}$ s^{-1} (n=4) for 50 nM PPIX and $1.02 \times 10^{-2} \pm 7.9 \times 10^{-4}$ s^{-1} (n=2) for 100 nM PPIX. As a result a positive linear relationship between the $k_{Fe(II)PPIX}$ and the concentration PPIX was found, increasing with 9.9×10^{-5} nM^{-1} PPIX. The rate constant normalized to 1 nM PPIX is: $K_{Fe(II)PPIX} = (k_{overall} - k_{ox})/[PPIX] = 1.04 \times 10^{-4} \pm 1.53 \times 10^{-5}$ (n=8).

Plot with $y = 9.9 \times 10^{-5} x + 1.4 \times 10^{-4}$ and $R^2 = 0.981$.
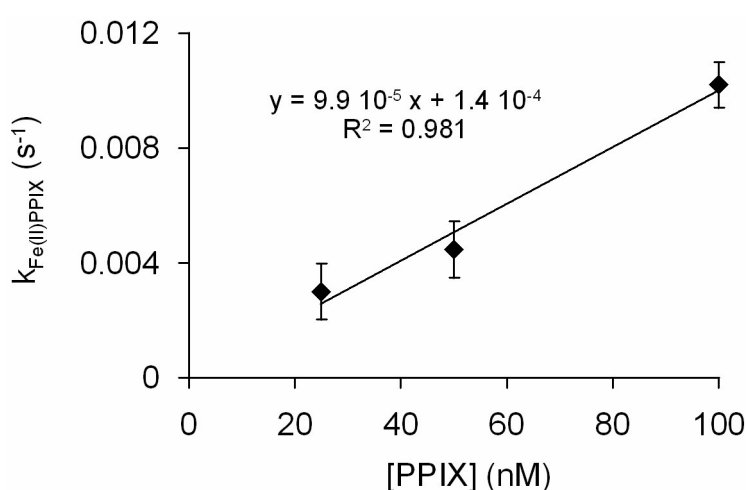
Figure 12. The rate constant of the binding of Fe(II) by PPIX ($k_{Fe(II)PPIX}$) versus the total concentration of added PPIX.

Because PPIX in seawater did not bind Fe(III) but Fe(II) instead, an addition of PPIX concentrations between 65 and 130 nM would always be in excess compared to 2.81 nM Fe(II) (100 nM Fe, no ligand), which explains why we did not see any effects of increasing concentrations of PPIX (Table 6).

Dark reduction of Fe apparently plays an important role in the reduction of Fe(III) to Fe(II). The experimental characteristic that was noticeably different between the photochemical experiments was the increase in Fe(II) concentration after turning off the light. Upon turning the light off, the Fe(II) concentration decreased quickly until a minimum after which the Fe(II) concentration increased again. Comparing the increase in the concentration of Fe(II) in the dark period after irradiance with the concentration of InEqDark Fe(II) in the other experiments revealed that the irradiance treatment had induced a process of Fe reduction even after the light was switched off. A clear linear relationship was found by

plotting the Fe(II) production rate (nM/h) in the dark versus the duration of the irradiance treatment (Figure 13, Table 6). The Fe(II) production rate in the dark increased with 0.13 nM/h for each hour of irradiance ($R^2 = 0.93$) (Figure 13). Dark reduction of Fe is often assigned to reduction of Fe by photoproduced superoxide (Voelker and Sedlak, 1995; Emmenegger et al., 2001).

This distinct behavior of the concentration of Fe(II) versus time in photochemical experiments of Fe(III) and PPIX in seawater could be explained by assuming that four processes are dominating the Fe redox speciation: i) photoreduction of colloidal Fe(III) (reaction 1, Figure 14) (Waite and Morel, 1984; Wells et al., 1991; King et al., 1993), ii) the reduction of Fe(III)
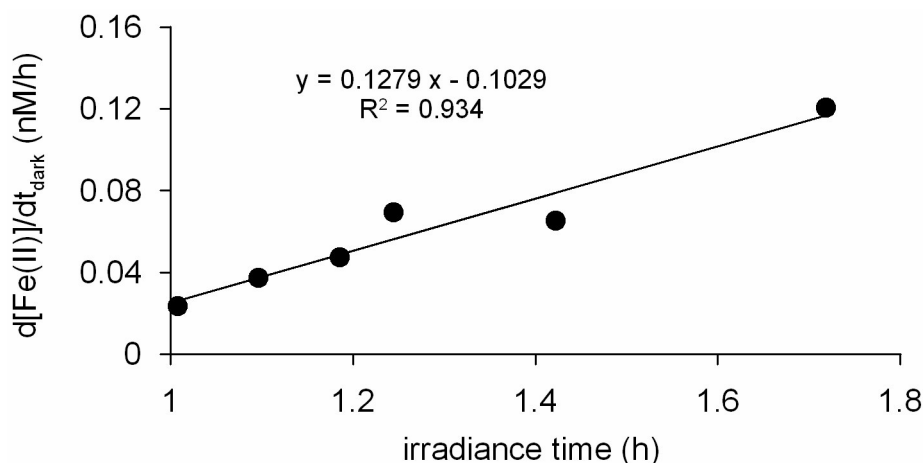
Figure 13. The Fe(II) production rate in the dark after irradiance, versus the irradiance time for Southern Ocean seawater containing 100 nM Fe(III) and various concentrations PPIX (though all in excess over Fe(II)).

by superoxide (reaction 2, Figure 14) (Voelker and Sedlak, 1995; Emmenegger et al., 2001) or free radical ligand species (reaction 3, Figure 14) (Ross and Neta, 1982; Faust, 1994), iii) oxidation of Fe(II) (reaction 4, Figure 14) (Millero et al., 1987; Millero and Sotolongo, 1989; King et al., 1995), and iv) the binding of Fe(II) by PPIX (reaction 5, Figure 14). Free radical ligand species can, depending on their competitive reactions with Fe(III) and O_2, result in Fe(II) or superoxide (reaction 6, Figure 14) (Faust, 1994).

The linear relationship between the duration of the irradiance treatment and the Fe(II) production rate in the dark hinted at a mechanism in which superoxide was involved in the reduction of Fe(III). The production of superoxide was confirmed by the concentration of H_2O_2 produced during irradiation of seawater containing Fe(III) and PPIX. Photochemical experiments (each with 100 nM Fe(III)) with 100 nM DFOB produced 2.85 nM H_2O_2 h^{-1},

Table 6. Experimental characteristics as the concentration InEqDark Fe(II), InPrRate Fe(II), the concentration Max Fe(II), Ox Fe(II), and the concentration FinEqDark Fe(II) for increasing concentrations PPIX added to Southern Ocean seawater. Standard errors are given for InEqDark Fe(II), Max Fe(II) and FinEqDark Fe(II).

	PPIX	PPIX	PPIX	PPIX	PPIX	PPIX
Ligand added (nM)	65	85	90	100	130	130
Fe added (nM)	100	100	100	100	100	100
InEqDark Fe(II) (nM)	0.21 ± 0.0012	0.24 ± 0.0045	0.24 ± 0.0027	0.23 ± 0.0020	0.23 ± 0.0016	0.31 ± 0.0006
InPrRate Fe(II) (nM/h)	11.31	4.31	4.84	4.05	5.47	7.02
Max Fe(II) (nM)	-	-	-	-	-	-
Ox Fe(II) (nM/h)	3.31	2.04	4.74	4.12	4.35	9.87
FinEqDark Fe(II) (slope: nM/h)	0.069	0.037	0.065	0.048	0.024	0.12
MaxProd Fe(II) (nM)	-	-	-	-	-	-
Net dark reduction (norm) (nM/$h_{irradiance}$)	-	-	-	-	-	-

with 100 nM phytic acid produced 1.53 nM H_2O_2 h^{-1} and 80 nM PPIX produced 6.85 H_2O_2 h^{-1}. The concentrations H_2O_2 produced during the experiments with PPIX are 2.5-4.5 times higher than with DFOB or phytic acid. Bimolecular dismutation of superoxide is postulated as the main source of hydrogen peroxide in the open ocean (Petasne and Zika, 1987). The fast oxidation of Fe(II) by superoxide also produces hydrogen peroxide (Weiss, 1935), although the reduction reaction of superoxide with trace metals is faster than the oxidation reaction in seawater (Voelker and Sedlak, 1995).

The photochemistry of metal porphyrins, in particular iron and manganese porphyrins, has attracted scientific interest because of the catalytic efficient behavior of those compounds which have been found to efficiently catalyze thermal redox reactions on organic substrates (Suslick and Watson, 1992; Maldotti et al., 1993). These complexes show photochemical activity which is due to a light induced intramolecular electron transfer involving the metal and the axial ligands. This is a way to induce redox processes in metal-porphyrin complexes which are known frequently to achieve their catalytic/enzymatic activity through reversible modification of the oxidation state of the metal centre (Frausto da Silva and Williams, 1994). Using organic solvents it is shown that irradiation is able to induce redox reactions in Fe-binding porphyrins like PPIX (Bartocci et al., 1980). In particular it has been demonstrated that the irradiation in the axial ligand to metal charge-transfer (LMCT) band results in an intramolecular electron transfer from the axial ligand, such as e.g. alcohols, azide, halides, pyridine, and imidazole (reaction 7, Figure 14) (Maldotti et al., 1993), to iron. This leads to the reduction of Fe(III) to Fe(II) and at the same time to the formation of a free-radical
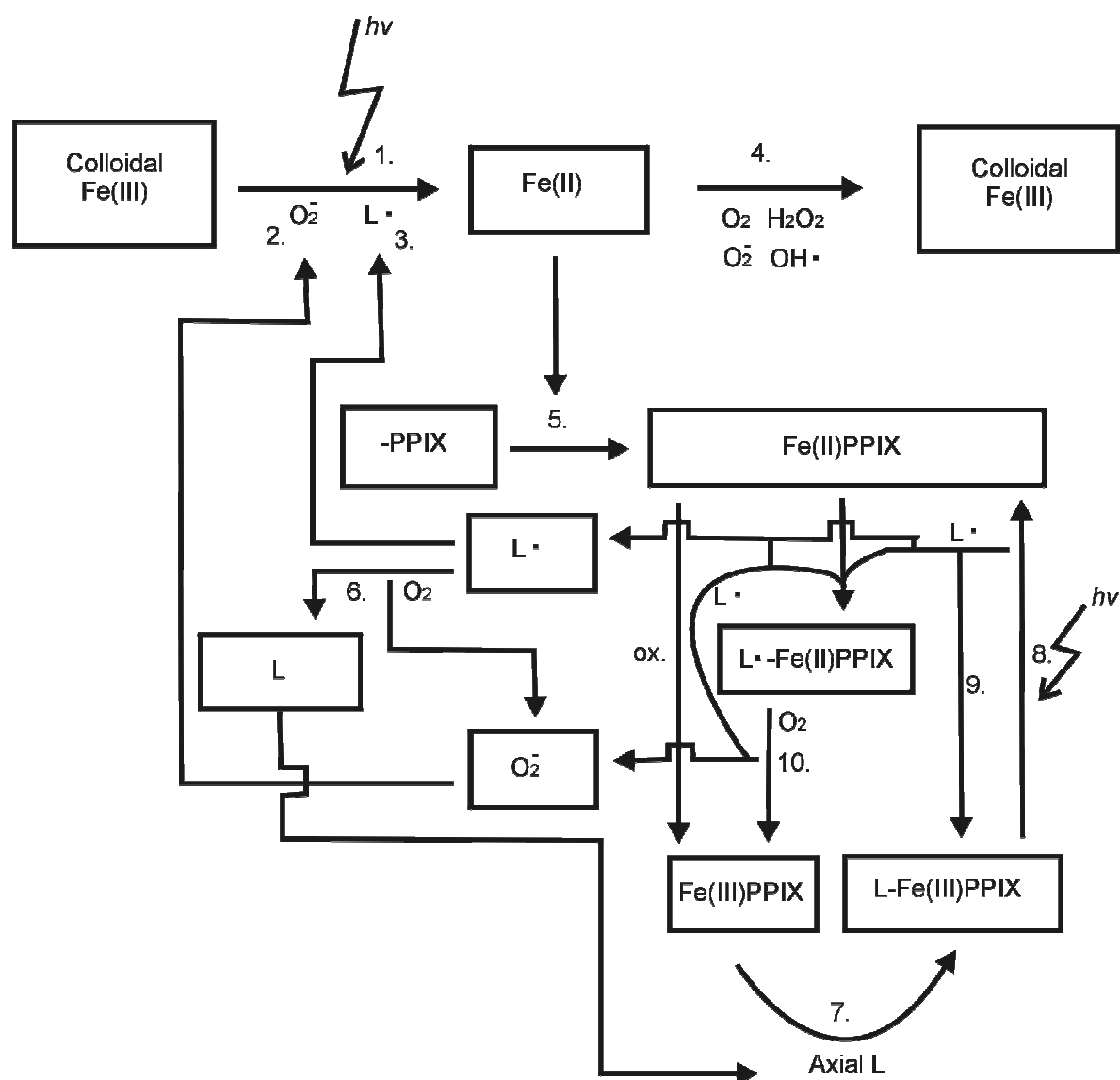
Figure 14. The reaction model as proposed to explain the concentration of Fe(II) as observed in photochemical experiments with PPIX. Key reactions are the photoreduction of Fe originating from amorphous Fe hydroxides (1), the binding of Fe(II) by PPIX (5) and the formation of superoxide (6,10) and eventually free radical ligand species (8,10) involved in the dark reduction of Fe. The formation of superoxide and free radical ligand species from the initial constituents via the formation of Fe(II)PPIX is based on literature of Fe-porphyrin complexes.

species from the axial ligand (7) (Bizet et al., 1981; Bartocci et al., 1985; Ozaki et al., 1987) (reaction 8, Figure 14).

$$L - Fe(III)Por \xrightarrow{\ hv\ } Fe(II)Por + L\cdot \qquad (7)$$

This primary photoredox process may be followed by the reoxidation of the ferrous porphyrin (Fe(II)Por) complex, thus realizing a photo-assisted cycle in which both the intermediates Fe(II)Por and the free radical can induce catalytic processes (8) (Suslick and Watson, 1992) (reaction 9, Figure 14).

$$Fe(II)Por + ox \xrightarrow{\ L\ } L - Fe(III)Por + red \qquad (8)$$

Using oxygenated aqueous ethanol as solvent, Maldotti et al. (1989) have shown that superoxide can be formed in a photo-induced reaction involving an Fe-porphyrin complex. Molecular oxygen is activated by coordination to Fe(II) in the ferrous porphyrin (9, 10) (reaction 10, Figure 14).
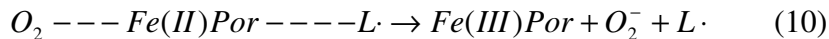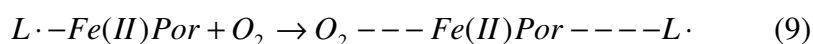
$$L\cdot - Fe(II)Por + O_2 \rightarrow O_2 - - - Fe(II)Por - - - - L\cdot \qquad (9)$$

$$O_2 - - - Fe(II)Por - - - - L\cdot \rightarrow Fe(III)Por + O_2^- + L\cdot \qquad (10)$$

The reactions shown here are leading to the production of superoxide and free radical ligand species which can explain the increased dark reduction of Fe observed with the addition of PPIX to seawater. We propose that similar reactions could occur in natural seawater containing organic matter suitable to complex FePPIX. This means that in the natural environment, the Fe complexed to porphyrin-like molecules can act as photosensitizing catalytic producers of superoxide.

4. Summary and conclusion

Addition of Fe(III) to Southern Ocean seawater resulted in the photoproduction of Fe(II) upon irradiance. The excellent linear increase of e.g. the concentration of MaxProd Fe(II) and InPrRate Fe(II) with the addition of increasing concentrations of Fe(III) revealed that after equilibration, processes such as hydrolization and colloid formation of the Fe did not influence the Fe(II) photoproduction within the experimental time frame (one day). More importantly, these linear relationships resulting from Fe(III) additions higher than the free natural organic Fe binding ligands present in the Southern Ocean seawater, now have shown us that the amorphous Fe hydroxides, and not the organically complexed Fe, were the main

source of the photoproduced Fe(II) pool. This does not mean that organic constituents were not involved in the Fe(II) photoproduction from amorphous Fe hydroxides in Southern ocean seawater. It is known that organic compounds such as e.g. oxalate and citrate adsorbed to colloidal Fe are able to improve the Fe photoredox cycle (Waite and Morel, 1984; Sulzberger and Laubscher, 1995). Yet, the observation of photoproduced Fe(II) after the addition of Fe(III) to artificial seawater showed that inorganic Fe species are also being photoreduced, as suggested by Waite and Morel (1984). These observations are especially important for the elucidation of the Fe chemistry after an Fe enrichment experiment leading to increased phytoplankton growth such as during EisenEx in the Southern Ocean. During EisenEx a fraction of about 13-40% of dissolved Fe was not bound by strong Fe(III)-binding forms and presumably formed inorganic colloids (Boye et al., in press). It is known that this fraction is being photoreduced (Chapter 3, Rijkenberg et al., 2005).

The influence of five ligands (phaeophytin, ferrichrome, DFOB, PPIX and phytic acid) on the photo-induced redox speciation of Fe in Southern Ocean seawater was found to be highly variable. Of the five ligands tested we investigated three Fe-binding ligands in more detail (DFOB, PPIX and phytic acid). The latter Fe-binding ligands each showed a different effect on the photo-induced Fe redox process. Each has its own environmental implications for the Fe chemistry in seawater and subsequent bioavailability for phytoplankton.

The DFOB caused a decrease of the photoproduced Fe(II) concentration in two ways. Firstly, DFOB binds Fe, thus resulting in lower concentrations of amorphous Fe hydroxides and consequently a lower Fe(II) production. Secondly, the DFOB removes the reoxidized Fe(III) from the photo-induced redox cycle by binding this Fe resulting in a decreasing photoreducible Fe fraction. This effect is shown by the linear relationship between the Fe(II) equilibrium developing in the light and the concentration of DFOB. The presence of DFOB and presumably also its marine variants (Martinez et al., 2001; Gledhill et al., 2004) results in lower equilibrium concentrations of Fe(II), and decreased formation of amorphous Fe hydroxides resulting from photocycling of more crystalline colloidal Fe. In the presence of organic ligands such as DFOB, the Fe is transferred into a non-bioavailable organically complexed Fe fraction (Timmermans et al., 2001; Wells and Trick, 2004). This instead of conversion into a more bioavailable amorphous Fe hydroxide fraction upon photo-induced redox cycling (Wells et al., 1991).

Phytic acid operates via another mechanism resulting in an increase in the Fe entering the photo-induced redox cycle. Phytic acid induces the formation of more irregular aggregates with the addition of Fe, increasing the Fe fraction available for photo-induced Fe reduction. This effect is less when the concentration of phytic acid considerably exceeds the Fe(III) concentration. This is probably due to shielding of the surface-bound Fe fraction from photo-induced reduction by adsorption of the phytic acid to the colloid surface. Phytic acid

makes up an important part of the phosphate entering the sea via rivers and could play an important role in the Fe chemistry of coastal waters.

Instead of complexation of PPIX with Fe(III) (Rue and Bruland, 1995; Witter et al., 2000), PPIX forms complexes with Fe(II), thereby decreasing the free Fe(II) concentration. In a photo-sensitizing catalytic reaction of Fe(II)PPIX with light, superoxide is formed, not only influencing the oxygen radical chemistry by enhancing the concentration of superoxide and the concentration of hydrogen peroxide, but also increasing the dark reduction of Fe(III). The latter finding is especially important for marine environments where the phytoplankton community is dependent on rapid Fe recycling of a very small iron pool (Cullen et al., 1992; Price et al., 1994). Much of the regenerated iron in these systems may be present in biological chelates such as porphyrin related molecules, whose release into seawater consequently could have an important influence on the redox speciation of Fe.

We conclude that the organic Fe-complexing ligands are not only important in the photochemistry of Fe as direct electron donors via ligand metal charge transfer reactions (Barbeau et al., 2001) but also via other modes of interaction, such as i) removal of reoxidized Fe(III) from the photo(induced) redoxcycle, ii) via influence on the aggregation of the amorphous Fe hydroxides, and iii) via photosensitizing reactions.

Acknowledgements

References

Anderson, G., 1963. Effect of iron/phosphorus ratio and acid concentration on precipitation of ferric inositol hexaphosphate. J. Sci. Food Agric., 14(5): 352-359.

Anderson, M.A. and Morel, F.M.M., 1980. Uptake of Fe(II) by a diatom in oxic culture medium. Mar. Biol. Let., 1: 263-268.

Anderson, M.A. and Morel, F.M.M., 1982. The influence of aqueous iron chemistry on the uptake of iron by the coastal diatom *Thalassiosira weissflogii*. Limnol. Oceanogr., 27(5): 789-813.

Barbeau, K., Rue, E.L., Bruland, K.W. and Butler, A., 2001. Photochemical cycling of iron in the surface ocean mediated by microbial iron(III)-binding ligands. Nature, 413(6854): 409-413.

Barbeau, K., Rue, E.L., Trick, C.G., Bruland, K.T. and Butler, A., 2003. Photochemical reactivity of siderophores produced by marine heterotrophic bacteria and cyanobacteria based on characteristic Fe(III) binding groups. Limnol. Oceanogr., 48(3): 1069-1078.

Bartocci, C., Maldotti, A., Carassiti, V., Traverso, O. and Ferri, A., 1985. Intramolecular photoredox reactions in iron(III) cytochrome-c and its azide derivative. Inorg. Chim. Acta, 107(1): 5-12.

Bartocci, C., Scandola, F., Ferri, A. and Carassiti, V., 1980. Photo-reduction of hemin in alcohol-containing mixed-solvents. J. Am. Chem. Soc., 102(23): 7067-7072.

Bizet, C., Morliere, P., Brault, D., Delgado, O., Bazin, M. and Santus, R., 1981. Photo-reduction of iron(III)porphyrins. Photochem. Photobiol., 34(3): 315-321.

Borer, P.M., Sulzberger, B., Reichard, P. and Kraemer, S.M., 2005. Effect of siderophores on the light induced dissolution of colloidal iron(III) (hydr)oxides. Mar. Chem., 93: 179-193.

Bowie, A.R., Achterberg, E.P., Sedwick, P.N., Ussher, S. and Worsfold, P.J., 2002. Real-time monitoring of picomolar concentrations of iron(II) in marine waters using automated flow injection-chemiluminescence instrumentation. Environ. Sci. Technol., 36(21): 4600-4607.

Boye, M., Aldrich, A.P., van den Berg, C.M.G., de Jong, J.T.M., Veldhuis, M. and de Baar, H.J.W., 2003. Horizontal gradient of the chemical speciation of iron in surface waters of the northeast Atlantic Ocean. Mar. Chem., 80(2-3): 129-143.

Boye, M., Nishioka, J., Croot, P.L., Laan, P., Timmermans, K.R. and de Baar, H.J.W., submitted. Major deviations of iron complexation during 22 days of a mesoscale iron enrichment in the open Southern Ocean. Mar. Chem.

Boye, M., van den Berg, C.M.G., de Jong, J.T.M., Leach, H., Croot, P.L. and de Baar, H.J.W., 2001. Organic complexation of iron in the Southern Ocean. Deep Sea Res. I, 48(6): 1477-1497.

Boye, M.e.a., in press. Major deviations of iron complexation during 22 days of a mesoscale iron enrichment in the open Southern Ocean. Marine Chemistry.

Bruland, K.W., Rue, E.L. and Smith, G.J., 2001. Iron and macronutrients in California coastal upwelling regimes: Implications for diatom blooms. Limnol. Oceanogr., 46(7): 1661-1674.

Celi, L., De Luca, G. and Barberis, E., 2003. Effects of interaction of organic and inorganic P with ferrihydrite and kaolinite-iron oxide systems on iron release. Soil Sci., 168(7): 479-488.

Cornell, R.M. and Schwertmann, U., 1996. The Iron Oxides. VCH Publishers, New York.

Croot, P.L., Bowie, A.R., Frew, R.D., Maldonado, M.T., Hall, J.A., Safi, K.A., la Roche, J., Boyd, P.W. and Law, C.S., 2001. Retention of dissolved iron and Fe-II in an iron induced Southern Ocean phytoplankton bloom. Geophys. Res. Lett., 28(18): 3425-3428.

Croot, P.L. and Johansson, M., 2000. Determination of iron speciation by cathodic stripping voltammetry in seawater using the competing ligand 2-(2- thiazolylazo)-p-cresol (TAC). Electroanalysis, 12(8): 565-576.

Cullen, J.J., Lewis, M.R., Davis, C.O. and Barber, R.T., 1992. Photosynthetic characteristics and estimated growth-rates indicate grazing is the proximate control of primary production in the equatorial Pacific. J. Geophys. Res., 97(C1): 639-654.

de Baar, H.J.W., Buma, A.G.J., Nolting, R.F., Cadee, G.C., Jacques, G. and Treguer, P.J., 1990. On iron limitation of the Southern Ocean - experimental- observations in the Weddell and Scotia seas. Mar. Ecol. Progr. Ser., 65(2): 105-122.

de Jong, J.T.M., den Das, J., Bathmann, U., Stoll, M.H.C., Kattner, G., Nolting, R.F. and de Baar, H.J.W., 1998. Dissolved iron at subnanomolar levels in the Southern Ocean as determined by ship-board analysis. Anal. Chim. Acta, 377(2-3): 113-124.

Emmenegger, L., Schonenberger, R.R., Sigg, L. and Sulzberger, B., 2001. Light-induced redox cycling of iron in circumneutral lakes. Limnol. Oceanogr., 46(1): 49-61.

Faust, B.C., 1994. A review of the photochemical redox reactions of iron(III) species in atmospheric, oceanic, and surface waters: Influences on geochemical cycles and oxidant formation. In: G.R. Helz, R.G. Zepp and D.G. Crosby (Editors), Aquatic Surface Photochemistry. CRC Press, Inc., London, pp. 3-37.

Frausto da Silva, J.J.R. and Williams, R.J.P., 1994. Haem iron: coupled redox reactions, The biological chemistry of the elements. Clarendon Press, Oxford, pp. 343-369.

Geider, R.J. and la Roche, J., 1994. The role of iron in phytoplankton photosynthesis, and the potential for iron-limitation of primary productivity in the sea. Photosynth. Res., 39(3): 275-301.

Geider, R.J., la Roche, J., Greene, R.M. and Olaizola, M., 1993. Response of the photosynthetic apparatus of *Phaeodactylum tricornutum* (Bacillariophyceae) to nitrate, phosphate, or iron starvation. J. Phycol., 29(6): 755-766.

Gerringa, L.J.A., Herman, P.M.J. and Poortvliet, T.C.W., 1995. Comparison of the linear van den Berg Ruzic transformation and a nonlinear fit of the Langmuir isotherm applied to Cu speciation data in the estuarine environment. Mar. Chem., 48(2): 131-142.

Gerringa, L.J.A., Rijkenberg, M.J.A., Timmermans, K.R. and Buma, A.G.J., 2004. The influence of solar ultraviolet radiation on the photochemical production of H_2O_2 in the equatorial Atlantic Ocean. J. Sea Res., 51(1): 3-10.

Gledhill, M., McCormack, P., Ussher, S., Achterberg, E.P., Mantoura, R.F.C. and Worsfold, P.J., 2004. Production of siderophore type chelates by mixed bacterioplankton populations in nutrient enriched seawater incubations. Mar. Chem., 88(1-2): 75-83.

Gledhill, M. and van den Berg, C.M.G., 1994. Determination of complexation of iron(III) with natural organic complexing ligands in seawater using cathodic stripping voltammetry. Mar. Chem., 47(1): 41-54.

Gledhill, M., van den Berg, C.M.G., Nolting, R.F. and Timmermans, K.R., 1998. Variability in the speciation of iron in the northern North Sea. Mar. Chem., 59(3-4): 283-300.

Granger, J. and Price, N.M., 1999. The importance of siderophores in iron nutrition of heterotrophic marine bacteria. Limnol. Oceanogr., 44(3): 541-555.

Greene, R.M., Geider, R.J. and Falkowski, P.G., 1991. Effect of iron limitation on photosynthesis in a marine diatom. Limnol. Oceanogr., 36(8): 1772-1782.

Harrison, G.I. and Morel, F.M.M., 1986. Response of the marine diatom *Thalassiosira weisflogii* to iron stress. Limnol. Oceanogr., 31: 989-997.

Hudson, R.J.M., Covault, D.T. and Morel, F.M.M., 1992. Investigations of iron coordination and redox reactions in seawater using Fe-59 radiometry and ion-pair solvent-extraction of amphiphilic iron complexes. Mar. Chem., 38(3-4): 209-235.

Hutchins, D.A. and Bruland, K.W., 1998. Iron-limited diatom growth and Si: N uptake ratios in a coastal upwelling regime. Nature, 393(6685): 561-564.

Hutchins, D.A., Franck, V.M., Brzezinski, M.A. and Bruland, K.W., 1999. Inducing phytoplankton iron limitation in iron-replete coastal waters with a strong chelating ligand. Limnol. Oceanogr., 44(4): 1009-1018.

Johnson, K.S., Coale, K.H., Elrod, V.A. and Tindale, N.W., 1994. Iron photochemistry in seawater from the equatorial Pacific. Mar. Chem., 46(4): 319-334.

Johnson, K.S., Gordon, R.M. and Coale, K.H., 1997. What controls dissolved iron concentrations in the world ocean? Mar. Chem., 57(3-4): 137-161.

King, D.W., Aldrich, R.A. and Charnecki, S.E., 1993. Photochemical redox cycling of iron in NaCl solutions. Mar. Chem., 44(2-4): 105-120.

King, D.W., Lounsbury, H.A. and Millero, F.J., 1995. Rates and mechanism of Fe(II) oxidation at nanomolar total iron concentrations. Environ. Sci. Technol., 29(3): 818-824.

Kuma, K., Nakabayashi, S. and Matsunaga, K., 1995. Photoreduction of Fe(III) by hydroxycarboxylic acids in seawater. Water Res., 29(6): 1559-1569.

Kuma, K., Nishioka, J. and Matsunaga, K., 1996. Controls on iron(III) hydroxide solubility in seawater: The influence of pH and natural organic chelators. Limnol. Oceanogr., 41(3): 396-407.

Kunkely, H. and Vogler, A., 2001. Photoreduction of aqueous ferrioxamine B by oxalate induced by outer-sphere charge transfer excitation. Inorg. Chem. Commun., 4(4): 215-217.

Liu, X.W. and Millero, F.J., 1999. The solubility of iron hydroxide in sodium chloride solutions. Geochim. Cosmochim. Acta, 63(19-20): 3487-3497.

Liu, X.W. and Millero, F.J., 2002. The solubility of iron in seawater. Mar. Chem., 77(1): 43-54.

Macrellis, H.M., Trick, C.G., Rue, E.L., Smith, G. and Bruland, K.W., 2001. Collection and detection of natural iron-binding ligands from seawater. Mar. Chem., 76(3): 175-187.

Maldonado, M.T. and Price, N.M., 2000. Nitrate regulation of Fe reduction and transport by Fe-limited *Thalassiosira oceanica*. Limnol. Oceanogr., 45(4): 814-826.

Maldonado, M.T. and Price, N.M., 2001. Reduction and transport of organically bound iron by *Thalassiosira oceanica* (Bacillariophyceae). J. Phycol., 37(2): 298-309.

Maldotti, A., Amadelli, R., Bartocci, C., Carassiti, V., Polo, E. and Varani, G., 1993. Photochemistry of iron-porphyrin complexes - biomimetics and catalysis. Coord. Chem. Rev., 125(1-2): 143-154.

Maldotti, A., Bartocci, C., Amadelli, R. and Carassiti, V., 1989. Photocatalytic reactions in the 2,3,7,8,12,13,17,18-octaethyl-porphyrinatoiron(III) ethanol carbon-tetrachloride system. J. Chem. Soc., Dalton Trans.(6): 1197-1201.

Martin, J.H., Coale, K.H., Johnson, K.S., Fitzwater, S.E., Gordon, R.M., Tanner, S.J., Hunter, C.N., Elrod, V.A., Nowicki, J.L., Coley, T.L., Barber, R.T., Lindley, S., Watson, A.J., Vanscoy, K., Law, C.S., Liddicoat, M.I., Ling, R., Stanton, T., Stockel, J., Collins, C., Anderson, A., Bidigare, R., Ondrusek, M., Latasa, M., Millero, F.J., Lee, K., Yao, W., Zhang, J.Z., Friederich, G., Sakamoto, C., Chavez, F., Buck, K., Kolber, Z., Greene, R., Falkowski, P., Chisholm, S.W., Hoge, F., Swift, R., Yungel, J., Turner, S., Nightingale, P., Hatton, A., Liss, P. and Tindale, N.W., 1994. Testing the iron hypothesis in ecosystems of the equatorial Pacific Ocean. Nature, 371(6493): 123-129.

Martin, J.H. and Fitzwater, S.E., 1988. Iron-deficiency limits phytoplankton growth in the northeast Pacific subarctic. Nature, 331(6154): 341-343.

Martin, J.H., Gordon, R.M. and Fitzwater, S.E., 1990. Iron in Antarctic waters. Nature, 345(6271): 156-158.

Martinez, J.S., Haygood, M.G. and Butler, A., 2001. Identification of a natural desferrioxamine siderophore produced by a marine bacterium. Limnol. Oceanogr., 46(2): 420-424.

McCormack, P., Worsfold, P.J. and Gledhill, M., 2003. Separation and detection of siderophores produced by marine bacterioplankton using high-performance liquid chromatography with electrospray ionization mass spectrometry. Anal. Chem., 75(11): 2647-2652.

Miller, W.L. and Kester, D., 1994. Photochemical iron reduction and iron bioavailability in seawater. J. Mar. Res., 52: 325-343.

Miller, W.L. and Kester, D.R., 1988. Hydrogen peroxide measurement in seawater by (para-hydroxyphenyl)acetic acid dimerization. Anal. Chem., 60(24): 2711-2715.

Miller, W.L. and Kester, D.R., 1994. Peroxide variations in the Sargasso sea. Mar. Chem., 48(1): 17-29.

Millero, F.J., 1998. Solubility of Fe(III) in seawater. Earth. Planet. Sci. Let., 154(1-4): 323-329.

Millero, F.J. and Sotolongo, S., 1989. The oxidation of Fe(II) with H_2O_2 in seawater. Geochim. Cosmochim. Acta, 53(8): 1867-1873.

Millero, F.J., Sotolongo, S. and Izaguirre, M., 1987. The oxidation-kinetics of Fe(II) in seawater. Geochim. Cosmochim. Acta, 51(4): 793-801.

Moffett, J.W., 2001. Transformations among different forms of iron in the ocean. In: D.R. Turner and K.A. Hunter (Editors), The Biogeochemistry of Iron in Seawater. IUPAC series on analytical and physical chemistry of environmental systems. John Wiley & Sons, LTD, New York, pp. 343-372.

Monzyk, B. and Crumbliss, A.L., 1982. Kinetics and mechanism of the stepwise dissociation of iron(III) from ferrioxamine-B in aqueous acid. J. Am. Chem. Soc., 104(18): 4921-4929.

Nishioka, J., Takeda, S., de Baar, H.J.W., Laan, P., Croot, P.L., Boye, M. and Timmermans, K.R., in press. Change in the concentrations of iron in different size fractions during an iron fertilization experiment in the Southern Ocean, EisenEx study. Mar. Chem.

Nolting, R.F., Gerringa, L.J.A., Swagerman, M.J.W., Timmermans, K.R. and de Baar, H.J.W., 1998. Fe(III) speciation in the high nutrient, low chlorophyll Pacific region of the Southern Ocean. Mar. Chem., 62(3-4): 335-352.

O'Sullivan, D.W., Hanson, A.K. and Kester, D.R., 1995. Stopped-flow luminol chemiluminescence determination of Fe(II) and reducible iron in seawater at subnanomolar levels. Mar. Chem., 49(1): 65-77.

Ognalaga, M., Frossard, E. and Thomas, F., 1994. Glucose-1-phosphate and myoinositol hexaphosphate adsorption mechanisms on goethite. Soil Sci. Soc. Am. J., 58(2): 332-337.

Ozaki, Y., Iriyama, K., Ogoshi, H. and Kitagawa, T., 1987. Ligand-aided photoreduction of iron porphyrin complexes probed by resonance raman-spectroscopy. J. Am. Chem. Soc., 109(19): 5583-5586.

Parfitt, R.L., 1989. Phosphate reactions with natural allophane, ferrihydrite and goethite. J. Soil Sci., 40(2): 359-369.

Pehkonen, S.O., Siefert, R., Erel, Y., Webb, S. and Hoffmann, M.R., 1993. Photoreduction of iron oxyhydroxides in the presence of important atmospheric organic-compounds. Environ. Sci. Technol., 27(10): 2056-2062.

Pehkonen, S.O., Siefert, R.L. and Hoffmann, M.R., 1995. Photoreduction of iron oxyhydroxides and the photooxidation of halogenated acetic-acids. Environ. Sci. Technol., 29(5): 1215-1222.

Petasne, R.G. and Zika, R.G., 1987. Fate of superoxide in coastal seawater. Nature, 325(6104): 516-518.

Price, N.M., Ahner, B.A. and Morel, F.M.M., 1994. The equatorial Pacific Ocean - grazer-controlled phytoplankton populations in an iron-limited ecosystem. Limnol. Oceanogr., 39(3): 520-534.

Pullin, M.J. and Cabaniss, S.E., 2003. The effects of pH, ionic strength, and iron-fulvic acid interactions on the kinetics of non-photochemical iron transformations. II. The kinetics of thermal reduction. Geochim. Cosmochim. Acta, 67(21): 4079-4089.

Raven, J.A., 1990. Predictions of Mn and Fe use efficiencies of phototrophic growth as a function of light availability for growth and of C assimilation pathway. New Phytologist, 116(1): 1-18.

Rijkenberg, M.J.A., Fischer, A.C., Kroon, J.J., Gerringa, L.J.A., Timmermans, K.R., Wolterbeek, H.T. and de Baar, H.J.W., 2005. The influence of UV irradiation on the photoreduction of iron in the Southern Ocean. Mar. Chem., 93: 119-129.

Rose, A.L. and Waite, T.D., 2002. Kinetic model for Fe(II) oxidation in seawater in the absence and presence of natural organic matter. Environ. Sci. Technol., 36(3): 433-444.

Ross, A.B. and Neta, P., 1982. Rate constants for reactions of aliphatic carbon-centered radicals in aqueous solution. *Natl. Stand. Ref. Data Ser.*, NSRDS-NBS-70: U.S. National Bureau of Standards.

Rue, E.L. and Bruland, K.W., 1995. Complexation of iron(III) by natural organic-ligands in the central north Pacific as determined by a new competitive ligand equilibration adsorptive cathodic stripping voltammetric method. Mar. Chem., 50(1-4): 117-138.

Rue, E.L. and Bruland, K.W., 1997. The role of organic complexation on ambient iron chemistry in the equatorial Pacific Ocean and the response of a mesoscale iron addition experiment. Limnol. Oceanogr., 42(5): 901-910.

Rueter, J.G. and Ades, D.R., 1987. The role of iron nutrition in photosynthesis and nitrogen assimilation in *Scenedesmus quadricauda* (Chlorophyceae). J. Phycol., 23(3): 452-457.

Rueter, J.G., Ohki, K. and Fujita, Y., 1990. The effect of iron nutrition on photosynthesis and nitrogen- fixation in cultures of *Trichodesmium* (Cyanophyceae). J. Phycol., 26(1): 30-35.

Santana-Casiano, J.M., Gonzalez-Davila, M. and Millero, F.J., 2004. The oxidation of Fe(II) in NaCl-HCO_3- and seawater solutions in the presence of phthalate and salicylate ions: a kinetic model. Mar. Chem., 85(1-2): 27-40.

Santana-Casiano, J.M., Gonzalez-Davila, M., Rodriguez, M.J. and Millero, F.J., 2000. The effect of organic compounds in the oxidation kinetics of Fe(II). Mar. Chem., 70(1-3): 211-222.

Schwertmann, U. and Fischer, W.R., 1973. Natural amorphous ferric hydroxide. Geoderma, 10: 237-247.

Schwertmann, U. and Taylor, R.M., 1972. The transformationof lepidocrocite to goethite. Clays Clay Miner., 20: 151-158.

Schwertmann, U. and Thalmann, H., 1976. The influence of [FeII], [Si], and pH on the formation of lepidocrocite and ferrihydrite during oxidation of aqueous $FeCl_2$ solutions. Clay Miner., 11: 189-200.

Seitz, W.R. and Hercules, D.M., 1972. Determination of trace amounts of iron (II) using chemiluminescence analysis. Anal. Chem., 44: 2143-2149.

Siffert, C. and Sulzberger, B., 1991. Light-induced dissolution of hematite in the presence of oxalate - a case-study. Langmuir, 7(8): 1627-1634.

Steeneken, S.F., Buma, A.G.J. and Gieskes, W.W.C., 1995. Changes in transmission characteristics of polymethylmethacrylate and cellulose-(III) acetate during exposure to ultraviolet-light. Photochem. Photobiol., 61(3): 276-280.

Strzepek, R.F. and Harrison, P.J., 2004. Photosynthetic architecture differs in coastal and oceanic diatoms. Nature, 431(7009): 689-692.

Sulzberger, B. and Laubscher, H., 1995. Reactivity of various types of iron(III) (hydr)oxides towards light-induced dissolution. Mar. Chem., 50(1-4): 103-115.

Sunda, W.G., Swift, D.G. and Huntsman, S.A., 1991. Low iron requirement for growth in oceanic phytoplankton. Nature, 351(6321): 55-57.

Suslick, K.S. and Watson, R.A., 1992. The photochemistry of chromium, manganese, and iron porphyrin complexes. New J. Chem., 16(5): 633-642.

Suzumura, M. and Kamatani, A., 1995. Origin and distribution of inositol hexaphosphate in estuarine and coastal sediments. Limnol. Oceanogr., 40(7): 1254-1261.

Takeda, S. and Kamatani, A., 1989. Photoreduction of Fe(III)-EDTA complex and its availability to the coastal diatom *Thalassiosira weissflogii*. Red Tides: Biol., Environ. Sci., Toxicol.: 349-352.

Theis, T.L. and Singer, P.C., 1974. Complexation of iron(II) by organic matter and its effect on iron(II) oxygenation. Environ. Sci. Technol., 8(6): 569-573.

Timmermans, K.R., Gerringa, L.J.A., de Baar, H.J.W., van der Wagt, B., Veldhuis, M.J.W., de Jong, J.T.M., Croot, P.L. and Boye, M., 2001. Growth rates of large and small Southern Ocean diatoms in relation to availability of iron in natural seawater. Limnol. Oceanogr., 46(2): 260-266.

Tipping, E., Thompson, D.W. and Woof, C., 1989. Iron-oxide particulates formed by the oxygenation of natural and model lakewaters containing Fe(II). Archiv Fur Hydrobiologie, 115(1): 59-70.

Trick, C.G., 1989. Hydroxamate-siderophore production and utilization by marine eubacteria. Curr. Microbiol., 18: 375-378.

van den Berg, C.M.G., 1995. Evidence for organic complexation of iron in seawater. Mar. Chem., 50(1-4): 139-157.

Voelker, B.M., Morel, F.M.M. and Sulzberger, B., 1997. Iron redox cycling in surface waters: Effects of humic substances and light. Environ. Sci. Technol., 31(4): 1004-1011.

Voelker, B.M. and Sedlak, D.L., 1995. Iron reduction by photoproduced superoxide in seawater. Mar. Chem., 50(1-4): 93-102.

Waite, D.T. and Morel, F.M.M., 1984. Photoreductive dissolution of colloidal iron oxides in natural waters. Environ. Sci. Technol., 18: 860-868.

Waite, T.D., 2001. Thermodynamics of the iron system in seawater. In: D.R. Turner and K.A. Hunter (Editors), The biogeochemistry of iron in seawater. IUPAC series on Analytical and Physical Chemistry of Environmental Systems. John Wiley & Sons, LTD, pp. 291-342.

Waite, T.D. and Morel, F.M.M., 1984. Photoreductive dissolution of colloidal iron-oxide - effect of citrate. J. Colloid Interface Sci., 102(1): 121-137.

Waite, T.D. and Torikov, A., 1987. Photo-assisted dissolution of colloidal iron-oxides by thiol-containing compounds.2. Comparison of lepidocrocite (gamma- FeOOH) and hematite (alpha-Fe_2O_3) dissolution. J. Colloid Interface Sci., 119(1): 228-235.

Waite, T.D., Torikov, A. and Smith, J.D., 1986. Photoassisted dissolution of colloidal iron-oxides by thiol- containing compounds.1. Dissolution of hematite (alpha-Fe_2O_3). J. Colloid Interface Sci., 112(2): 412-420.

Weiss, J., 1935. Elektronenübergangsprozesse im Mechanismus von Oxidations- und Reduktionsreaktionen in Lösungen. Die Naturwissenschaften, 4: 64-69.

Wells, M.L., 1999. Manipulating iron availability in nearshore waters. Limnol. Oceanogr., 44(4): 1002-1008.

Wells, M.L. and Mayer, L.M., 1991. The photoconversion of colloidal iron oxyhydroxides in seawater. Deep Sea Res. I, 38(11): 1379-1395.

Wells, M.L., Mayer, L.M., Donard, O.F.X., Sierra, M.M.D. and Ackelson, S.G., 1991. The photolysis of colloidal iron in the oceans. Nature, 353(6341): 248-250.

Wells, M.L., Price, N.M. and Bruland, K.W., 1994. Iron limitation and the cyanobacterium *Synechococcus* in equatorial Pacific waters. Limnol. Oceanogr., 39(6): 1481-1486.

Wells, M.L. and Trick, C.G., 2004. Controlling iron availability to phytoplankton in iron-replete coastal waters. Mar. Chem., 86(1-2): 1-13.

Wilhelm, S.W. and Trick, C.G., 1994. Iron-limited growth of cyanobacteria: multiple siderophore production is a common response. Limnol. Oceanogr., 39(8): 1979-1984.

Witter, A.E., Hutchins, D.A., Butler, A. and Luther, G.W., 2000. Determination of conditional stability constants and kinetic constants for strong model Fe-binding ligands in seawater. Mar. Chem., 69(1-2): 1-17.

Witter, A.E., Lewis, B.L. and Luther, G.W., 2000. Iron speciation in the Arabian Sea. Deep Sea Res. II, 47(7-8): 1517-1539.

Witter, A.E. and Luther, G.W., 1998. Variation in Fe-organic complexation with depth in the northwestern Atlantic Ocean as determined using a kinetic approach. Mar. Chem., 62(3-4): 241-258.

Wu, J.F. and Luther, G.W., 1995. Complexation of Fe(III) by natural organic-ligands in the northwest Atlantic Ocean by a competitive ligand equilibration method and a kinetic approach. Mar. Chem., 50(1-4): 159-177.

Xiao, C.B., Palmer, D.A., Wesolowski, D.J., Lovitz, S.B. and King, D.W., 2002. Carbon dioxide effects on luminol and 1,10-phenanthroline chemiluminescence. Anal. Chem., 74(9): 2210-2216.

Chapter 6

Diatoms enhance the reactive Fe pool: increasing Fe-photoreduction and light-independent modification of strong Fe-binding ligands

Micha J.A. Rijkenberg, Loes J.A. Gerringa, Klaas R. Timmermans, Astrid C. Fischer, Koos J. Kroon, Anita G.J. Buma, Bert Th. Wolterbeek and Hein J.W. de Baar

Abstract

Short term (2 days) laboratory studies showed the modification of Fe speciation in seawater by two open oceanic Antarctic diatom species, *Thalassiosira* sp. and *Chaetoceros brevis*. Three light conditions were used during these experiments: the total spectrum (visible light (VIS; 400-700 nm) + ultraviolet B (UVB; 280-315 nm) + ultraviolet A (UVA; 315-400 nm)) and the others by exclusion of UVB and UVB+UVA, respectively. An increase in the Fe(II) concentration during the second day of the experiments in concert with an increasing importance of VIS suggests a modification of the photoreducible Fe fraction due to organic substances released by the diatoms. Furthermore, *C. brevis* modifies part of the strong Fe-binding ligand assemblage resulting in weaker Fe-binding ligands. This effect has not been observed in cultures with *Thalassiosira* sp. Overall, these diatoms appear to actively enhance the reactive Fe pool and improve the biological availability of Fe.

1. Introduction

Iron, Fe, present in high concentrations in seawater during the anoxic past of the earth (Falkowski and Raven, 1997; Turner et al., 2001), evolved to be a key element in many biochemical reactions, e.g. nitrogen fixation and photosynthesis (Rueter and Ades, 1987; Geider et al., 1993). With the ensuing oxygenation of the oceans and the atmosphere (Holland, 1984; Turner and Hunter, 2001), the dissolved Fe was removed from the oceans and became a "hard to get essential" (Martin and Fitzwater, 1988), inducing the evolution of specialized Fe harvesting strategies in marine organisms (Price and Morel, 1998). The Southern Ocean is an example of a modern marine environment where Fe, next to light and grazing, is strongly limiting primary production (de Baar et al., 1990; Martin et al., 1990) and affecting biogeochemical cycles, notably that of carbon dioxide (de Baar and Boyd, 2000).

The Fe(III) has a very low solubility in seawater and rapidly becomes hydrolyzed into various Fe(III) oxyhydroxides (Millero, 1998; Liu and Millero, 1999; Liu and Millero, 2002). Organic complexation of Fe(III) into an Fe-ligand complex (FeL) in seawater increases its

solubility (Kuma et al., 1996; Johnson et al., 1997). These organic ligands are often found in excess over the dissolved Fe pool (Boye et al., 2001). The reduced Fe(II), although better soluble in seawater, becomes rapidly oxidized by O_2 and H_2O_2 (Millero et al., 1987; Millero and Sotolongo, 1989; King et al., 1995).

Redox reactions and speciation have shown to be important for the bioavailability of Fe for phytoplankton. The Fe(II) is suggested to be suitable for biological uptake (Anderson and Morel, 1980; Anderson and Morel, 1982; Takeda and Kamatani, 1989; Maldonado and Price, 2001). Furthermore, the Fe redox cycle initiated by photochemical processes is mentioned as an important mechanism by which (colloidal) Fe is converted into more reactive species (defined by the research method applied) resulting in a higher bioavailability to phytoplankton (Finden et al., 1984; Wells and Mayer, 1991; Johnson et al., 1994; Miller and Kester, 1994).

Photo-induced production of Fe(II) is the major source for the production of Fe(II) in the marine environment (Hong and Kester, 1986; Croot et al., 2001; Chapter 3, Rijkenberg et al., 2005). However, various reports describe Fe(II) maxima coinciding with chlorophyll-*a* maxima (O'Sullivan et al., 1991; Emmenegger et al., 2001; Shaked et al., 2002). The ability of different phytoplankton species to enzymatically reduce Fe(III) at the cell surface is known for a long time (Allnut and Bonner, 1987; Jones and Morel, 1988; Maldonado and Price, 2000). Furthermore, Kuma et al. (1992) noticed high concentrations of Fe(II) during spring blooms in Funka Bay (Japan) and relates this to the release of organic components from phytoplankton inducing the photoreduction of Fe. The presence of various dissolved organic substances, generally considered to be released by phytoplankton, e.g. sugar acids, indeed improved the photoreduction of Fe (Kuma et al., 1995).

Marine Fe(III)-siderophore complexes, which are high affinity Fe(III) binding ligands secreted by e.g. marine bacteria to scavenge and transport Fe (Trick, 1989; Wilhelm and Trick, 1994; Granger and Price, 1999), have shown to be photo-reactive producing Fe(II) in the light (Barbeau et al., 2001; Barbeau et al., 2002; Barbeau et al., 2003). Photoredox reactions of Fe ligand complexes occur via a ligand to metal charge transfer (LMCT) reaction resulting in the production of Fe(II) and a non-reversible decomposed organic ligand (Waite and Morel, 1984). This suggests that the concentration of photo-reactive Fe binding ligands would decrease under irradiance, thus leaving behind the non-photoreactive Fe binding ligands present (Boye et al., 2001; Powell and Wilson-Finelli, 2003). Yet, the importance of siderophores or other strong Fe-binding ligands in the photoproduction of Fe(II) in the marine environment is still uncertain (Chapter 8).

In this study we investigated the influence of two typical open oceanic Antarctic diatoms species, *Thalassiosira* sp. and *Chaetoceros brevis*, on the photo(induced) changes in Fe speciation in Southern Ocean seawater. We describe three experiments varying the

phytoplankton species and/or Fe concentration. Short term experiments were chosen as it allows observation of an immediate, or at least short-term, response of Fe speciation within 24-36 hours while the plankton community remains relatively uniform (Timmermans et al., 1998).

2. Materials and methods

2.1 Diatoms

C. brevis is a small diatom, 4-6 μm, with a k_m for Fe of 0.6 x 10^{-12} nM and a maximal growth rate of 0.39 d^{-1}, growing as single cells (Timmermans et al., 2001). *Thalassiosira* sp. is a big chain forming diatom, 70 μm, with a k_m for Fe of 0.62 nM and a maximal growth rate of 0.31 d^{-1} (Timmermans et al., 2004). The *C. brevis* and *Thalassiosira* sp. cells were pre-cultivated in the same Southern Ocean seawater as used during the experiments, however with a 5 nM Fe addition. It was impossible to grow the diatoms under Fe limitation and still be able to collect enough biomass to perform the experiments.

Thalassiosira sp. cells were taken from Southern Ocean seawater with silicon tubing as follows: one opening of the silicon tubing was covered with a fine acid-cleaned. ~36 µm polyamide (ZBF, Mesh + Technology, Switzerland) filter. The culture was then gently sucked through the filter with a vacuum pump leaving the diatom cells behind on the filter. Cells were subsequently rinsed and gently resuspended in Southern Ocean seawater. The cells were counted, followed by inoculation in the PMMA bottles. The *C. brevis* culture was dense enough to inoculate the PMMA bottles directly.

Thalassiosira sp. cells were counted in 5 ml settling chambers under an inverted microscope; *C. brevis* was counted using an Epics XL flowcytometer.

2.2 Seawater

Clean Southern Ocean surface water (51ºS 20ºE, 1 November 2000) was pumped into an over-pressurized class 100 clean air container using a Teflon diaphragm pump (Almatec A-15, Germany) driven by a compressor (Jun-Air, Denmark, model 600-4B) connected via acid-washed braided PVC tubing to a torpedo towed at approximately 5 m alongside the ship (Polarstern, ANTXVIII/2). The seawater was filtered in-line by a filter (Sartorius Sartobran filter capsule 5231307H8) with a cut-off of 0.2 μm. Back in the laboratory the tank (volume of 1 m^3) was stored at room temperature. The Southern Ocean seawater contained 0.32 nM dissolved Fe and 1.69 ± 0.19 equivalents of nM Fe of natural ligands with a conditional stability constant (log K') of 21.43 ± 0.24 (given errors show the 95% confidence interval). Nutrient concentrations were: 26 µM NO_3^-, 24.45 µM Si, 1.82 µM P.

2.3 Light

Philips UVB (TL-12), UVA (TL' 40W/05) and VIS (TL'D 36W/33) lamps were used in combination with Mylar, 50% cut-off at 320 nm, and UV-opaque PMMA filter, 50% cut-off at 380 nm, to create the three different optical treatments: UVB+UVA+VIS, UVA+VIS and VIS. Spectral conditions were measured for every bottle using a MACAM Spectroradiometer SR9910 with a small spherical 4π sensor. Spectra were recorded from 280-700 nm. The two spectra of the duplicate bottles of the UVB+UVA+VIS and VIS optical conditions were very similar. The two spectra of the duplicate bottles receiving UVA+VIS showed an intensity difference (Figure 1). Integrated values of the irradiance of UVB, UVA and VIS as measured from inside the bottles are given in Table 1.

Table 1. Integrated values of UVB, UVA and VIS irradiance as measured within the PMMA bottles receiving different wavelength ranges of irradiance.

	UVB+UVA+VIS		UVA+VIS		VIS	
	bottle 1	bottle 2	bottle 1	bottle 2	bottle 1	bottle 2
UVB (Wm^{-2})	0.38	0.41	0.02	0.02	0.01	0.01
UVA (Wm^{-2})	3.45	3.77	2.77	3.52	0.98	0.96
VIS (Wm^{-2})	8.71	8.61	6.75	8.98	8.52	8.71

2.4 Experimental

The experiments were performed in a temperature controlled class 100 clean container. The temperature was constant at 4°C. A 20 µM Fe(III) stock solution was made with ammonium Fe(III) sulfate ($NH_4Fe^{(III)}(SO_4)_2 \cdot 12H_2O$, Baker Analyzed, reagent grade) in 0.012 M three times quartz distilled (3xQD) HCl using 18 MΩ nanopure water.

Three experiments were performed: Experiment A with *Thalassiosira* sp. and an addition of 5 nM Fe(III), experiment B with *Thalassiosira* sp. without Fe(III) addition and experiment C with *C. brevis* and an addition of 5 nM Fe(III). The walls of the 2 liter, UV transparent, polymethylmetacrylate (PMMA) bottles (Steeneken et al., 1995) were equilibrated prior to use with Southern Ocean seawater containing the same concentration Fe(III) as during the experiment. Addition of 5 nM Fe(III) in experiments A and C resulted in the formation of amorphous ferric hydroxides after a 12 hour equilibration period (Chapter 5). No Fe(III) was added in experiment B. Each experiment started with the addition of an equal amount of algae to 7 PMMA bottles containing Southern Ocean seawater. One bottle (t=0) was immediately sampled for dissolved Fe, Fe ligands and cell numbers. The other bottles were sampled during the experiments. At regular intervals the bottles were shaken gently.
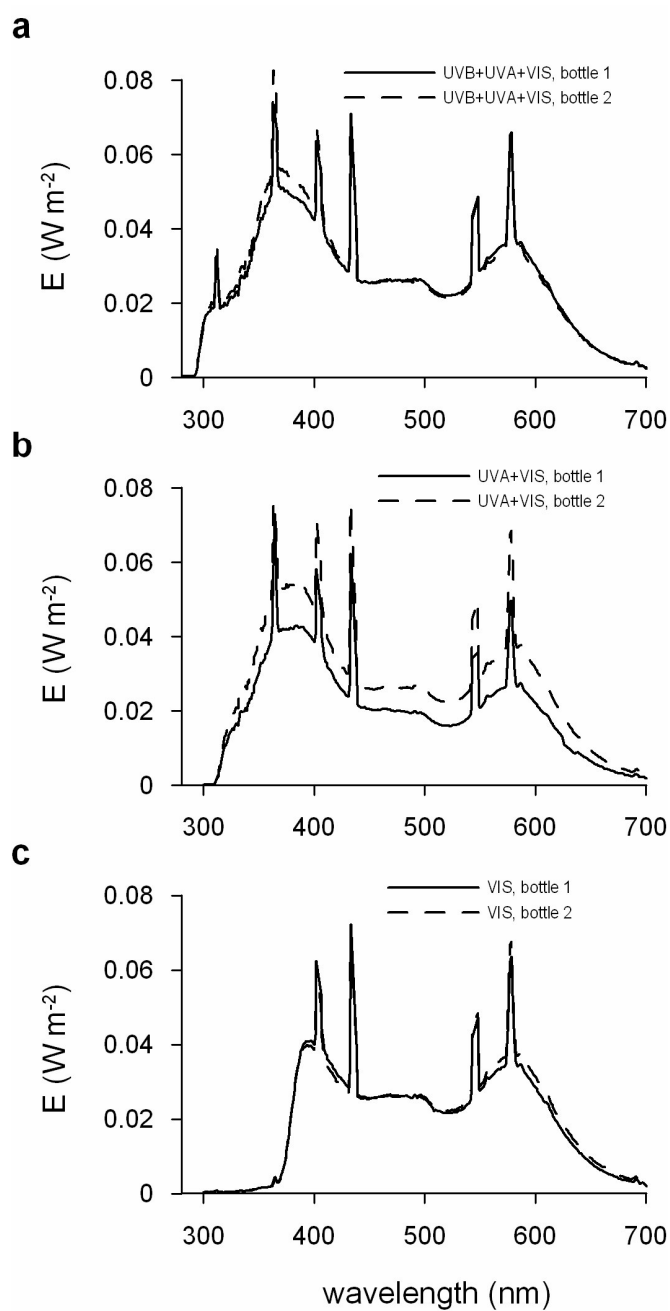
Figure 1. The light spectra as measured in the PMMA bottles receiving UVB+UVA+VIS (a), UVA+VIS (b) and VIS (c).

Samples for dissolved Fe and FeL were gently filtered inside a flow bench using acid cleaned 0.22 µm polycarbonate filters (Micron Separations Inc.) in an acid-cleaned filter

holder (Nalgene) connected to a vacuum pump. Samples for Fe(II) were sampled inline and immediately measured (see below).

2.5 Iron(II) analysis

Concentrations of Fe(II) were measured inline via an acid cleaned 0.2 μm acrodisc filter (refreshed each day) using an automated flow injection analysis system employing a luminol-based chemiluminescence detection of Fe(II) (Seitz and Hercules, 1972; King et al., 1995; O'Sullivan et al., 1995). An alkaline luminol solution is mixed with the sample in a spiral shaped flow cell in front of a Hamamatsu HC135 photon counter. At pH 10, Fe(II) is rapidly oxidized by oxygen on a millisecond time scale causing the oxidation of luminol and producing blue light (Xiao et al., 2002).

Samples were transported in-line from the PMMA bottle to a sample loop. Then the sample was, by introducing it in MQ, transported into the flow cell every 93 seconds.

The complete analysis system was built in a light-tight wooden box. The luminol reagent and the carrier were kept in light tight bags (used for storage of photographic films). The tubing was covered with aluminum foil and the tubing of the peristaltic pump was shaded by black plastic.

The alkaline luminol solution was prepared weekly with 15 mM 5-amino-2,3-dihyfro-1,4-phthal-azinedione (Luminol) (SIGMA) in 20 mM Na_2CO_3. The 50 μM luminol reagent solution was made in 0.5 M NH_3 (suprapur, Merck) and 0.1 M HCl (suprapur, Merck). The luminol reagent solution was stored in the dark for at least 24 hours before use, to ensure that the reagent properties had stabilized. A 0.01 M Fe(II) stock was prepared monthly by dissolving ferrous ammonium sulfate hexahydrate ($Fe^{(II)}(NH_4SO_4)_2 \cdot 6H_2O$) (Baker Analyzed, reagent grade) in 0.012 M 3xQD HCl. Working solutions were prepared daily. All Fe(II) stock solutions were kept refrigerated in the dark at 4°C when not in use.

Calibration was performed by the standard addition of known concentrations of Fe(II) to the sample matrix. The time delay between Fe(II) addition and measurement caused an oxidation effect. This oxidation effect was accounted for by extrapolating the data back to time zero using the fact that the oxidation of Fe(II) in seawater very closely approximates pseudo-first-order kinetics.

2.6 Dissolved Fe analysis

Dissolved Fe, defined as the Fe fraction passing a 0.2 μm filter, was determined using flow injection analysis with luminol chemiluminescence and H_2O_2 (de Jong et al., 1998).

2.7 CLE-ACSV

Determination of the organic speciation of Fe in seawater water was performed using competitive ligand exchange-adsorptive cathodic stripping voltammetry (CLE-ACSV). The reagent 2-(2-Thiazolylazo)-p-cresol (TAC) (Aldrich, used as received) was used as competing ligand (Croot and Johansson, 2000). All solutions were prepared using 18.2 MΩ nanopure water. The equipment consisted of a µAutolab voltammeter (Ecochemie, Netherlands), a static mercury drop electrode (Metrohm Model VA663), a double-junction Ag/saturated AgCl reference electrode with a salt bridge containing 3 M HCl and a counter electrode of glassy carbon. The titration was performed using 0.01 M stock solution of TAC in 3xQD methanol, 1 M boric acid (Suprapur, Merck) in 0.3 M ammonia (Suprapur, Merck) to buffer the samples to a pH of 8.05 and a 10^{-6} M Fe(III) stock solution acidified with 0.012 M HCl (3xQD). Fe was removed from the borate buffer by the addition of TAC and subsequent binding of TAC and $Fe(TAC)_2$ on a C_{18} SepPak column. Aliquots of 15 ml were spiked with Fe(III) with final concentrations between 0 and 20 nM and allowed to equilibrate overnight (> 15 hours) with 5 mM borate buffer and 10 µM TAC. The concentration $Fe(TAC)_2$ in the samples were measured using the following procedure: i) removal of oxygen from the samples for 200 seconds with dry nitrogen gas, a fresh Hg drop was formed at the end of the purging step, ii) a deposition potential of -0.40 V was applied for 30-60 seconds depending on the sample measured, the solution was stirred to facilitate the adsorption of the $Fe(TAC)_2$ to the Hg drop, iii) at the end of the adsorption period the stirrer was stopped and the potential was scanned using the differential pulse method from -0.40 to -0.90 V at 19.5 mV s^{-1} and the stripping current from the adsorbed $Fe(TAC)_2$ recorded.

The ligand concentration and the conditional stability constant were calculated using the non-linear fit of the Langmuir isotherm (Gerringa et al., 1995).

3. Results and discussion

3.1 Diatoms

A 5 nM Fe(III) addition (experiment A) resulted in *Thalassiosira* sp. growth restricted to 1 doubling over the 36 hours of the experiment. Cells increased from 52 ± 14 (n=7) to 100 ± 15 (n=6) cells ml^{-1} (Figure 2). In experiment B, where no additional Fe(III) was added, a smaller increase in cells was observed, 48 ± 11 (n=7) to 72 ± 17 (n=6) cells ml^{-1} over 36 hours (Figure 2). However, the difference in growth of *Thalassiosira* sp. in experiment A and experiment B was too small to relate it to the initial Fe addition and subsequent Fe speciation.

A 5 nM Fe(III) addition (experiment III) resulted in the growth of *C. brevis* with cell numbers increasing from 10433 ± 754 cells ml^{-1} (n=6) to 17673 ± 2720 cells ml^{-1} (n=5) in 36

hours (Figure 2). No significant difference in growth was observed between the different optical conditions in the three experiments.

3.2 Total dissolved Fe

The Southern Ocean seawater contained 0.32 nM total dissolved Fe (Fe_{diss}) and 1.69 equivalents of nM Fe (eq nM Fe) ligand concentration with an excess ligand concentration of 1.37 eq nM Fe (excess L). Assuming that 1.37 nM of the added 5 nM Fe is organically complexed, 3.63 nM Fe(III) can precipitate as inorganic Fe overnight. After addition of the diatoms we found a Fe_{diss} concentration of ~ 3.7 nM in experiment A and C. This means that only 1.6 nM (5.32 nM Fe_{diss} – 3.7 nM Fe_{diss}) was probably present as precipitated Fe after the addition of diatoms.
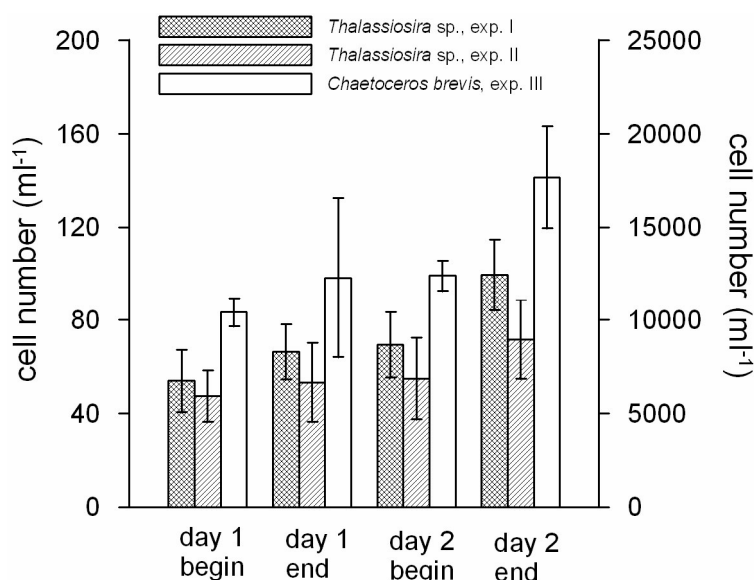
Figure 2. *Thalassiosira* sp. cell numbers (left y-axis) in experiment A and B and *Chaetoceros brevis* cell numbers (right y-axis) in experiment C. The error bars give the standard deviation (n=6).

In experiment B the Fe_{diss} concentration was lower than the total ligand concentration. Theoretically all Fe in experiment B was organically complexed but, as observed before, non-negligible amounts of amorphous Fe oxyhydroxides apparently persist in spite of the presence of organic ligands with high conditional stability constants (Chapter 5).

The concentrations of Fe_{diss} as function of the light treatments were too variable to draw conclusions with regard to co-variance between Fe_{diss} and Fe(II) concentrations (Figure

3). This suggests that no clear relation exists between the photoreducible Fe fraction and the Fe_{diss} concentration. The Fe_{diss} is an operationally defined Fe fraction based on filtration (0.4 or 0.2 µm). It consists of different chemical Fe forms including a small colloidal phase as well as inorganic ions and organically complexed Fe (Wells and Goldberg, 1992; Rue and Bruland, 1995; Nishioka et al., 2001). Although organically complexed Fe can be photoreducible (Barbeau et al., 2001), its importance in Fe photoreduction in the field and in e.g. phytoplankton cultures with natural seawater has not been convincingly shown yet (Barbeau et al., 2003; Chapter 5, 8). The colloidal Fe fraction was shown to be a source for photoreducible Fe (Wells and Mayer, 1991; Waite et al., 1995; Ozturk et al., 2003; Chapter 3, Rijkenberg et al., 2005).

The Fe_{diss} concentration decreased during the experiments A, B and C (Figure 3). The formation of Fe(II) cannot be responsible for this decrease because the Fe(II) in samples for dissolved Fe was allowed to oxidize before acidification and subsequent measurement. Adsorption of Fe on the wall of the bottle (Fischer et al., submitted) should be minimal because the bottles were equilibrated with the same seawater containing the same Fe concentration as during the experiments. Thus, the decrease in the Fe_{diss} concentration can only be ascribed to the combination of uptake by diatoms and colloid formation.

3.3 Fe(II)

When the Fe(II) concentration versus time was compared for the three experiments we see that in all three cases the concentration Fe(II) on the second day was higher than on the first day (Figure 4, 5, 6). Furthermore we observed a wavelength dependency at the first day which disappeared at the second day.

The photoproduced Fe(II) concentration is strongly dependent on the intensity (Chapter 3, Rijkenberg et al., 2005) and wavelength of the irradiance used (Chapter 4, Rijkenberg et al., 2004). We predicted the relative Fe(II) concentrations as expected in each bottle using the experimental irradiance data and the weighting function describing the wavelength dependency of the photo-production of Fe(II) from amorphous Fe hydroxides in Antarctic seawater (Chapter 4, Rijkenberg et al., 2004) (Table 2). The concentrations Fe(II) during the three experiments were compared (within each experiment separately) with their expected Fe(II) production rates predicted by the weighting function.
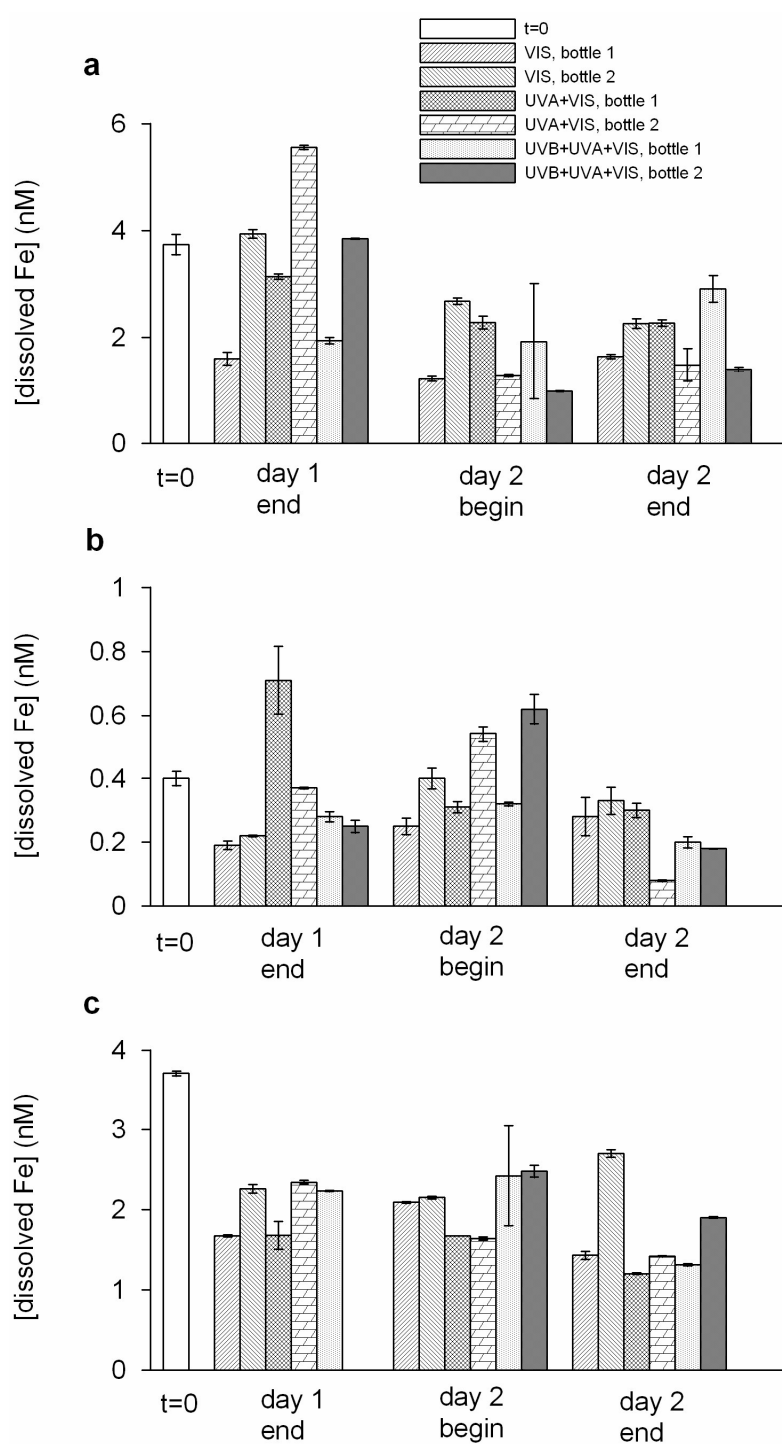
Figure 3. The concentrations dissolved Fe (Fe_{diss}) (nM) for A) experiment A (+5 nM Fe, +*Thalassiosira* sp.), B) experiment B (+*Thalassiosira* sp.), and C) experiment C (+5 nM Fe, +*C. brevis*). The concentration of dissolved Fe for t=0 was sampled directly after the addition of the phytoplankton. The error bars give the standard deviation of the analysis (n=2).

Table 2. The initial Fe(II) photoproduction rates as predicted for the 6 offered irradiance spectra using the weighting function (Chapter 4, Rijkenberg et al., 2004). Bottle 1 and bottle 2 are the replicate bottles receiving the same wavelengths of irradiance. The weighting function calculates Fe(II) production rates upon turning on the light using 10 nM Fe in the form of amorphous Fe hydroxides and can in the context of this article only be used as a relative comparison.

	UVB+UVA+VIS (x 10^{-6} M Fe(II) s^{-1})	UVA+VIS (x 10^{-6} M Fe(II) s^{-1})	VIS (x 10^{-6} M Fe(II) s^{-1})
bottle 1	6.11	3.88	1.79
bottle 2	6.56	4.92	1.75

At the first day of experiment A (+ 5 nM Fe(III), *Thalassiosira* sp.) (Figure 4) more Fe(II) was produced in the bottle receiving UVB+UVA+VIS compared to the bottle receiving UVA+VIS and VIS respectively (Figure 4D). This was expected according to the weighting function. Also the Fe(II) production with time under constant irradiance was as expected, a steep rise in the concentration Fe(II) until a maximum is reached followed by a decrease in Fe(II) concentration. This process was repeatedly observed in experiments with inorganic colloidal Fe (Chapter 4, Rijkenberg et al., 2004; Chapter 3, Rijkenberg et al., 2005; Chapter 5), also reported by others (Waite and Morel, 1984; Miller et al., 1995) and even induced by pre-irradiating water, destroying all organic substances (Emmenegger et al., 2001). According to Wells and Mayer (1991) the decreasing Fe(II) concentration during irradiance is caused by the modification of the colloidal Fe surface by photochemical processes which cause a decrease of the amount of photoreducible Fe upon irradiance.

Experiment B (*Thalassiosira* sp., no Fe(III) addition) (Figure 5) had very low concentrations of Fe$_{diss}$ (~ 0.32 nM) and very low concentrations of Fe(II) at the first day of the experiment (Figure 5), ~ 20 pM Fe(II). No wavelength effect in the concentration Fe(II) could be distinguished. The UVA and UVB did not play a major role in the Fe(II) production (Figure 5D). This is in contrast with the predicted differences (Table 2). Possible explanations for these discrepancies are: i) the measured Fe(II) concentrations were too low to distinguish differences by the different wavelength regions offered, and ii) no Fe(III) was added to the seawater and therefore no inorganic colloidal Fe was formed. All the Fe present may be organically complexed.

In experiment C (*C. brevis* + 5 nM dissolved Fe) we expected, according to the weighting function and the irradiance data (Table 2), the Fe(II) concentration to decrease from UVB+UVA+VIS to UVA+VIS to VIS. We did not see this very clearly in experiment C (Figure 6). The Fe(II) concentration in the bottle receiving VIS showed an increase from the start of the experiment without reaching a maximum as far as this can be distinguished from
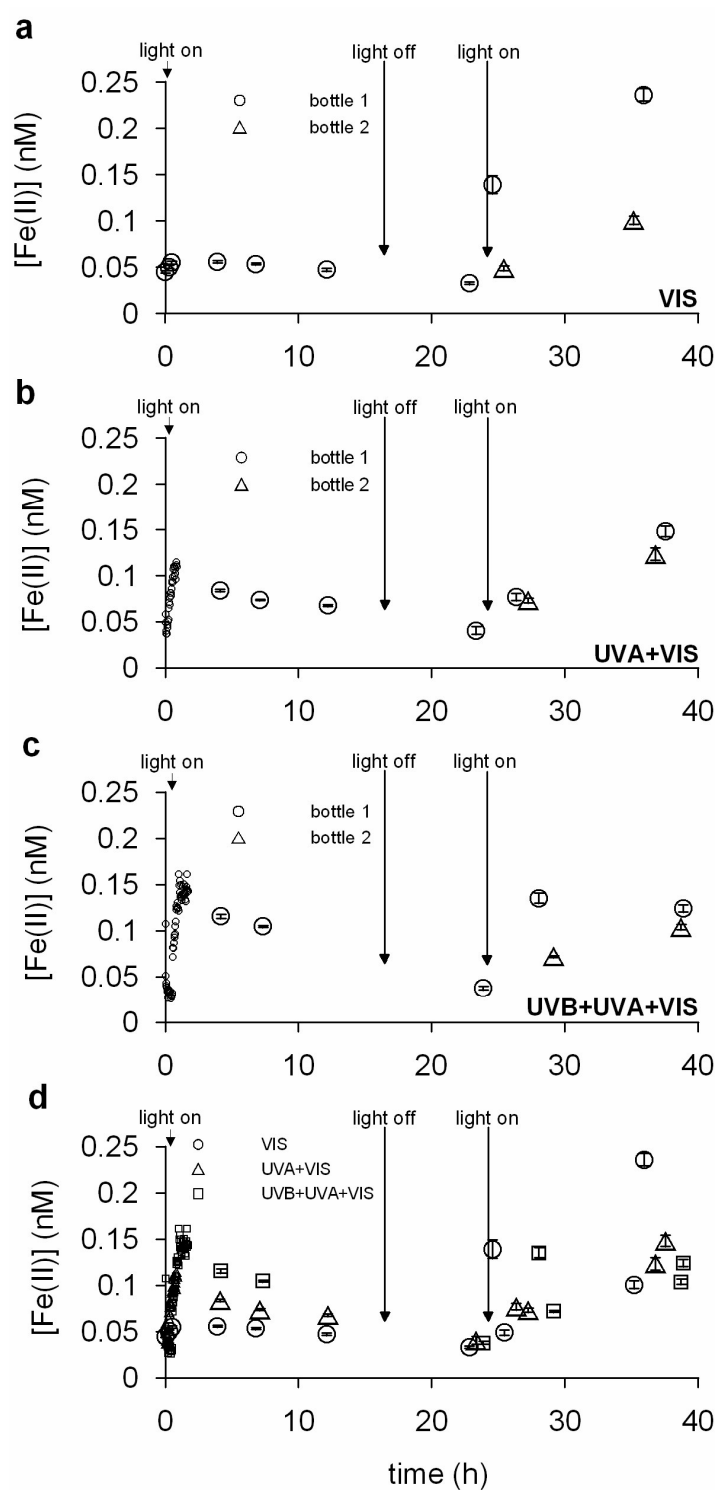
Figure 4. The concentration of Fe(II) (nM) in experiment A (addition of 5 nM Fe(III) and *Thalassiosira* sp.) receiving a) VIS in bottle 1 and bottle 2, b) UVA+VIS in bottle 1 and bottle 2, c) UVB+UVA+VIS in bottle 1 and bottle 2, and d) the Fe(II) concentration for bottle 1 and 2 of VIS, UVA+VIS and UVB+UVA+VIS. The error bars show the standard error.

the modest number of data points (Figure 6A). The Fe(II) concentration in the bottle receiving UVA+VIS showed a decrease in Fe(II) concentration after reaching a maximum but started to increase already at the first day (Figure 6B). The bottle receiving UVB+UVA+VIS showed a decrease in Fe(II) concentration after reaching the Fe(II) maximum and no increase yet (Figure 6C). Surprisingly, the Fe(II) concentration at the end of the dark period is higher than the concentration Fe(II) during the first day. In the case of the bottle receiving UVA+VIS it was even higher than the concentration Fe(II) during irradiance at the second day. These high Fe(II) concentrations in the dark may be ascribed to three different conceivable mechanisms: reduction of Fe(III) in the dark by either i) photoproduced superoxide (Voelker and Sedlak, 1995) or ii) carbon containing radicals (Ross and Neta, 1982; Faust, 1994), produced during the first light period, or iii) the reduction of Fe by extra-cellular enzymes (Maldonado and Price, 2000) produced by *C. brevis*.

The Fe(II) concentrations of experiments A and B increased during the second day even above the concentrations measured at the first day (Figure 4, 5). The Fe(II) concentrations at the second day of experiment C did not show an increase but were still higher than the Fe(II) concentrations of the first day (Figure 6). The Fe(II) concentration in experiment C is only increasing in the bottle receiving UVB+UVA+VIS. The bottles receiving VIS and UVA+VIS showed a decreasing and stabilizing Fe(II) concentration respectively. This increase in the concentration Fe(II) at the second day was not expected. A control experiment where no diatoms were added to the seawater showed at the second day no increase but a steady state in the Fe(II) concentration (Figure 7).

Kuma et al. (1992) explained high Fe(II) concentrations found during a spring bloom by the release of organic components from phytoplankton in Funka Bay (Japan) inducing photoproduction of Fe(II). In laboratory experiments Kuma et al. (1992) showed that the Fe(II) production increased after the addition of hydroxycarboxylic acids, such as sugar acids. The colloidal fraction is seen as an important candidate to contain a photoreducible Fe fraction (Wells and Mayer, 1991; Waite et al., 1995; Emmenegger et al., 2001; Ozturk et al., 2003). Dissolved organic substances may adsorb on and associate with ferric colloidal material during and after formation (Wells and Goldberg, 1992; Wells and Goldberg, 1993). We assume that the increasing Fe(II) concentrations in experiments A, B and C are caused by more effective Fe photoreduction due to organic substances released by the diatoms.

Assuming equilibrium, all Fe in experiment B was probably organically complexed. On the one hand, the observation of increasing Fe(II) concentrations at day 2 could indicate that inorganic colloidal Fe was present in experiment B. On the other hand, there is the possibility that the released organic substances are involved in the photoredox reaction of organically complexed Fe as for example has been observed for desferrioxamine B. Compounds such as oxalate are able to induce the photoreduction of Fe(III) complexed with
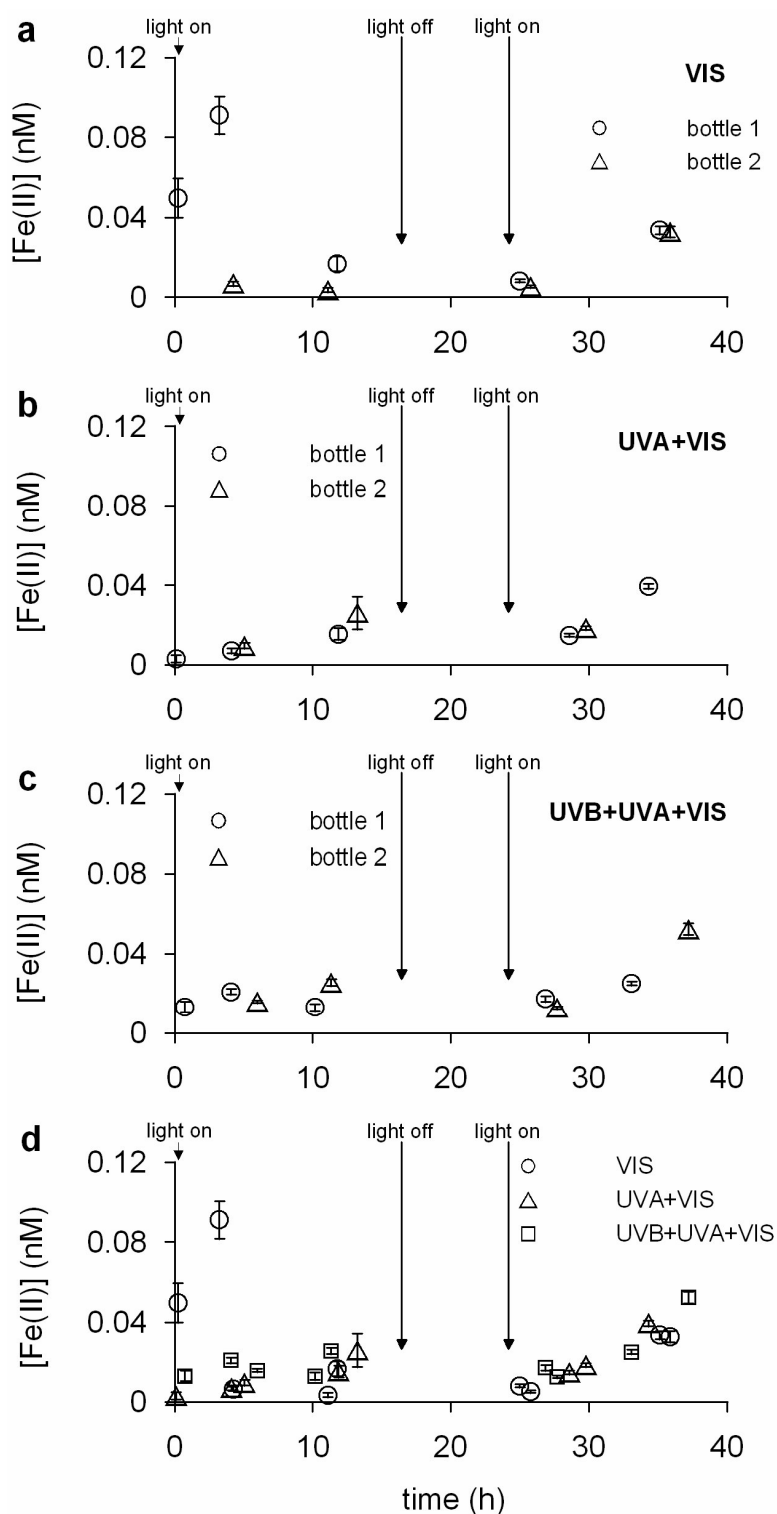
Figure 5. The concentration Fe(II) (nM) during experiment B (in the presence of *Thalassiosira* sp., no addition of Fe) receiving a) VIS in bottle 1 and bottle 2, b) UVA+VIS in bottle 1 and bottle 2, c) UVB+UVA+VIS in bottle 1 and bottle 2, and d) the Fe(II) concentration for bottle 1 and 2 of VIS, UVA+VIS and UVB+UVA+VIS. The error bars show the standard error.
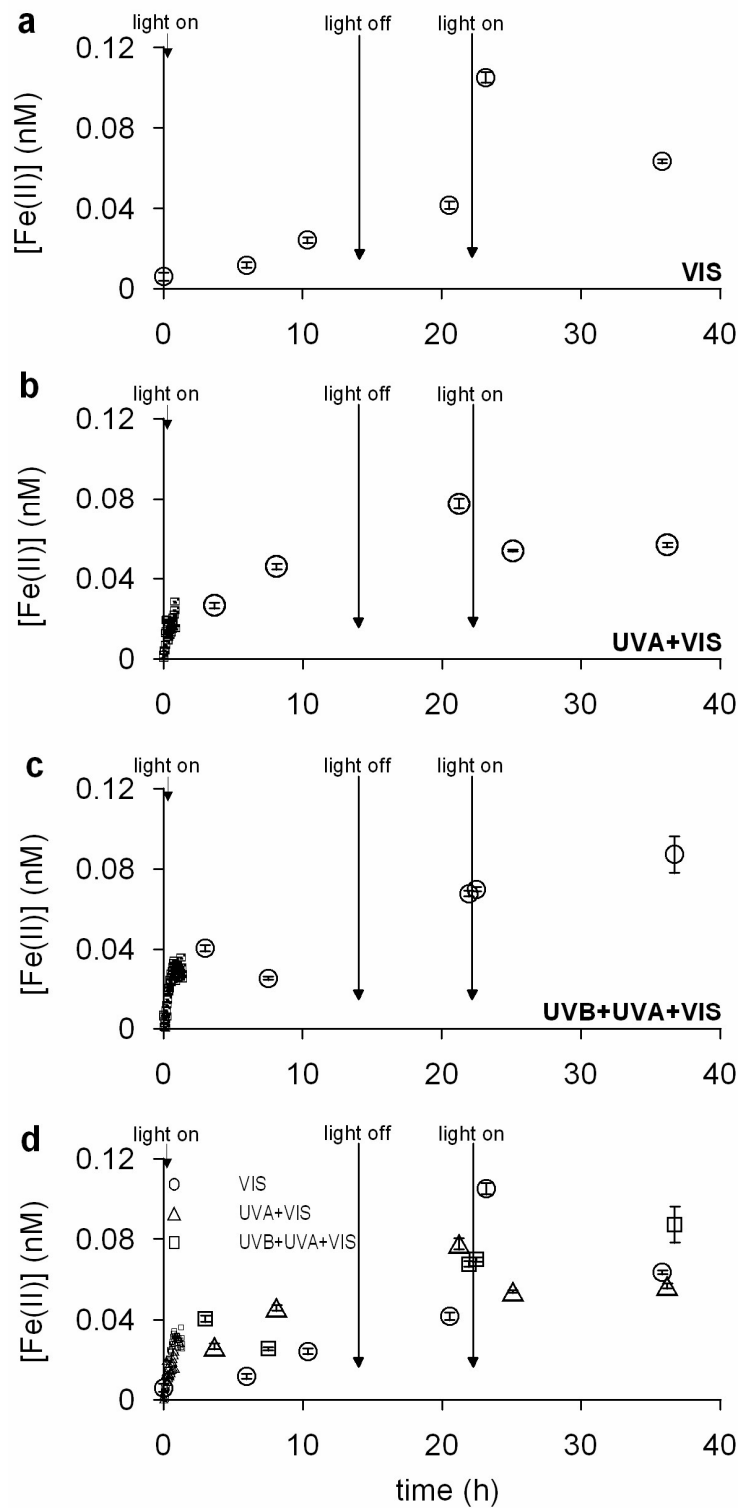
Figure 6. The concentration Fe(II) (nM) in experiment C (in the presence of *C. brevis*, addition of 5 nM Fe(III)) receiving a) VIS, b) UVA+VIS, c) UVB+UVA+VIS, and d) the Fe(II) concentration for VIS, UVA+VIS and UVB+UVA+VIS. The error bars show the standard error.
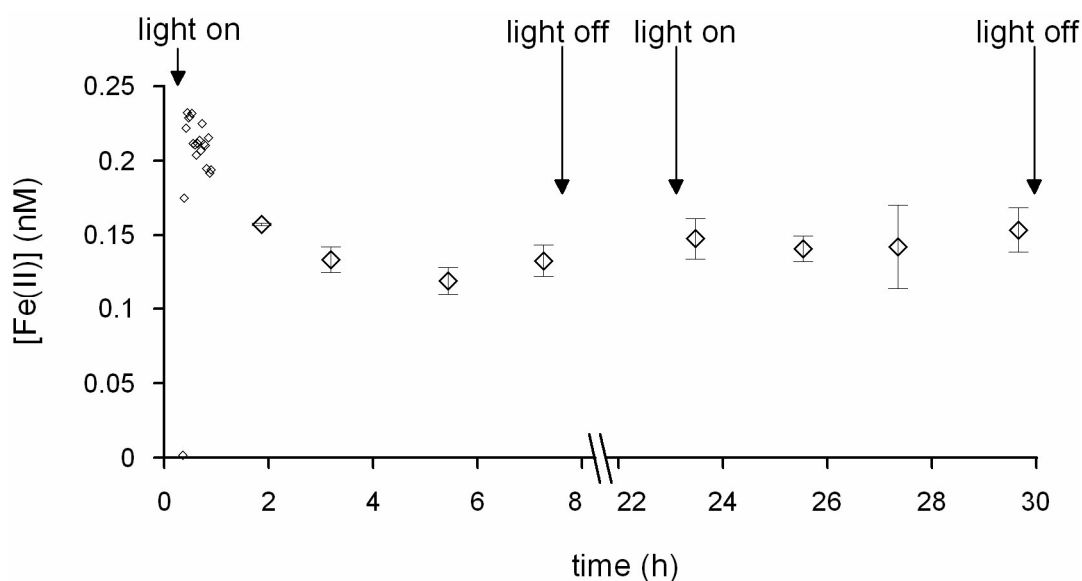
Figure 7. Control experiment showing the concentration of Fe(II) (nM) during 2 days in seawater without diatoms. The change with time during the first day is typically a rapid increase until a maximum Fe(II) concentration is reached, this followed by a decrease in Fe(II) concentration during the light period until an equilibrium is approached. The concentration of Fe(II) at the second day is similar to the concentration of the approached equilibrium during the first day. The error bars show the standard error.

the otherwise photostable desferrioxamine B (Gao and Zepp, 1998) by an outer-sphere charge transfer excitation leaving DFOB intact (Kunkely and Vogler, 2001).

Apart from an increase in the concentration Fe(II) at the second day we also observed an increase in the relative importance of VIS in the Fe(II) production (Figure 8). This effect has been observed before with the complexation of Fe by oxalate, present in dust, extending the absorption band of Fe(III) into the visible light (Zuo, 1995). It could also be possible that UVB has a negative effect on the photoproduction of Fe(II) due to the photodegradation of the organic constituents responsible for the increase in the photoreducible Fe fraction. Overall, a decrease in the concentration Fe(II) produced due to the UVB+UVA+VIS led to an increase in the relative importance of VIS (Figure 8). These two processes were observed in experiment A, experiment B and to a lesser extent also in experiment C.

The UV part of the spectrum, particularly UVB, attenuates fast with increasing depth in the water column (Boucher and Prezelin, 1996). So, the release of organic substances, which are photoreactive in combination with the trace metal Fe, could be a mechanism to improve the biological availability of colloidal/particulate Fe in the watercolumn. If so, the question rises why this effect is only visible at the second day of the experiment?
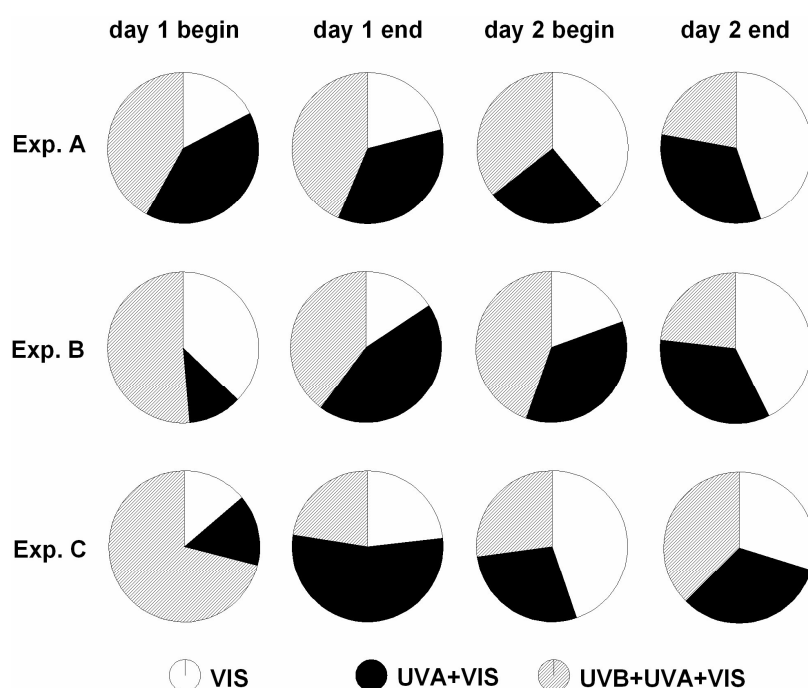
Figure 8. The attribution of VIS, UVA+VIS and UVB+UVA+VIS to the total concentration of Fe(II) as percentage of the sum of the concentration of Fe(II) due to all three different light conditions together for the experiments A, B and C.

Possible explanations are: i) oxidation of photoproduced Fe(II) induces formation of fresh colloidal Fe incorporating the organic substances released, resulting in a higher photoproduction of Fe(II). Only at day 2 the resulting Fe(II) production due to this process overrides the decreasing concentration photoreducible Fe from the amorphous Fe hydroxides. Or ii) the diatoms started only after 1 day to produce these organic substances influencing the Fe photochemistry. The increases in cell numbers were higher at day 2 compared to day 1 in all experiments (Figure 2). This explanation is further confirmed by the observation that although the number of *C. brevis* cells was higher in experiment C compared to the number

Table 3. Average cell numbers, calculated total cell surface and total cell volume for experiment A, B (*Thalassiosira* sp.) and experiment C (*C. brevis*).

	Cells ml^{-1}		Surface (μm^2)			Volume (μm^3)		
	t=0	t=end	1 cell[a]	t=0	t=end	1 cell[a]	t=0	t=end
Exp. A	52	100	$12 \ 10^3$	$6.2 \ 10^5$	$1.2 \ 10^6$	$7.7 \ 10^4$	$4.0 \ 10^6$	$7.7 \ 10^6$
Exp. B	48	72	$12 \ 10^3$	$5.8 \ 10^5$	$8.6 \ 10^5$	$7.7 \ 10^4$	$3.7 \ 10^6$	$5.5 \ 10^6$
Exp. C	10433	17673	61	$6.4 \ 10^5$	$1.1 \ 10^6$	50	$7.2 \ 10^4$	$8.8 \ 10^5$

[a] (Timmermans et al., 2004)

of *Thalassiosira* sp. cells in experiment A and B, in terms of cell membrane surface area and cell volume the values were respectively fairly similar or much lower for *C. brevis* in comparison to *Thalassiosira* sp. (Table 3). The different response of the Fe(II) concentration under different light regimes in combination with the similar and lower values for cell surface area and cell volume respectively, indicates that *C. brevis* started faster, but irradiance wavelength dependent, with the release of organic substances.

When Fe(II) is expressed as percentage of the Fe_{diss} concentration a clear trend is visible: the Fe(II) concentration as percentage of the Fe_{diss} concentration increased with time (Figure 9).
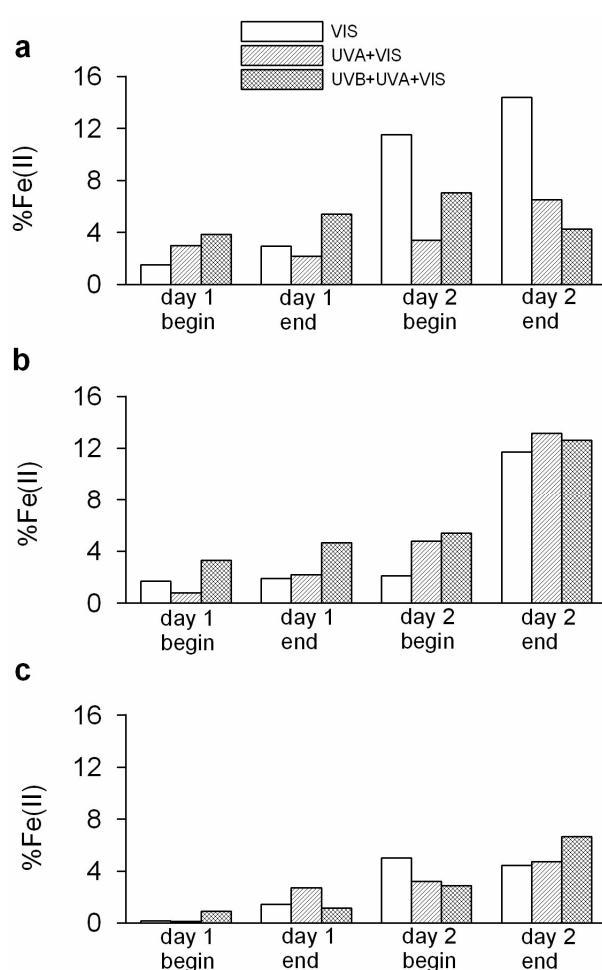
Figure 9. The concentration of Fe(II) as percentage of the concentration Fe_{diss} for a) experiment A (+5 nM Fe, +*Thalassiosira* sp.), b) experiment B (+*Thalassiosira* sp.), and c) experiment C (+5 nM Fe, +*C. brevis*). For the %Fe(II) in experiment B the bottle 2 was used because unrealistic Fe(II) concentrations were observed in bottle 1.

3.4 Organically complexed Fe

The experiments A, B and C contained an assemblage of organic Fe binding ligands with an average of the logarithm of the conditional stability constants (log K') of 21.55 ± 0.16 (n=6), 21.13 ± 0.13 (n=6) and 20.29 ± 0.13 (n=6) respectively. These values are in good agreement with the conditional stability constants as found in various oceans (van den Berg, 1995; Wu and Luther, 1995; Rue and Bruland, 1997; Gledhill et al., 1998; Witter et al., 2000; Boye et al., 2001) and with model ligands (Witter et al., 2000).

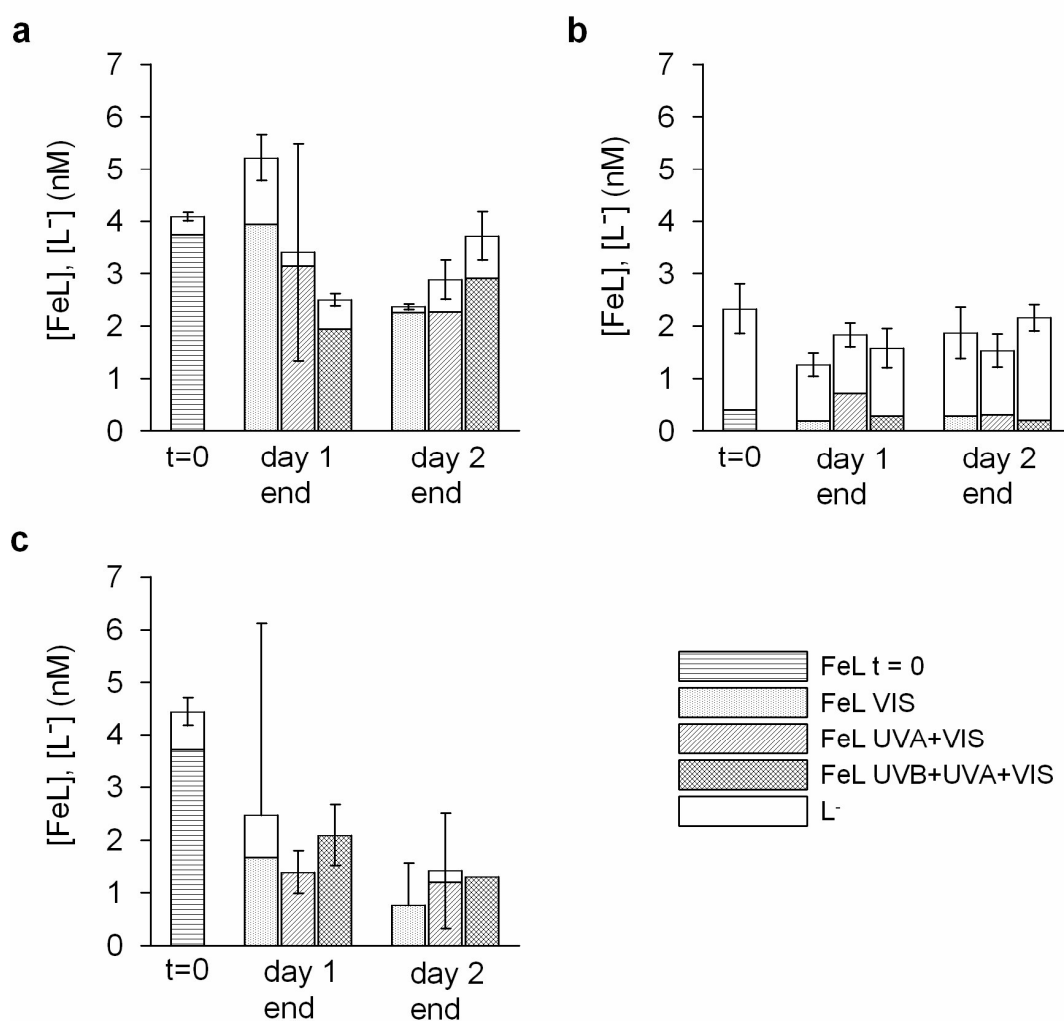**Figure 10.** The concentrations of FeL and excess ligand L in a) experiment A (+5 nM Fe, +*Thalassiosira* sp.), b) experiment B (+*Thalassiosira* sp.), and c) experiment C (+5 nM Fe, +*C. brevis*). The error bars show the 95% confidence interval.

The average total concentration L in experiment A (containing 5.32 nM Fe) was 3.35 ± 1.05 eq nM Fe (n=7) and for t=0, just after addition of the diatoms, 4.09 eq nM Fe, roughly twofold higher than the concentration L in experiment B, average 1.71 ± 0.31 eq nM Fe (n=7) and 2.33 eq nM Fe at t=0 (Figure 10). This high concentration of ligands in experiment A could according to Boye et al. (in press) be explained by an increased Fe-binding capacity due to the formation of inorganic colloids. The colloidal Fe(III) oxyhydroxides resulting from the Fe addition in experiment A could precipitate and form surface active amorphous colloids that appeared as a (saturated) strong Fe-binding capacity upon titration. The observation that the concentration excess L was less in experiment A, 0.57 ± 0.39 eq nM Fe (n=7), than in experiment B, 1.46 ± 0.37 eq nM Fe (n=7), was expected as 5 nM Fe was added to the seawater of experiment A. In contrast to experiment A and B the total concentration L decreased during experiment C (Figure 10). This could mean that Fe-binding ligands in the *C. brevis* culture were degraded or utilized while this effect was not detected in the culture containing *Thalassiosira* sp.

No correlation between excess L and/or FeL and the different optical treatments were observed in any of the experiments (Figure 10). Also, no relation was found between the concentration of FeL and/or excess L and the photoproduction of Fe(II). Experiment C showed an initial decrease in L concentration but no further significant decrease during the second day. These findings are in agreement with the observation that Fe-binding ligands were not photo-degraded as shown for the Scheldt estuary (Chapter 8).
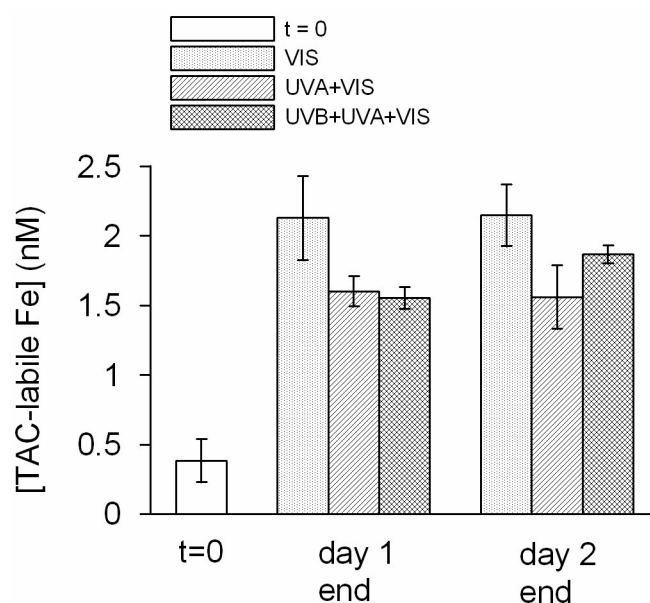

Figure 11. The concentration of TAC-labile Fe in experiment C (+5 nM Fe, +*C. brevis*). The error bars show the standard deviation (n = 2 or 3).

Remarkably the excess L concentration was very low or not present in experiment C when compared to experiment A and B (Figure 10). In addition we observed a high TAC-labile Fe concentration, compared to the concentrations of TAC-labile Fe close to zero in experiment A and B (TAC-labile Fe being the Fe bound by TAC (10 μM) during >12 hours equilibration). This TAC-labile Fe was ~ 0.4 nM at t=0 but increased during the first day to ~ 1.5 – 2.1 nM and did not increase anymore during the second day (Figure 11). We have indications that this TAC-labile Fe, observed during titrations, represents a weak ligand class (log K' < 18), which cannot compete with TAC (Chapter 7, 8). The lower log K' found for the stronger ligand class present in experiment C compared to the log K' of the stronger ligand class in experiment A and B confirms the presence of this weaker ligand class. The conditional stability constant is an average of the conditional stability constants of a range of organic ligands present in natural seawater. Analysis of the log K' by analysis of variance (ANOVA) revealed significant differences between the three experiments (Table 4 A). Post-hoc analysis using Tukey's method (Montgomery, 1997) showed that the log K' of experiment C was significantly lower than in experiment A and B (Table 4 B). The variation in the decrease in the concentration of the strong ligand L with respect to its concentration strong L at t=0 ($[L]_{t=0} - [L]_{t=x}$) varied linearly with the TAC-labile Fe (R^2 of 0.95, see Figure 12). This means that possibly the stronger ligand class is the source of the weaker ligand class. Barbeau et al. (2001) found a decrease in the log K' of 0.7 (from 22.2 to 21.5) after the photoreduction and release of Fe initially bound to an organic siderophore. There are two reasons why we believe that the photoreduction of Fe bound by an organic ligand was not the cause of the increased TAC-labile Fe concentrations in our

Table 4 A. Analysis of the log K' by analysis of variance (ANOVA). The test revealed significant differences between the experiments.

source	d.f.	S.S.	M.S.	F	P
Exp. A-C	2	4.914	2.457	21.08	0.001*
Residual	15	1.748	0.117		
Total	17	6.663			

* denotes a significant result P ≤ 0.001

Table 4 B. Post-hoc analysis, using Tukeys test, showed significant (yes) (P ≤ 0.05) and non-significant differences (no) in the log K' between experiments.

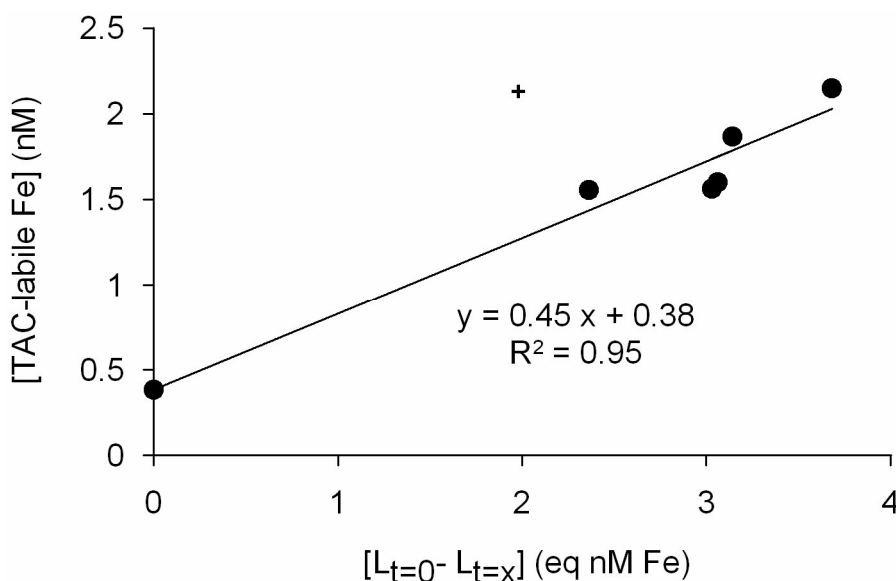| source	Log K'	Exp. A	Exp. B	Exp. C
Exp. A	21.55 ± 0.16		no	yes
Exp. B	21.13 ± 0.13	-		yes
Exp. C	20.29 ± 0.13	-	-	

Figure 12. The concentration of TAC-labile Fe as function of the decrease in ligand concentration at t=0 ($[L]_{t=x} - [L]_{t=0}$) in experiment C. One data point (+) was not used for the calculation of the function ($R^2 = 0.95$) because of the high error in the measurement of L_{total} (see Figure 10 day 1).

experiments, namely: i) there was no relation between the offered optical conditions and the TAC-labile Fe concentration, and ii) we would have observed the same effect in the cultures with *Thalassiosira* sp. However, similar high TAC-labile Fe concentrations have been reported during bloom situations (Croot and Johansson, 2000; Chapter 8) and could be the result of scavenging of organically complexed Fe. This modification of the Fe into a more reactive Fe species could be the result of Fe uptake and/or could increase the bioavailability of Fe.

The diatom cultures used during these experiments were not axenic. However, bacteria counts in other experiments with *C. brevis* were low (pers. communication K. R. Timmermans). Furthermore similar effects were not observed in experiments with *Thalassiosira* sp. suggesting that *C. brevis* was responsible for the modification of the strong ligand class.

4. Summary and conclusions

There was no relation between the concentration Fe_{diss}, FeL and differences in the wavelength of the light spectra offered under the experimental irradiance conditions. The presence of diatoms had more influence on the speciation, both on Fe(II) and FeL. The Fe(II) concentration in the first day light period was found to be wavelength dependent although

this wavelength dependency surprisingly disappeared at the second day of the experiments. The increased photoproduction of Fe(II) coincides with an increase in the relative importance of VIS in this process. It is known that the photo-induced reduction of Fe from Fe-colloids keeps this Fe pool more amorphous and more reactive and therefore better available for biological uptake (Wells and Mayer, 1991; Johnson et al., 1994). The release of carbohydrates and/or other organic compounds to induce Fe photoreduction (Hudson et al., 1992; Kuma et al., 1992) in the visible part of the spectrum results in the reduction and solubilisation of Fe from colloidal material and possibly from organically complexed Fe. This would confirm the finding of Nishioka and Takeda (2000) who found that the small colloidal size class was the most dynamic Fe pool in a *Chaetoceros* sp. culture and would provide a mechanism for the supply of biological available Fe from colloidal material (Chen and Wang, 2001). This study shows that diatoms act on the colloidal Fe pool and possibly also on the organically complexed Fe pool in the euphotic zone. Diatoms probably increase the availability of Fe for uptake by enhancing the photochemical processes.

The relation between the variation in TAC-labile Fe and the variation in the decrease in the strong ligand class as compared to t=0 suggests that *C. brevis* modified a part of the strong ligand class, this resulting in the presence of a weaker class of ligands. It can be speculated that this transformation is caused during uptake of the complexed Fe or that *C. brevis* modifies the strong Fe binding ligands to make the complexed Fe more kinetically labile with respect to ligand exchange and subsequently improve its biological availability (Morel et al., 1991).

Laboratory studies show that it is difficult for a small diatom species such as *C. brevis* to be forced into Fe-limitation (Timmermans et al., 2001). The diffusion limitation of Fe becomes more important with increasing cell diameter (Sunda and Huntsman, 1995). Small cells with relative large cell surface to volume ratios have the lowest half-saturation values with respect to dissolved Fe (Timmermans et al., 2004), in other words small diatoms have a higher affinity for dissolved Fe. Modification of the strongly bound Fe-ligand pool by the small *C. brevis* as compared to the large *Thalassiosira sp.* could be an additional explanation.

Acknowledgements

References

Allnut, F.C.T. and Bonner, W.D., 1987. Evaluation of reductive release as a mechanism for iron uptake from ferrioxamine B by *Chlorella vulgaris*. Plant Physiol., 85: 751-756.

Anderson, M.A. and Morel, F.M.M., 1980. Uptake of Fe(II) by a diatom in oxic culture medium. Mar. Biol. Let., 1: 263-268.

Anderson, M.A. and Morel, F.M.M., 1982. The influence of aqueous iron chemistry on the uptake of iron by the coastal diatom *Thalassiosira weissflogii*. Limnol. Oceanogr., 27(5): 789-813.

Barbeau, K., Rue, E.L., Bruland, K.W. and Butler, A., 2001. Photochemical cycling of iron in the surface ocean mediated by microbial iron(III)-binding ligands. Nature, 413(6854): 409-413.

Barbeau, K., Rue, E.L., Trick, C.G., Bruland, K.T. and Butler, A., 2003. Photochemical reactivity of siderophores produced by marine heterotrophic bacteria and cyanobacteria based on characteristic Fe(III) binding groups. Limnol. Oceanogr., 48(3): 1069-1078.

Barbeau, K., Zhang, G.P., Live, D.H. and Butler, A., 2002. Petrobactin, a photoreactive siderophore produced by the oil- degrading marine bacterium *Marinobacter hydrocarbonoclasticus*. J. Am. Chem. Soc., 124(3): 378-379.

Boucher, N.P. and Prezelin, B.B., 1996. Spectral modeling of UV inhibition of in situ Antarctic primary production using a field-derived biological weighting function. Photochemistry and Photobiology, 64(3): 407-418.

Boye, M., Nishioka, J., Croot, P.L., Laan, P., Timmermans, K.R. and de Baar, H.J.W., in press. Major deviations of iron complexation during 22 days of a mesoscale iron enrichment in the open Southern Ocean. Mar. Chem.

Boye, M., van den Berg, C.M.G., de Jong, J.T.M., Leach, H., Croot, P.L. and de Baar, H.J.W., 2001. Organic complexation of iron in the Southern Ocean. Deep Sea Res. I, 48(6): 1477-1497.

Chen, M. and Wang, W.X., 2001. Bioavailability of natural colloid-bound iron to marine plankton: Influences of colloidal size and aging. Limnology and Oceanography, 46(8): 1956-1967.

Croot, P.L., Bowie, A.R., Frew, R.D., Maldonado, M.T., Hall, J.A., Safi, K.A., la Roche, J., Boyd, P.W. and Law, C.S., 2001. Retention of dissolved iron and Fe-II in an iron induced Southern Ocean phytoplankton bloom. Geophys. Res. Lett., 28(18): 3425-3428.

Croot, P.L. and Johansson, M., 2000. Determination of iron speciation by cathodic stripping voltammetry in seawater using the competing ligand 2-(2- thiazolylazo)-p-cresol (TAC). Electroanalysis, 12(8): 565-576.

de Baar, H.J.W. and Boyd, P.W., 2000. The role of iron in plankton ecology and carbon dioxide transfer of the global oceans. In: R.B. Hanson, H.W. Ducklow and J.G. Field (Editors), The dynamic ocean carbon cycle; A midterm synthesis of the joint global ocean flux study. University Press Cambridge, Cambridge.

de Baar, H.J.W., Buma, A.G.J., Nolting, R.F., Cadee, G.C., Jacques, G. and Treguer, P.J., 1990. On iron limitation of the Southern Ocean - experimental- observations in the Weddell and Scotia seas. Mar. Ecol. Progr. Ser., 65(2): 105-122.

de Jong, J.T.M., den Das, J., Bathmann, U., Stoll, M.H.C., Kattner, G., Nolting, R.F. and de Baar, H.J.W., 1998. Dissolved iron at subnanomolar levels in the Southern Ocean as determined by ship-board analysis. Anal. Chim. Acta, 377(2-3): 113-124.

Emmenegger, L., Schonenberger, R.R., Sigg, L. and Sulzberger, B., 2001. Light-induced redox cycling of iron in circumneutral lakes. Limnol. Oceanogr., 46(1): 49-61.

Falkowski, P.G. and Raven, J.A., 1997. Aquatic Photosynthesis. Blackwell Science, Malden, MA.

Faust, B.C., 1994. A review of the photochemical redox reactions of iron(III) species in atmospheric, oceanic, and surface waters: Influences on geochemical cycles and oxidant formation. In: G.R. Helz, R.G. Zepp and D.G. Crosby (Editors), Aquatic Surface Photochemistry. CRC Press, Inc., London, pp. 3-37.

Finden, D.A.S., Tipping, E., Jaworski, G.H.M. and Reynolds, C.S., 1984. Light-induced reduction of natural iron(III) oxide and its relevance to phytoplankton. Nature, 309(5971): 783-784.

Fischer, A.C., Kroon, J.J., Verburg, T.G., Teunissen, T. and Wolterbeek, H.T., submitted. Radio-iron measurements in vessels: Exchange of iron with the wall.

Gao, H.Z. and Zepp, R.G., 1998. Factors influencing photoreactions of dissolved organic matter in a coastal river of the southeastern United States. Environ. Sci. Technol., 32(19): 2940-2946.

Geider, R.J., la Roche, J., Greene, R.M. and Olaizola, M., 1993. Response of the photosynthetic apparatus of *Phaeodactylum tricornutum* (Bacillariophyceae) to nitrate, phosphate, or iron starvation. J. Phycol., 29(6): 755-766.

Gerringa, L.J.A., Herman, P.M.J. and Poortvliet, T.C.W., 1995. Comparison of the linear van den Berg Ruzic transformation and a nonlinear fit of the Langmuir isotherm applied to Cu speciation data in the estuarine environment. Mar. Chem., 48(2): 131-142.

Gledhill, M., van den Berg, C.M.G., Nolting, R.F. and Timmermans, K.R., 1998. Variability in the speciation of iron in the northern North Sea. Mar. Chem., 59(3-4): 283-300.

Granger, J. and Price, N.M., 1999. The importance of siderophores in iron nutrition of heterotrophic marine bacteria. Limnol. Oceanogr., 44(3): 541-555.

Holland, H.D., 1984. The chemical evolution of the atmosphere and oceans. Princeton University Press, Princeton, NJ.

Hong, H. and Kester, D.R., 1986. Redox state of iron in the offshore waters of Peru. Limnol. Oceanogr., 31: 512-524.

Hudson, R.J.M., Covault, D.T. and Morel, F.M.M., 1992. Investigations of iron coordination and redox reactions in seawater using Fe-59 radiometry and ion-pair solvent-extraction of amphiphilic iron complexes. Mar. Chem., 38(3-4): 209-235.

Johnson, K.S., Coale, K.H., Elrod, V.A. and Tindale, N.W., 1994. Iron photochemistry in seawater from the equatorial Pacific. Mar. Chem., 46(4): 319-334.

Johnson, K.S., Gordon, R.M. and Coale, K.H., 1997. What controls dissolved iron concentrations in the world ocean? Mar. Chem., 57(3-4): 137-161.

Jones, G.J. and Morel, F.M.M., 1988. Plasmalemma redox activity in the diatom *Thalassiosira*. Plant Physiol., 87: 143-147.

King, D.W., Lounsbury, H.A. and Millero, F.J., 1995. Rates and mechanism of Fe(II) oxidation at nanomolar total iron concentrations. Environ. Sci. Technol., 29(3): 818-824.

Kuma, K., Nakabayashi, S. and Matsunaga, K., 1995. Photoreduction of Fe(III) by hydroxycarboxylic acids in seawater. Water Res., 29(6): 1559-1569.

Kuma, K., Nakabayashi, S., Suzuki, Y., Kudo, I. and Matsunaga, K., 1992. Photo-reduction of Fe (III) by dissolved organic-substances and existence of Fe (II) in seawater during spring blooms. Mar. Chem., 37(1-2): 15-27.

Kuma, K., Nishioka, J. and Matsunaga, K., 1996. Controls on iron(III) hydroxide solubility in seawater: The influence of pH and natural organic chelators. Limnol. Oceanogr., 41(3): 396-407.

Kunkely, H. and Vogler, A., 2001. Photoreduction of aqueous ferrioxamine B by oxalate induced by outer-sphere charge transfer excitation. Inorg. Chem. Commun., 4(4): 215-217.

Liu, X.W. and Millero, F.J., 1999. The solubility of iron hydroxide in sodium chloride solutions. Geochim. Cosmochim. Acta, 63(19-20): 3487-3497.

Liu, X.W. and Millero, F.J., 2002. The solubility of iron in seawater. Mar. Chem., 77(1): 43-54.

Maldonado, M.T. and Price, N.M., 2000. Nitrate regulation of Fe reduction and transport by Fe-limited *Thalassiosira oceanica*. Limnol. Oceanogr., 45(4): 814-826.

Maldonado, M.T. and Price, N.M., 2001. Reduction and transport of organically bound iron by *Thalassiosira oceanica* (Bacillariophyceae). J. Phycol., 37(2): 298-309.

Martin, J.H. and Fitzwater, S.E., 1988. Iron-deficiency limits phytoplankton growth in the northeast Pacific subarctic. Nature, 331(6154): 341-343.

Martin, J.H., Gordon, R.M. and Fitzwater, S.E., 1990. Iron in Antarctic waters. Nature, 345(6271): 156-158.

Miller, W.L. and Kester, D., 1994. Photochemical iron reduction and iron bioavailability in seawater. J. Mar. Res., 52: 325-343.

Miller, W.L., King, D.W., Lin, J. and Kester, D.R., 1995. Photochemical redox cycling of iron in coastal seawater. Mar. Chem., 50(1-4): 63-77.

Millero, F.J., 1998. Solubility of Fe(III) in seawater. Earth. Planet. Sci. Let., 154(1-4): 323-329.

Millero, F.J. and Sotolongo, S., 1989. The oxidation of Fe(II) with H_2O_2 in seawater. Geochim. Cosmochim. Acta, 53(8): 1867-1873.

Millero, F.J., Sotolongo, S. and Izaguirre, M., 1987. The oxidation-kinetics of Fe(II) in seawater. Geochim. Cosmochim. Acta, 51(4): 793-801.

Montgomery, D.C., 1997. Design and analysis of experiments. John Wiley & Sons, Inc., USA.

Morel, F.M.M., Hudson, R.J.M. and Price, N.M., 1991. Limitation of productivity by trace-metals in the sea. Limnol. Oceanogr., 36(8): 1742-1755.

Nishioka, J. and Takeda, S., 2000. Change in the concentrations of iron in different size fractions during growth of the oceanic diatom Chaetoceros sp.: importance of small colloidal iron. Marine Biology, 137(2): 231-238.

Nishioka, J., Takeda, S. and Wong, C.S., 2001. Change in the concentrations of iron in different size fractions during a phytoplankton bloom in controlled ecosystem enclosures. Journal of Experimental Marine Biology and Ecology, 258(2): 237-255.

O'Sullivan, D.W., Hanson, A.K. and Kester, D.R., 1995. Stopped-flow luminol chemiluminescence determination of Fe(II) and reducible iron in seawater at subnanomolar levels. Mar. Chem., 49(1): 65-77.

O'Sullivan, D.W., Hanson, A.K., Miller, W.L. and Kester, D.R., 1991. Measurement of Fe(II) in surface-water of the equatorial Pacific. Limnol. Oceanogr., 36(8): 1727-1741.

Ozturk, M., Bizsel, N. and Steinnes, E., 2003. Iron speciation in eutrophic and oligotrophic Mediterranean coastal waters; impact of phytoplankton and protozoan blooms on iron distribution. Mar. Chem., 81(1-2): 19-36.

Ozturk, M., Bizsel, N. and Steinnes, E., 2003. Iron speciation in eutrophic and oligotrophic Mediterranean coastal waters; impact of phytoplankton and protozoan blooms on iron distribution. Mar. Chem., 81: 19-36.

Powell, R.T. and Wilson-Finelli, A., 2003. Photochemical degradation of organic iron complexing ligands in seawater. Aquat. Sci., 65(4): 367-374.

Price, N.M. and Morel, F.M.M., 1998. Biological cycling of iron in the ocean, Metal Ions in Biological Systems, Vol 35, pp. 1-36.

Rijkenberg, M.J.A., Fischer, A.C., Kroon, J.J., Gerringa, L.J.A., Timmermans, K.R., Wolterbeek, H.T. and de Baar, H.J.W., 2005. The influence of UV irradiation on the photoreduction of iron in the Southern Ocean. Mar. Chem., 93: 119-129.

Rijkenberg, M.J.A., Gerringa, L.J.A., Neale, P.J., Timmermans, K.R., Buma, A.G.J. and de Baar, H.J.W., 2004. UVA variability overrules UVB ozone depletion effects on the photoreduction of iron in the Southern Ocean. Geophys. Res. Lett., 31: L24310, doi:10.1029/2004GL020829.

Rijkenberg, M.J.A., Gerringa, L.J.A., Neale, P.J., Timmermans, K.R., Buma, A.G.J. and de Baar, H.J.W., 2004. UVA variability overrules UVB ozone depletion effects on the photoreduction of iron in the Southern Ocean. Geophys. Res. Lett., 31(24): [doi:24310.21029/22004GL020829].

Ross, A.B. and Neta, P., 1982. Rate constants for reactions of aliphatic carbon-centered radicals in aqueous solution. *Natl. Stand. Ref. Data Ser.*, NSRDS-NBS-70: U.S. National Bureau of Standards.

Rue, E.L. and Bruland, K.W., 1995. Complexation of iron(III) by natural organic-ligands in the central north Pacific as determined by a new competitive ligand equilibration adsorptive cathodic stripping voltammetric method. Mar. Chem., 50(1-4): 117-138.

Rue, E.L. and Bruland, K.W., 1997. The role of organic complexation on ambient iron chemistry in the equatorial Pacific Ocean and the response of a mesoscale iron addition experiment. Limnol. Oceanogr., 42(5): 901-910.

Rueter, J.G. and Ades, D.R., 1987. The role of iron nutrition in photosynthesis and nitrogen assimilation in *Scenedesmus quadricauda* (Chlorophyceae). J. Phycol., 23(3): 452-457.

Seitz, W.R. and Hercules, D.M., 1972. Determination of trace amounts of iron (II) using chemiluminescence analysis. Anal. Chem., 44: 2143-2149.

Shaked, Y., Erel, Y. and Sukenik, A., 2002. Phytoplankton-mediated redox cycle of iron in the epilimnion of Lake Kinneret. Environ. Sci. Technol., 36(3): 460-467.

Steeneken, S.F., Buma, A.G.J. and Gieskes, W.W.C., 1995. Changes in transmission characteristics of polymethylmethacrylate and cellulose-(III) acetate during exposure to ultraviolet-light. Photochem. Photobiol., 61(3): 276-280.

Sunda, W.G. and Huntsman, S.A., 1995. Iron uptake and growth limitation in oceanic and coastal phytoplankton. Mar. Chem., 50(1-4): 189-206.

Takeda, S. and Kamatani, A., 1989. Photoreduction of Fe(III)-EDTA complex and its availability to the coastal diatom *Thalassiosira weissflogii*. Red Tides: Biol., Environ. Sci., Toxicol.: 349-352.

Timmermans, K.R., Gerringa, L.J.A., de Baar, H.J.W., van der Wagt, B., Veldhuis, M.J.W., de Jong, J.T.M., Croot, P.L. and Boye, M., 2001. Growth rates of large and small Southern Ocean

diatoms in relation to availability of iron in natural seawater. Limnol. Oceanogr., 46(2): 260-266.

Timmermans, K.R., Gledhill, M., Nolting, R.F., Veldhuis, M.J.W., de Baar, H.J.W. and van den Berg, C.M.G., 1998. Responses of marine phytoplankton in iron enrichment experiments in the northern North Sea and northeast Atlantic Ocean. Marine Chemistry, 61(3-4): 229-242.

Timmermans, K.R., van der Wagt, B. and de Baar, H.J.W., 2004. Growth rates, half-saturation constants, and silicate, nitrate, and phosphate depletion in relation to iron availability of four large, open-ocean diatoms from the Southern Ocean. Limnol. Oceanogr., 49(6): 2141-2152.

Trick, C.G., 1989. Hydroxamate-siderophore production and utilization by marine eubacteria. Curr. Microbiol., 18: 375-378.

Turner, D.R. and Hunter, K.A. (Editors), 2001. The Biogeochemistry of Iron in Seawater. IUPAC series on analytical and physical chemistry of environmental systems., 7. John Wiley & Sons, LTD., Chichester. New York. Weinheim. Brisbane. Singapore. Toronto.

Turner, D.R., Hunter, K.A. and de Baar, H.J.W., 2001. Introduction. In: D.R. Turner, Hunter, K.A. (Editor), The Biogeochemistry of Iron in Seawater. IUPAC series on analytical and physical chemistry of environmental systems. John Wiley & Sons, LTD., Chichester. New York. Weinheim. Brisbane. Singapore. Toronto, pp. 1-7.

van den Berg, C.M.G., 1995. Evidence for organic complexation of iron in seawater. Mar. Chem., 50(1-4): 139-157.

Voelker, B.M. and Sedlak, D.L., 1995. Iron reduction by photoproduced superoxide in seawater. Mar. Chem., 50(1-4): 93-102.

Waite, D.T. and Morel, F.M.M., 1984. Photoreductive dissolution of colloidal iron oxides in natural waters. Environ. Sci. Technol., 18: 860-868.

Waite, T.D., Szymczak, R., Espey, Q.I. and Furnas, M.J., 1995. Diel variations in iron speciation in northern Australian shelf waters. Mar. Chem., 50(1-4): 79-91.

Wells, M.L. and Goldberg, E.D., 1992. Marine Submicron Particles. Marine Chemistry, 40(1-2): 5-18.

Wells, M.L. and Goldberg, E.D., 1993. Colloid aggregation in seawater. Mar. Chem., 41(4): 353-358.

Wells, M.L. and Mayer, L.M., 1991. The photoconversion of colloidal iron oxyhydroxides in seawater. Deep Sea Res. I, 38(11): 1379-1395.

Wilhelm, S.W. and Trick, C.G., 1994. Iron-limited growth of cyanobacteria: multiple siderophore production is a common response. Limnol. Oceanogr., 39(8): 1979-1984.

Witter, A.E., Hutchins, D.A., Butler, A. and Luther, G.W., 2000. Determination of conditional stability constants and kinetic constants for strong model Fe-binding ligands in seawater. Mar. Chem., 69(1-2): 1-17.

Witter, A.E., Lewis, B.L. and Luther, G.W., 2000. Iron speciation in the Arabian Sea. Deep Sea Res. II, 47(7-8): 1517-1539.

Wu, J.F. and Luther, G.W., 1995. Complexation of Fe(III) by natural organic-ligands in the northwest Atlantic Ocean by a competitive ligand equilibration method and a kinetic approach. Mar. Chem., 50(1-4): 159-177.

Xiao, C.B., Palmer, D.A., Wesolowski, D.J., Lovitz, S.B. and King, D.W., 2002. Carbon dioxide effects on luminol and 1,10-phenanthroline chemiluminescence. Anal. Chem., 74(9): 2210-2216.

Zuo, Y.G., 1995. Kinetics of photochemical chemical cycling of iron coupled with organic-substances in cloud and fog droplets. Geochim. Cosmochim. Acta, 59(15): 3123-3130.

Chapter 7

Kinetic study reveals new Fe-binding ligand which affects the solubility of Fe in the Scheldt estuary

Loes J.A. Gerringa, Micha J.A. Rijkenberg, Bert Th. Wolterbeek, Tona G. Verburg, Marie Boye, Hein J.W. de Baar

Abstract

The chemistry of dissolved Fe(III) was studied in the Scheldt estuary (The Netherlands). Two discrete size fractions of the dissolved bulk (<0.2 μm and <1 kDa) and three salinities (S=26, 10 and 0.3) were considered.

Characteristics of dissolved organic Fe-binding ligands were determined by competitive ligand exchange adsorptive cathodic stripping voltammetry (CLE-ACSV) and by observing kinetic interactions. The conditional stability constant (K'), of the traditionally recognised dissolved organic Fe-binding ligands varies between $10^{20.4}$ and $10^{21.1}$ over the salinity range S=0.3 to S=26. For both size fractions the ligand concentrations are slightly lower than the dissolved Fe concentrations. Within the upper estuary where the fresh river water first meets seawater, the dissolved Fe and ligand concentrations decrease steeply with increasing salinity. Further downstream in the middle and lower estuary the decrease continues but far less pronounced. Since Fe is in excess over these ligands the solubility product of Fe(hydr)oxides apparently is exceeded in the whole estuary. The introduction of a new, relatively weak, ligand class and the study of kinetics between the different Fe(III) pools provided an explanation of the existence of high dissolved "labile" concentrations of Fe. We concluded that weak ligands (P) prevented precipitation of Fe(hydr)oxides. It's α value (binding potential = K'*[P]) varies between 10^{11} and $10^{11.5}$. The relatively weak ligand is thought to retard direct precipitation of an extra input of Fe. The presence of the weak ligand influences the analysis by CLE-ACSV, masking a salinity dependence in K'_{FeL}. It is the dissociation rate constant of FeL that causes this salinity dependence, but this can only partly be ascribed to the change in ionic strength. Changes in the origin of the organic ligands must take place as well, hence serve as the complementary explanation.

Rate constants of Fe with the competing ligand TAC were also measured in relation to salinity. Both rate constants, formation and dissociation of $Fe(TAC)_2$ decreased with salinity, in such a way that $K'_{Fe(TAC)2}$ remained constant between S=10 and S=26 with the value known from the literature ($\log\beta'_{Fe(TAC)2}$=22.4; Croot and Johansson, 2000). Yet the $\log\beta'_{Fe(TAC)2}$ is 26.8 at S=0.3, substantially higher than 22.4.

1. Introduction

Fe is essential for phytoplankton growth and is known to be limiting not only in the open ocean but also in coastal areas (Hutchins et al., 1998). To study the influence of the organic ligands on the solubility and reactivity of Fe may give valuable information to understand the biogeochemical behaviour of Fe. In this study we estimate the influence of dissolved organic ligands on the solubility and reactivity of Fe in the Scheldt estuary. Since the nature of organic ligands changes from terrestrial to marine environments, large solubility changes of the metals can be expected across salinity gradients (Baeyens et al., 1998).

The Scheldt estuary can be characterised as a system with strong hydrodynamic and physico-chemical gradients. The mixing zone of fresh and salt water extends over a distance of 70 to 100 km (Wollast, 1988). The upper part of the estuary has a high organic and nutrient load. Because most particulate matter is negatively charged, mixing of fresh water and seawater neutralises the surface charges resulting in a flocculation zone between S=1-5 (Sholkovitz, 1976; Wollast, 1988; Paucot and Wollast, 1997). Due to the large input of biodegradable organic matter during the summer, anoxia occurs (Duinker et al., 1983; Wollast, 1988). During the nineteen-eighties the quality of the estuary has been improved, reducing the nutrient and organic matter load, but still in summer anoxia occurs (Zwolsman and van Eck, 1993; Baeyens et al., 1998).

The residence time of water in the upper estuary is around 3 months during which non-refractory organic matter of terrestrial origin is almost completely mineralised (Wollast, 1988). Decrease in turbidity at salinities higher than 5 in combination with the large supply of nutrients by the river Scheldt produces phytoplankton blooms in spring and summer. During these periods the produced organic matter almost equals the amount of terrestrial organic carbon removed by respiration and sedimentation in the upper part (Wollast and Peters, 1978). Most of this freshly formed organic matter is transported to the North Sea.

Processes influencing metal solubility in the Scheldt estuary have been studied extensively in the past. The concentration of dissolved metals, like Zn, Cd, Mn, Cu and Fe, depends for 100% on the combination of redox conditions and organic ligand content (Chapter 8, Duinker and Nolting, 1978; van den Berg et al., 1987; Regnier and Wollast, 1993; Zwolsman and van Eck, 1993; Gerringa et al., 1996; Paucot and Wollast, 1997). In the upper estuary, where anoxia can occur, the dissolved Fe concentrations are relatively high (Duinker and Nolting, 1978; Zwolsman and van Eck, 1993). Metals like Zn and Cd easily precipitate as sulphides, since the solubility product of these solid sulphides is low (Emerson et al., 1983; Comans and van Dijk, 1988; Gerringa et al., 2001). In contrast Fe sulphides have a relatively high solubility product and their precipitation is unlikely in the Scheldt estuary, since the dissolved sulphide concentrations are not high enough. Concentration of dissolved organic

ligands are thought to determine the concentration of dissolved Fe above the solubility product of solid phases stable at the redox potential of the system (van den Berg et al., 1987).

However, Whitworth et al. (1999) could not explain the dissolved Fe concentrations in the Scheldt estuary with their model considering binding with dissolved organic ligands on the one hand and adsorption on particles on the other hand. The dissolved Fe concentrations were too high according to their model. From other studies it is known that high labile (with respect to the applied method) Fe concentrations occur in seawater which cannot be easily explained (Croot and Johansson, 2000; Boye et al., in press; Powell, personal communication; Chapter 8). The existence of a weak ligand, outside the detection window of the method applied to determine dissolved ligands, may constitute a perfect explanation for both "too high" dissolved Fe concentrations in the Scheldt estuary and relatively high labile Fe concentrations. To examine a possible existence of other ligand groups than the organic ones commonly found with K' between 10^{19} and $10^{23.5}$ (Gledhill and van den Berg, 1994; Croot et al., 2004), the complexation characteristics were studied in the Scheldt estuary in combination with a kinetic study.

We sampled three specific regions: **a**. upstream of the high turbidity zone, where terrestrial organic matter is present in high concentration (S=0.3); **b**. the zone where high primary production of plankton blooms generates fresh organic matter (S=10); **c**. the zone with predominantly coastal marine organic matter (S=26). Characteristics, like the dissolved organic ligand concentration L, the conditional stability constant K' of organic Fe complexes, and its dissociation and formation rate constants were determined in two size fractions (<0.2 μm and <1 kDa).

2. Methods

2.1. Sampling, filtration and measurement of dissolved Fe

In April 2002, samples were taken during a cruise on the ship Navicula (Royal-NIOZ) in the estuary of the river Scheldt in the south of the Netherlands (Figure 1). A torpedo towed alongside the ship was used to pump (Teflon diaphragm pump, Almatec A-15, Germany, driven by a compressor, Jun-Air model 600-4B, Denmark) water from 1 a 2 meter depth via acid-washed braided PVC tubing to an overpressurized class 100 clean container. The samples were filtered inline using 0.2 μm polycarbonate filter-cartridges (Sartorius Sartobran filter capsule 5231207H8). Salinity was measured with a simple TS meter.

Samples to characterise the dissolved organic Fe-binding ligands were collected from three stations in the Scheldt estuary at S=0.3, upstream of Antwerp, at S=10 near Hansweert and at S=26 where the river outlet enters the North Sea (Figure1). Part of these samples was then ultra-filtrated using an acid-cleaned Amicon SP60 cartridge (<1 kDa fraction) and a peristaltic pump of Watson Marlow (604S/R), enabling filtration of large sample volumes. Samples for the determination of dissolved Fe (<0.2 μm and <1 kDa) were immediately acidified to pH=2 with concentrated 3 x quartz-distilled (3xQD) HNO_3 and stored at room temperature. Dissolved Fe in samples at high salinity (S=26) was measured with flow injection analysis (FIA) (de Jong et al., 1998). Samples of medium and low salinity (0.3 and 10) were directly measured by graphite furnace atomic absorption spectroscopy GFAAS (Perkin Elmer). Samples taken for the characterisation of the dissolved organic ligands were frozen immediately after sampling.
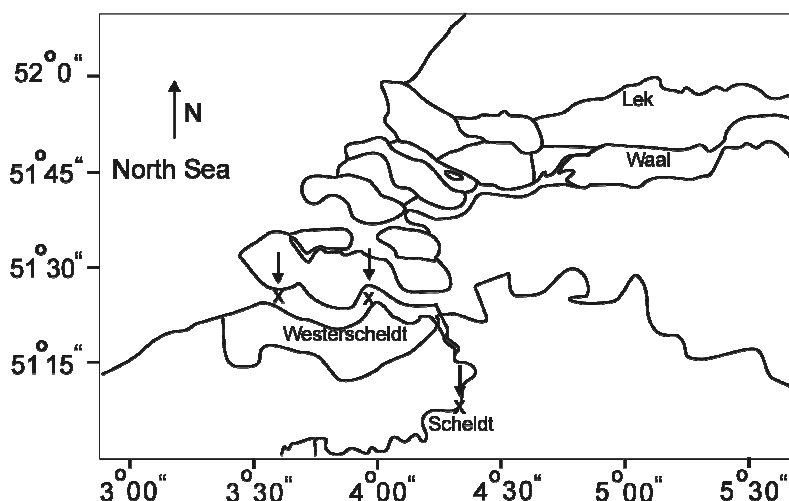

Figure 1. The estuary of the river Scheldt in the southwest of The Netherlands. The three sampling sites are indicated.

2.2 Complexation characterisation

2.2.1 Titration with Fe to estimate [L] and K' after equilibration of the samples

Determination of the organic speciation of iron in seawater water was performed using Competing Ligand Exchange-Absorptive Cathodic Stripping Voltammetry (CLE-ACSV). The 2-(2-Thiazolylazo)-p-cresol (TAC) was used as competing ligand (Croot and Johansson, 2000). All solutions were prepared using 18.2 MΩ nanopure water. The equipment consisted of a μAutolab voltammeter (Ecochemie, The Netherlands), a static mercury drop electrode (Metrohm Model VA663), a double-junction Ag/saturated AgCl reference electrode with a salt bridge containing 3 M KCl and a counter electrode of glassy carbon. The titration was performed using 0.01 M stock solution of TAC in 3xQD methanol, 1 M boric acid (Suprapur, Merck) in 0.3 M 3x QD ammonia (Suprapur, Merck) (extra cleaning by the addition of TAC after which TAC and $Fe(TAC)_2$ was removed with a C18 SepPak column) to buffer the samples to a pH of 8.05 (Boye et al., 2003) and a 10^{-6} M Fe(III) stock solution acidified with 0.012 M HCl (3xQD). Aliquots of 15 ml were spiked with Fe(III) until final concentrations between 0 and 20 nM and allowed to equilibrate overnight (> 15 hours) with 5 mM borate buffer and 10 μM TAC. The borate buffer was adapted to samples of differing salinities and pH's.

The concentration $Fe(TAC)_2$ in the samples was measured using the following procedure: i) removal of oxygen from the samples for 200 seconds with dry nitrogen gas, a fresh Hg drop was formed at the end of the purging step, ii) a deposition potential of –0.40 V was applied for 30-60 seconds according to the sample measured, the solution was stirred to facilitate the adsorption of the $Fe(TAC)_2$ to the Hg drop, iii) at the end of the adsorption period the stirrer was stopped and the potential was scanned using the differential pulse method from -0.40 to -0.90 V at 19.1 mV s^{-1} and the stripping current from the adsorbed $Fe(TAC)_2$ recorded.

The Fe bound by TAC (10 μM) after equilibration overnight (>15 hours) is defined as Fe labile with respect to TAC.

2.2.2 Kinetic characterisation of the dissolved ligands

To determine dissociation and formation rate constants of the natural organic Fe-complexes a slightly modified method as described by Wu and Luther (1995) was used. Instead of 1-nitroso-2-naphtol (NN) TAC was used as competing ligand (Croot and Johansson, 2000). The Fe or TAC is added to the sample and the changes imposed by these additions are followed with time until equilibrium is reached. All reactions considered are

assumed to go via inorganic Fe (Fe'), direct formation of one complex of Fe out of another complex of Fe are ignored, i.e. assumed only to exist via dissociation from one complex followed by the formation of the other complex.

The frozen samples were thawed directly before the kinetic experiments.

To measure the binding and precipitation after an addition of Fe, 20 nM of Fe is added to 250 ml seawater and 15 sub-samples were taken in time. Labile Fe, defined as that pool of Fe complexed with TAC within 120 s after addition of 10 µM TAC, was measured. The TAC was added to the sample after the 200 s nitrogen bubbling (measuring procedure is described in section 2.2.1) to remove oxygen and before an extra period of 30 s of nitrogen bubbling and a collection period of 90 s. This is the shortest time used to measure labile Fe in these samples. The observed decrease with time after Fe addition of labile Fe is explained by the formation of Fe complexes (FeL and FeP) and the precipitation of oxyhydroxides (FeX) (Figure 2 A, B).
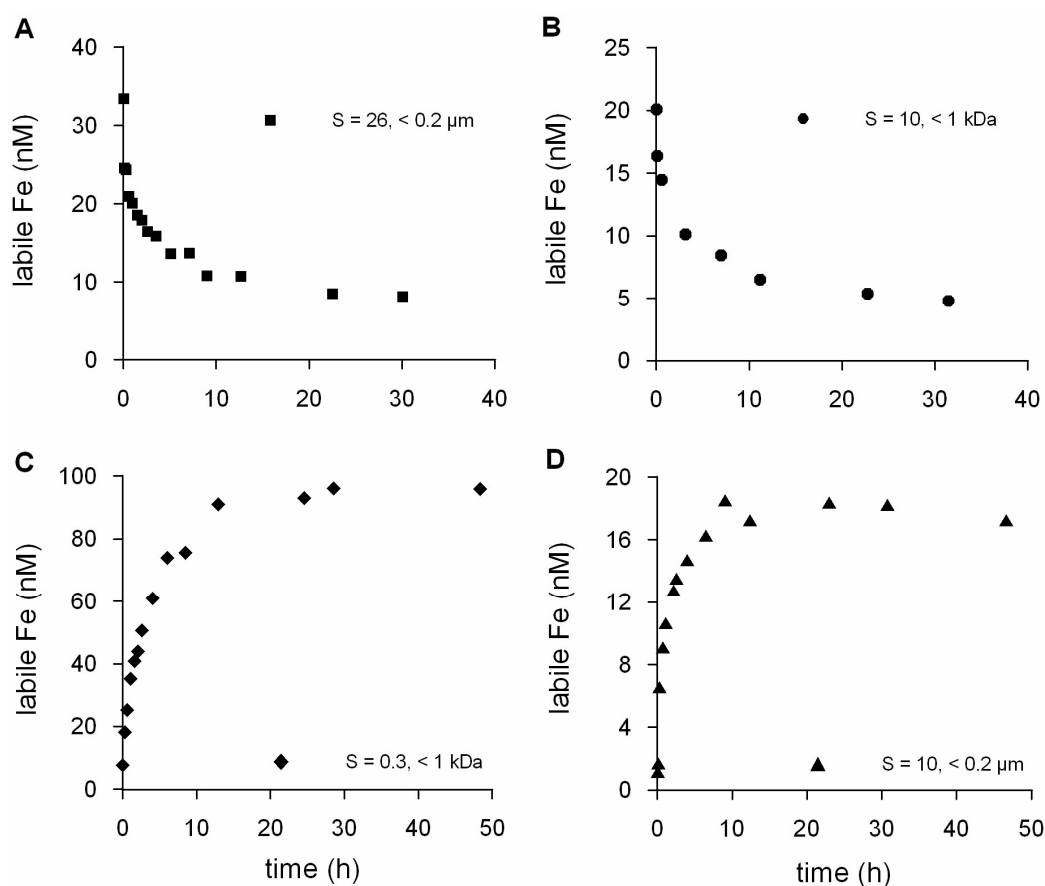

Figure 2. Changing Fe concentrations with time after an addition of Fe (A and B) and TAC (C and D). In figures A and B the presence of TAC was as short as possible (120 s), therefore the measured Fe concentration is called labile. In figures C and D TAC is competing with the natural ligands for Fe and the measured Fe concentration is called labile with respect to TAC ([TAC]$=10^{-5}$M).

The classical titration with Fe followed by an equilibration period (section 2.2.1.) is assumed to represent the equilibration situation with the ligand L ($K'=10^{19}$-$10^{23.5}$). (Obviously in the case that a second ligand exists as well, as here reported, this assumption is not necessarily valid, as discussed below). To measure the effect of addition of a competing ligand with time, 10 µM TAC was added to the seawater forcing the dissociation of dissolved Fe-complexes. The subsequent increase of the concentration Fe(TAC)$_2$ with time is measured as reflection of the dissociation of natural Fe complexes on the one hand and formation of Fe(TAC)$_2$ on the other hand (Figure 2 C, D). The formation and dissociation rate constants of Fe(TAC)$_2$ can be estimated this way and a relation of these rate constants with salinity can be studied.

2.3 Modelling

In order to formulate models for the calculation of rate constants, some general assumptions have to be made. The inorganic speciation of Fe was described by: inorganic Fe= Fe'= 10^{10}*Fe^{3+} (Hudson et al., 1992) and the solubility product of iron-oxyhydroxides FeX is assumed to be 0.2 nM (Byrne and Kester, 1976; Kuma et al., 1996; Liu and Millero, 2002). After filtration the samples were frozen immediately preventing chemical reactions to take place, only during thawing of the samples precipitation could happen. Although this possible precipitation cannot be ruled out, it was assumed that the initial concentration of oxyhydroxides is [FeX]=0 at t=0. Whether this assumption is valid will be discussed in the discussion section.

2.3.1 Model 1: addition of Fe

Addition of Fe will cause formation of Fe complexes and possibly precipitation of an Fe(hydr)oxide (hereafter called FeX). Titration analyses, used to obtain the ligand characteristics, showed that the Fe-binding ligand sites were saturated with Fe. Thus the assumption is that, upon addition of 20 nM Fe, labile Fe would decrease due to formation of FeX. Since the labile Fe concentration was too high to fit the above mentioned assumptions, the presence of a relative weak ligand called P is assumed. This is discussed extensively in the results section. We do not have any information on the concentration of P. Since P is not detected during the titrations analyses, it must be below the detection window of TAC (10 µM) (αFe(TAC)$_2$ = β* [TAC]^2 = $10^{22.4}$ *10^{-10} = $10^{12.4}$ thus αFeP $\leq 10^{11.4}$). Here it is assumed that due to the short time TAC is present in the sample, that it does not influence the concentrations of either FeL or FeX.

Furthermore it is implicitly assumed that FeP dissociates within 120 s in the presence of 10 µM TAC. Measured labile Fe would thus contain [Fe'] + [FeP], which needs to be

tested. Moreover the FeL, FeP and FeX all have been defined as having the simple 1:1 coordination, where the free concentration of the constituents is annotated with a prime ([L']).

The reactions which take place after addition of Fe can be described by,

$$[FeL] \quad \underset{k2}{\overset{k1}{\rightleftarrows}} \quad [Fe'] + [L'] \tag{1}$$

$$[FeP] \quad \underset{k4}{\overset{k3}{\rightleftarrows}} \quad [Fe'] + [P'] \tag{2}$$

$$[FeX]\downarrow \quad \underset{k6}{\overset{k5}{\rightleftarrows}} \quad [Fe'] + [X'] \tag{3}$$

Total [L] is known from the titration analysis. Total dissolved [Fe] is known and 20 nM Fe is added at t=0 as Fe'. The k_1, k_3, and k_5 are the dissociation rate constants and the k_2, k_4 and k_6 are the formation rate constant of FeL, FeP and FeX, respectively (Figure. 3). Thus the changes in concentration of all species are defined by the following suite of equations

$$d[Fe']/dt = k_1*[FeL] + k_3*[FeP] + k_5*[FeX] -$$
$$k_2*[Fe']*[L'] - k_4*[Fe']*[P'] - k_6*[Fe']*[X'] \tag{4}$$

$$d[FeL]/dt = k_2*[Fe']*[L'] - k_1*[FeL] \tag{5}$$

$$d[L']/dt = k_1*[FeL] - k_2*[Fe']*[L'] \tag{6}$$

$$d[FeP]dt = k_4*[Fe']*[P'] - k_3*[FeP] \tag{7}$$

$$d[P]/dt = k_3*[FeP] - k_4*[Fe']*[P'] \tag{8}$$

$$d[FeX]/dt = k_6*[Fe']*[X'] - k_5*[FeX] \tag{9}$$

$$d[X']/dt = k_5*[FeX] - k_6*[Fe']*[X'] \tag{10}$$

Together with the boundary conditions these 7 equations (4-10) can be used to solve the 6 rate constants and 2 species concentrations. Modelling was done using Excel (Microsoft) and Scientific software (Micromath Scientific software) and the calculations were performed using a least squares fit.
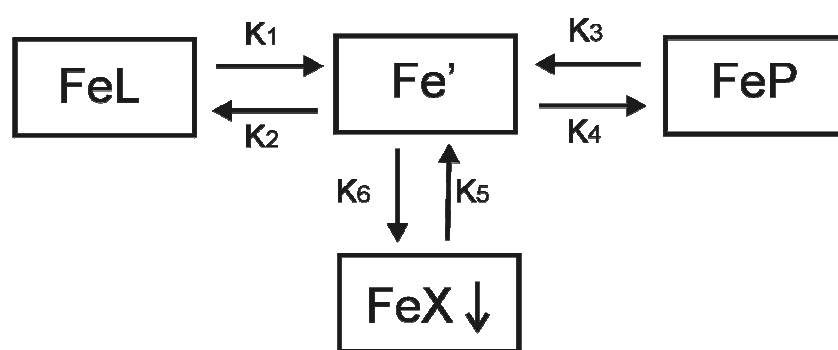
Figure 3. Model 1 representing the reactions taking place after addition of Fe between inorganic Fe (Fe'), the complexes FeL and FeP, and the precipitate FeX. X represents an oxyhydroxide molecule. With k_1, k_3 and k_5 as dissociation or dissolution rate constants and k_2, k_4 and k_6 as formation rate constants.

The following boundary conditions were used for the concentrations of X and P:

A). For the results in Table 2 a conditional statement was used, to let FeX only be formed if [Fe']>0.2 nM. A similar conditional statement of a maximum metal concentration before precipitation can take place was also used by Laan et al. (2004). A concentration for total P was chosen as three times the total dissolved Fe concentration. This choice is rather arbitrary and is based on the results of Nolting et al. (1998), they found in the Southern Ocean that the ligand concentration was larger or equal to three times the dissolved Fe concentration ([Fe$_{diss}$]).

B). For the results in Table 3 it was assumed that total [X] at t=0 was so large, that formation of FeX would not change its concentration, implying [X']≈constant and d[X']/dt≈0, such that equation 10 can be eliminated from the model. At constant pH and assuming a kind of oxyhydroxide to form, a constant [X'] is a credible assumption since [OH$^-$]≈10^{-6}M. The advantage above the preceding assumption (case A above, where a threshold value is applied before formation of FeX can occur), is the possibility of the formation and dissociation (dissolution in this case) of FeX independently of [Fe']. Moreover the term k_6*X' then can be substituted by k_6' such that a conditional statement in the formation of FeX is not necessary anymore. This changes the equations 4 and 9 into,

$$[Fe'] = k_1*[FeL]+k_3*[FeP]+k_5*[FeX]-$$
$$k_2*[Fe']*[L^{'}]-k_4*[Fe']*[P^{'}]- k_6'* [Fe'] \qquad (4b)$$

$$[FeX] = k_6'* [Fe']-k_5*[FeX] \qquad (9b)$$

As second assumption a very high total [P] was chosen, being 10 μM, implying [P$^{'}$]≈constant and d[P]/dt≈0 resulting in the elimination of equation 8 from the model.

C). As described above (B) the assumptions [X']≈constant and d[X']/dt≈0 were used for the results given in Table 4. For the total P concentration the assumption described in A was used, $[P]=3*[Fe_{diss}]$.

2.3.2 Model 2: addition of TAC.

Here no Fe was added, only 10 μM TAC as competing ligand. In this research the changes in [Fe(TAC)$_2$] are followed until equilibrium is reached. An extra reaction has to be taken into account for model 2,

$$[Fe(TAC)_2] \quad \xrightleftharpoons[k8]{k7} \quad [Fe'] + 2[TAC^{'}] \tag{12}$$

with two new rate constants, changing eq. 4 into 4c and adding eq. 13 and 14 to eq. 4-10 in the model (Figure 4).
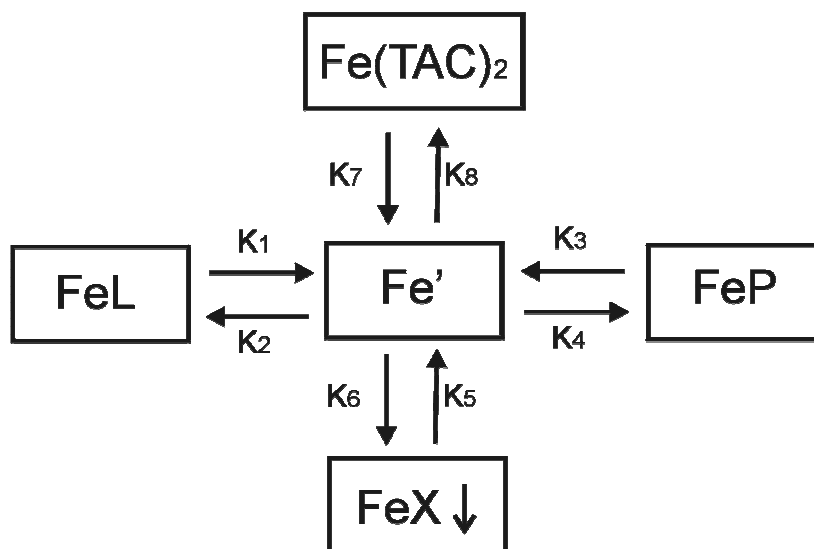

Figure 4. Model 2 representing the reactions taking place after addition of TAC between inorganic Fe (Fe'), the natural Fe complexes FeL, FeP, the added complex Fe(TAC)$_2$ and the precipitate FeX. X represents an oxyhydroxide molecule. With k_1, k_3, k_5 and k_7 as dissociation or dissolution rate constants and k_2, k_4, k_6 and k_8 as formation rate constants.

$$d[Fe']/dt = k_1*[FeL] + k_3*[FeP] + k_5*[FeX] + k_7*[Fe(TAC)_2]$$
$$-k_2*[Fe']*[L^{'}] - k_4*[Fe']*[P^{'}] - k_6'*[Fe'] - k_8*[Fe']*[TAC^{'}]^2 \qquad (4c)$$

$$d[Fe(TAC)_2]/dt = k_8*[Fe']*[TAC^{'}]^2 - k_7*[Fe(TAC)_2] \qquad (13)$$

$$d[TAC']/dt = k_7*[Fe(TAC)_2] - k_8*[Fe']*[TAC^{'}]^2 \qquad (14)$$

The program Scientist was used to fit the data. We had chosen the rate constants k_1-k_6' from Table 3 in order to calculate the rate constants of TAC, k_7 and k_8. The choice to use these rate constants and not the ones from Table 2 or 5 is explained in the results section.

3. Results

3.1 Dissolved Fe

Data on dissolved Fe in the Scheldt estuary are scarce (van den Berg et al., 1987; Herzl, 1999; Nolting et al., 1999). Otherwise Nolting et al. (1999) presented dissolved Fe concentrations from 1978 which were much higher than the values found in this work. Their Fe concentrations ranged from 50 nM at salinity 30, via 300 nM at S=10 to >1 μM at S=1. This is more than twofold higher than our data (Table 1). Van den Berg et al. (1987) measured comparable Fe concentrations as Duinker et al. (1983) and Nolting et al. (1999) , ranging from 400 nM at S=10 to 30 nM at S=27. For a large part the higher dissolved Fe concentrations are due to a higher organic load during the nineteen seventies-eighties, exemplified by the oxygen depletion reached up to S=15 (Duinker et al., 1983). Dissolved and colloidal Fe concentrations from 1993 to 1997 are presented by Herzl (1999). She found mean dissolved Fe concentrations in the upper estuary (S=0.3) of 524 nM, near Vlissingen (S≈30) a mean Fe concentration of 28 nM was observed.

The dissolved Fe concentrations decrease very steeply in the upper estuary due to flocculation and possibly oxidation (Sholkovitz, 1976; Duinker et al., 1983; Zwolsman and van Eck, 1993; Herzl, 1999) followed by a more gradual decrease at higher salinities (Table 1). The soluble Fe fraction <1 kDa is 3 to 6 times smaller than the total dissolved Fe (<0.2 μm), suggesting a high content of colloidal Fe (>1 kDa - <0.2 μm) in the estuary. This is in line with results from Galveston Bay where 80% of dissolved Fe was >1 kDa (Wen et al., 1999), similar to the Venice Lagoon (Martin et al., 1995) and other estuaries (Powell et al., 1996). Herzl (1999) filtered Scheldt water over two size fractions <0.45 μm and <0.05 μm. She found that almost all dissolved Fe was <0.05 μm. Only during high river discharge high concentrations of Fe between 0.45 and 0.05 μm were measured.

Table 1. The dissolved Fe concentrations (nM), conditional stability constants (K') and the dissolved organic ligand concentrations (nano-equivalents of M Fe = neq of M Fe) of the three salinities in the Scheldt estuary. The 0.2/1kDa denotes the ratio of the concentrations of Fe and L between the two size fractions <0.2 μm and <1 kDa, respectively. Since the ligand sites were saturated with Fe, the estimation of K' and L could not be done with the usual accuracy (see method section) and errors on these calculations could not be estimated. The log K' and the ligand concentrations are mean values of n determinations. The α value is the product of the conditional stability constant and the concentration ($\alpha = K' * [L_t]$).

	$[Fe_{diss}]$ (nM)	Log K'	Ligand (neq M Fe)	$[Fe_{diss}]/[L_t]$	Log α
S=26					
<0.2μm	12.2	20.4 (n=5)	8	1.5	12.3
<1kDa	2	20.5 (n=4)	1.3	1.5	11.6
(0.2/1kDa)	6.1		6.1		
S=10					
<0.2μm	104.5	21.1 (n=2)	95	1.1	14.1
<1kDa	36	20.6 (n=3)	30	1.2	13.1
(0.2/1kDa)	3		3		
S=0.3					
<0.2μm	536	21.2 (n=2)	525	1.02	14.9
<1kDa	102	20.8 (n=3)	85	1.2	13.7
(0.2/1kDa)	5.3		6.2		

3.2 Complexation characteristics of Fe

3.2.1 [L] and K' estimated by titration with Fe after equilibration of the samples

The concentrations of organic Fe-binding ligands in size fractions, <0.2 μm and <1 kDa, and at all three salinities (S=26, 10 and 0.3) are slightly lower than the concordant dissolved Fe concentrations (Table 1). Thus, the Fe-binding ligand sites of all samples are saturated with Fe. A titration curve is therefore seldom found, most titrations resulted thus in a straight line and in all cases the concentration of Fe labile with respect to TAC is relatively high. Estimation of the ligand characteristics by nonlinear regression is not possible (Gerringa et al., 1995). Instead the linearization of van den Berg/Ružić is used (van den Berg, 1982), but an error estimation of the parameters is not possible. Reasoning from experience the error of

the estimation of log K_{FeL}' must be large, near 1; the error of the estimation of the ligand concentration near 10%. The relatively high error of K' is due to statistical causes since calculation of K_{FeL}' is hardly possible when no curvature is found in the titration curve (Gerringa et al., 1995).

For both size fractions considered, the K_{FeL}' was estimated to be around 10^{21} with respect to Fe^{3+} (Table 1). This value is in concert with other findings in the open ocean and the Mediterranean Sea (Gledhill and van den Berg, 1994; Rue and Bruland, 1995; van den Berg, 1995; Rue and Bruland, 1997; Nolting et al., 1998; Boye et al., 2001; Boye et al., 2003). In this estuary with a gradient in salinity and in the origin and characteristics of the dissolved organic matter the conditional stability constant is surprisingly constant. An excess of dissolved Fe over the ligand concentration is found, at S=26 even 1.5 times more Fe than ligand is present, at the other salinities this ratio is around 1.1 (Table 1). It appears that a colloidal ligand group with the same binding characteristics exists.

It is probable that a weaker ligand group exists in both size fractions, since otherwise the solubility product, 0.2 nM (Liu and Millero, 2002), of solid Fe(oxy)hydroxides is exceeded. However, only one strong ligand group was detected. Thus the conceivable weak ligand group falls outside the detection window, product of concentration and stability constant, of our method. According to Apte et al. (1988) the detection window of CSV is 2 to 3 orders of magnitude wide, thus with a centre of the detection window, of $10^{12.4}$ meaning that ligands with an α value lower than about $10^{10.9}$ cannot be detected. During the analysis of the ligand characteristics K' and the total ligand concentration [L], TAC had more than 15 hours time to compete with the natural organic ligands present. The method of the titration is based on measuring the competition between TAC and the natural ligands until the point in the titration where the ligands are filled with Fe and only TAC is complexing the added excess Fe. Weaker ligands below the detection window of TAC cannot compete, and dissociate within the time of the equilibration period. Ligands within the detection window used do compete with TAC for the added Fe in the titration, but also dissociate to a small extent assuming reversible complexation. Since TAC was selected to compete with these ligands, the centre of the detection window equals more or less with the α value (K_{FeL}'*total [L]) of the complexing ligands. Therefore even when strong ligands are saturated with Fe, a small horizontal part in the titration curve is possible. This horizontal part represents the filling of the empty spaces L^- as created by dissociation of the natural ligand due to competition with TAC during the overnight equilibration period.

High concentrations of Fe labile with respect to TAC have been reported by Boye et al. (in press) in the open ocean, by Croot and Johansson (2000) in coastal water, by Rijkenberg et al. (Chapter 8) in coastal areas and estuaries and after a dust deposition (Powell, personal communication). High concentration of Fe labile with respect to TAC means that within the equilibration time (overnight) $Fe(TAC)_2$ is formed to a substantial concentration.

The most logical explanation is that TAC is stronger than the natural ligands. Interpretation becomes problematic when, as in these samples, high concentrations of Fe labile with respect to TAC do occur in samples in which a titration curve was found with a horizontal part steeply curving into the linear part of the titration. The horizontal part reflects the filling of empty ligand sites with Fe, the form of the curving represents the strength of the binding, a smooth curve a relative weak binding, a sharp curve a relatively strong binding strength. A combination of high concentrations of Fe labile with respect to TAC with a relative strong binding strength of the ligands can only be explained when two ligands are present, a relatively weak ligand, causing a high concentration of Fe labile with respect to TAC, falling outside the detection window of the method and a relatively strong ligand reflected by the sharp curvature in the titration graph. For the relatively weak ligand this implies α values must be less than $10^{10.9}$. Assuming concentrations of the weak ligand P three times the dissolved Fe concentration, then for S=26, K_{FeP}' has a maximum value of $10^{18.3}$ ($10^{10.9}/3*12.2*10^{-9}$) and for S=0.3 K_{FeP}' has a maximum value of $10^{16.7}$ ($10^{10.9}/3*536*10^{-9}$). An alternative assumption being used here is for [P] to be at an even larger overdose here arbitrarily taken to be 1000 nM, this resulting in a maximum K_{FeP}' of $10^{16.9}$.

3.2.2 Kinetic characterisation of the dissolved ligands

Until now the method of Wu and Luther (1995) had been applied to open ocean samples with low concentrations of dissolved Fe (<1-2 nM Fe) and low concentrations of organic ligands (≈ 5 nano-equivalents of M Fe), or been applied to low concentrations of organic model ligands in open ocean samples (Witter et al., 2000). The samples of the Scheldt estuary are different from open ocean samples, since the concentrations of Fe and organic matter are much higher, the salinity is lower and varies (S=26, 10 and 0.3 in our samples) and the organic ligands sites of L (K'=10^{21}) are saturated with Fe.

Since the dissolved organic ligands L are filled with Fe in the Scheldt samples, addition of Fe should theoretically result in precipitation of Fe-(hydr)oxides. For the ocean it is assumed that the solubility product (SP) of Fe-(hydr)oxides is 0.2 nM (Byrne and Kester, 1976; Kuma et al., 1996; Liu and Millero, 2002). The SP of inorganic Fe(hydr)oxides depends, apart from pH and temperature, also on salinity. According to Liu and Millero (2002) the SP decreases from 0.3 nM Fe' at S=26 to 0.16 nM Fe' at S=10, after which it increases to 0.4 nM Fe' at S=0.03 (pH=8.1 and 25 °C). We used 0.2 nM for all salinities in our calculations. However, as discussed before, the concentration Fe labile with respect to TAC was so high that a relatively weak ligand P is assumed to exist. During the kinetic measurements high labile Fe concentrations were measured (Figure 2 A). Moreover, in the samples from S=0.3 and the fraction <0.2 μm, after addition of 20 nM of Fe no decrease with

time of labile Fe was observed. This would mean that this 20 nM of added Fe did not form precipitates as oxy-hydroxides within 48 hours.

3.2.2.1 Model 1: addition of Fe

A decline in labile Fe with time was observed in all samples except for the samples of S=0.3, in the fraction <0.2 μm (Figure 2A, B). The decline in labile Fe cannot be the result of the formation of FeL since these ligand sites are saturated with Fe. On the other hand, the decrease in labile Fe could be due to the formation of FeP complexes, but this effect would not have been detected since FeP is assumed to be labile with respect to 10 μM TAC in 120 s. It is very likely that Fe was precipitating as Fe(hydr)oxides. A precipitation of Fe is expected to be Fe-(hydr)oxides of amorphous colloidal nature. This precipitate must then be so stable that it cannot be dissolved after addition of TAC by formation of $Fe(TAC)_2$ within 120 s. Rijkenberg et al. (Chapter 5) showed in open ocean Antarctic water that indeed these fresh precipitates were stable with respect to the conditions of the measurement. Unpublished results in estuarine water from the Wadden Sea also showed that fresh Fe-precipitates were stable with respect to the 120 s exposure of TAC. Moreover dissolution by prolonged presence of TAC showed a relatively slow dissolution process. The decrease in labile Fe over time observed in samples from S=26 and S=10 and from the fraction <1 kDa in S=0.3 (Figure 2A, B) is assumed to result from Fe(hydr)oxides precipitation, annotated as FeX.

In the samples of S=0.3, in the fraction <0.2 μm apparently no precipitation took place; the high labile Fe cannot be explained by relatively high concentrations of P. Due to high variance in the data of the samples S=0.3, the <0.2 μm fraction could not be modelled. Initially the measured concentrations of labile Fe increased with time after which it remained constant. An increase with time is not the expected result (see for comparison Figures 2A and B). However, the concentrations were very low with respect to the total dissolved Fe concentration (10 nM compared to 525 nM Fe_{diss}). Moreover at low salinity and high organic matter the chemical analysis is operating at the borders of what is possible. It was decided to discard the data from the samples S=0.3, <0.2 μm.

A. Formation of FeX if [Fe']>0.2 nM; [P]=3*[Fe$_{diss}$]

For the results in Table 2 a conditional statement was used, to let FeX only be formed if [Fe']>0.2 nM as used by Laan et al. (2004). The theoretical drawback of this model is that

Table 2. Results of model 1, which assume that formation of FeX is only possible if [Fe']>0.2 nM. The K' values and α values are given with respect to [Fe^{3+}], the rate constants with respect to [Fe']. The concentrations (P, L, X) are in nM, the k_f in $M^{-1} s^{-1}$, the k_d in s^{-1}, and the K' in M^{-1}.

	S=26		S=10		S=0.3	
	0.2µm	1kDa	0.2µm	1kDa	0.2µm	1kDa
k_d1	1.41E-05	3.82E-05	2.85E-07	2.99E-07		8.08E-05
k_f2	3.13E+05	8.32E+05	1.28E+06	1.13E+06		1.14E+06
k_d3	7.47E-05	1.49E-04	6.29E-05	4.54E-05		6.28E-05
k_f4	4.65E+03	1.12E+05	6.24E+03	6.75E+03		4.80E+03
k_d5	4.91E-06	4.68E-06	2.39E-07	2.48E-07		7.02E-06
k_f6	5.52E+04	4.37E+05	1.00E+05	1.05E+05		4.08E+04
init[X]	37	19.3	49.1	36.8		35
[L]	8	2	95	30	525	85
[P]	150	40	400	180		350
LogK'$_{FeL}$	20.35	20.34	22.65	22.58		20.15
LogK'$_{FeP}$	17.79	18.87	18.00	18.18		17.89
k6/k5 FeX	20.05	20.97	21.62	21.63		19.77
Log αFeL	12.25	11.64	15.63	15.05		13.08
Log α FeP	10.97	11.48	11.60	11.43		11.43
Log αFeX	12.62	13.26	14.31	14.19		12.31

the assumption that Fe' should be smaller than 0.2 nM is an assumption belonging to the equilibrium conditions domain, yet here used in kinetics. Moreover precipitation and dissolution also occurs when Fe < 0.2 nM. The fact that in Table 2 the conditional stability constant of the precipitate FeX can be higher than the conditional stability constant of FeL and FeP and still that not all Fe is precipitated is due to the 'if then' statement used. Latter statement is meaning that FeX can only be formed if Fe' > 0.2 nM. Here please notice the fact that the concentration of X is also fitted and if X is related to the pH the concentration of X must remain constant. However, in these calculations [X'] decreases while forming FeX. Table 2 shows that K'$_{FeL}$ of the samples S=10 are substantially higher. This is not found by the equilibrium method (Table 1). The values found for K'$_{FeP}$ are a little higher than expected considering that FeP was expected to fall outside the detection window of TAC. Furthermore, Table 2 shows rate constants of the three different species that are not very specific per species. For all species the k_d varies around values of $10^{-5} s^{-1}$, similar values as found by Witter et al. (2000) and Witter et al. (2000). These results suggest that the value of 10^{-5} to $10^{-6} s^{-1}$ is a mean value for the dissociation rate constant, applicable for all Fe species. The formation rate constant shows more variation, making discrimination between FeL, with $k_f=3*10^5- 10^6$, and FeP, with $k_f=4*10^3-10^5$, possible.

B. [X']≈ constant, d[X']/dt≈ 0, [P']≈ constant, d[P']/dt≈ 0

The results in Table 3 show K'_{FeL} values that vary negatively with salinity and thus with ionic strength. Such lower K' values with higher ionic strength is in agreement with the thermodynamic theory stating that activity coefficients become lower at higher ionic strength, this effect increases with increasing charge of the species (Stumm and Morgan, 1996). The decrease in K'_{FeL} is caused by the increase of the dissociation rate constant of FeL and a decrease of the formation rate constant with increasing salinity (Table 3). The increase in dissociation rate of FeL can be shown considering the half life times, $t_{1/2}= 0.693/k_d$ (Stone and Morgan, 1990). At S=26 the half life time is 48 to 100 s; at S=10 the half life varies between 582 and 1155 s (9.7-19 min); at S=0.3 (<1 kDa) the half life time is 814 s (13.5 min.). For each salinity the dissociation rate of FeL of the size fraction <1 kDa is smaller than for the <0.2 μm fraction. The formation rate constant of FeL decreases with S with a factor 100 between S=26 and S=0.3 <1 kDa.

The K'_{FeP} values are substantially lower than K'_{FeL}, the K'_{FeP} and the rate constants of FeP do not show a trend with S, (Table 3). The dissociation half life is between 1.8 and 3.6 h.

A distinct differentiation in dissociation rate constants between the two ligand groups L and P exists, ranging from $10^{-2} – 10^{-4}$ s^{-1} for FeL to 10^{-5} s^{-1} for FeP. The dissolution rate

Table 3. Results from model 1, assuming [X]≈ constant and [P]=10μM. The $k_f'6$ is $k_f6*[X']$. The concentrations (P, L) are in nM, the k_f in M^{-1} s^{-1}, the k_d in s^{-1}, and the K' in M^{-1}. The K' values and α values are given with respect to [Fe^{3+}] and the rate constants with respect to [Fe'].

	S=26,		S=10		S=0.3	
	0.2μm	1kDa	0.2μm	1kDa	0.2μm	1kDa
k_d1	1.42E-02	5.94E-03	1.19E-03	5.97E-04		8.51E-04
k_f2	1.13E+07	1.91E+07	7.00E+08	9.15E+07		1.09E+09
k_d3	7.72E-05	2.31E-04	1.19E-04	5.25E-05		6.84E-05
k_f4	7.80E+01	6.81E+02	3.02E+02	1.61E+02		3.61E+02
k_d5	4.84E-05	8.46E-05	9.28E-05	3.18E-05		9.18E-05
$k_f'6$	2.38E-03	7.61E-03	4.53E-03	3.65E-03		5.15E-03
[L]	8	2	95	30	525	85
logK'$_{FeL}$	18.9	19.51	21.77	21.19		22.11
logK'$_{FeP}$	16.00	16.47	16.40	16.49		16.72
Log αFeL	10.81	10.81	14.75	13.66		15.04
Log αFeP	11.00	11.47	11.40	11.49		11.72
Log αFeX	11.69	11.95	11.69	12.06		11.75

constant of FeX is also in the order of 10^{-5} to 10^{-4} s^{-1}. This value is at least 100 times faster than found by Kuma et al. (1992). Rose and Waite (2003) observed comparable dissolution rates as obtained in this research, they found that the k_d depends on the ageing of the Fe-precipitate, and measured dissolution rates of $2.3*10^{-4}$ s^{-1} from freshly precipitated iron and $4.6*10^{-6}$ s^{-1} for precipitates aged for one week. The formation rate constants differ considerably, with fast formation kinetics for FeL and substantially slower formations kinetics for FeP. Note the relatively low α value for FeL at S=26, especially when compared with the α value of FeP. The α values of FeL, FeX and FeP indicate the distribution of Fe over these species when equilibrium is reached.

C. $[X']\approx$ constant, $d[X']/dt\approx 0$, $[P]=3*[Fe_{diss}]$

We know that a negative salinity relationship exists for DOC and for the total concentration of L. If P is of an organic nature it is sensible to assume such a relationship also for P. By assuming [P] to be related to [Fe$_{diss}$] a relationship between P and S is created in an indirect way. In Table 4 the result are shown. The α values do remain as given in Table 3, but

Table 4. Results from model 1, assuming $[X]\approx$constant and $[P]=3*[Fe_{diss}]$. The kf'6 is kf6*[X']. The K' values and α values are given with respect to $[Fe^{3+}]$, the rate constants with respect to [Fe']. The concentrations (P, L) are in nM, the k_f in M^{-1} s^{-1}, the k_d in s^{-1} and the K' in M^{-1}.

	S=26		S=10		S=0.3	
	0.2μm	1kDa	0.2μm	1kDa	0.2μm	1kDa
k_d1	9.08E-03	5.27E-03	1.14E-03	5.70E-04		7.02E-04
k_f2	1.06E+07	1.59E+07	6.51E+08	8.74E+07		9.05E+08
k_d3	7.49E-05	2.03E-04	1.18E-04	5.15E-05		7.22E-05
k_f4	5.56E+03	1.55E+05	7.61E+03	8.80E+03		1.01E+04
k_d5	4.64E-05	7.44E-05	8.47E-05	3.12E-05		7.51E-05
$k_f'6$	2.19E-03	6.88E-03	4.52E-03	3.58E-03		4.97E-03
[L]	8	2	95	30		85
[P]	150	40	400	180		350
LogK'$_{FeL}$	19.07	19.48	21.76	21.19		22.11
LogK'$_{FeP}$	17.87	18.88	17.81	18.23		18.15
Log α FeL	10.97	10.78	14.73	13.66		15.04
Log α FeP	11.05	11.48	11.41	11.49		11.69
Log α FeX	11.67	11.97	11.73	12.06		11.82

the formation rate constant of FeP and thus K'$_{FeP}$ changed with the assumptions of [P]. A relationship between salinity and the total concentration of P does not create a relation between kinetics and salinity.

3.2.2.2 Model 2: addition of TAC.

The addition of TAC to the samples introduces two new rate constants, k_d7 and k_f8 (equations 4c, 12 and 13 and Figure 4). The kinetic rate constants obtained applying boundary condition set B ([X']≈ constant, d[X']/dt≈ 0, [P']≈ constant, d[P']/dt≈ 0; results shown in Table 3) were used to calculate the formation and dissociation rate constants of Fe(TAC)$_2$. As shown before the results using boundary condition set A (Table 2) did not allow a distinction between two ligands (L and P). The choice between the rate constants displayed in Tables 3 and 4 is rather arbitrary. In principle these results do not differ from each other, only the assumed [P] does. Since the results in Table 4 do not give any confirmation that [P] is related to S and/or [Fe$_{diss}$], the results obtained with boundary condition set B (Table 3) were used.

The thus calculated rate constants of Fe(TAC)$_2$ have a distinct relation with salinity. The formation rate constant of Fe(TAC)$_2$ increases with decreasing S and varies from $2*10^7$ M^{-2} s^{-1} at S=26 to $8*10^8$ M^{-2} s^{-1} at S=10. The dissociation rate constant of Fe(TAC)$_2$ increases with decreasing S, and varies from $4*10^{-6}$ s^{-1} at S=26 to $1*10^{-4}$ s^{-1} at S=10. The β'$_{Fe(TAC)2}$ remains constant at $10^{22.7}$, varying between 10^{23} and 10^{22}, very close to the value given by Croot and Johansson (2000) of $10^{22.4}$. Although only one calculation was done for S=0.3 and it is not very secure to draw conclusions, we observed the same trend with salinity continuing to increasing k_f and decreasing k_d. However, at S=0.3 the value of β'$_{Fe(TAC)2}$ also changes, increasing to $10^{26.3}$.

4. Discussion

4.1 The assumptions and the methods

Application of a threshold [Fe'] for precipitation of FeX did not give satisfactory results since a distinction between the different Fe species was not possible (Table 2). The rate constants are more or less the same for the different Fe species and the result of a mean value of the existing Fe species. However these rate constants do coincide with those found for model ligands and natural ligands in the Arabian Sea (Witter et al., 2000; Witter et al., 2000). The assumption of a high and thus more or less constant concentration of X resulted in three distinct sets of rate constants for the three Fe species.

Table 5. The estimated rate constants and stability constant of $Fe(TAC)_2$ according to model 2. The rate constants k_1-k_6 from Table 3 were used together with the assumption that $[P] = 10000$ nM. The k_f is in $M^{-2}\,s^{-1}$, the k_d in s^{-1}, and the K' in M^{-2}. The K' values and α values are given with respect to $[Fe^{3+}]$ and the rate constants with respect to [Fe']. The $\alpha_{Fe(TAC)2}$ is $\beta_{Fe(TAC)2}*[TAC']^2$.

sample	Log β Fe(TAC)$_2$	k_f	k_d	Log α Fe(TAC)$_2$
S=**26**, <0.2μm	22.62	2.71E+07	6.43E-06	12.62
S=**26**, <0.2μm	22.69	1.97E+07	4.00E-06	12.69
S=**26**, <1kDa	23.00	1.36E+07	1.38E-06	13
S=**26**, <1kDa	22.84	1.47E+07	2.12E-06	12.84
S=**10**, < 0.2μm	22.98	1.00E+09	1.06E-04	12.98
S=**10**, <0.2μm	23.08	8.50E+08	7.11E-05	13.08
S=**10**, <1kDa	21.98	8.78E+07	9.09E-05	11.98
S=**10**, <1kDa	22.34	2.90E+08	1.31E-04	12.34
S=**0.3**, <1kDa	26.28	3.25E+10	1.74E-06	16.28

Table 1 shows the binding characteristics of FeL determined by the titration, although no trend in K'$_{FeL}$ with S is present. However, the α values do show a trend with S as observed by the kinetic experiments (Tables 4 and 5). No distinction could be made between the ligand groups with the equilibration method of titration (Table 1); a mean K' value of more than one ligand group was obtained. This value of K' represents both the ligands L and P. The ligand P is only just outside the detection window of TAC and it will interfere to some extent during the titration method. The technique of ligand equilibration is vulnerable for these interferences.

According to Table 5 the conditional stability constant of $Fe(TAC)_2$ at S=0.3 is much higher than for the higher salinities, thus the K'$_{FeL}$ values in Table 1 for the samples at S=0.3 are an underestimation since all these samples are calculated with $\beta_{Fe(TAC)2}=10^{22.4}$ given by Croot and Johansson (2000). This underestimation is indeed confirmed by the K'$_{FeL}$ obtained from the kinetic experiments (Tables 3 and 4).

Model 2 produced for S=26 and S=10 the binding characteristics of Fe and TAC that are very close to the values from the literature (Croot and Johansson, 2000). Knowing the rate constants for Fe binding and dissociation with TAC we can discuss the meaning of labile Fe and Fe labile with respect to TAC. The formation rate constants of $Fe(TAC)_2$ are fast but not fast enough to complex all labile Fe within the time of the measurement. Different collection times will result in different labile Fe concentrations and thus the resulting labile Fe measured as $Fe(TAC)_2$ is very sensitive to the conditions during the measurement. Thus labile Fe is not necessarily the same as excess Fe with respect to L.

The data from S=0.3, <0.2 μm could not be modelled. No decline in labile Fe after an addition of Fe was observed. This can not be explained by the formation of FeP. The constant

high Fe concentration in this practically fresh water can only be explained by formation of instable colloidal Fe species of unknown composition. The concentration of colloidal Fe is higher than 400 nM here (Table 1).

4.2 Comparison with literature values

The FeL is the traditionally known complexed Fe species with fast formation rates, more or less 10 times faster than the model ligands used by Witter et al. (2000) and the surface samples of Witter and Luther (1998) (Table 6). The k_d values found by Witter and Luther (1998) and Witter et al. (2000) are more comparable to the values we find for the relatively weak ligand P. Since this investigation considers estuarine samples and not open ocean water as was used by Witter and Luther (1998) and Witter et al. (2000) the discrepancy might also be due to the presence of coastal ligands differing form truly marine organic ligands. Another reason for differences in rate constants might be because the method of calculation in this research is an improvement of the method copied from Wu and Luther (1995), the latter also used in the papers of Witter and co-authors. Our improvement made it possible to distinguish between two ligands. We found for the strong ligand L (that also might consist of more than one ligand group as found by Rue and Bruland (1995, 1997) that the k_d values are between $8*10^{-4}$ and $1.42*10^{-2}$ s^{-1} and for the weak ligand P k_d values between $5*10^{-5}$ and $2.3\ 10^{-4}$ s^{-1}. The relatively strong ligand L dissociates faster than the relatively weak ligand P (Table 3). Rose and Waite (2003) studied kinetics of Fe with ligands from terrigenous organic matter from coastal areas. They distinguished two classes, a ligand class with k_d constants between $3.24*10^{-4}$ to $3.4*10^{-3}$ and a ligand class with k_d between 10^{-6} and 10^{-4} s^{-1} (Table 6). So the k_d of the so-called weak ligand from the data of Rose and Waite (2003) coincides with the k_d of our strong ligand L and the k_d of the so-called strong ligand of Rose and Waite (2003) coincides with k_d values of our weak ligand P.

The k_f for the strong ligand L found in the Scheldt varies between 10^7 to 10^9 M^{-1}s^{-1}, with the highest value occurring in the almost fresh water part of the estuary (Table 3). Rose and Waite (2003) found formation rate constants between 10^6 to 10^8 M^{-1}s^{-1}. The most estuarine samples in our research have k_f values close to values found by Rose and Waite (2003) in coastal organic matter and the surface values in the NW Atlantic Ocean of Witter and Luther (1998). Witter et al. (2000) found values in the Arabian Sea which are a little higher (Table 6).

The dissolution rate of FeX is between $3.2*10^{-5}$ and $9.3*10^{-5}$ s^{-1}, almost exactly the same value of $3.5*3.2*10^{-5}$ s^{-1} as found by Witter and Luther (1998) for dissolution of added (and then assumed to be precipitated) Fe to UV-oxidized North-western Atlantic Ocean water. The dissolution rate compares less well with the dissolution rate measured by Kuma et al., (1992) at pH=8.06, they found more than 10 times higher values in seawater.

Table 6. Comparison of the rate constants found in this research with other publications. All rate constants are given with respect to [Fe']. The data of this research are given for both size fractions; first the values for the fraction <0.2 μm and then the values of <1 kDA according to the salinity. The formation rate constant of FeP depends on the assumed concentration for P, therefore they are not given in this table (see Tables 3 and 4).

sample	k_f in M^{-1} s^{-1}	k_d in s^{-1}	references
<u>Natural marine ligands</u>			
NW Atlantic	$2 \cdot 10^6$	$3 \cdot 10^{-5}$	Wu and Luther , 1995
NW Atlantic 200m	$1.13 \cdot 10^6$	$3.9 \cdot 10^{-5}$	Witter and Luther, 1998
NW Atlantic 2874m	$4.21 \cdot 10^4$	$1 \cdot 10^{-7}$	
<u>Model ligands in</u>			
NW Atlantic water	$1 \cdot 10^5 - 2 \cdot 10^6$	$5 \cdot 10^{-8} - 1.2 \cdot 10^{-5}$	Witter et al., 2000a
Arabian Sea	$5 \cdot 10^5 - 10^4$	$10^{-6} - 2 \cdot 10^{-5}$	Witter et al., 2000b
<u>Terrigenous NOM in</u>			
<u>Offshore Sydney, S=36</u>			
Strong ligand	$2.1 \cdot 10^5 - 9.6*10^7$	$1 \cdot 10^{-6} - 1.3 \cdot 10^{-4}$	Rose and Waite, 2003b
Weak ligand		$2 \cdot 10^{-4} - 4 \cdot 10^{-3}$	
<u>Scheldt Estuary S=26</u>			
Strong ligand L	$1.1 - 2 \cdot 10^7$	$1.4 \cdot 10^{-2} - 6 \cdot 10^{-3}$	This research*
Weak ligand P		$7.7 \cdot 10^{-5}$	
<u>Scheldt Estuary S=10</u>			
Strong ligand L	$7 \cdot 10^8 - 9.1 \cdot 10^7$	$1.2 \cdot 10^{-3} - 6 \cdot 10^{-4}$	This research*
Weak ligand P		$1.2 \cdot 10^{-4} - 5.2 \cdot 10^{-5}$	
<u>Scheldt Estuary S=0.3</u>			
Strong ligand L	$1 \cdot 10^9$	$8.5 \cdot 10^{-4}$	This research*
Weak ligand P		$6.8 \cdot 10^{-5}$	

4.4. Salinity

The kinetic rate constants were found to depend on salinity resulting in a salinity-related K'. Yet no variation in K' with salinity was found upon application of the classical titration using CLE-ACSV. This coincides with the results obtained by Witter and Luther (1998) when they observed a relation between K' and depth using the kinetic approach and no relation between K' and depth using the titration method.

The K'_{FeL} values increase from $10^{18.9}$ at S=26 to $10^{22.11}$ at S=0.3. Whether the change of K'_{FeL} with S is related to changes in ionic strength and the activity coefficients of the reacting species, or that the origin of the organic ligands changes is an interesting question that we want to address now. According to Stone and Morgan (1990) an increase in the ionic strength lowers the reaction rate between a cation and an anion and has little effect on reaction rate when one or both of the reactants are uncharged. Here we assume that Fe is bound in a 1:1 coordination to the ligand in ionic binding. According to Hering and Morel (1990) the formation rate constant of metal chelation is decreasing with increasing strength for charged metals, although this also depends on the type of complex formation and the therefore on the rate-limiting reactions. The dissociation rate constant is related to the formation rate constant through the principle of micro reversibility, hence proportional to the formation rate constant by division through the conditional stability constant. The observed increase in K'_{FeL} in Table 3 can partially be explained by the decrease of the ionic strength. Since the complex is supposed to have no charge and the ionic species are assumed to have a charge of three, the effect on changing activity coefficients is thus higher on the formation rate constant. At the salinities 26, 10 and 0.3 the ionic strengths are 0.47, 0.23, and 0.03 respectively. According to the Davies equation the activity coefficients for ions with a charge of three are 0.0115, 0.056 and 0.21 respectively (Stumm and Morgan, 1996). A difference of factor 324 in formation rate constants between S=26 and S=0.3 can be accounted for by salinity (0.21/0.0115=18, a difference of 18 for Fe^{3+} and for the assumed L^{3-} or P^{3-} and thus 18^2). The actual difference is factor 100 (Table 3) and is thus of the order of magnitude that it can be explained by ionic strength alone. However, a difference exists also between the size fractions per salinity, which apart from ligand concentration is the only difference that can be found with size fraction as discrimination. The presence of colloidal molecules increases the dissociation of the two ligand classes (FeL and FeP) with a factor of 2 (Tables 3 and 4). This is also an indication for a difference in the origin of the organic ligands. Moreover, a faster dissociation with increasing S cannot be explained by means of ionic strength and this probably reflects the changing origin of the organic ligands, which in this estuary should be quite large. At S=0.3 the organic material is terrestrial of nature since it is upstream of the area with maximum turbidity, terrestrial organic matter prevails here and the conditions may differ considerably with more saline water downstream where most of the terrestrial organic matter has already been lost due to flocculation. Therefore it is quite possible that we cannot compare data from S=0.3 with the other data. Although Rose and Waite (2003) also used organic matter of terrigenous origin, a comparison is difficult since they measured at a constant high salinity in their experiments. It is thus not surprising to find differences in organic ligands, although until now since everybody found the same K' values, a distinction to source of the organic ligands was hardly possible. A faster dissociation of Fe from the organic ligands is favourable for

uptake by phytoplankton, since the Fe concentration can be limited in seawater, so this might be essential for the role of Fe in plankton growth.

4.4. The new ligand P

The ligand P was distinguished and since no information was present about this ligand a concentration had to be assumed. An assumed high concentration of 1000 nM implying no changes in P' worked very well. It has to be remembered however, that the estimated K'_{FeP} must always be considered in combination with the assumed total concentration of P, the α value (product of total ligand concentration and conditional stability constant) remains constant. A change in the concentration of P is reflected by changes in the formation rate constant and so in the value of K', whereas α remains constant. The influence of salinity cannot be found in the estimated characteristics of this ligand. When constructing the models it was assumed that labile Fe consisted of Fe' and FeP, since the dissociation was assumed to be relatively fast. To verify this hypothesis let us use the time 120 s of the measurement and the rate constants from tables 3 and 5, $[TAC] = 10^{-5}$ M, $[Fe'] = 20*10^{-9}$ M, $[Fe(TAC)_2] = 0$ at t=0 and for the sake of simplicity let us assume that equal concentrations of FeL and L' and equal concentrations of FeP and P' exist. Then 4.8 and 7800 nM $Fe(TAC)_2$ can be formed (depending on the salinity), no dissociation occurred, 500 times more FeP is dissociated than formed, and 14 times more FeL is formed than dissociated, using equations 13, 7 and 5 respectively. High labile Fe concentrations can thus be attributed to the dissociation of the relatively weak ligand. The measured $[Fe(TAC)_2]$ is due to added Fe' (20 nM) and the dissociating FeP. The dissociation of FeP is slow compared to FeL, but the formation is very much slower compared to FeL and slower than FeX. Thus after an Fe addition first FeL would be formed, which is not possible here since the sites were already saturated with Fe, then FeX will precipitate and in a later stage FeP can be formed.

4.5 Consequences for the mobility of Fe in the Scheldt

The α value of FeL is lower at S=26 but higher at the other salinities than the other two α values of FeP and FeX, which are of the same order of magnitude. The FeX as species was treated in the same way as the ligands, with a constant concentration of X, which might be close to the truth thinking of OH^- linked species (oxyhydroxides). Thus at high salinity in the estuary, L', P' and X' compete with each other for Fe', and part of the Fe will precipitate as FeX. Upstream in the estuary at lower salinities, L must be saturated before any formation of FeP or precipitation as FeX can occur. There, equal amounts of excess Fe will be precipitated as FeX and exist as FeP according to the more or less equal α values (Tables 3 and 4). Thus half of the excess Fe with respect to L remains in the dissolved phase!

As much as 90% of the Fe complexes had dissociated by competition with TAC at t≈∞ in the samples S=26 (both fractions) as well as in S=0.3 in the fraction <1 kDa (Figure 2C). Dissociation of organic Fe complexes in samples of S=10 (both fractions) and S=0.3, <0.2 μm occurred only for 20% (Figure 2D). These results are well explained when the α values of FeL, FeP, FeX and $Fe(TAC)_2$ are considered. At S=26 and S=0.3 <1 kDa the α values of the ligands L and P and of the precipitate FeX (Table 3) are all below those of $Fe(TAC)_2$ (Table 5) and indeed around 10% of the α value of $Fe(TAC)_2$. On the other hand for the samples at S=10 the α value of FeL is larger than of $Fe(TAC)_2$ (Tables 3 and 5). According to equilibrium assumptions and the fact that α of FeL is around 10 times larger than α $Fe(TAC)_2$, only 10% of total Fe should exist as $Fe(TAC)_2$ at the end of the experiment, and indeed this varies between 11 and 20% for the samples at S=10 (results not shown).

It is also apparent from the relatively high α values of FeX in Table 3 that some Fe will precipitate after disturbing the equilibrium with the solid phase due to filtration and removal of the colloidal size fraction. The α values of the Fe species FeL, FeP, FeX and $Fe(TAC)_2$ suggest that Fe will even precipitate in the presence of TAC.

Whitworth et al. (1999) described the binding constants of several metals on suspended particulate matter in the Scheldt estuary. With these binding constants and those of dissolved organic ligands they can model the competition between ligands and particles and predict the dissolved metal concentration. This was impossible for Fe because the conditional stability constants for the adsorption on particles (logK'=15) differed too much from the conditional stability constant of the dissolved organic ligands (logK'=18-23). With our results on the ligand P and FeX, we fill this gap.

Ligands like the here called P might be of minor importance in the open ocean where free ligand sites of the strong ligand are still in excess. In coastal areas however, or in the open ocean after a sudden input of Fe these relatively weak ligands can become important. The presence of weak ligands can be indicated by high labile Fe or Fe concentrations in excess over the ligand concentrations (Croot and Johansson, 2000; Boye et al., in press; Powell, personal communication; Chapter 8).

5. Conclusions

Modelling of the kinetic data of Fe in natural estuarine waters gave new insight in the chemistry and mobility of Fe. A distinction could be made in rate constants between three different Fe species. A strong well known ligand, L, with fast formation kinetics, 10 to 100 times faster than the model ligands found by Witter et al. (2000), is accompanied by a relatively weak ligand, P, and a precipitate of Fe, FeX. The existence of this relatively weak ligand P was not detected before. Calculations pointed out that half of excess Fe (with respect

to L) was kept in the dissolved phase by the weak ligand P. The presence of P explained the high concentrations of Fe labile with respect to TAC in the estuary.

The K', and both rate constants of the strong ligand L are dependent on the salinity. The formation rate constant decreases with salinity, which could for the largest part be explained by ionic strength and related changes in activity coefficients. The positive relation between salinity and the dissociation rate constant indicates a changing origin of the ligands, which in the Scheldt estuary is not surprising.

The formation rate constant of $Fe(TAC)_2$ is not as fast as expected by its high stability constant. The detection window for 10 μM TAC allows interferences with the relatively weak ligand P. TAC can be used in samples of all salinities. Until S=10 the $\beta_{Fe(TAC)2}$ value of $10^{22.4}$ from Croot and Johansson (2000) can be used, at lower salinities $\beta_{Fe(TAC)2}$ value increases considerably ($10^{26.3}$ at S=0.3).

The influence of size fractions was found, except on Fe and ligand concentrations, also on the dissociation rate constant of FeL. Fe from the colloidal fraction dissociates faster than from the truly dissolved phase.

Finally, precipitation cannot be neglected in filtered, non-acidified samples, even in the presence of excess strong ligands.

Acknowledgements

References

Apte, S.C., Gardner, M.J. and Ravenscroft, J.E., 1988. An evaluation of voltammetric titration procedures for the determination of trace-metal complexation in natural-waters by use of computer-simulation. Anal. Chim. Acta, 212(1-2): 1-21.

Baeyens, W., Goeyens, L., Monteny, F. and Elskens, M., 1998. Effect of organic complexation on the behaviour of dissolved Cd, Cu and Zn in the Scheldt estuary. Hydrobiologia, 366: 81-90.

Baeyens, W., Parmentier, K., Goeyens, L., Ducastel, G., De Gieter, M. and Leermakers, M., 1998. The biogeochemical behaviour of Cd, Cu, Pb and Zn in the Scheldt estuary: results of the 1995 surveys. Hydrobiologia, 366: 45-62.

Boye, M., Aldrich, A.P., van den Berg, C.M.G., de Jong, J.T.M., Veldhuis, M. and de Baar, H.J.W., 2003. Horizontal gradient of the chemical speciation of iron in surface waters of the northeast Atlantic Ocean. Mar. Chem., 80(2-3): 129-143.

Boye, M., Nishioka, J., Croot, P.L., Laan, P., Timmermans, K.R. and de Baar, H.J.W., in press. Major deviations of iron complexation during 22 days of a mesoscale iron enrichment in the open Southern Ocean. Mar. Chem.

Boye, M., van den Berg, C.M.G., de Jong, J.T.M., Leach, H., Croot, P.L. and de Baar, H.J.W., 2001. Organic complexation of iron in the Southern Ocean. Deep Sea Res. I, 48(6): 1477-1497.

Byrne, R.H. and Kester, D.R., 1976. Solubility of hydrous ferric oxide and iron speciation in seawater. Mar. Chem., 4: 255-274.

Comans, R.N.J. and van Dijk, C.P.J., 1988. Role of complexation processes in cadmium mobilization during estuarine mixing. Nature, 336(6195): 151-154.

Croot, P.L., Andersson, K., Ozturk, M. and Turner, D.R., 2004. The distribution and speciation of iron along 6[deg]E in the Southern Ocean. Deep Sea Research Part II: Topical Studies in Oceanography, 51(22-24): 2857-2879.

Croot, P.L. and Johansson, M., 2000. Determination of iron speciation by cathodic stripping voltammetry in seawater using the competing ligand 2-(2- thiazolylazo)-p-cresol (TAC). Electroanalysis, 12(8): 565-576.

de Jong, J.T.M., den Das, J., Bathmann, U., Stoll, M.H.C., Kattner, G., Nolting, R.F. and de Baar, H.J.W., 1998. Dissolved iron at subnanomolar levels in the Southern Ocean as determined by ship-board analysis. Anal. Chim. Acta, 377(2-3): 113-124.

Duinker, J.C. and Nolting, R.F., 1978. Mixing, removal and mobilization of trace-metals in the Rhine estuary. Neth. J. Sea Res., 12(2): 205-223.

Duinker, J.C., Nolting, R.F. and Michel, D., 1983. Effects of salinity, pH and redox conditions on the behaviour of Cd, Zn, Ni and Mn in the Scheldt estuary. Thalassia Jugosl., 18: 120-191.

Emerson, S., Jacobs, L. and Tebo, B., 1983. The behaviour of trace metals in marine anoxic waters: solubilities at the oxygen-hydrogen sulphide interface. In: C.S. Wong, E. Boyle, K.W. Bruland, J.D. Bruland and E.D. Goldberg (Editors), Trace metals in seawater. Plenum Press, New York, pp. 579-608.

Gerringa, L.J.A., de Baar, H.J.W., Nolting, R.F. and Paucot, H., 2001. The influence of salinity on the solubility of Zn and Cd sulphides in the Scheldt estuary. J. Sea Res., 46(3-4): 201-211.

Gerringa, L.J.A., Herman, P.M.J. and Poortvliet, T.C.W., 1995. Comparison of the linear van den Berg Ruzic transformation and a nonlinear fit of the Langmuir isotherm applied to Cu speciation data in the estuarine environment. Mar. Chem., 48(2): 131-142.

Gerringa, L.J.A., Poortvliet, T.C.W. and Hummel, H., 1996. Comparison of chemical speciation of copper in the Oosterschelde and Westerschelde estuaries, The Netherlands. Est. Coastal Shelf Sci., 42(5): 629-643.

Gledhill, M. and van den Berg, C.M.G., 1994. Determination of complexation of iron(III) with natural organic complexing ligands in seawater using cathodic stripping voltammetry. Mar. Chem., 47(1): 41-54.

Hering, J.G. and Morel, F.M.M., 1990. The kinetics of trace metal complexation: Implications for metal reactivity in natural waters. In: W. Stumm (Editor), Aquatic Chemical Reactions. Reaction rates of processes in natural wtaers. Wiley Interscience, New York, pp. 145-173.

Herzl, V., 1999. The dissolved metal speciation may be affected by the particle/water interactions existing within the turbidity maximum zone of an estuary. PhD thesis Thesis, Universite Libre de Bruxelles, Bruxelles.

Hudson, R.J.M., Covault, D.T. and Morel, F.M.M., 1992. Investigations of iron coordination and redox reactions in seawater using Fe-59 radiometry and ion-pair solvent-extraction of amphiphilic iron complexes. Mar. Chem., 38(3-4): 209-235.

Hutchins, D.A., DiTullio, G.R., Zhang, Y. and Bruland, K.W., 1998. An iron limitation mosaic in the California upwelling regime. Limnol. Oceanogr., 43(6): 1037-1054.

Kuma, K., Nakabayashi, S., Suzuki, Y. and Matsunaga, K., 1992. Dissolution rate and solubility of colloidal hydrous ferric-oxide in seawater. Mar. Chem., 38(1-2): 133-143.

Kuma, K., Nishioka, J. and Matsunaga, K., 1996. Controls on iron(III) hydroxide solubility in seawater: The influence of pH and natural organic chelators. Limnol. Oceanogr., 41(3): 396-407.

Laan, R.G.W., Verburg, T.G., Wolterbeek, H.T. and de Goeij, J.J.M., 2004. Photodegradation of iron(III)-EDTA: Iron speciation and domino effect on cobalt availability. Environ. Chem., 1: 107-115.

Liu, X.W. and Millero, F.J., 2002. The solubility of iron in seawater. Mar. Chem., 77(1): 43-54.

Martin, J.M., Dai, M.H. and Cauwet, G., 1995. Significance of colloids in the biogeochemical cycling of organic-carbon and trace-metals in the Venice lagoon (Italy). Limnol. Oceanogr., 40(1): 119-131.

Nolting, R.E., Helder, W., de Baar, H.J.W. and Gerringa, L.J.A., 1999. Contrasting behaviour of trace metals in the Scheldt estuary in 1978 compared to recent years. J. Sea Res., 42(4): 275-290.

Nolting, R.F., Gerringa, L.J.A., Swagerman, M.J.W., Timmermans, K.R. and de Baar, H.J.W., 1998. Fe(III) speciation in the high nutrient, low chlorophyll Pacific region of the Southern Ocean. Mar. Chem., 62(3-4): 335-352.

Paucot, H. and Wollast, R., 1997. Transport and transformation of trace metals in the Scheldt estuary. Mar. Chem., 58(1-2): 229-244.

Powell, R.T., personal communication. High TAC-labile Fe concentrations after dust input. In: L.J.A. Gerringa (Editor).

Powell, R.T., Landing, W.M. and Bauer, J.E., 1996. Colloidal trace metals, organic carbon and nitrogen in a southeastern US estuary. Mar. Chem., 55(1-2): 165-176.

Regnier, P. and Wollast, R., 1993. Distribution of trace-metals in suspended matter of the Scheldt estuary. Mar. Chem., 43(1-4): 3-19.

Rijkenberg, M.J.A., Gerringa, L.J.A., Carolus, V.E., Velzeboer, I. and de Baar, H.J.W., Chapter 5. Individual ligands have different effects on the photoreduction of iron in natural seawater of the Southern Ocean.

Rose, A.L. and Waite, T.D., 2003. Kinetics of hydrolysis and precipitation of ferric iron in seawater. Environ. Sci. Technol., 37(17): 3897-3903.

Rose, A.L. and Waite, T.D., 2003. Kinetics of iron complexation by dissolved natural organic matter in coastal waters. Mar. Chem., 84(1-2): 85-103.

Rue, E.L. and Bruland, K.W., 1995. Complexation of iron(III) by natural organic-ligands in the central north Pacific as determined by a new competitive ligand equilibration adsorptive cathodic stripping voltammetric method. Mar. Chem., 50(1-4): 117-138.

Rue, E.L. and Bruland, K.W., 1997. The role of organic complexation on ambient iron chemistry in the equatorial Pacific Ocean and the response of a mesoscale iron addition experiment. Limnol. Oceanogr., 42(5): 901-910.

Sholkovitz, E.R., 1976. Flocculation of dissolved organic and inorganic matter during mixing of river water and seawater. Geochim. Cosmochim. Acta, 40(7): 831-845.

Stone, A.T. and Morgan, J.J., 1990. Kinetics of chemical transformations in the environment. In: W. Stumm (Editor), Aquatic Chemical Kinetics. Reaction rates of processes in natural waters. Wiley Interscience, New York, pp. 1-43.

Stumm, W. and Morgan, J.J., 1996. Aquatic Chemistry. Chemical equilibria and rates in natural waters. Wiley Interscience, New York.

van den Berg, C.M.G., 1982. Determination of copper complexation with natural organic-ligands in sea-water by equilibration with MnO_2.1. Theory. Mar. Chem., 11(4): 307-322.

van den Berg, C.M.G., 1995. Evidence for organic complexation of iron in seawater. Mar. Chem., 50(1-4): 139-157.

van den Berg, C.M.G., Merks, A.G.A. and Duursma, E.K., 1987. Organic complexation and its control of the dissolved concentrations of copper and zinc in the Scheldt estuary. Estuar. Coastal Shelf Sci., 24(6): 785-797.

Wen, L.S., Santschi, P., Gill, G. and Paternostro, C., 1999. Estuarine trace metal distributions in Galveston Bay: importance of colloidal forms in the speciation of the dissolved phase. Mar. Chem., 63(3-4): 185-212.

Whitworth, D.J., Achterberg, E.P., Herzl, V., Nimmo, M., Gledhill, M. and Worsfold, P.J., 1999. Development of a simple extraction procedure using ligand competition for biogeochemically available metals of estuarine suspended particulate matter. Anal. Chim. Acta, 392(1): 3-17.

Witter, A.E., Hutchins, D.A., Butler, A. and Luther, G.W., 2000. Determination of conditional stability constants and kinetic constants for strong model Fe-binding ligands in seawater. Mar. Chem., 69(1-2): 1-17.

Witter, A.E., Lewis, B.L. and Luther, G.W., 2000. Iron speciation in the Arabian Sea. Deep Sea Res. II, 47(7-8): 1517-1539.

Witter, A.E. and Luther, G.W., 1998. Variation in Fe-organic complexation with depth in the northwestern Atlantic Ocean as determined using a kinetic approach. Mar. Chem., 62(3-4): 241-258.

Wollast, R., 1988. The Scheldt estuary. In: W. Salomons, B.L. Bayne, E.K. Duursma and U. Förstner (Editors), Pollution of the North Sea, an assessment. Springer, Berlin, pp. 183-194.

Wollast, R. and Peters, J.J., 1978. Biogeochemical properties of an estuarine system: the river Scheldt, United Nations, Paris.

Wu, J.F. and Luther, G.W., 1995. Complexation of Fe(III) by natural organic-ligands in the northwest Atlantic Ocean by a competitive ligand equilibration method and a kinetic approach. Mar. Chem., 50(1-4): 159-177.

Zwolsman, J.J.G. and van Eck, G.T.M., 1993. Dissolved and particulate trace metal geochemistry in the Scheldt estuary, S.W. Netherlands (water column and sediments). Neth. J. Aquat. Ecol., 27: 287-300.

Chapter 8

Iron-binding ligands in Dutch estuaries are not affected by UV induced photochemical degradation

Micha J.A. Rijkenberg, Loes J.A. Gerringa, Ilona Velzeboer, Klaas R. Timmermans, Anita G.J. Buma, Hein J.W. de Baar

Abstract

This study shows that ultraviolet B (UV-B: 280-315 nm) and ultraviolet A (UVA: 315-400 nm) have no significant influence on the photo-degradation of organic Fe-binding ligands in estuarine waters from Marsdiep and Scheldt (The Netherlands). High salinity estuarine seawater from the Marsdiep and Scheldt contain concentrations of organic Fe-binding ligands as high as 24.4 equivalents of nM Fe (eq nM Fe) and ~ 4.6 eq nM Fe respectively with conditional stability constants (K') of $10^{21.0}$ and $10^{20.1}$ respectively. Investigation of the relation between the organically bound iron fraction and the photo-production of Fe(II) in the estuarine Marsdiep and Scheldt water showed that the concentration of Fe(II) produced was very low (< 240 pM). This demonstrates that the major part of the organically complexed Fe is not involved in photo-induced Fe redox cycling. Consequently UV has no influence on the transport of dissolved organically complexed Fe from the estuarine environment to the coastal zone.

1. Introduction

The overall dissolved iron (Fe) input of rivers in the world oceans is estimated to be 26 x 10^9 mol y^{-1} (de Baar and de Jong, 2001). The majority of dissolved Fe in river water exist as small colloid particles (Fox, 1988). Flocculation of these colloids, due to the change in ionic strength upon mixing of fresh river water with salt seawater, causes a massive removal of the freshly formed particulate Fe (Sholkovitz, 1978; Sholkovitz et al., 1978). In the Schedlt estuary flocculation occurs between salinities of 1-5 (Wollast and Peters, 1980).

Organic complexation is an important factor in the biogeochemistry of Fe in estuarine waters, as it maintains iron in the dissolved phase at high salinities after the flocculation zone. The dissolved phase will be flushed from the estuary while the non-organically complexed fraction tends to aggregate and adsorb to particles, thereby residing within the internal cycle of the estuary for a longer time (Morris et al., 1986). Thus organically complexed iron of estuarine systems can act as a source of dissolved iron for coastal zone waters (Powell and Wilson-Finelli, 2003). Despite its importance in the geochemical Fe cycle and despite the fact

that primary production can be limited by Fe availability in coastal environments (Glover, 1978; Hutchins and Bruland, 1998; Hutchins et al., 1998; Kirchman et al., 2000; Bruland et al., 2001), data on the organic complexation of Fe in estuaries is scarce.

The chemistry of Fe in the more saline estuarine waters is complex. Dissolved Fe can exist in two different oxidation states, Fe(II) and Fe(III). The Fe(III) is the thermodynamically stable form in oxygenated waters and has a very low solubility in high saline water (Millero, 1998; Liu and Millero, 2002). Fe(III) becomes rapidly hydrolyzed into various Fe(III) oxyhydroxides. The low solubility of Fe oxyhydroxides and the tendency to form colloids contributes to the scarcity of directly bioavailable Fe species in the marine environment (Martin et al., 1995; Powell et al., 1996; Sanudo-Wilhelmy et al., 1996; Wen et al., 1999).

Dissolved Fe(III) occurs for a major part as complexes (FeL) with strong organic ligands (Gledhill and van den Berg, 1994; Hutchins et al., 1999; Waite, 2001). This organic complexation is normally described in terms of concentration and conditional stability constants (K'_{FeL}) for various oceans (Gledhill and van den Berg, 1994; Rue and Bruland, 1995; Wu and Luther, 1995; Rue and Bruland, 1997; Gledhill et al., 1998; Nolting et al., 1998; Witter and Luther, 1998; Witter et al., 2000) and coastal seas (Gledhill and van den Berg, 1994; Croot and Johansson, 2000; Macrellis et al., 2001). The conditional stability constants of FeL complexes range in magnitude between 10^{18} and 10^{23} (Witter et al., 2000). Although the K'_{FeL} of organic complexes between different oceans may range over 5 orders of magnitude it is not possible to use the K'_{FeL} to identify organic ligands using the K'_{FeL} of known model ligands (Witter et al., 2000). Instead Witter et al. (2000) suggested that, based on a comparison of formation- and dissociation rate constants between model ligands and field samples, most unknown ligands in seawater originate from porphyrin and siderophore-like compounds. Porphyrins are molecules that relate to the photosynthetic pigments of autotrophic organisms, e.g. chlorophyll-*a*. Siderophores are low-molecular weight, high affinity Fe(III) binding ligands secreted by e.g. marine cyanobacteria and heterotrophic bacteria under Fe limiting circumstances to bind and transport Fe for uptake (Wilhelm and Trick, 1994; Martinez et al., 2000). Furthermore, Macrellis et al. (2001) found hydroxamate or catecholate Fe-binding functional groups, characteristic for siderophores, present in different size classes of samples taken along the Californian coast. The presence of Fe-binding compounds in the low molecular weight classes (<300 Da) was suggested to be caused by UV induced degradation of larger Fe-binding siderophores in the surface waters.

Photochemical (-induced) reactions of Fe(III)-siderophore complexes can result in the decomposition of the siderophores and the production of Fe(II) in sunlit waters (Barbeau et al., 2001). Furthermore, organic Fe-binding ligands can increase or decrease Fe photoreducibility by affecting Fe aggregation and by binding of Fe resulting in photostable complexes (Chapter 5). Iron(II), although well soluble in seawater, becomes rapidly oxidized

by O_2 and H_2O_2 (Millero et al., 1987; Millero and Izaguirre, 1989; Millero and Sotolongo, 1989; King et al., 1991; King et al., 1995; King, 1998) but at the same time Fe(II) is thought to be an important biological available species (Anderson and Morel, 1980; Takeda and Kamatani, 1989; Auclair, 1995; Croot et al., 2001). The redox cycling of (colloidal) iron hydroxides and iron chelates initiated by photochemical processes is mentioned as an important mechanism by which iron bioavailability for phytoplankton is enhanced by increasing the concentration of reactive inorganic species of Fe(II) and Fe(III) (Anderson and Morel, 1982; Finden et al., 1984; Rich and Morel, 1990; Wells and Mayer, 1991; Johnson et al., 1994; Miller and Kester, 1994; Sunda and Huntsman, 1995; Barbeau et al., 2001).

There is still much controversy about the importance of photodegradation and subsequent Fe(II) production of organically complexed Fe in the natural environment. Siderophores may be photodegradable, but until recently none of the depth profiles of Fe(III) chelators reported (Gledhill and van den Berg, 1994; Rue and Bruland, 1995; Wu and Luther, 1995) exhibit shallow mixed layer minima or any other features which would suggest a surface/photochemical sink (Moffett, 2001). Yet, Boye et al. (2001) recently reported depth profiles, where lower concentrations of organic Fe-binding ligands in Southern Ocean surface waters suggest photodegradation. Furthermore, Powell and Wilson-Finelli (2003) reported photodegradation of organic Fe-binding ligands at the timescale of hours in the Gulf of Mexico.

Photodegradation of organically bound Fe will influence the biogeochemical cycle of iron and could increase its biological availability and reactivity. Here we report experiments performed with high saline estuarine Marsdiep and Scheldt waters to investigate the influence of light on the presence of organic Fe-binding ligands. Furthermore, we show that although high concentrations organic Fe-binding ligands are present in the Marsdiep and Scheldt water, upon irradiation the Fe(II) production is relatively low as compared with the fraction of Fe bound to organic ligands.

2. Materials and methods

2.1 Samples

Marsdiep water (0.2 μm filtered) was collected at the 8th of May 2003 at 11:50 from the NIOZ jetty during high tide (Figure 1). The salinity was 29.1 versus the practical salinity
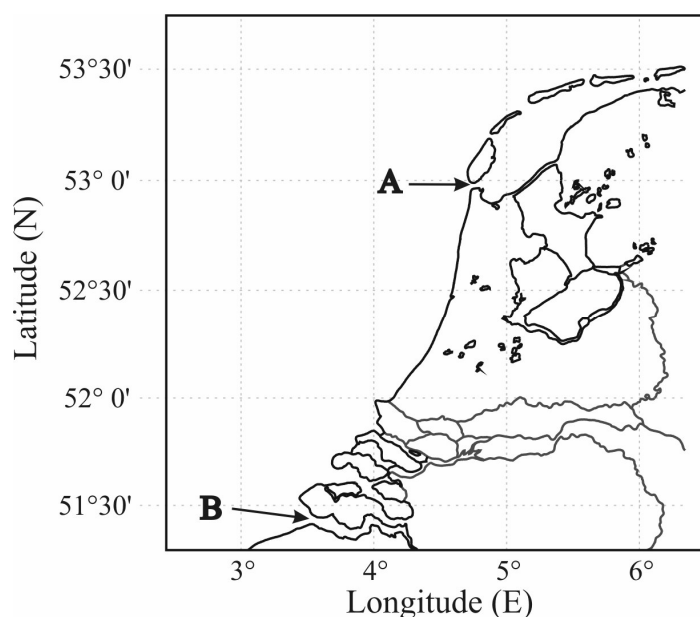
Figure 1. The coastline of the Netherlands. Samples were taken in the Marsdiep (A) and in the Westerschelde (Scheldt) (B).

scale, and the DOC concentration was 298 ± 14.6 μM C. The Marsdiep water was collected in an acid cleaned 20 liter carboy using a portable flow bench (Interflow) and acid cleaned tubing. The carboy was stored in the dark at 4°C. The collected Marsdiep water was used within a week after collection.

Scheldt water (0.2 μm filtered) was collected in the Westerschelde near Vlissingen at the 5th of April 2001 (Figure 1). Surface seawater was pumped into an over-pressurized class 100 clean air container using a Teflon diaphragm pump (Almatec A-15, Germany) driven by a compressor (Jun-Air, Denmark, model 600-4B) connected via acid-washed braided PVC tubing to a torpedo towed at approximately 3 m depth alongside the ship (Navicula, Royal NIOZ). The seawater was filtered in-line by a (Sartorius Sartobran filter capsule 5231307H8) with a cut-off of 0.2 μm. The <1 kDa fraction was filtered using an acid-cleaned Amicon SP60 cartridge and a peristaltic pump of Watson Marlow (604S/R). The salinity of the Scheldt water was 26 and the DOC concentration was 217.6 μM. The collected Scheldt water was used the next day for the deck-incubations.

2.2 Experimental

The influence of irradiance on the organic Fe-binding ligands in Marsdiep water was investigated in the laboratory. Before use, acid-cleaned UV transparent polymethylmetacrylate (PMMA) bottles (Steeneken et al., 1995) were conditioned overnight with Marsdiep water (0.2 μm filtered) at 15°C, the temperature of the water in the field at the

time of collection. The experiments were performed in a temperature controlled class 100 clean container. The pH of the Marsdiep samples was 8.14 +/- 0.006 (Metrohm 713 pH meter). To investigate the influence of UV on the photodegradation of organic Fe-binding ligands a PMMA bottle containing Marsdiep water was placed in the light and another PMMA bottle containing Marsdiep water was placed in the dark. Samples were taken at t = 0 and t = 18.5 h. The samples were frozen and used within a week for competitive ligand exchange-adsorptive cathodic stripping voltammetry (CLE-ACSV) to determine the concentration and the log K' of the organic Fe-binding ligands (equivalents of Fe-binding places).

The influence of irradiance on the organic Fe-binding ligands in Scheldt water was performed by means of deck incubations. The incubations were performed using acid cleaned PMMA and pre-conditioned bottles in UV transparent PMMA incubators. The bottles, incubated between 8:45 and 22:40 at the 7th of April 2001, were kept at a constant ambient temperature of 12°C using running seawater from the ship's pumping system. The pH of the Scheldt water was 8.8 (Metrohm 713 pH meter). Sampling was performed in a laminar flow bench in a class 100 clean container. Samples for the determination of the concentration organic iron binding ligands and their log K' were immediately frozen. Stored samples for dissolved iron were acidified with 100 μl 3x quartz distilled HCl per 100 ml sample (pH = 2).

Investigation of the photoproduction of Fe(II) was performed in a temperature controlled class 100 clean container. The PMMA bottles were pre-conditioned with the water as used during the experiments and at the temperatures as used during the experiments. Water was continuously stirred using a magnetic induced, Teflon stirring bean during the experiment. An experiment typically started with measuring the background signal in the dark, after which the lamps were switched on. During 90-120 minutes the production of Fe(II) was followed. When enough sample volume was available, the oxidation of Fe(II) was followed for 30 minutes after having turned off the light.

2.3 Light

Philips UVB (TL-12), UVA (TL' 40W/05) and VIS (TL'D 36W/33) lamps were used to simulate the solar spectrum in the experiments with Marsdiep water. Spectral conditions were measured using a MACAM Spectroradiometer SR9910 with a small spherical 4π sensor. All sides of the box shaped PMMA bottle, except the top, were covered with black plastic to prevent focussing effects. Spectra were recorded from 280-700 nm.

Fe(III) siderophore complexes have been shown to absorb light in the high UVB and low UVA range (Barbeau et al., 2001; Barbeau et al., 2003). Therefore, we used mainly UVB

Table 1. The doses of UVB, UVA and VIS irradiance received by the coastal Marsdiep water during the incubation of 18.5 hours. As comparison the doses of solar UVB and UVA irradiance detected nearby (within 300 m) at the Royal NIOZ during a whole day (14.75 hours of daylight) are given.

wavelength region	Incubation (kJ m^{-2})	solar irradiance 8th of May (kJ m^{-2})
UVB	204.39	48.02
UVA	377.04	1170.71
VIS	919.24	$1.98 \cdot 10^6$

and UVA lamps during the incubation, but VIS lamps were included as well. Table 1 shows the doses of UVB, UVA and VIS received by the Marsdiep water during the incubation. The doses of solar UVB and UVA as measured by a hyperspectral radiometer (280-680 nm) containing a cosine collector (TriOS Optical Sensors) at the roof of the Royal NIOZ at 300 m from the Marsdiep sample station, and the dose of solar VIS as measured with TriOS Ramses ACC irradiation meter with cosine collector at the Marsdiep sample station, for the 8th of May 2003, are included for comparison. During the experiments an UVB irradiance dose 4 times higher, an UVA dose 3 times lower and a VIS dose 2200 times lower than the dose which estuarine seawater could receive during a day at the water surface (8th May 2003) were used (Table 1). Because we hereby ignored the effect of mixing and the strong light attenuation in these estuarine waters the applied UVB dose and probably also UVA irradiance are likely higher than *in situ* UVB and UVA doses.

A PUV 500 surface sensor (Biospherical Instruments) was used to measure the irradiance during the deck-incubation of the Scheldt seawater. The PUV measured irradiance between 9:15 and 16:05 (local time, 7th of April 2001). The irradiance values, given as dose, were measured at 305 nm (0.14 kJ m^{-2} nm^{-1}), 320 nm (3.09 kJ m^{-2} nm^{-1}), 340 nm (6.04 kJ m^{-2} nm^{-1}), 380 nm (7.91 kJ m^{-2} nm^{-1}) and VIS (400-700 nm, 20.49 E m^{-2}). The deck-incubations of the Scheldt seawater were performed between 8:45 and 22:40 so the actual dose of irradiance received by the Scheldt sample was somewhat higher than measured with the PUV.

2.4 CLE-ACSV

Determination of the organic speciation of iron in the Marsdiep and Scheldt water was performed using CLE-ACSV. The 2-(2-Thiazolylazo)-p-cresol (TAC) (Aldrich, used as received) reagent was used as competing ligand (Croot and Johansson, 2000). All solutions were prepared using 18.2 MΩ nanopure water. The equipment consisted of a μAutolab voltammeter (Ecochemie, Netherlands), a static mercury drop electrode (Metrohm Model VA663), a double-junction Ag/saturated AgCl reference electrode with a salt bridge

containing 3 M HCl and a counter electrode of glassy carbon. The titration was performed using 0.01 M stock solution of TAC in 3x quartz distilled (QD) methanol, 1 M boric acid (Suprapur, Merck) in 0.3 M ammonia (Suprapur, Merck) (extra cleaning by the addition of TAC after which TAC and $Fe(TAC)_2$ was removed with a C18 SepPak column) to buffer the samples to a pH of 8.05 and a 10^{-6} M Fe(III) stock solution acidified with 0.012 M HCl (3xQD). Aliquots of 15 ml were spiked with Fe(III) up to final concentrations between 0 and 20 nM and allowed to equilibrate overnight (> 15 hours) with 5 mM borate buffer and 10 μM TAC. The concentration $Fe(TAC)_2$ in the samples was measured using the following procedure: i) removal of oxygen from the samples for 200 seconds with dry nitrogen gas, after which a fresh Hg drop was formed, ii) a deposition potential of –0.40 V was applied for 30-60 seconds according to the sample measured, the solution was stirred to facilitate the adsorption of the $Fe(TAC)_2$ to the Hg drop, iii) at the end of the adsorption period the stirrer was stopped and the potential was scanned using the differential pulse method from -0.40 to -0.90 V at 19.5 mV s^{-1} and the stripping current from the adsorbed $Fe(TAC)_2$ recorded.

The ligand concentration and the conditional stability constants were calculated using the non-linear fit of the Langmuir isotherm (Gerringa et al., 1995).

2.5 Iron(II) analysis

Concentrations of Fe(II) were followed using an automated flow injection analysis system employing a luminol-based chemiluminescence detection of Fe(II) (Seitz and Hercules, 1972; King et al., 1995; O'Sullivan et al., 1995). An alkaline luminol solution is mixed with the Fe(II) sample in a spiral shaped flow cell in front of a Hamamatsu HC135 photon counter. At pH 10, Fe(II) is rapidly oxidized by oxygen on a millisecond time scale causing the oxidation of luminol and producing blue light (Xiao et al., 2002).

Samples were transported in-line from the PMMA bottle to a sample loop. Then the sample was, by introducing it in a pure water carrier (18.2 MΩ nanopure water), transported into the flow cell every 93 seconds.

The complete analytic system was built inside a light-tight wooden box. The luminol reagent and the carrier were kept in light-tight bags (as used for storage of photographic films). The tubing was covered by aluminum foil and the tubing of the peristaltic pump was shaded by black plastic.

A 15 mM 5-amino-2,3-dihyfro-1,4-phthal-azinedione (Luminol) (SIGMA) stock solution was prepared weekly in 20 mM Na_2CO_3. The 50 μM luminol reagent solution was made in 0.5 M NH_3 (Suprapur, Merck) and 0.1 M HCl (Suprapur, Merck). The luminol reagent solution was stored in the dark for at least 24 hours before use to ensure that the reagent properties had stabilized. An 0.01 M Fe(II) stock was prepared monthly by dissolving ferrous ammonium sulfate hexahydrate ($Fe^{(II)}(NH_4SO_4)_2 \cdot 6H_2O$) (Baker Analyzed, reagent

grade) in 0.012 M (3xQD) HCl. Working solutions were prepared daily. All Fe(II) stock solutions were refrigerated in the dark at 4°C when not in use.

Calibration was performed by the standard addition of known concentrations of Fe(II) to the sample matrix. The standard addition for the experiments with Scheldt water was performed in Southern Ocean seawater because of a lack of sample. The time delay between Fe(II) addition and measurement caused an oxidation effect. This oxidation effect was accounted for by extrapolating the data back to time zero using the fact that Fe(II) oxidation in seawater very closely approximates pseudo-first-order kinetics.

2.6 Fe(III) analysis

Dissolved iron, defined as the Fe fraction passing an 0.2 μm filter, was determined using flow injection analysis with luminol chemiluminescence and H_2O_2 (de Jong et al., 1998).

3. Results and discussion

3.1 Iron speciation of the Marsdiep and Scheldt estuary samples

Marsdiep water was sampled during the last stage of a phytoplankton springbloom with low cell numbers caused by an early depletion of the nutrients phosphate and nitrate. The bloom developed from the 16th of March until the 15th of May, 2003. The Marsdiep water contained 25.4 nM dissolved iron and 24.4 eq nM Fe of dissolved ligands with a log K'_{FeL} of 21.0 ± 0.18 (n=4). Some 4 nM Fe is present as TAC-labile Fe (TAC-labile Fe being the Fe bound by 10 μM TAC after >12 hours equilibration) (Table 2). Samples from the Scheldt estuary contained concentrations dissolved Fe of 12-15 nM and a relatively high concentration of TAC-labile Fe: 11-12 nM. The Fe-binding ligand concentration was 4.6 eq nM Fe with a log K'_{FeL} of 20.1 (n=1) (Table 2).

Similar values for the log K'_{FeL} in coastal waters were reported by (Rose, 2003) using a kinetic approach and by Powell and Wilson-Finelli (2003) using CLE-ACSV. Croot and Johansson (2000) found similar values for the log K' and the initial concentration TAC-labile Fe during an algal bloom at Valö, Sweden. However, (Gobler et al., 2002) found extremely high conditional stability constants, log $K' \sim 23$, for organic iron binding ligands at similar salinities in the Peconic Estuary (Long Island, USA).

Table 2. Dissolved Fe, TAC-labile Fe, total ligand concentration and the logarithm of the conditional stability constant (K') for the Marsdiep-, Scheldt samples and the UV destruction of Marsdiep water. The $[Fe]_{dissolved}$ is the fraction iron determined in 0.2 μm filtered seawater as measured by flow injection analysis using luminol chemiluminescence (de Jong et al., 1998). The TAC-labile Fe is the labile iron concentration recoverable by adding 10 μM TAC, allowing the sample to equilibrate overnight, this value is an average of the first few values of the titration. The [L], the concentration of Fe-binding ligand, and log $K_{Fe'L}$, the conditional stability constant of the iron binding ligand expressed with respect to Fe^{3+}, and their 95% confidence interval were estimated using non-linear least squares analysis (Systat) (Gerringa et al., 1995).

samples	$[Fe]_{dissolved}$ (nM)	[TAC-labile Fe](nM)	$[L]_{total}$ (nM)	±95% confidence interval	log K'_{FeL}	±95% confidence interval
Marsdiep samples						
dark (t = 0)	25.39	4.30	22.89	0.78	21.23	0.27
light (t = 0)	25.42	4.46	25.89	0.82	20.83	0.11
dark (t = 18.5 h)	25.21	3.49	23.49	0.55	21.37	0.22
light (t = 18.5 h)	25.59	3.52	25.07	0.84	21.17	0.19
Scheldt samples						
dark	12.34	11.04	4.19	2.62	20.09	1.04
light	14.68	11.62	5.01	1.36	20.56	1.10
UV destruction						
A (t=0)	26.09	6.01	23.62	1.32	20.89	0.26
B (t=0)	26.61	6.15	22.73	1.41	21.03	0.40
A (t=10 h)	18.55	2.75	18.01	0.79	21.42	0.34
B (t=10 h)	18.38	2.39	17.92	0.51	21.41	0.21

3.2 TAC-labile Fe concentrations and their response to irradiance

In open ocean waters the concentration of ligands are always higher than the concentration of dissolved Fe (Gledhill and van den Berg, 1994; Rue and Bruland, 1995; van den Berg, 1995). This means that after equilibration (>12 hours) all dissolved iron is complexed by organic ligands and not available for TAC. Titration with Fe result typically in low TAC-labile Fe concentrations for the first few Fe additions in open ocean water (Figure 2).

The curvature in the titration curves of Marsdiep and Scheldt water (Figures 2, 3) indicating competition between the natural ligands and the added concentration TAC revealed the presence of strong ligands. The concentration of TAC-labile Fe of titrations with estuarine seawater was higher then observed for titrations of open ocean water.
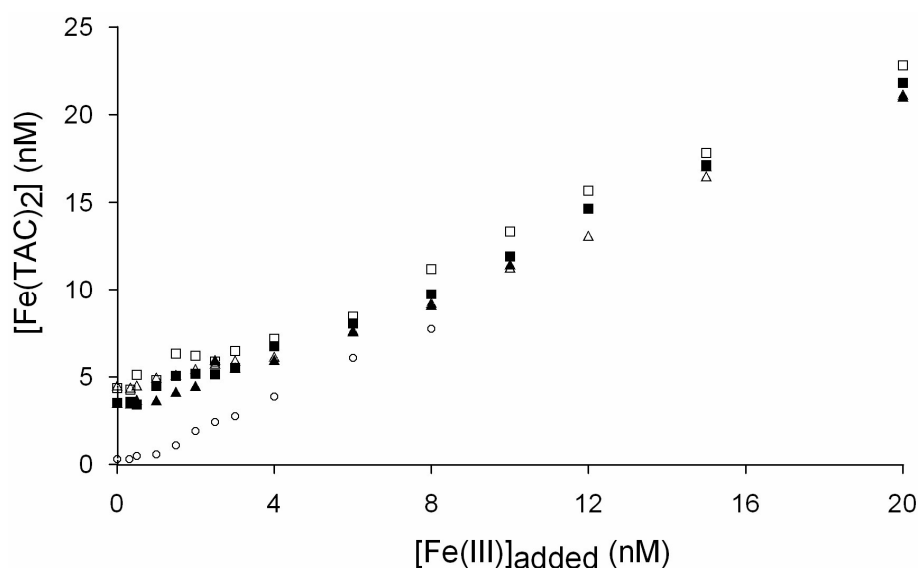
Figure 2. The CLE-ACSV Fe titration data from the Marsdiep and from Southern Ocean seawater (○). The titration curves for the coastal Marsdiep water were determined before and after the sample received 18.5 hours irradiance or darkness: t = 0 light (△), t = 0 dark (□), t = 18.5 h light (▲) and t = 18.5 dark (■).

Croot and Johansson (2000) reported TAC-labile Fe values of ~ 6.2 nM during a bloom and ~ 4.6 nM after a bloom (10 μM TAC, overnight equilibration) at Valö, Sweden. The TAC-labile Fe concentrations determined during this study were between 3.5 and 4.5 nM for Marsdiep water and between 11 and 12 nM for water sampled in the Scheldt estuary.

The high TAC-labile Fe concentrations are explained by the existence of weak Fe-binding compounds in the coastal seawater samples. These weak Fe-binding ligands cannot compete with TAC and lose their Fe to TAC (Chapter 7). Furthermore, in competition with the strong Fe-binding ligands, TAC is able to catch some of the Fe initially bound by the natural strong ligands and so creating a pool of iron free ligands which were subsequently titrated (Chapter 7). This explains why the titration shows a curve in the presence of Fe bound by weaker ligands.

Comparing 1 kDa filtered Scheldt samples with 0.2 μm filtered Scheldt samples showed us that the initial TAC-labile Fe fraction decreased with filter pore size, indicating that at least part of the TAC-labile Fe fraction had a relationship with the colloidal iron fraction (Figure 4).

The TAC-labile iron concentration in Marsdiep water decreased in time independent of the irradiance treatment (Figure 5). Marsdiep water incubated in the dark for 18.5 hours showed the same decrease in TAC-labile Fe as Marsdiep water incubated during 18.5 hours in the light. This time-dependent decrease was probably caused by degradation of weak organic iron binding ligands or by Fe-binding places related to colloidal material subject to
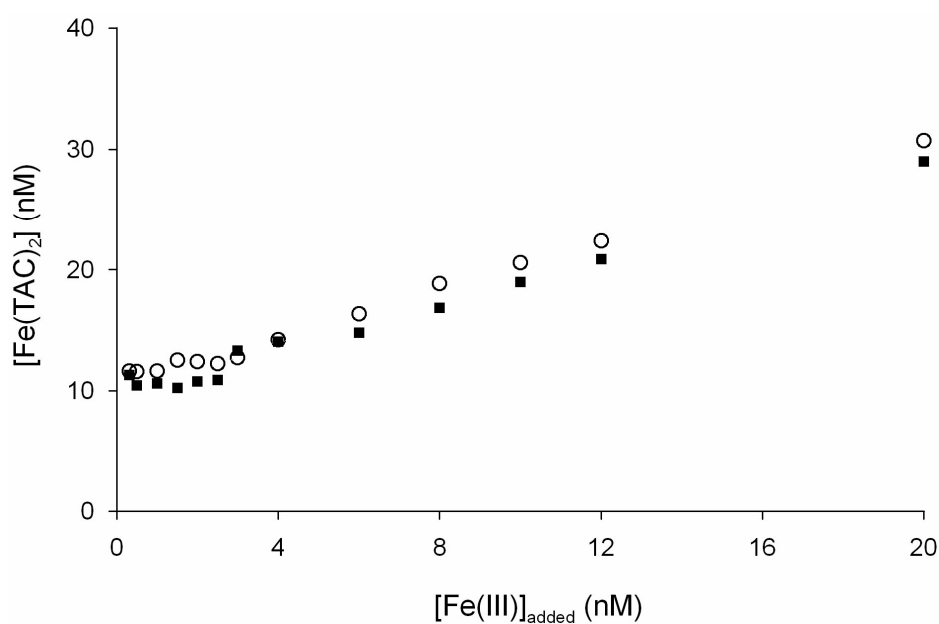
Figure 3. The CLE-ACSV Fe titration data from the Westerschelde. The titration curves for the Scheldt water were determined after a sample received 12 hours of daylight in spring (7th of April, 2001) (○) and after being incubated for 12 hours in the dark (■).

processes as ageing (Cornell and Schwertmann, 1996), adsorption of organic material (Kreller et al., 2003) and aggregation (Wells and Goldberg, 1993; Hunter et al., 1997).
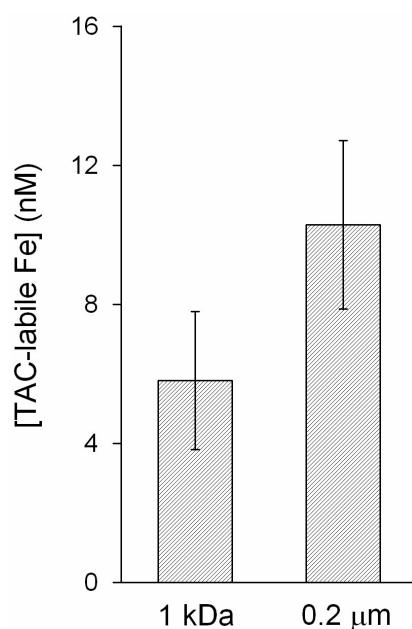

Figure 4. The TAC-labile Fe concentrations for two size fractions of Scheldt water; <1000 Da filtered (n=3) and <0.2 μm filtered (n=4).
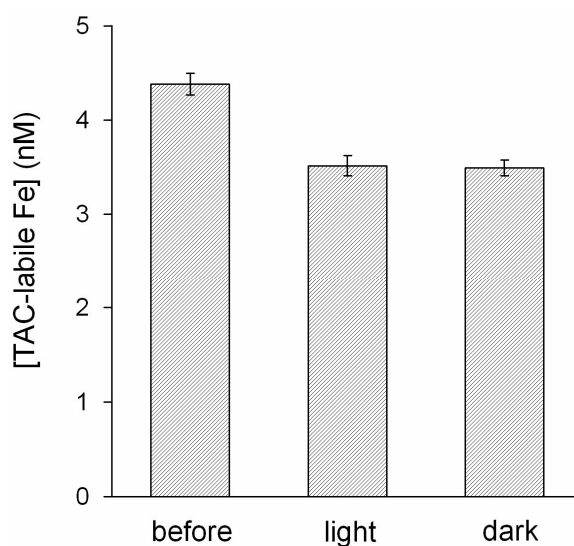
Figure 5. The TAC-labile Fe values determined for Marsdiep water, before and after incubation during 18.5 hours in the light or in the dark.

3.3 The influence of UV on the organic Fe-binding ligands

Irradiation with UVC (254 nm) during UV-destruction of the Marsdiep water resulted in a 22% decrease in the concentration of Fe(III) chelators. Also a decrease in the dissolved Fe concentration was observed (Figure 6A, Table 2). The high UV irradiance inducing the degradation of the Fe(III) chelators and increasing the concentration of free iron in the Marsdiep water probably caused an increase in inorganic Fe resulting in the precipitation of particulate iron to the bottom of the quartz tubes. Also the concentration TAC-labile Fe decreased during the UV-exposure (Figure 6B, Table 2). This indicates that particularly the weaker ligand class is UV degraded. The use of a high, unnatural UVC irradiance level, shows the Fe chemical effects of photo-induced degradation of Fe-binding ligands.

However, exposure of estuarine water sampled in the Marsdiep with simulated solar irradiance showed no significant decrease in the concentration organic Fe-complexing ligands or change in the log K'_{FeL}, (Figure 2, 7). Additionally, organic Fe-complexing ligands in Scheldt water (S=26) showed no decrease in concentration after incubation under natural sunlight for a whole day as compared to incubation in the dark (Figure 3, 8).

Our results are consistent with the absence of vertical gradients of Fe(III) chelators in open ocean waters, i.e. the absence of minima within the shallow mixed layer minima, or any other feature which would suggest a surface/photochemical sink (Gledhill and van den Berg, 1994; Rue and Bruland, 1995; Wu and Luther, 1995; Moffett, 2001). On the other hand, it was reported recently that a weak Fe-binding ligand class (log K' 20-22, <1 kDa) in the Gulf
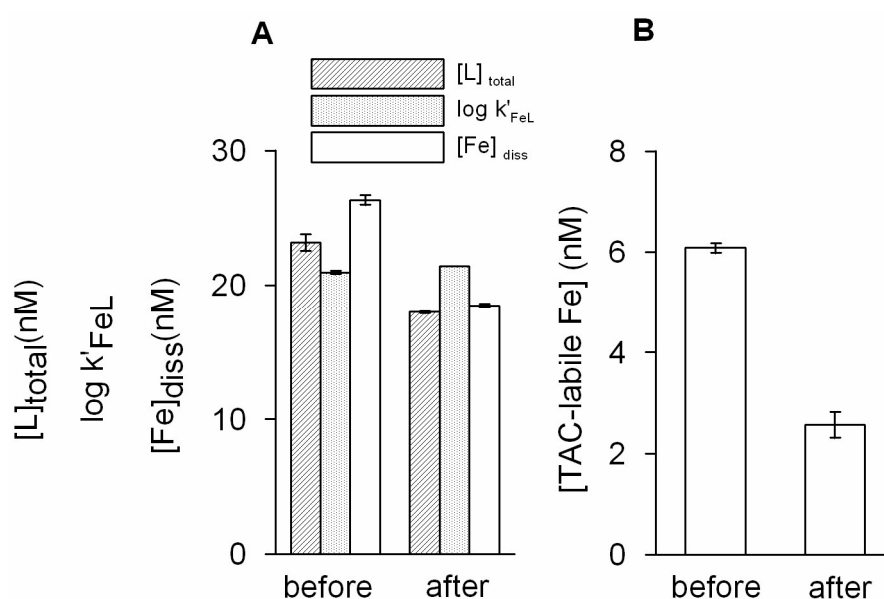
Figure 6. (A) The total concentration of Fe-binding ligand, log K'$_{FeL}$ and the concentration dissolved Fe of Marsdiep water before and after 10 hours of UV destruction. (B) The TAC-labile Fe concentration before and after 10 hours of UV destruction of the Marsdiep water. The error bars give the standard errors (n = 2).

of Mexico is being photodegraded (Powell and Wilson-Finelli, 2003). Powell and Wilson-Finelli (2003) demonstrated that organic Fe-complexing ligands change little in the surface samples of the stratified Mississippi plume. Yet they explained the steady presence of the

ligands with the continuous production of new ligands replacing the photo-degraded organic Fe-binding ligands. Production of organic Fe-binding ligands to compensate for the photo-degraded ligands can not explain the constant Fe-binding capacity in our experiments because phytoplankton and the majority of bacteria were filtered out.

Macrellis et al. (2001) had suggested larger iron binding siderophores to be photo-degraded to smaller Fe-binding molecules. This has been postulated to explain the detection of molecules with siderophore-like characteristics in a size class smaller then the defined size range for siderophores (300-1000 Da) in surface waters (Macrellis et al., 2001). Reduction of Fe(III) with photo-degradation of the siderophore and a significant drop in Fe(III) binding strength was also shown by Barbeau et al. (2001). The reason that we did not measure photo-degradation of the Fe-binding capacity could be that the overall input of photo-sensitive Fe(III) chelators was low. Related to this the photo-reactive fraction could already have been quickly photo-degraded during river transport or in the shallow well mixed coastal seawaters. Estuarine waters continuously receive new organic material originating from river input and
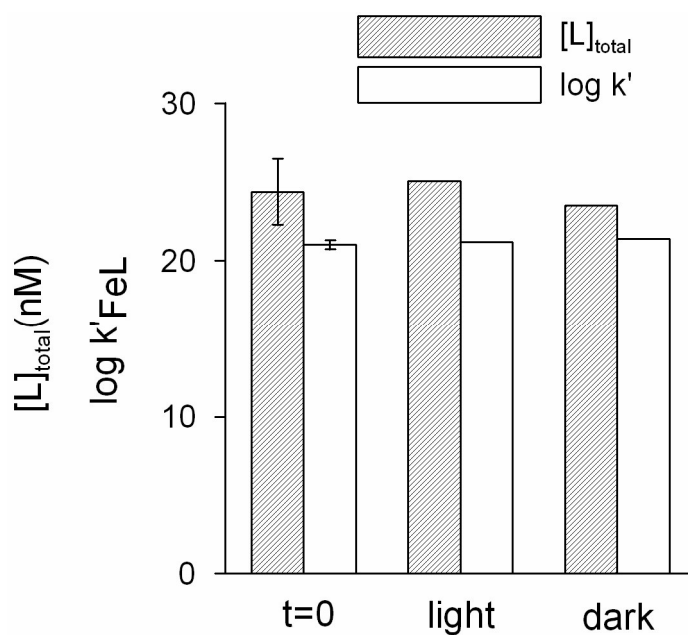
Figure 7. The total concentration of Fe-binding ligand and log K'_{FeL} for Marsdiep water at t=0 (n=2) and before and after 18.5 hours in the light (n=1) or in the dark (n=1).

biological activity. The fraction of photo-degradable Fe(III) chelators within this organic material appears to be low.

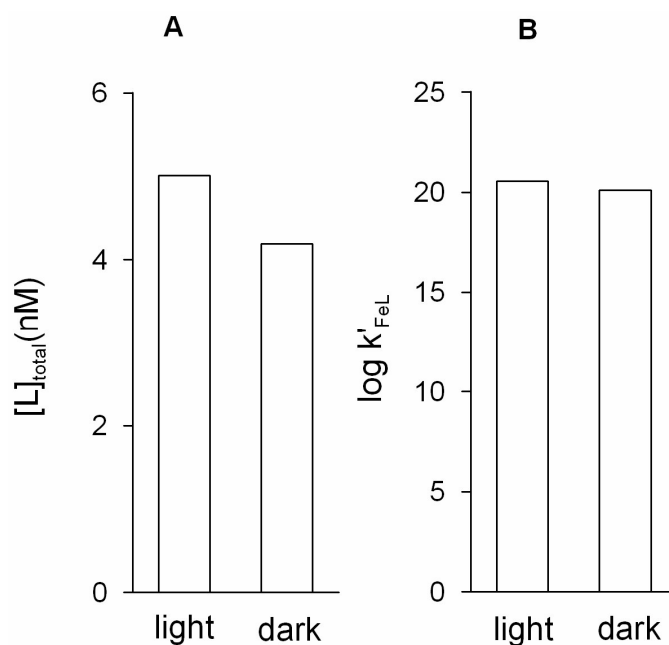**Figure 8.** (A) The total concentration of Fe-binding ligand and (B) log K'_{FeL} of Scheldt water after 12 hours of natural sunlight or 12 hours in the dark.

3.4 Fe(II) photo-production in Marsdiep and Scheldt water

Although there was no significant influence of light on the photo degradation of the Fe(III) chelators, the Fe(II) was still photoproduced (Figure 9). The photo-production of Fe(II) in Marsdiep water was investigated under three different optical treatments (Figure 9). The 0.2 μm and 1 kDa filtered Scheldt water was only irradiated with the total spectrum (280-700 nm) (Figure 10).

The Fe(II) concentration in the dark for Marsdiep water was 43 ± 9 pM Fe(II) and for the Scheldt water 57 ± 4 pM Fe(II). Comparison of the Fe(II) production of the Marsdiep and Scheldt water receiving the same optical treatment showed a "steady state" value of 177 ± 8 pM for the 0.2 μm Marsdiep water and 239 ± 4 pM and 131 ± 8 pM for 0.2 μm and 1 kDa filtered Scheldt water respectively.

We have no knowledge about the nature and concentrations of the photo-reactive Fe(III) species but these experiments show that the concentrations Fe(II) formed during irradiation experiments were very low. The determined concentrations of FeL were a factor 100 higher than the concentration Fe(II) for the Marsdiep water and a factor of 20 higher than
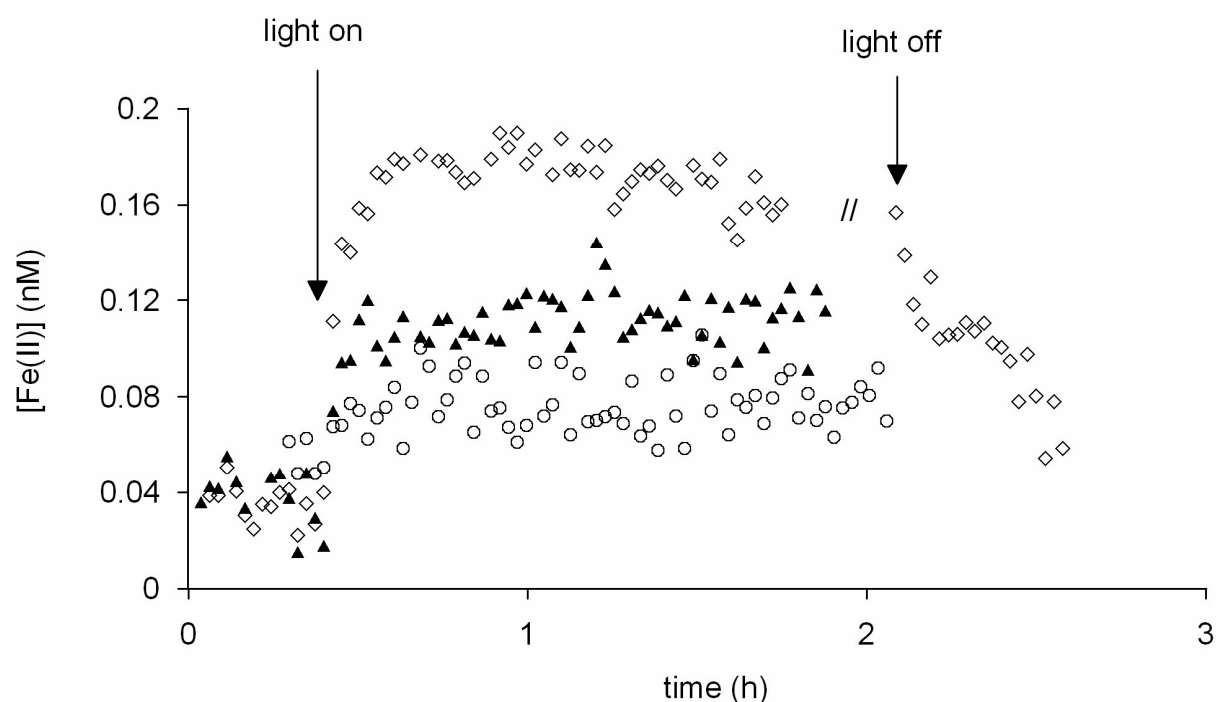

Figure 9. The concentration of Fe(II) formed during irradiation of Marsdiep water with three different wavelength regions: 280-700 nm (◇), 320-700 nm (▲) and 360-700 nm (○).

the concentration of Fe(II) in the Scheldt water. This means that the majority of the organic complexed iron is not involved in the photo-production of Fe(II).

The Fe(II) photoproduction in Marsdiep water showed the typical pattern seen during experiments with inorganic iron colloids (Waite and Morel, 1984; Wells and Mayer, 1991). The pattern observed when the light is on, namely a rapid increase until a maximum, followed by a slow decrease in the Fe(II) concentration during further continued irradiance, has been reported before in experiments using colloidal Fe (Wells and Mayer, 1991; Miller et al., 1995; Emmenegger et al., 2001). Wells and Mayer (1991) found that the photoconversion rates diminished with continued irradiation when ferrihydrite was irradiated. Waite and Morel (1984) found the same effect for the photodissolution rate of lepidocrocite. This pattern was explained by the presence of a limited amount of chromophoric colloidal Fe species (Wells and Mayer, 1991; Kimball et al., 1992; Chapter 3, Rijkenberg et al., 2005; Chapter 5). The occurrence of this similar pattern in the production of Fe(II) with time suggests that the produced Fe(II) could originate from a colloidal Fe fraction. Our results support this suggestion clearly when UVB was included in the irradiance spectra offered.

Moreover, we found that the production of Fe(II) was lower in the truly dissolved fraction (1 kDa filtered) of Scheldt water, 131 ± 8 pM Fe(II) compared to the Fe(II) produced in the dissolved fraction (0.2 μm filtered), 239 ± 4 pM Fe(II). This means that part of the Fe(II) produced results from a photo-reactive colloidal Fe fraction. We cannot conclude that the Fe(II) formed in the truly dissolved Scheldt water fraction is the result of a photo-reactive
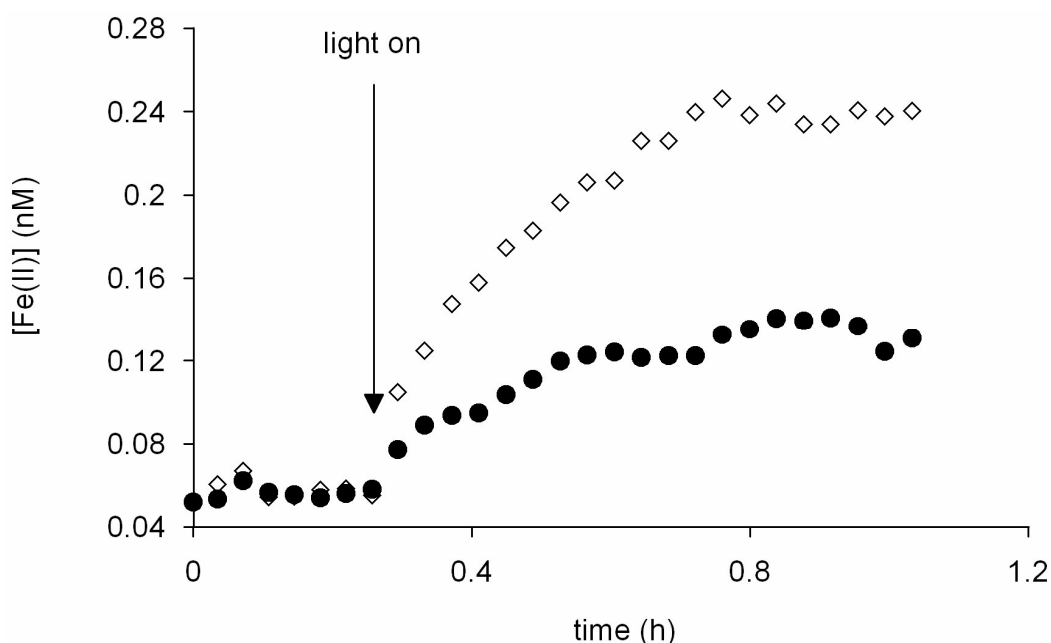

Figure 10. The concentration Fe(II) in Scheldt water formed upon irradiation of 0.2 μm filtered (◇) and 1 kDa filtered (●) water with irradiance between the wavelengths 280 and 700 nm.
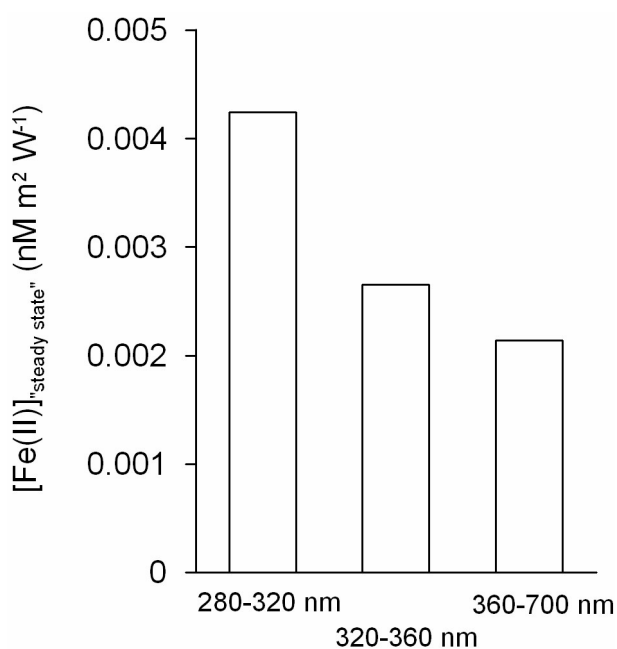
Figure 11. The mean Fe(II) concentration in Marsdiep at steady state/highest point due to the wavelength regions 280-320 nm, 320-360 nm and 360-700 nm normalised to 1 W m^{-2}.

organic complexed iron or of an inorganic truly soluble fraction, because colloids could have formed in this sample during sample handling in the laboratory. Enclosing a sample of (coastal) seawater in a container causes a decrease in the concentration of soluble iron and an increase in the concentration of particulate iron (Lewin and Chen, 1973). Another effect possibly increasing the colloidal iron fraction is the observation that iron is less soluble in warmer waters (Kuma et al., 1996). The colloidal iron fraction could increase when the estuarine seawater was kept in a warmer laboratory environment during various stages of the process.

Changing the wavelength range of the optical treatments of the Marsdiep water showed that less Fe(II) was formed upon excluding the lower wavelength regions UVB and UVA from the optical treatment. Comparing the values for the steady state normalized to 1 Wm^{-2} between the different wavelength regions shows us that UVB produces most Fe(II), followed by UVA and VIS, respectively (Figure 11).

4. Summary and conclusion

We conclude from the present study that UV does not significantly photo-degrade the organic Fe-binding ligands in the waters of the Marsdiep and the Scheldt estuary. The UV light has no influence on the organically complexed Fe fraction and will not influence the transport of the dissolved organically complexed Fe phase to the coastal zone.

The concentrations of Fe(II) formed during irradiation experiments were very low (<240 pM). The concentrations of organic Fe-binding ligands are in the order of 24.4 nM for the Marsdiep and 4.6 nM for the Scheldt. Thus, the majority of the organically complexed iron in the Marsdiep water is not involved in the photo-production of Fe(II) and is not being photo-degraded during the process of photo-reduction of Fe bound to organic ligands. The pattern of Fe(II) production resembled the pattern observed during irradiation experiments with inorganic colloidal iron like ferrihydrite and goethite (Waite and Morel, 1984; Wells and Mayer, 1991) or amorphous iron oxyhydroxides (Chapter 5), suggesting that it might be a colloidal Fe fraction responsible for the photoproduced Fe(II).

Acknowledgements

References

Anderson, M.A. and Morel, F.M.M., 1980. Uptake of Fe(II) by a diatom in oxic culture medium. Mar. Biol. Let., 1: 263-268.

Anderson, M.A. and Morel, F.M.M., 1982. The influence of aqueous iron chemistry on the uptake of iron by the coastal diatom *Thalassiosira weissflogii*. Limnol. Oceanogr., 27(5): 789-813.

Auclair, J.C., 1995. Implications of increased UV-B induced photoreduction - Iron(II) enrichment stimulates picocyanobacterial growth and the microbial food-web in clear-water acidic Canadian shield lakes. Can. J. Fish. Aquat. Sci., 52(8): 1782-1788.

Barbeau, K., Rue, E.L., Bruland, K.W. and Butler, A., 2001. Photochemical cycling of iron in the surface ocean mediated by microbial iron(III)-binding ligands. Nature, 413(6854): 409-413.

Barbeau, K., Rue, E.L., Trick, C.G., Bruland, K.T. and Butler, A., 2003. Photochemical reactivity of siderophores produced by marine heterotrophic bacteria and cyanobacteria based on characteristic Fe(III) binding groups. Limnol. Oceanogr., 48(3): 1069-1078.

Boye, M., van den Berg, C.M.G., de Jong, J.T.M., Leach, H., Croot, P.L. and de Baar, H.J.W., 2001. Organic complexation of iron in the Southern Ocean. Deep Sea Res. I, 48(6): 1477-1497.

Bruland, K.W., Rue, E.L. and Smith, G.J., 2001. Iron and macronutrients in California coastal upwelling regimes: Implications for diatom blooms. Limnol. Oceanogr., 46(7): 1661-1674.

Cornell, R.M. and Schwertmann, U., 1996. The Iron Oxides. VCH Publishers, New York.

Croot, P.L., Bowie, A.R., Frew, R.D., Maldonado, M.T., Hall, J.A., Safi, K.A., la Roche, J., Boyd, P.W. and Law, C.S., 2001. Retention of dissolved iron and Fe-II in an iron induced Southern Ocean phytoplankton bloom. Geophys. Res. Lett., 28(18): 3425-3428.

Croot, P.L. and Johansson, M., 2000. Determination of iron speciation by cathodic stripping voltammetry in seawater using the competing ligand 2-(2- thiazolylazo)-p-cresol (TAC). Electroanalysis, 12(8): 565-576.

de Baar, H.J.W. and de Jong, J.T.M., 2001. Distributions, sources and sinks of iron in seawater. In: D.R. Turner and K.A. Hunter (Editors), The biogeochemistry of iron in seawater. John Wiley & sons, New York, pp. 123-253.

de Jong, J.T.M., den Das, J., Bathmann, U., Stoll, M.H.C., Kattner, G., Nolting, R.F. and de Baar, H.J.W., 1998. Dissolved iron at subnanomolar levels in the Southern Ocean as determined by ship-board analysis. Anal. Chim. Acta, 377(2-3): 113-124.

Emmenegger, L., Schonenberger, R.R., Sigg, L. and Sulzberger, B., 2001. Light-induced redox cycling of iron in circumneutral lakes. Limnol. Oceanogr., 46(1): 49-61.

Finden, D.A.S., Tipping, E., Jaworski, G.H.M. and Reynolds, C.S., 1984. Light-induced reduction of natural iron(III) oxide and its relevance to phytoplankton. Nature, 309(5971): 783-784.

Fox, L.E., 1988. The solubility of colloidal ferric hydroxide and its relevance to iron concentrations in river water. Geochim. Cosmochim. Acta, 52(3): 771-777.

Gerringa, L.J.A., Herman, P.M.J. and Poortvliet, T.C.W., 1995. Comparison of the linear van den Berg Ruzic transformation and a nonlinear fit of the Langmuir isotherm applied to Cu speciation data in the estuarine environment. Mar. Chem., 48(2): 131-142.

Gledhill, M. and van den Berg, C.M.G., 1994. Determination of complexation of iron(III) with natural organic complexing ligands in seawater using cathodic stripping voltammetry. Mar. Chem., 47(1): 41-54.

Gledhill, M., van den Berg, C.M.G., Nolting, R.F. and Timmermans, K.R., 1998. Variability in the speciation of iron in the northern North Sea. Mar. Chem., 59(3-4): 283-300.

Glover, H.E., 1978. Iron in Maine coastal waters; seasonal variation and its apparent correlation with a dinoflagellate bloom. Limnol. Oceanogr, 23: 534-537.

Gobler, C.J., Donat, J.R., Consolvo, J.A. and Sanudo-Wilhelmy, S.A., 2002. Physicochemical speciation of iron during coastal algal blooms. Mar. Chem., 77(1): 71-89.

Hunter, K.A., Leonard, M.R., Carpenter, P.D. and Smith, J.D., 1997. Aggregation of iron colloids in estuaries: A heterogeneous kinetics study using continuous mixing of river and sea waters. Colloid Surf. A-Physicochem. Eng. Asp., 120(1-3): 111-121.

Hutchins, D.A. and Bruland, K.W., 1998. Iron-limited diatom growth and Si: N uptake ratios in a coastal upwelling regime. Nature, 393(6685): 561-564.

Hutchins, D.A., DiTullio, G.R., Zhang, Y. and Bruland, K.W., 1998. An iron limitation mosaic in the California upwelling regime. Limnol. Oceanogr., 43(6): 1037-1054.

Hutchins, D.A., Witter, A.E., Butler, A. and Luther, G.W., 1999. Competition among marine phytoplankton for different chelated iron species. Nature, 400(6747): 858-861.

Johnson, K.S., Coale, K.H., Elrod, V.A. and Tindale, N.W., 1994. Iron photochemistry in seawater from the equatorial Pacific. Mar. Chem., 46(4): 319-334.

Kimball, B.A., McKnight, D.M., Wetherbee, G.A. and Harnish, R.A., 1992. Mechanisms of iron photoreduction in a metal-rich, acidic stream (St-Kevin Gulch, Colorado, USA). Chem. Geol., 96(1-2): 227-239.

King, D.W., 1998. Role of carbonate speciation on the oxidation rate of Fe(II) in aquatic systems. Environ. Sci. Technol., 32(19): 2997-3003.

King, D.W., Lin, J. and Kester, D.R., 1991. Spectrophotometric determination of iron(II) in seawater at nanomolar concentrations. Anal. Chim. Acta, 247(1): 125-132.

King, D.W., Lounsbury, H.A. and Millero, F.J., 1995. Rates and mechanism of Fe(II) oxidation at nanomolar total iron concentrations. Environ. Sci. Technol., 29(3): 818-824.

Kirchman, D.L., Meon, B., Cottrell, M.T., Hutchins, D.A., Weeks, D. and Bruland, K.W., 2000. Carbon versus iron limitation of bacterial growth in the California upwelling regime. Limnol. Oceanogr., 45(8): 1681-1688.

Kreller, D.I., Gibson, G., Novak, W., Van Loon, G.W. and Horton, J.H., 2003. Competitive adsorption of phosphate and carboxylate with natural organic matter on hydrous iron oxides as investigated by chemical force microscopy. Colloid Surf. A-Physicochem. Eng. Asp., 212(2-3): 249-264.

Kuma, K., Nishioka, J. and Matsunaga, K., 1996. Controls on iron(III) hydroxide solubility in seawater: The influence of pH and natural organic chelators. Limnol. Oceanogr, 41(3): 396-407.

Lewin, J. and Chen, C., 1973. Changes in the concentration of soluble and particulate iron in seawater enclosed in containers. Limnol. Oceanogr, 18: 590-596.

Liu, X.W. and Millero, F.J., 2002. The solubility of iron in seawater. Mar. Chem., 77(1): 43-54.

Macrellis, H.M., Trick, C.G., Rue, E.L., Smith, G. and Bruland, K.W., 2001. Collection and detection of natural iron-binding ligands from seawater. Mar. Chem., 76(3): 175-187.

Martin, J.M., Dai, M.H. and Cauwet, G., 1995. Significance of colloids in the biogeochemical cycling of organic-carbon and trace-metals in the Venice lagoon (Italy). Limnol. Oceanogr., 40(1): 119-131.

Martinez, J.S., Barbeau, K. and Butler, A., 2000. Marine bacterial siderophores. Abstracts of Papers of the American Chemical Society, 219: 522-INOR.

Miller, W.L. and Kester, D., 1994. Photochemical iron reduction and iron bioavailability in seawater. J. Mar. Res., 52: 325-343.

Miller, W.L., King, D.W., Lin, J. and Kester, D.R., 1995. Photochemical redox cycling of iron in coastal seawater. Mar. Chem., 50(1-4): 63-77.

Millero, F.J., 1998. Solubility of Fe(III) in seawater. Earth. Planet. Sci. Let., 154(1-4): 323-329.

Millero, F.J. and Izaguirre, M., 1989. Effect of ionic-strength and ionic interactions on the oxidation of Fe(II). J. Solut. Chem., 18(6): 585-599.

Millero, F.J. and Sotolongo, S., 1989. The oxidation of Fe(II) with H_2O_2 in seawater. Geochim. Cosmochim. Acta, 53(8): 1867-1873.

Millero, F.J., Sotolongo, S. and Izaguirre, M., 1987. The oxidation-kinetics of Fe(II) in seawater. Geochim. Cosmochim. Acta, 51(4): 793-801.

Moffett, J.W., 2001. Transformations among different forms of iron in the ocean. In: D.R. Turner and K.A. Hunter (Editors), The Biogeochemistry of Iron in Seawater. IUPAC series on analytical

and physical chemistry of environmental systems. John Wiley & Sons, LTD, New York, pp. 343-372.

Morris, A.W., Bale, A.J., Howland, R.J.M., Millward, G.E., Ackroyd, D.R., Loring, D.H. and Rantala, R.T.T., 1986. Sediment mobility and its contribution to trace-metal cycling and retention in a macrotidal estuary. Water Sci. Technol., 18(4-5): 111-119.

Nolting, R.F., Gerringa, L.J.A., Swagerman, M.J.W., Timmermans, K.R. and de Baar, H.J.W., 1998. Fe(III) speciation in the high nutrient, low chlorophyll Pacific region of the Southern Ocean. Mar. Chem., 62(3-4): 335-352.

O'Sullivan, D.W., Hanson, A.K. and Kester, D.R., 1995. Stopped-flow luminol chemiluminescence determination of Fe(II) and reducible iron in seawater at subnanomolar levels. Mar. Chem., 49(1): 65-77.

Powell, R.T., Landing, W.M. and Bauer, J.E., 1996. Colloidal trace metals, organic carbon and nitrogen in a southeastern US estuary. Mar. Chem., 55(1-2): 165-176.

Powell, R.T. and Wilson-Finelli, A., 2003. Importance of organic Fe complexing ligands in the Mississippi River plume. Est. Coast. Shelf Sci., 58(4): 757-763.

Powell, R.T. and Wilson-Finelli, A., 2003. Photochemical degradation of organic iron complexing ligands in seawater. Aquat. Sci., 65(4): 367-374.

Rich, H.W. and Morel, F.M.M., 1990. Availability of well-defined iron colloids to the marine diatom *Thalassiosira weissflogii*. Limnol. Oceanogr., 35(3): 652-662.

Rijkenberg, M.J.A., Fischer, A.C., Kroon, J.J., Gerringa, L.J.A., Timmermans, K.R., Wolterbeek, H.T. and de Baar, H.J.W., 2005. The influence of UV irradiation on the photoreduction of iron in the Southern Ocean. Mar. Chem., 93: 119-129.

Rose, A.L., Waite, T.D., 2003. Kinetics of iron complexation by dissolved natural organic matter in coastal waters. Mar. Chem., xx: xx-xx.

Rue, E.L. and Bruland, K.W., 1995. Complexation of iron(III) by natural organic-ligands in the central north Pacific as determined by a new competitive ligand equilibration adsorptive cathodic stripping voltammetric method. Mar. Chem., 50(1-4): 117-138.

Rue, E.L. and Bruland, K.W., 1997. The role of organic complexation on ambient iron chemistry in the equatorial Pacific Ocean and the response of a mesoscale iron addition experiment. Limnol. Oceanogr., 42(5): 901-910.

Sanudo-Wilhelmy, S.A., RiveraDuarte, I. and Flegal, A.R., 1996. Distribution of colloidal trace metals in the San Francisco Bay estuary. Geochim. Cosmochim. Acta, 60(24): 4933-4944.

Seitz, W.R. and Hercules, D.M., 1972. Determination of trace amounts of iron (II) using chemiluminescence analysis. Anal. Chem., 44: 2143-2149.

Sholkovitz, E.R., 1978. Flocculation of dissolved Fe, Mn, Al, Cu, Ni, Co and Cd during estuarine mixing. Earth. Planet. Sci. Let., 41(1): 77-86.

Sholkovitz, E.R., Boyle, E.A. and Price, N.B., 1978. Removal of dissolved humic acids and iron during estuarine mixing. Earth. Planet. Sci. Lett., 40(1): 130-136.

Steeneken, S.F., Buma, A.G.J. and Gieskes, W.W.C., 1995. Changes in transmission characteristics of polymethylmethacrylate and cellulose-(III) acetate during exposure to ultraviolet-light. Photochem. Photobiol., 61(3): 276-280.

Sunda, W.G. and Huntsman, S.A., 1995. Iron uptake and growth limitation in oceanic and coastal phytoplankton. Mar. Chem., 50(1-4): 189-206.

Takeda, S. and Kamatani, A., 1989. Photoreduction of Fe(III)-EDTA complex and its availability to the coastal diatom *Thalassiosira weissflogii*. Red Tides: Biol., Environ. Sci., Toxicol.: 349-352.

van den Berg, C.M.G., 1995. Evidence for organic complexation of iron in seawater. Mar. Chem., 50(1-4): 139-157.

Waite, T.D., 2001. Thermodynamics of the iron system in seawater. In: D.R. Turner and K.A. Hunter (Editors), The biogeochemistry of iron in seawater. IUPAC series on Analytical and Physical Chemistry of Environmental Systems. John Wiley & Sons, LTD, pp. 291-342.

Waite, T.D. and Morel, F.M.M., 1984. Photoreductive dissolution of colloidal iron-oxide - effect of citrate. J. Colloid Interface Sci., 102(1): 121-137.

Wells, M.L. and Goldberg, E.D., 1993. Colloid aggregation in seawater. Mar. Chem., 41(4): 353-358.

Wells, M.L. and Mayer, L.M., 1991. The photoconversion of colloidal iron oxyhydroxides in seawater. Deep Sea Res. I, 38(11): 1379-1395.

Wen, L.S., Santschi, P., Gill, G. and Paternostro, C., 1999. Estuarine trace metal distributions in Galveston Bay: importance of colloidal forms in the speciation of the dissolved phase. Mar. Chem., 63(3-4): 185-212.

Wilhelm, S.W. and Trick, C.G., 1994. Iron-limited growth of cyanobacteria: multiple siderophore production is a common response. Limnol. Oceanogr., 39(8): 1979-1984.

Witter, A.E., Hutchins, D.A., Butler, A. and Luther, G.W., 2000. Determination of conditional stability constants and kinetic constants for strong model Fe-binding ligands in seawater. Mar. Chem., 69(1-2): 1-17.

Witter, A.E., Lewis, B.L. and Luther, G.W., 2000. Iron speciation in the Arabian Sea. Deep Sea Res. II, 47(7-8): 1517-1539.

Witter, A.E. and Luther, G.W., 1998. Variation in Fe-organic complexation with depth in the northwestern Atlantic Ocean as determined using a kinetic approach. Mar. Chem., 62(3-4): 241-258.

Wollast, R. and Peters, J.J., 1980. Transfer of materials in estuarine zones, Symposium on transport processes in estuarine and near-shore zones. International Counsil for the Expplaration of the Sea. 68th Statutory Meeting, Copenhagen, Denmark, pp. 20 pp.

Wu, J.F. and Luther, G.W., 1995. Complexation of Fe(III) by natural organic-ligands in the northwest Atlantic Ocean by a competitive ligand equilibration method and a kinetic approach. Mar. Chem., 50(1-4): 159-177.

Xiao, C.B., Palmer, D.A., Wesolowski, D.J., Lovitz, S.B. and King, D.W., 2002. Carbon dioxide effects on luminol and 1,10-phenanthroline chemiluminescence. Anal. Chem., 74(9): 2210-2216.

Chapter 9

Summary and recommendations

1. Summary

The chemistry of the biological limiting trace metal Fe in seawater is a prominent subject in the elucidation of the biological mechanisms controlling CO_2 uptake and release in so called High Nutrient Low Chlorophyll regions as e.g. the Southern Ocean. The photoreduction of Fe is an important mechanism to convert colloidal and chelated Fe species in more kinetically labile inorganic Fe species, resulting in a higher bioavailability to phytoplankton (Wells et al., 1991; Miller and Kester, 1994). A possible positive influence of enhanced ultraviolet B (UVB: 280-315 nm), due to the yearly austral spring ozone depletion, on the primary production via the chemistry of Fe and subsequent possible change into a more biological available Fe fraction is studied here. Furthermore, we investigated the influence of light on different chemical forms of Fe, varied by the presence of different Fe-binding ligands, and moreover, the effect of two typical Antarctic diatom species on the Fe photochemistry. The influence of UV on natural organic Fe-complexes was investigated in the Dutch estuarine waters of the Scheldt and Marsdiep.

As clearly shown during deck-incubations of open Southern Ocean seawater, where a distinct diel cycle in iron photoreduction was observed, UVB produces most Fe(II) per $W^{-1}m^{+2}$ followed by ultraviolet A (UVA: 315-400 nm) and the visible part of the light spectrum (VIS: 400-700 nm) respectively (Chapter 3, Rijkenberg et al., 2005). Similar conclusions were made for the production of the important Fe(II) oxidant H_2O_2 as determined in the eastern equatorial Atlantic Ocean (Chapter 2, Gerringa et al., 2004). The production of H_2O_2 increased with shorter wavelength and light intensity. The UVB is 228 times more effective and UVA 6.5 times more effective than VIS in the production of 1 nM H_2O_2. Therefore, UVB is not only the most effective wavelength region in the photoproduction of Fe(II) but also in the production of H_2O_2. However, surprisingly, as H_2O_2 is regarded as an important Fe(II) oxidant (Croot et al., in press), the excellent linear relationship between Fe(II) production and irradiance during deck-incubations in the Southern Ocean show that the Fe(II) oxidation rate remained constant (Chapter 3, Rijkenberg et al., 2005). No increase in Fe(II) oxidation rate due to photoproduced H_2O_2 was detected.

We know now that UVB plays an important role but it is not yet possible to evaluate the relative impact of enhanced UVB on the Fe photochemistry. Ozone depletion not only causes increased UVB irradiance but also a shift towards lower wavelengths. To evaluate the influence of enhanced UVB we assessed the influence of each wavelength on the photoproduction of Fe(II) in the Southern Ocean seawater (Chapter 4, Rijkenberg et al.,

2004). A spectral weighting function describing the wavelength dependency of the photoproduction of Fe(II) in Antarctic seawater was established. The strong wavelength-dependent photoproduction of Fe(II) from amorphous ferric hydroxides is described as an exponential function: $\varepsilon(\lambda) = 3.57 \cdot 10^3 \cdot e^{-0.02(\lambda-300)}$. Solar spectra recorded during the Antarctic ozone depletion season of year 2000 were used to demonstrate that daily and seasonal variability of the UVA and VIS dominates Fe(II) production rates in surface waters (respectively >60% and about 30%) in all seasons and at all depths. Although UVB is the most effective wavelength region for Fe(II) photoproduction, the impact of UVB was small due to the relatively low flux of UVB into the ocean surface waters. Nevertheless, the impact of UVB did indeed increase significantly from 3.54 to 6.15 % during the austral ozone minimum. Conclusively, the effect of enhanced UVB is relatively small compared to UVA and VIS and consequently of minor importance for the production of biological available Fe for phytoplankton in the Southern Ocean.

Organic Fe-binding ligands play an important role in the chemistry of Fe in seawater. More than 99% of the dissolved Fe concentration is organically complexed (Rue and Bruland, 1995; van den Berg, 1995). Organic Fe-binding ligands increase the solubility of Fe in seawater (Kuma et al., 1996). Furthermore, it is reported that Fe bound by certain siderophores can be photoreduced (Barbeau et al., 2003). We investigated two aspects of the influence of light on organically complexed Fe: i) the influence of organic Fe-complexing ligands (model and natural) on the photoreduction of Fe, and ii) the influence of light, and especially UV, on the photodegradation of natural organic Fe-binding ligands.

The addition of model Fe-binding ligands as desferrioxamine B (DFOB), phytic acid and protoporphyrin IX (PPIX) led to changes in Fe photochemistry each according to a different mechanism either increasing or decreasing the Fe(II) photoproduction (Chapter 5). Desferrioxamine B caused a decrease of the initial photoreducible Fe fraction and captured re-oxidized Fe, thus decreasing the Fe(II) steady-state concentration. Consequently DFOB, and presumably also its other marine variants, prevents the photo-transformation of crystalline Fe into a potentially more bioavailable amorphous Fe fraction, where instead the Fe is transformed in an organically complexed Fe fraction which is known to be not available for uptake by phytoplankton (Wells, 1999; Timmermans et al., 2001).

Phytic acid operates by another mechanism resulting in an increase in the Fe entering the photo-induced redox cycle. Phytic acid influenced the colloid formation of Fe by the formation of more irregular aggregates with Fe (Anderson, 1963), increasing the Fe fraction available for photo-induced Fe reduction. This effect of phytic acid on the photoreduction of Fe from an amorphous colloidal Fe pool disappears when the phytic acid concentration becomes too high. Then the phytic acid appears to shield the surface-bound Fe fraction from photo-induced reduction by adsorption of the phytic acid to the colloid surface (Ognalaga et al., 1994). Phytic acid makes up an important part of the phosphate pool entering the sea via

the rivers (Suzumura and Kamatani, 1995) and consequently plays an important role in the Fe photochemistry in coastal waters.

The PPIX doesn't bind Fe(III) in seawater as suggested by Rue and Bruland (1995) and Witter et al. (2000), but instead binds Fe(II) under seawater conditions. The PPIX acts as a photosensitizing catalytic producer of superoxide and possibly free radical ligand species, thus increasing the dark reduction of Fe(III) to Fe(II). The PPIX does not only influence the Fe chemistry in seawater but also the oxygen radical chemistry increasing the concentration of superoxide and subsequent via dismutation also the concentration of hydrogen peroxide. This finding is especially important for marine environments where the phytoplankton community is dependent on rapid Fe cycling with a very low iron pool (Cullen et al., 1992; Price et al., 1994). Much of the regenerated iron in these open ocean systems may be present in biological chelates such as porphyrin related molecules, whose release into seawater indeed has an important influence on the chemical speciation of Fe (Sunda, 2001).

In conclusion, organic ligands affect the photochemistry of Fe in seawater. We do not know if these model ligands are present in significant concentrations in the oceans and especially in the Southern Ocean.

To investigate the photodegradation of natural organic Fe-binding ligands leading to the production of Fe(II) we used organic rich estuarine waters (Chapter 8). The water collected in the Marsdiep as well as in the Scheldt estuary contained concentrations of Fe-binding ligands as high as 24.4 eq nM Fe and ~ 4.6 eq nM Fe with conditional stability constants K' of 10^{21} and $10^{20.1}$, respectively.

The organic Fe-binding ligands in the Marsdiep and Scheldt water were not significantly photodegraded by UVA and UVB (Chapter 8). No significant photodegradation or changes in concentration or conditional stability constant of the strong Fe-binding ligands were observed. These findings were confirmed by the production of very low concentrations Fe(II) (< 240 pM) compared to the concentration of organic iron ligand complexes. Furthermore, the observation that the Fe(II) production versus time showed a similar pattern as the Fe(II) production from inorganic Fe colloids (Wells and Mayer, 1991; Emmenegger et al., 2001) suggests that the Fe(II) originates mainly from an inorganic colloidal Fe fraction. Also the natural organic Fe-binding ligands in the Southern Ocean seawater were insensitive for UV destruction (Chapter 5). The observation that even the relatively fresh organic Fe-binding ligands from coastal and estuarine waters are not photodegraded confirms further that in contrast to the effect of model ligands, the effect of photodegradation of natural ligands only plays a minor role within the Fe photochemistry.

Organic complexation plays also an important role in the biogeochemistry of Fe in estuaries. As it keeps iron in the dissolved phase. The dissolved phase will be flushed from the estuary while the non-organically complexed phase tends to aggregate and adsorb to particles staying within the internal cycle of the estuary (Morris et al., 1986; Dai and Martin,

1995; Wen et al., 1999). Here we show that UV irradiance has no influence on the transport of dissolved organically complexed Fe from the estuarine environment to the coastal zone.

Surprisingly we observed besides strong Fe-binding ligands also concentrations of TAC-labile Fe (Fe complexed by 10 μM TAC after >12 hours of equilibration) of 4 and 12 nM in the Marsdiep and Scheldt, respectively. These TAC-labile Fe concentrations were lower after 1 kDa ultrafiltration indicating that at least part of the TAC-labile Fe is colloidal. Furthermore, the TAC-labile Fe concentration decreased during irradiance as well as in the dark. We do not know which process could be responsible for this decrease in the concentration of TAC-labile Fe. We suggest that the degradation of weak Fe-binding ligands or maybe colloidal material subject to aging (Cornell and Schwertmann, 1996), adsorption of organic material (Kreller et al., 2003) or aggregation (Wells and Goldberg, 1993) could be responsible.

The high dissolved concentrations of TAC-labile Fe are well above the concentration of dissolved Fe-binding ligands and the solubility product of Fe. This excess of Fe could be explained with the presence of a relative weak ligand class with an estimated conditional stability constant outside the detection window of the voltammetric method using TAC as competing ligand. A kinetic approach resulted in an estimated conditional stability constant between 10^{16} and 10^{18} (Chapter 7). We concluded that this class of weak ligands (P) prevented precipitation of Fe(hydr)oxides. These high TAC-labile Fe concentrations have been observed before, during algae blooms (Croot and Johansson, 2000; Chapter 8) and incubations with single diatom species (Chapter 6) indicating that biological processes might be involved. It is not yet possible to draw conclusions about the identity of the weaker ligand P. Yet, there are clues hinting at colloidal Fe as shown by using ultra filtration of Scheldt water (Chapter 8) and the detection of high TAC-labile Fe concentration after input of large quantities of Fe during an Fe enrichment experiment (Boye et al., in press).

We discussed the photochemistry of amorphous Fe (hydr)oxides and organically complexed Fe and left the last words to the diatoms. We performed many photochemical experiments to investigate the relation between different iron species and irradiance trying to elucidate the role of light in the enhancement of a biological available Fe fraction. But the diatoms took the last word. *Thalassiosira* sp. and *Chaetoceros brevis*, two typical Antarctic diatoms actively modify the photo-induced Fe chemistry (Chapter 6). An increase in the Fe(II) concentration during the second day of the experiments, together with a relative increase in the importance of VIS suggested a modification of the photoreducible Fe fraction by released organic substances. This would improve the photochemical processes, resulting in the reduction and solubilisation of Fe from colloidal material, and increase the biological availability of Fe in the euphotic zone. Although UVB is the most effective wavelength, it forms the least significant source, and although UVA plays the dominant role in the

photoreduction of amorphous Fe (hydr)oxides, the diatoms modify the photoreducible Fe source, thus increasing the role of VIS.

The diatoms not only surprised us with the improvement of the photoreducibility of the Fe fraction but *C. brevis* also transformed strong organic Fe-binding ligands into a weaker Fe-binding ligand class. Recently, biological uptake of Fe complexed by organic Fe-binding ligands was shown, visualized by the uptake of radio-isotopic Fe (Hutchins et al., 1999; Maldonado and Price, 2001). This study shows that the binding characteristics of the organic Fe-complexing ligands are changed by the presence of the phytoplankton species *C. brevis* (Chapter 6). It can be speculated that this transformation is caused during uptake of the complexed Fe, or that *C. brevis* modifies the strong Fe-binding ligands to make the complexed Fe more biologically available. Thus there is a possibility that *C. brevis* as a small diatom species (4-6 μm) not only benefits from its surface to volume ratio as compared to large diatoms as *Thalassiosira* sp. (70 μm) (Sunda and Huntsman, 1995) but also from their ability to modify the Fe-binding ligand fraction (Chapter 6).

A more rigorous study of the immense complexity and diversity of the Fe chemistry in seawater is only possible using detailed and controlled experiments. This being stated, the results should however be verified under natural conditions. We found that UVB is the most effective wavelength region to photoreduce Fe originating from freshly formed Fe (hydr)oxides, however, in the whole solar spectrum its importance is relatively small. Furthermore, model ligands gave us very clear and interesting results upon irradiation with light, however, these processes were not directly identified in coastal seawater containing natural ligands. Finally, in experiments with diatoms the studied processes in the laboratory were extremely useful in interpreting the modification of the Fe speciation induced by diatoms.

2. Recommendations

The chemistry of Fe in seawater is complex which means that additional experiments and questions to answer have been piling up during this study. We used a weighting function for the photoproduction of Fe(II) from amorphous Fe (hydr)oxides in Southern Ocean seawater to evaluate the influence of an anthropogenic increase in UVB on the Fe photochemistry. Although a good approach, it can be improved by performing these experiments at the location itself using fresh natural seawater without addition of Fe and under the natural solar irradiance.

The photochemistry of amorphous Fe (hydr)oxides as a result of the addition of Fe(III) to seawater needs to be investigated into more detail. The process of aging of Fe colloids needs to be investigated for changes in the photoreducible Fe fraction. Furthermore, the change in reactivity of the crystalline Fe for binding by TAC (Fe reactivity) during aging

could tell us about its potential availability for biological uptake. These experiments will give us more insight in the processes occurring after a fresh input of Fe via dust or iron enrichment experiments.

We investigated the photodegradation of organic Fe-binding ligands in the Marsdiep and Scheldt. Similar experiments need to be performed for an open ocean environment such as the Southern Ocean. The concentration of ligands is low in an open ocean environment and eventual photodegradation of ligands will have more impact on the solubility of Fe.

A new class of weak ligands (P) has consequences for our view on the solubility of Fe. We deduced its existence from kinetic experiments but we do not know anything yet about its identity or even if it is organic or inorganic. We do not know where and when this class of ligands occurs. High TAC-labile Fe has been found during springblooms but we do not know if these weaker ligands (P) were present before and after these spring blooms. High concentrations TAC-labile Fe have been found in incubations with *C. brevis*. However, we have no explanation for the difference of occurrence of high TAC-labile Fe in incubations with *C. brevis* as compared to the incubations with *Thalassiosira* sp. It will be an important step forward when TAC-labile Fe, as suggested, can be related to biological uptake of Fe.

Experiments performed in Chapter 6 where Fe was added to incubation experiments with diatoms resulted in a doubling of the concentration of Fe-binding ligands. A similar effect was observed during EisenEx (Boye et al., in press). This would suggest that inorganic colloidal Fe can bind Fe with similar conditional stability constants as the strong Fe-binding ligands. Experiments where Fe is added to organic-free seawater and samples are taken in time and measured for Fe-binding places by voltammetry can give us the answer. Did *C. brevis* transform a strong organic Fe-binding ligand class or a strong inorganic Fe-binding class as a result of the addition of Fe? And if *C. brevis* transforms a strong inorganic Fe-binding class does that result in the weak Fe-binding class P?

Not much is known about the importance of photo(induced) reduction of Fe for the speciation and biological availability of Fe in the world oceans. A field study is necessary to measure the relative importance of Fe photochemistry of different oceanic environments from coastal via shelf to open oceanic waters. A combination of size fractionation, subsequent determination of organic Fe-complexing compounds and of the photoreducible Fe fraction will give us insight in the identity and quantity of the Fe fractions susceptible for photoreduction. After evaluation of these results more detailed studies can be performed to increase our knowledge of Fe photochemistry in relation to Fe chemistry and biological availability. Above all photochemistry of Fe must be investigated in relation to organic as well as inorganic speciation and the aging of colloidal and crystalline Fe.

References

Anderson, G., 1963. Effect of iron/phosphorus ratio and acid concentration on precipitation of ferric inositol hexaphosphate. J. Sci. Food Agric., 14(5): 352-359.

Barbeau, K., Rue, E.L., Trick, C.G., Bruland, K.T. and Butler, A., 2003. Photochemical reactivity of siderophores produced by marine heterotrophic bacteria and cyanobacteria based on characteristic Fe(III) binding groups. Limnol. Oceanogr., 48(3): 1069-1078.

Boye, M., Nishioka, J., Croot, P.L., Laan, P., Timmermans, K.R. and de Baar, H.J.W., in press. Major deviations of iron complexation during 22 days of a mesoscale iron enrichment in the open Southern Ocean. Mar. Chem.

Cornell, R.M. and Schwertmann, U., 1996. The Iron Oxides. VCH Publishers, New York.

Croot, P.L. and Johansson, M., 2000. Determination of iron speciation by cathodic stripping voltammetry in seawater using the competing ligand 2-(2- thiazolylazo)-p-cresol (TAC). Electroanalysis, 12(8): 565-576.

Croot, P.L., Laan, P., Nishioka, J., Strauss, V., Boye, M., Timmermans, K.R., Bellerby, R.G., Goldson, L., Nightingale, P. and de Baar, H.J.W., in press. Spatial and temporal distribution of Fe(II) and H_2O_2 during EisenEx, an open ocean mesoscale iron enrichment. Marine Chemistry.

Cullen, J.J., Lewis, M.R., Davis, C.O. and Barber, R.T., 1992. Photosynthetic characteristics and estimated growth-rates indicate grazing is the proximate control of primary production in the equatorial Pacific. J. Geophys. Res., 97(C1): 639-654.

Dai, M.H. and Martin, J.M., 1995. First data on trace-metal level and behavior in 2 major Arctic river-estuarine systems (Ob and Yenisey) and in the adjacent Kara Sea, Russia. Earth Planet. Sci. Lett., 131(3-4): 127-141.

Emmenegger, L., Schonenberger, R.R., Sigg, L. and Sulzberger, B., 2001. Light-induced redox cycling of iron in circumneutral lakes. Limnol. Oceanogr., 46(1): 49-61.

Gerringa, L.J.A., Rijkenberg, M.J.A., Timmermans, K.R. and Buma, A.G.J., 2004. The influence of solar ultraviolet radiation on the photochemical production of H_2O_2 in the equatorial Atlantic Ocean. J. Sea Res., 51(1): 3-10.

Hutchins, D.A., Witter, A.E., Butler, A. and Luther, G.W., 1999. Competition among marine phytoplankton for different chelated iron species. Nature, 400(6747): 858-861.

Kreller, D.I., Gibson, G., Novak, W., Van Loon, G.W. and Horton, J.H., 2003. Competitive adsorption of phosphate and carboxylate with natural organic matter on hydrous iron oxides as investigated by chemical force microscopy. Colloid Surf. A-Physicochem. Eng. Asp., 212(2-3): 249-264.

Kuma, K., Nishioka, J. and Matsunaga, K., 1996. Controls on iron(III) hydroxide solubility in seawater: The influence of pH and natural organic chelators. Limnol. Oceanogr., 41(3): 396-407.

Maldonado, M.T. and Price, N.M., 2001. Reduction and transport of organically bound iron by *Thalassiosira oceanica* (Bacillariophyceae). J. Phycol., 37(2): 298-309.

Miller, W.L. and Kester, D., 1994. Photochemical iron reduction and iron bioavailability in seawater. J. Mar. Res., 52: 325-343.

Morris, A.W., Bale, A.J., Howland, R.J.M., Millward, G.E., Ackroyd, D.R., Loring, D.H. and Rantala, R.T.T., 1986. Sediment mobility and its contribution to trace-metal cycling and retention in a macrotidal estuary. Water Sci. Technol., 18(4-5): 111-119.

Ognalaga, M., Frossard, E. and Thomas, F., 1994. Glucose-1-phosphate and myoinositol hexaphosphate adsorption mechanisms on goethite. Soil Sci. Soc. Am. J., 58(2): 332-337.

Price, N.M., Ahner, B.A. and Morel, F.M.M., 1994. The equatorial Pacific Ocean - grazer-controlled phytoplankton populations in an iron-limited ecosystem. Limnol. Oceanogr., 39(3): 520-534.

Rijkenberg, M.J.A., Fischer, A.C., Kroon, J.J., Gerringa, L.J.A., Timmermans, K.R., Wolterbeek, H.T. and de Baar, H.J.W., 2005. The influence of UV irradiation on the photoreduction of iron in the Southern Ocean. Mar. Chem., 93: 119-129.

Rijkenberg, M.J.A., Gerringa, L.J.A., Neale, P.J., Timmermans, K.R., Buma, A.G.J. and de Baar, H.J.W., 2004. UVA variability overrules UVB ozone depletion effects on the photoreduction of iron in the Southern Ocean. Geophys. Res. Lett., 31: L24310, doi:10.1029/2004GL020829.

Rue, E.L. and Bruland, K.W., 1995. Complexation of iron(III) by natural organic-ligands in the central north Pacific as determined by a new competitive ligand equilibration adsorptive cathodic stripping voltammetric method. Mar. Chem., 50(1-4): 117-138.

Sunda, W.G., 2001. Bioavailability and bioaccumulation of iron in the sea. In: D.R. Turner, Hunter, K.A. (Editor), The biogeochemistry of iron in seawater. John Wiley & sons, New York, pp. 41-84.

Sunda, W.G. and Huntsman, S.A., 1995. Iron uptake and growth limitation in oceanic and coastal phytoplankton. Mar. Chem., 50(1-4): 189-206.

Suzumura, M. and Kamatani, A., 1995. Origin and distribution of inositol hexaphosphate in estuarine and coastal sediments. Limnol. Oceanogr., 40(7): 1254-1261.

Timmermans, K.R., Gerringa, L.J.A., de Baar, H.J.W., van der Wagt, B., Veldhuis, M.J.W., de Jong, J.T.M., Croot, P.L. and Boye, M., 2001. Growth rates of large and small Southern Ocean diatoms in relation to availability of iron in natural seawater. Limnol. Oceanogr., 46(2): 260-266.

van den Berg, C.M.G., 1995. Evidence for organic complexation of iron in seawater. Mar. Chem., 50(1-4): 139-157.

Wells, M.L., 1999. Manipulating iron availability in nearshore waters. Limnol. Oceanogr., 44(4): 1002-1008.

Wells, M.L. and Goldberg, E.D., 1993. Colloid aggregation in seawater. Mar. Chem., 41(4): 353-358.

Wells, M.L. and Mayer, L.M., 1991. The photoconversion of colloidal iron oxyhydroxides in seawater. Deep Sea Res. I, 38(11): 1379-1395.

Wells, M.L., Mayer, L.M., Donard, O.F.X., Sierra, M.M.D. and Ackelson, S.G., 1991. The photolysis of colloidal iron in the oceans. Nature, 353(6341): 248-250.

Wen, L.S., Santschi, P., Gill, G. and Paternostro, C., 1999. Estuarine trace metal distributions in Galveston Bay: importance of colloidal forms in the speciation of the dissolved phase. Mar. Chem., 63(3-4): 185-212.

Witter, A.E., Hutchins, D.A., Butler, A. and Luther, G.W., 2000. Determination of conditional stability constants and kinetic constants for strong model Fe-binding ligands in seawater. Mar. Chem., 69(1-2): 1-17.

Samenvatting

Het spoor-metaal ijzer (Fe) speelt in grote delen van de oceaan een belangrijke rol in de limitatie van algengroei. De chemie van Fe is daarom ondermeer van belang voor het koolstofdioxide budget in de Zuidelijke IJszee. De fotoreductie van ijzer is essentieel in de transformatie van colloidaal en organisch gebonden ijzer naar een reactievere Fe vorm die beter beschikbaar is voor opname door algen. Iedere lente ontstaat boven Antarctica een gat in de ozonlaag resulterend in een verhoogde intensiteit ultaviolet-B licht (UVB: 280-315 nm) die het aard- en zeeoppervlak bereikt. Onderzocht werd of deze hogere intensiteit aan UVB de fotoreductie van Fe(III) bevordert, resulterend in hogere concentraties biologisch beschikbaar Fe. Daarnaast werd onderzocht hoe de aanwezigheid van Fe-bindende organische moleculen (liganden) en twee typische Antarctische algen van invloed zijn op de fotoreductie van Fe. Natuurlijke organische liganden, zoals die voorkomen in de Westerschelde en het Marsdiep, werden onderzocht op hun gevoeligheid voor afbraak door ultraviolet licht.

Dekincubaties van zeewater in de Zuidelijke IJszee tonen aan dat de concentratie Fe(II) (het resultaat van de fotoreductie van Fe) een dagelijkse cyclus vertoont en dat de Fe(II) productie ten gevolge van UVB het hoogst is gevolgd door ultraviolet-A licht (UVA: 315-400 nm) en zichtbaar licht (VIS: 400-700 nm) (Hoofdstuk 3). Vergelijkbare conclusies konden worden getrokken met betrekking tot de golflengte afhankelijkheid van de productie van H_2O_2 in de oostelijke equatoriale Atlantische Oceaan (Hoofdstuk 2). H_2O_2 is een belangrijke oxidator van Fe en transformeert Fe(II) terug naar Fe(III). De hoogste concentraties H_2O_2 worden geproduceerd door het licht met de laagste golflengte. Het UVB is 228 keer beter en het UVA is 6,5 keer beter dan het VIS in het produceren van 1 nM H_2O_2. UVB is dus niet alleen het meest effectief in de fotoproductie van Fe(II) maar ook in de productie van H_2O_2. Verbazingwekkend was echter dat de oxidatie van Fe(II) door het H_2O_2, dat als de belangrijkste oxidator van Fe(II) wordt beschouwd, constant bleef tijdens de dekincubaties. De oxidatie van Fe(II) nam tijdens het experiment niet toe door fotoproductie van H_2O_2.

Alhoewel we nu weten dat UVB een belangrijke rol speelt in de fotochemie van Fe, kunnen we nog niets zeggen over de invloed van een hogere intensiteit UVB op de Fe fotochemie. Afnemende concentraties ozon zorgen niet alleen voor een hogere intensiteit van het UVB dat het zee-oppervlak bereikt maar ook voor een verschuiving van het lichtspectrum naar lagere golflengten. Om de invloed van zowel de hogere intensiteit UVB als de verschuiving van het lichtspectrum naar lagere golflengten op de fotoreductie van Fe in het zeewater te kunnen bepalen werd de golflengte afhankelijkheid van de invloed van het licht op de fotoreductie van Fe onderzocht door het opstellen van een weegfunctie. Deze weegfunctie beschrijft de golflengte afhankelijkheid van de fotoproductie van Fe(II) in

zeewater afkomstig uit de Zuidelijke IJszee (Hoofdstuk 4). De sterk golflengte afhankelijke Fe(II) fotoproductie uit amorphe Fe(III) (hydr)oxiden kan worden beschreven als een exponentiele functie: $\varepsilon(\lambda) = 3.57 \cdot 10^3 \cdot e^{-0.02(\lambda - 300)}$. Gebruik makend van zonnespectra gemeten tijdens het Antarctische ozon minimum in het jaar 2000 laat toepassing van de weegfunctie zien dat de Fe(II) fotoproductie gedomineerd wordt door de dagelijkse variatie in het UVA en VIS. Dit geldt gedurende alle seizoenen voor zowel het zee-oppervlak (respectievelijk >60% en 30%) als dieper in de water kolom. Alhoewel UVB het meest effectieve golflengte gebied is in de fotoproductie van Fe(II), was de uiteindelijk invloed van UVB erg klein door de relatief lage intensiteit van het UVB dat de oppervlakte van de zee bereikt. Desalnietemin was de invloed van het verhoogde UVB op de Fe(II) fotoproductie statistisch significant. De invloed van het UVB als percentage van de Fe(II) fotoproductie door het gehele zonnespectrum steeg van 3,54% naar 6,15% gedurende het ozon minimum. Geconcludeerd kan worden dat de invloed van het verhoogde UVB relatief klein is in vergelijking met de invloed van het UVA en VIS op de productie van biologisch beter beschikbaar Fe voor de algen in de Zuidelijke IJszee.

Organische Fe liganden spelen een belangrijke rol in de chemie van Fe in zeewater. Meer dan 99% van de concentratie opgelost Fe is gebonden aan organische liganden. Deze organische liganden zorgen ervoor dat het slecht oplosbare Fe in zeewater toch in concentraties hoger dan het oplosbaarheidproduct van inorganisch Fe oxiden opgelost kan zijn. In dit proefschrift onderzochten wij twee aspecten van de interactie tussen licht en Fe gebonden door organische liganden, namelijk: i) de invloed van zowel individuele model liganden als de assemblage aan natuurlijke organische Fe liganden op de fotoreductie van Fe, en ii) de invloed van licht, en met name het UV, op de afbraak van deze natuurlijke organische liganden.

Het toevoegen van de Fe bindende liganden desferrioxamine B (DFOB), phytic acid en protoporphyrine IX (PPIX) leidde tot veranderingen in de fotochemie van het ijzer die ieder volgens een ander mechanisme resulteerde in een verhoging of een verlaging van de Fe(II) fotoproductie (Hoofdstuk 5). De fotoreduceerbare Fe fractie nam af na toevoeging van DFOB. Daarnaast werd het gevormde Fe(II) nadat het terug oxideerde tot Fe(III) door DFOB gebonden waardoor bij hoger wordende concentraties DFOB de evenwichtsconcentratie Fe(II) omlaag ging. Geconcludeerd kan worden dat DFOB samen met zijn mariene varianten de transformatie van kristalijn Fe naar een mogelijk biologisch beschikbare Fe fractie voorkomt. In plaats daarvan wordt het Fe getransformeerd van een kristalijne Fe fractie naar een organisch gebonden Fe fractie waarvan bekend is dat deze niet biologisch beschikbaar is.

Het toevoegen van phytic acid leidde juist tot een verhoging van de fotoreduceerbare Fe fractie. Doordat het Fe en de phytic acid onregelmatige aggregaten vormen ontstaat een groter oppervlakte waardoor meer Fe gefotoreduceerd kan worden. Echter, wanneer de concentratie phytic acid te hoog wordt, verdwijnt dit effect en neemt de fotoreduceerbare Fe

fractie juist af. Het lijkt erop dat phytic acid in die situatie het Fe aan het oppervlakte van de aggregaten afschermt door aan het oppervlak van colloidale Fe deeltjes te binden. Een belangrijk deel van het fosfaat dat via de rivieren in zee terecht komt bestaat uit phytic acid. Phytic acid kan dus een belangrijke rol spelen in de chemie van Fe in de kustwateren.

Het PPIX bind geen Fe(III) in zeewater zoals in de wetenschappelijke literatuur werd gesuggereerd, maar bindt in plaats daarvan Fe(II). Het PPIX gedraagt zich als een lichtgevoelige katalysator in de productie van superoxide en mogelijk van vrije radicalen gevormd uit aanwezige Fe liganden. Superoxide en de vrije radicalen gevormd uit aanwezige Fe liganden kunnen Fe(III) ook in het donker reduceren to Fe(II). Het PPIX beinvloedt niet alleen de Fe chemie in zeewater maar ook de chemie van zuurstof en zijn radicalen en dus de concentratie van waterstof peroxide dat via dismutatie uit superoxide kan ontstaan. Deze resultaten zijn erg belangrijk voor het Fe gelimiteerde mariene milieu waarin de algen afhankelijk zijn van het hergebruik van Fe. Veel van het Fe in deze milieus is namelijk gebonden door biologische moleculen, zoals porphyrines en gerelateerde moleculen, die in het water terecht komen na het stuk gaan van de algen cellen.

Geconcludeerd kan worden dat de organische Fe bindende liganden van groot belang zijn voor de fotochemie van het Fe in zeewater. We weten echter niet of de gebruikte individuele organische Fe bindende liganden in relevante concentraties in het mariene milieu en meer specifiek de Zuidelijke IJszee voorkomen.

Om onderzoek te kunnen doen naar de afbraak van natuurlijk Fe bindende liganden door licht werd gebruik gemaakt van water, rijk aan organisch materiaal, afkomstig uit estuaria (Hoofdstuk 8). Het water afkomstig uit het Marsdiep bevatte 24,4 eq nM Fe aan liganden met een conditionele stabiliteits constante (K') van 10^{21}. Het water van de Westerschelde bevatte ongeveer 4,6 eq nM Fe aan liganden met een conditionele stabiliteits constante (K') van $10^{20.1}$.

De organische Fe liganden in het water afkomstig uit de Westerschelde en het Marsdiep werden niet meetbaar afgebroken door UVA en UVB. Er werden geen veranderingen in de concentraties of de conditionele stabiliteits constanten geconstateerd. Deze observaties werden bevestigd door de lage fotoproductie van Fe(II) (<240 pM) in vergelijking met de concentraties organische Fe liganden. Verder suggereert de grote gelijkenis tussen het verloop van de concentratie Fe(II) met de tijd in dit water en de concentratie Fe(II) afkomstig van colloidaal Fe, zoals aangegeven in de wetenschappelijke literatuur, dat het Fe(II) waarschijnlijk afkomstig is van colloidaal Fe. Bovendien bleken de natuurlijke organische Fe bindende liganden in water afkomstig uit de Zuidelijke IJszee ongevoelig te zijn voor destructie door UV (Hoofdstuk 5). De observatie dat ook de relatief verse organische Fe liganden in het estuariene water niet worden afgebroken bevestigt verder dat de natuurlijk voorkomende organische Fe bindende liganden, in tegenstelling tot de model Fe liganden, geen grote rol spelen binnen de fotochemie van Fe.

De complexatie van Fe door organische liganden speelt ook een belangrijke rol in de geochemie van estuariene milieus aangezien daardoor het Fe in de opgeloste fase wordt gehouden. Het opgelost Fe zal vanuit het estuarium in de kustwateren stromen terwijl het Fe dat niet door organische liganden wordt gebonden zal aggregeren tot, en adsorberen aan, deeltjes die een veel langere verblijftijd in het estuarium hebben. We laten in dit hoofdstuk uit het proefschrift zien dat UV geen invloed heeft op het transport van opgelost organisch materiaal vanuit de estuarium naar de kustwateren (Hoofdstuk 8).

Verrassend genoeg vonden we naast de sterke organische Fe bindende liganden ook concentraties van 4 (Mardiep) en 12 nM (Westerschelde) TAC-labiel Fe (Fe dat na een periode van > 12 uur gebonden is door het Fe bindende ligand TAC, 10 µM). De concentratie TAC-labiel Fe was lager in de fractie < 1 kDa. Een gedeelte van het TAC-labiel Fe is dus colloidaal.

De concentratie TAC-labiel Fe was veel hoger dan de concentratie Fe bindende liganden en zeker hoger dan het oplosbaarheids product van Fe oxiden in het estuariene water. De overmaat aan Fe, die het TAC-labiel Fe vormt, zou verklaard kunnen worden door de aanwezigheid van een relatief zwak Fe bindend ligand met een conditionele stabiliteits constante die buiten het bereik van de voltammetrische methode met TAC als competerend ligand ligt. Door het probleem kinetsch te benaderen werd een schatting verkregen van de conditionele stabiliteits constante liggend tussen de 10^{16} en 10^{18} (Hoofdstuk 7). We concluderen dat deze zwakke Fe bindende liganden de precipitatie van Fe(hydr)oxiden voorkomt. De hoge concentraties TAC-labiel Fe zijn in de wetenschappelijke literatuur al een keer eerder beschreven en waargenomen tijdens een algen bloei en daarnaast ook tijdens experimenten met een Antarctische alg (Hoofdstuk 6). Deze waarnemingen wijzen op de mogelijkheid dat biologische processen een rol spelen in het ontstaan van deze zwakke Fe bindende liganden. Het is echter niet mogelijk om conclusies te trekken over de identiteit van deze zwakke Fe bindende ligand klasse, alhoewel resultaten met ultrafiltratie en de detectie van hoge concentraties TAC-labiel Fe na het toevoegen van grote hoeveelheden Fe aan het zeewater tijdens een Fe verrijkings experiment er op wijzen dat colloidaal Fe hier een rol kan spelen.

We hebben het nu gehad over de fotochemie van amorfe Fe (hydr)oxiden en organische Fe liganden maar we laten het laatste woord aan de algen zelf. We hebben heel veel fotochemische experimenten uitgevoerd in relatie tot verschillende vormen van Fe om te achterhalen hoe en of licht de biologisch beschikbare Fe fractie verhoogt, maar de algen hebben inderdaad het laatste woord. *Thalassiosira* sp. en *Chaetoceros brevis*, twee Antarctische algen beïnvloeden direct de fotochemie van Fe (Hoofdstuk 6).

Een verhoging van de gefotoreduceerde concentratie Fe(II) tegelijkertijd met een relatieve toename in het belang van VIS in de Fe fotochemie suggereert een verandering in de Fe fotochemie door organisch materiaal uitgescheiden door de Antarctische algen. Hierdoor

werd het fotochemische proces verbeterd resulterend in een hogere concentratie reactief en biologisch beschikbaar Fe. Alhoewel UVB de meest effectieve golflengte is en UVA de hoofdrol speelt in de fotoreductie van amorfe Fe (hydr)oxides, lijkt de aanwezigheid van organisch materiaal uitgescheiden door algen de rol van VIS in de fotoreductie van Fe te vergroten.

De algen verrasten ons niet alleen met het verbeteren van de fotoreduceerbaarheid van de Fe fractie maar *C. brevis* veranderde ook een gedeelte van de sterke organische Fe bindende liganden in een zwakker Fe bindende ligand klasse. In de wetenschappelijke literatuur wordt in onderzoek met behulp van radio-isotopisch Fe aangetoond dat algen Fe gebonden door organische Fe bindende liganden op kunnen nemen. Hoofdstuk 6 laat zien dat de bindings karakteristieken van de organische Fe bindende liganden veranderen door de aanwezigheid van de alg *C. brevis*. Er kan over gespeculeerd worden of deze verandering optreedt gedurende de biologische opname van het gecomplexeerde Fe, of dat *C. brevis* de sterke Fe bindende liganden zodanig verandert dat het gecomplexeerde Fe beter beschikbaar wordt. De mogelijkheid bestaat dat *C. brevis*, als kleine alg onder Fe limiterende omstandigheden, niet alleen voordeel heeft van zijn oppervlakte tot volume verhouding maar ook door de mogelijkheid om de organische gebonden Fe fractie te beïnvloeden (Hoofdstuk 6).

Een beter begrip van de enorme complexiteit en diversiteit van de Fe chemie in zeewater is alleen mogelijk wanneer gebruik gemaakt wordt van meer gedetailleerde en gecontroleerde experimenten. Daarnaast moeten resultaten wel geverifieerd worden aan de processen zoals deze in de natuur voorkomen. We hebben aangetoond dat UVB het meest effectieve golflengte gebied is in de fotoreductie van Fe afkomstig van vers gevormde amorfe Fe (hydr)oxiden, hoewel het UVB afkomstig van de zon vergeleken met de de golflengte regionen UVA en VIS het minst belangrijk is. Verder gaf de toevoeging van individuele liganden aan zeewater duidelijke en interessante resultaten. Deze processen konden echter niet direct gerelateerd worden aan processen die in de kustwateren met hoge concentraties Fe bindende liganden plaatsvinden. Uiteindelijk waren al deze experimenten van groot belang voor het begrip van de processen, die in aanwezigheid van algen, de fotoreductie van het Fe veroorzaakten.

Dankwoord

Dit dankwoord vind ik het moeilijkste gedeelte om te schrijven. Zoveel mensen hebben direct of indirect aan dit proefschrift bijgedragen, dat er ongewild het gevaar dreigt dat je iemand niet noemt. Verder vind ik het moeilijk om mijn dankbaarheid op de juiste manier onder woorden te brengen. Maar hieronder volgt een poging.....

Allereerst natuurlijk mijn dank aan mijn co-promotors Loes Gerringa en Anita Buma die mij vanaf het begin door dik en dun gesteund hebben. Met goed geplaatste zetjes op de juiste momenten heeft Loes mij door mijn PhD heen geduwd. Anita was altijd beschikbaar om mijn werk te lezen en van commentaar te voorzien. Daarnaast gaat mijn dank uit naar mijn promotor Prof. Hein de Baar die mij vooral in de laatste fase van mijn PhD heeft geholpen. Verder worden natuurlijk alle andere (ex)collegas van de ijzer afdeling, Patrick Laan, Jurjen Kramer, Marie Boye, Peter Croot, Klaas Timmermans en Bas van der Wagt bedankt voor hun medewerking en enthousiasme. Waarbij vooral ook Klaas en Patrick mij met raad en daad bijstonden. En degenen die ik vooral niet zal vergeten zijn de stage-studenten die zowel voor mij als voor Loes aan het werk zijn geweest. Zij hebben allen, Vicky Carolus, Ilona Velzeboer, Annelies Hommersom en Justin Swart, een wezelijke bijdrage geleverd aan het tot stand komen van dit proefschrift. Het was altijd een plezier om met jullie samen te werken. Verder heb ik veel geleerd van Patrick Neale die mij heeft geholpen om de weegfunctie te construeren.

Het enthousiasme van Astrid Fischer en Koos Kroon aan boord van de Polarstern maakte het erg plezierig om met hen samen te werken. Een samenwerking die werd voortgezet gedurende de dagen en nachten van de experimenten in Delft onder de rook (bij wijze van spreken) van de nucleaire reactor van het IRI. Hierbij werd ook de hulp van Ursula Woroniecka zeer gewaardeerd. Verder wordt Bert Wolterbeek hartstikke bedankt voor zijn kritisch commentaar en de voor mij zo leerzame discussies. En Tona Verburg wordt natuurlijk bedankt voor haar geduld bij het modeleren van onze data.

Ik ben mee geweest op vier wetenschappelijke vaartochten. Ik wil alle opvarenden, bemanning en wetenschappers, van de Polarstern (ANT 18 I, ANT 18 II), de Pelagia (Ironages III) en de Navicula (COMET) bedanken voor hun hulp bij het uitvoeren van mijn experimenten. Specifiek heb ik hierbij de samenwerking met Saad el Naggar, Tim van Oijen, Fleur Visser, Thomas Reinthaler en Gerard Herndl op prijs gesteld.

De leescommissie, Prof. Jef Huisman, Prof. Herman van Leeuwen en Prof. Patrick Neale bedank ik voor hun bereidheid om mijn proefschrift te beoordelen en mijn paranimfen Tanya Compton en Jack Terra bedank ik alvast voor hun steun tijdens de verdediging van mijn proefschrift.

De Potvis wordt helaas afgebroken! Vijf jaar heb ik met veel plezier in de Potvis gewoond en samengewoond. Een hele stoet aan mensen zijn de afgelopen jaren aan mij

voorbij getrokken. A single one, my girlfriend Tanya Compton, even got stuck. Ik wil allereerst natuurlijk mijn bungalow-genoten Ben Abbas, Joana Cardoso en Anne-Claire Baudoux bedanken voor hun jaren lange betrokkenheid en het erg prettige samenwonen. Natuurlijk zijn er nog heel veel meer mensen die het leven in de Potvis veraangenaamden: onze buren Seb en Nicola, Francois en Judith + kinderen, Marco en Cornelia, Piet, Eva, Thomas en Barbara, Denis, Khalid en Jasper samen met al die ex-Potvissers en Texel bewoners: Kai, Ishmael, Isabelle, Christina, Delphine, Phil, Yann, Alina, Marie-Aude, Pedro, Furu, Teresa, Oscar, Luisa, Genoveva, Marjolijn, Eva, Txetxu, Christian, Jerome, Neven, Inès, Fedor, Ellen, Conny en Geraldine.

Het dankwoord is bedoeld voor diegenen die een bijdrage leverden aan het proefschrift. Die bijdrage kan op vele manieren zijn geleverd in zowel het heden als het verleden: mijn ouders Han en Riet, Sung, Tanya, familie, vrienden en Wadwayers, bedankt!

Name	Micha J.A. Rijkenberg
Home address	De Dageraad 1 b5 1797 SK Den Hoorn, Texel The Netherlands phone: +31-6-27295999
Work address	Royal NIOZ Department of Marine Chemistry and Geology P.O. Box 59, 1790 AB Den Burg The Netherlands phone: +31-222-369489
E-mail	rijken@nioz.nl
Date and place of birth	June 3rd 1972, Amsterdam, The Netherlands
Citizenship	Dutch

EDUCATION

2000-*present*	Ph.D. candidate in Marine Chemistry, University of Groningen, the Netherlands
1992-1998	M.Sc. in Chemistry (molecular microbiology), University of Amsterdam, the Netherlands

EXPERIENCE

2000-*present*   Ph.D. candidate in a NOW/NAAP (Dutch Antarctic Program) funded project: Positive feedback of enhanced UV-B via iron chemistry of seawater on phytoplankton growth and CO_2 drawdown in the Southern Ocean.

Subject:	The influence of UV, organic Fe binding ligands and biology on the photochemistry of Fe in seawater.
Institute:	Royal NIOZ, University of Groningen
Supervisors:	Prof. Hein J.W. de Baar, Dr. Loes J.A. Gerringa, Dr. Anita G.J. Buma

1997   Research assistant in molecular microbiology (M.Sc. candidate).

Subject:	Cloning of the gene coding for the Photoactive Yellow Protein (PYP) from *Rhodobacter capsulatus*.
Institute:	University of British Columbia, Vancouver, Canada
Supervisor:	Prof. J.T Beatty

1996   Research assistant in molecular microbiology (M.Sc. candidate).

Subject:	Characterization of an alkaliphilic non-phototrophic bacterium.
Institute:	University of Amsterdam
Supervisor:	Prof. Klaas J Hellingwerf, Dr. Remco Kort

GRADUATE COURSES

2002	"Speciation and Bioavailability", Wageningen University, the Netherlands
2001	"Presentation" Course, Royal NIOZ, the Netherlands
2000	"Radioactivity safety course", level 5B, Interfacultair Reactor Institute, University of Delft

TEACHING EXPERIENCE

1998	"Molecular microbiology" (undergraduate practical course, University of Amsterdam)
	"Molecular techniques" (undergraduate practical course, University of Amsterdam)
2005	Coordination of the Oceanography course (undergraduate practical course, Royal NIOZ/University of Groningen)

CRUISE EXPERIENCE

2002	"Ironages III" Iron from above, Canaries basin, Ship: Pelagia (Royal NIOZ, the Netherlands), 4 weeks
2001	"Canoba I" (leg 2), The continental shelf pump. North Sea, Ship: Pelagia (Royal NIOZ, the Netherlands), 1 week
2001	"Comet" Fe and light in estuaries and rivers, Scheldt estuary, the Netherlands, Ship: Navicula (Royal NIOZ, the Netherlands), 10 days
2000	ANT 18/2, "EisenEx" Iron fertilization experiment, Southern Polar Frontal Zone, Ship: RV Polarstern (Alfred Wegener Institute Bremer-Haven, Germany), 6 weeks
2000	ANT 18/1, "Ironages I" Intercomparison Fe analysis, South-East Atlantic, Ship: RV Polarstern (Alfred Wegener Institute Bremer-Haven, Germany), 3 weeks

PUBLICATIONS (REFEREED JOURNALS)

Gerringa, L.J.A., **Rijkenberg, M.J.A.**, Wolterbeek, H.Th., Verburg, T.G., Boye, M., de Baar, H.J.W. Kinetic study reveals new Fe-binding ligand which affects the solubility of Fe in the Scheldt estuary *Submitted to Marine Chemistry*

Rijkenberg, M.J.A., Gerringa, L.J.A., Velzeboer, I., Timmermans, K.R., Buma, A.G.J., de Baar, H.J.W. Iron-binding ligands in Dutch estuaries are not affected by UV induced photochemical degradation *Submitted to Marine Chemistry*

Rijkenberg, M.J.A., Gerringa, L.J.A., Carolus, V.E., Velzeboer, I., Timmermans, K.R., de Baar, H.J.W. Individual ligands have different effects on the photoreduction of iron in natural seawater of the Southern Ocean *Submitted to Geochimica et Cosmochimica Acta*

de Baar, H.J.W., Boyd, P.W., Coale, K.H., Landry, M.R., Tsuda, A., Assmy, P., Bakker, D.C.E., Bozec, Y., Barber, R.T., Brzezinski, M.A., Buesseler, K.O., Boye, M., Croot, P.L., Gervais, F., Gorbunov, M.Y., Harrison, P.J., Hiscock, W.T., Laan, P., Lancelot, C., Levasseur, M., Marchetti, A., Millero, F.J., Nishioka, J., Nojiri, Y., van Oijen, T., Riebesell, U., **Rijkenberg, M.J.A.**, Saito, H., Takeda, S., Timmermans, K.R. and Veldhuis, M.J.W., 2005. Synthesis of 8 iron fertilization experiments: from the Iron Age in the age of enlightenment. *Accepted by Journal of Geophysical Research*

Rijkenberg, M.J.A., Fischer, A.C., Kroon, J.J., Gerringa, L.J.A., Timmermans, K.J., de Baar, H.J.W. (2005) The influence of UV irradiation on the photoreduction of iron in the Southern Ocean *Marine Chemistry* 93, 119-129

Rijkenberg, M.J.A., Gerringa, L.J.A., Neale, P.J., Timmermans, K.R., Buma, A.G.J., de Baar, H.J.W. (2004) UV-A variability overrules UV-B ozone hole effects on the photoreduction of iron in the Southern Ocean *Geophysical Research Letters* Vol. 31, L24310, doi: 10.1029/2004GL020829

Gerringa, L.J.A., **Rijkenberg, M.J.A.**, Timmermans K.R., Buma, A.G.J. (2004) The influence of UV on photochemical production of hydrogen peroxide formation in equatorial Atlantic Ocean water. *J. Sea Research*. 51, 3-10

Rijkenberg, M.J.A., Kort, R., Hellingwerf, K.J. (2001) *Alkalispirillum mobile* gen. Nov., spec. Nov., an alkaliphilic non-phototrophic member of the *Ectothiorhodospiraceae Arch. Microbiol.* 175:369-375

OTHER REFEREED PUBLICATIONS

Van Oijen, T., **Rijkenberg, M.J.A.** (2004) Control of phytoplankton growth by iron in the Southern Polar Frontal Zone: results of deck incubation during an *in situ* iron enrichment experiment (EisenEx/CARUSO), Ph.D. thesis, Groningen.

PUBLICATIONS IN PREPARATION

Rijkenberg, M.J.A., Gerringa, L.J.A., Timmermans, K.R., Fischer, A.C., Wolterbeek, H.Th., Buma, A.G.J., de Baar, H.J.W. Diatoms enhance the reactive iron pool: increasing Fe-photoreduction and light-independent modification of strong iron-binding ligands

PRESENTATIONS

Rijkenberg, M.J.A., Gerringa, L.J.A., Carolus, V.E., Velzeboer, I., de Baar, H.J.W. Photo(induced) redox cycling of Fe in the Southern Ocean: the organic Fe-binding ligands, BIPED, University of Groningen, 16 December 2004, Haren, *oral*

Rijkenberg, M.J.A., Gerringa, L.J.A., Neale, P.J., Timmermans, K.R., Buma, A.G.J., de Baar, H.J.W. Impact of enhanced UVB on the Fe photochemistry in the Southern Ocean
- Polair Symposium, Dutch Polar Program (NWO) and SCAR (KNAW), 10 & 11 May 2004, Teylers Museum, Haarlem (the Netherlands), *oral*
- Symposium on Positive feedback of enhanced UV-B via iron chemistry of seawater on phytoplankton growth and CO_2 fixation in the Southern Ocean, 8th April 2004, Royal NIOZ (the Netherlands), *oral*

Rijkenberg, M.J.A., Gerringa, L.J.A., Timmermans, K.J., Fischer, A.C., Carolus, V., Maas, L.R.M., Neale, P.J., de Baar H.J.W. The photoreduction of iron in seawater
- EGS - AGU - EUG Joint Assembly, April 2003, Nice (France), *poster*

Rijkenberg, M.J.A., Fischer, A.C., Gerringa, L.J.A., Kroon, J.J., Timmermans, K.R., Buma, A.G.J., de Baar H.J.W. The influence of enhanced UV radiation on the diel cycle of iron photoreduction in the Southern Ocean
- 6e Dutch Earth-Scientific Symposium 18 & 19 April 2002 Koningshof, Veldhoven (the Netherlands), *poster*
- Verwey meeting 28 & 29 January 2002 Royal NIOZ (the Netherlands), *poster*
- International Global Change Open Science Conference, 10-13 July 2001, Amsterdam (the Netherlands), *poster*
- Antarctica Symposium NWO/NAAP, 12th April 2001, Trippenhuis, Amsterdam (the Netherlands), *poster*

OTHER ACTIVITIES

1993-*present*	Member of the international committee of the youth association "Jong Nederland" (similar to Scouting)
1992-2001	Group leader for children between 7 and 12 years old. Vice chairman (1994-1995), chairman (1995-1997) of a local association of "Jong Nederland"
1997-1998	student member of the board of the education committee of bio-molecular chemistry
1996-1997	student member of the education committee of bio-molecular chemistry

SKILLS

Languages	Dutch: native language
	English: excellent
Drivers license	Yes